



**UNIVERSITY of the  
WESTERN CAPE**

**‘Recommendations for the development of a framework for  
radiological imaging studies during implant therapy in SA’**

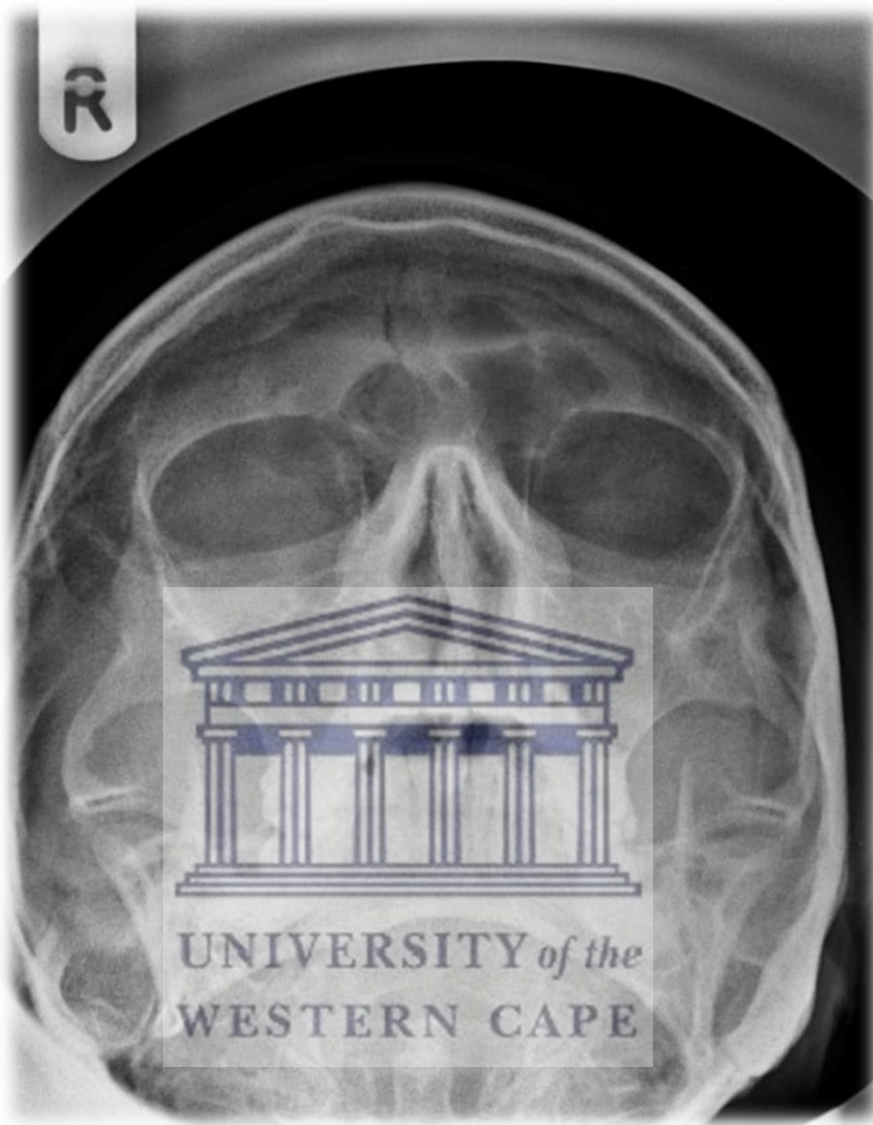


**Khaled Raed Beshtawi**

**Supervisor: Prof. M. Chetty**

**Co-supervisor: Dr. M. Peck**

"Submitted in fulfillment of the requirements of a Ph.D. degree in the Department of  
Diagnostics and Radiology, Faculty of Dentistry - University of the Western Cape."



*"The eye is always caught by light, but shadows have more to say." -Gregory Maguire.*

## DECLARATION

I declare that ‘Recommendations for the development of a framework for radiological imaging studies during implant therapy in SA’ is my own work, that it has not been submitted before for any degree or examination in any other university, and that all the sources I have used or quoted have been indicated and acknowledged as complete references.

Khaled Beshtawi: .....

Sept. 2020



UNIVERSITY *of the*  
WESTERN CAPE

## ACKNOWLEDGEMENTS

I would like to express my sincere thanks and appreciation to the following people for their respective contributions during this study:

- My supervisor and mentor, Professor M. Chetty for her insightful guidance and unwavering support.
- My co-supervisor Dr. M.T Peck for his assistance and constructive criticism.
- The medical physicist Dr.Christian Traunchet, Division of Medical Physics, Faculty of Health Sciences, Stellenbosch University.
- All the staff members at the Medical Physics Department, Groote Schuur Hospital, Cape Town.
- All the staff members at the Department of Radiology, Groote Schuur Hospital. Especial thanks go to Ms. Nazlea Behardien-Peters.
- The academic and administrative staff of the Department of Oral and Maxillofacial Radiology, Faculty of Dentistry, University of the Western Cape.
- Dr. Shoayeb Shaik for his support and advice over the last few years.
- Dr. Faheema Kimmie-Dhansay, for her assistance in statistical analysis, and support over the last few years.
- Gendent SA radiation inspection company, especially Mrs. Gillian Swart, for her generous assistance.
- Dr.Emad Qirresh for his endless support.
- Research Senate, Faculty of Dentistry, University of the Western Cape, South Africa for funding this project.

## DEDICATION

*This thesis is dedicated to my beloved family: My father, My mother, My brother.*

*To my extended family in South Africa*



UNIVERSITY *of the*  
WESTERN CAPE

## CONTENTS

|   |           |
|---|-----------|
| DECLARATION .....   | iii       |
| ACKNOWLEDGEMENTS .....  | iv        |
| DEDICATION .....  | v         |
| <b>PART 1 STUDY OVERVIEW .....</b>  | <b>1</b>  |
| CHAPTER 1   INTRODUCTION .....  | 2         |
| CHAPTER 2   AIM, OBJECTIVES, AND RATIONALE OF THE MAIN STUDY .....  | 6         |
| 2.1 Aim .....   | 6         |
| 2.2 Objectives .....  | 6         |
| 2.3 The rationale of the study .....  | 6         |
| CHAPTER 3   MATERIALS AND METHODS .....   | 8         |
| 3.1 Expected outcomes: Establishment of recommendations .....   | 8         |
| 3.2 Funding .....   | 8         |
| 3.3 Ethics .....  | 9         |
| <b>PART 2 NARRATIVE REVIEWS .....</b>   | <b>10</b> |
| CHAPTER 1   REVIEW OF RECENTLY PUBLISHED GLOBAL GUIDELINES AND<br>RECOMMENDATIONS ON IMAGING DURING IMPLANT THERAPY ..... | 11        |
| 1.1 Introduction .....  | 13        |
| 1.2 Recommendations by various organisational bodies .....  | 17        |
| 1.3 Conclusion .....  | 33        |
| 1.4 Limitations .....   | 33        |
| CHAPTER 2   REVIEW OF THE RADIOGRAPHIC MODALITIES USED DURING<br>DENTAL IMPLANT THERAPY: A NARRATIVE .....                | 34        |
| 2.1 Introduction .....  | 36        |
| 2.2 Current maxillofacial radiographic technologies (Table 2.7) .....   | 36        |
| 2.3 Phases of dental implant therapy where radiographic modalities are indicated (Table 2.9)<br>45                        |           |
| 2.4 Emerging technologies .....   | 53        |
| 2.5 Discussion & conclusion .....   | 54        |
| <b>PART 3 RADIOGRAPHIC PRESCRIPTION TRENDS AMONG SOUTH AFRICAN<br/>DENTISTS DURING DENTAL IMPLANT THERAPY .....</b>       | <b>55</b> |
| CHAPTER 1   INTRODUCTION .....  | 58        |
| CHAPTER 2   LITERATURE REVIEW .....   | 60        |
| 2.1 Dental implant radiographic prescription practices worldwide .....  | 60        |
| 2.2 Radiographic prescriptions in Africa .....  | 62        |

|  |  |           |
|--|--|-----------|
| CHAPTER 3  | AIMS AND OBJECTIVES.....                                 | 64        |
| 3.1  | Aim.....   | 64        |
| 3.2  | Objectives.....  | 64        |
| 3.3  | Rationale.....   | 64        |
| CHAPTER 4  | MATERIALS AND METHODS .....                              | 65        |
| 4.1  | Tools and methods.....                                   | 65        |
| 4.2  | Statistical overview and data analysis: .....            | 68        |
| CHAPTER 5  | RESULTS .....  | 69        |
| CHAPTER 6  | DISCUSSION .....   | 82        |
| CHAPTER 7  | CONCLUSION .....   | 85        |
| <b>PART 4    DIMENSIONAL ACCURACY OF VARIOUS RADIOGRAPHIC MODALITIES<br/>USED DURING IMPLANT THERAPY .....</b> |  | <b>86</b> |
| CHAPTER 1  | INTRODUCTION.....  | 89        |
| CHAPTER 2  | LITERATURE REVIEW.....                                   | 91        |
| 2.1  | Linear measurements accuracy: CBCT.....                  | 91        |
| 2.2  | Linear measurement accuracy: Panoramic radiographs ..... | 92        |
| CHAPTER 3  | AIMS AND OBJECTIVES.....                                 | 94        |
| 3.1  | Aim.....   | 94        |
| 3.2  | Objectives.....  | 94        |
| 3.3  | Rationale.....   | 94        |
| CHAPTER 4  | MATERIALS AND METHODS .....                              | 95        |
| 4.1  | Study design.....  | 95        |
| 4.2  | Methodology .....  | 95        |
| 4.3  | Data and statistical analysis.....                       | 103       |
| CHAPTER 5  | RESULTS .....  | 104       |
| CHAPTER 6  | DISCUSSION .....   | 109       |
| CHAPTER 7  | CONCLUSION .....   | 115       |
| <b>PART 5    RADIATION DOSES RECEIVED BY PATIENTS DURING DENTAL IMPLANT<br/>THERAPY 116</b>                    |  |           |
| CHAPTER 1  | INTRODUCTION.....  | 120       |
| CHAPTER 2  | LITERATURE REVIEW.....                                   | 122       |
| 2.1  | Absorbed and equivalent doses .....                      | 122       |
| 2.2  | Effective dose.....                                      | 122       |
| CHAPTER 3  | AIMS AND OBJECTIVES.....                                 | 130       |
| 3.1  | Aim.....   | 130       |

|               |  |            |
|---------------|--|------------|
| 3.2           | Objectives.....  | 130        |
| 3.3           | Rationale.....   | 130        |
| CHAPTER 4     | MATERIALS AND METHODS .....  | 131        |
| 4.1           | Study phases.....  | 131        |
| 4.2           | Data analysis .....  | 154        |
| CHAPTER 5     | RESULTS .....  | 155        |
| 5.1           | Phase I: TLD received doses .....  | 155        |
| 5.2           | Phase II: computer simulations .....   | 167        |
| CHAPTER 6     | DISCUSSION .....   | 173        |
| CHAPTER 7     | CONCLUSION .....   | 179        |
| <b>PART 6</b> | <b>RADIATION PROTECTION .....</b>  | <b>181</b> |
| CHAPTER 1     | INTRODUCTION.....  | 184        |
| CHAPTER 2     | LITERATURE REVIEW.....   | 186        |
| 2.1           | Biological risks.....  | 186        |
| 2.2           | Radiation protection measures .....  | 188        |
| CHAPTER 3     | AIMS AND OBJECTIVES.....   | 191        |
| 3.1           | Aim.....   | 191        |
| 3.2           | Objectives.....  | 191        |
| 3.3           | Rationale.....   | 191        |
| CHAPTER 4     | MATERIALS AND METHODS .....  | 192        |
| 4.1           | Methodology: .....   | 192        |
| CHAPTER 5     | RESULTS .....  | 198        |
| CHAPTER 6     | DISCUSSION .....   | 213        |
| CHAPTER 7     | CONCLUSION .....   | 219        |
| <b>PART 7</b> | <b>DISCUSSION AND CONCLUSION .....</b>   | <b>220</b> |
|               | Section 1: Discussion and conclusion .....   | 221        |
|               | Section 2: Proposed draft recommendations on implant imaging in SA (CHART 7-1).....          | 225        |
| <b>PART 8</b> | <b>REFERENCES.....</b>   | <b>233</b> |
| <b>PART 9</b> | <b>APPENDICES.....</b>   | <b>261</b> |
| 1)            | ETHICS APPROVAL LETTER.....  | 261        |
| 2)            | INFORMATION SHEET .....  | 262        |
| 3)            | CONSENT FORM: PARTICIPATION IN THE STUDY .....   | 265        |
| 4)            | SURVEY (Q1/2018): RADIOGRAPHIC TRENDS DURING DENTAL IMPLANT<br>THERAPY IN SOUTH AFRICA ..... | 266        |



## LIST OF TABLES:

|   |    |
|---|----|
| Table 1.1. PhD study at a glance.....   | 4  |
| Table 2.1. Selected relevant publications concerning implant imaging protocols and guidelines. ....   | 15 |
| Table 2.2. Clinical situations and the AAOMR recommendations 2012 (Tyndall et al., 2012).....   | 19 |
| Table 2.3. European Association for Osseointegration recommendations (Harris et al., 2002).....   | 20 |
| Table 2.4. Diagnostic properties of radiographic modalities (Harris et al., 2012). ....   | 21 |
| Table 2.5. European guidelines on radiation protection in dental radiology (Issue No 136) (European Commission, 2004). ....   | 24 |
| Table 2.6. Position statement of The American College of Prosthodontics (Ahmad & Chapokas, 2019).<br>.....  | 29 |
| Table 2.7. Radiographic modalities used during implant therapy .....  | 37 |
| Table 2.8. Indications, advantages, and disadvantages of radiographic modalities used in implant therapy consolidated by the author (Tyndall et al., 2012; Harris et al., 2012; Nagarajan et al., 2014; Gupta et al., 2015; Agrawal et al., 2014; Manisundar et al., 2014; Lingam et al., 2013; Sahai, 2015; Gray et al., 2003; Fokas et al., 2018). .... | 43 |
| Table 2.9. The radiographic indication of each treatment phase during dental implantology (Nagarajan et al., 2014; Gupta et al., 2015). ....  | 45 |
| Table 2.10. Estimated Hounsfield units for various bone types (Gupta et al., 2015). ....  | 49 |
| Table 3.1. Summary of survey results (Sakakura et al., 2003). ....  | 60 |
| Table 3.2. Survey results (Ramakrishnan et al., 2014). ....   | 61 |
| Table 3.3. Survey results (Alnahwi et al., 2017). ....  | 61 |
| Table 3.4. Factors influencing radiographic prescriptions (Rabi et al., 2017). ....   | 62 |
| Table 3.5. Survey results of prescription trends (Majid et al., 2014). ....   | 63 |
| Table 3.6. Factors influencing radiographic prescriptions (Majid et al., 2014).....   | 63 |
| Table 3.7. Distribution of the surveyees.....   | 69 |
| Table 3.8. Radiographic modalities preferred in various anatomical regions during the implant planning phase.....   | 71 |
| Table 3.9. Factors that influence radiographic preference during the implant planning phase. ....   | 74 |
| Table 3.10. Radiographic modalities preferred during and directly after the surgery. ....   | 75 |
| Table 3.11. The radiographic modalities preferred during follow-ups for symptomatic and asymptomatic patients.....  | 77 |
| Table 3.12. Factors that influence the radiographic preference during follow-up.....  | 78 |
| Table 3.13. The most frequently selected radiographic examinations during planning phase by various dental specialities. ....   | 80 |

|  |     |
|--|-----|
| Table 3.14. The most frequently selected radiographic examinations during surgical and post-surgical phases by various dental specialities. ....   | 80  |
| Table 3.15. The number of participants vs factors chosen by various dental specialities. ....  | 81  |
| Table 4.1. Exposure parameters, x-ray unit's specification, and distances measured. ....   | 102 |
| Table 4.2. Statistical overview showing the mean and standard deviation (SD) of the measured distances in various modalities. The mean difference (mm) between the radiographic modality and the corresponding physical measurements with the standard deviation (SD), and the <i>P</i> -value is also tabulated. .... | 105 |
| Table 4.3. An overview of the number of readings that showed differences attained by each radiographic modality, in both jaws. ....  | 106 |
| Table 4.4. Differences between physical linear and angular distances (linear – angular, mm).....   | 107 |
| Table 4.5. Inter-examiner and intra-examiner intraclass correlation coefficient. ....  | 108 |
| Table 5.1. Tissue weighting factor (ICRP 103 in 2007) (SCENIHR, 2012). ....  | 123 |
| Table 5.2. Published reports on the use of Monte-Carlo software for <i>E</i> calculations. ....  | 125 |
| Table 5.3. Reported ( <i>E</i> ) for selected CBCT machines. ....  | 127 |
| Table 5.4. Reported ( <i>E</i> ) for selected panoramic x-ray machines. ....   | 129 |
| Table 5.5. Technical specifications of the TLD-700 chips.....  | 133 |
| Table 5.6. Technical specifications of the annealing oven.....   | 134 |
| Table 5.7. Technical specifications of the dose-measuring device. ....   | 134 |
| Table 5.8. Technical specifications of the TLD chips' reader.....  | 134 |
| Table 5.9. TLDs' location in the phantom-head (adopted from (Ludlow, 2011)).....   | 135 |
| Table 5.10. Technical specifications of the first CBCT unit used. ....   | 136 |
| Table 5.11. Technical specifications of the second CBCT unit used. ....  | 137 |
| Table 5.12. Technical specifications of the panoramic x-ray machine used. ....   | 137 |
| Table 5.13. Exposure information during the radiographic examinations. ....  | 138 |
| Table 5.14. The fractions of tissue irradiated adapted by the author to measure FOV relevant to the study (Ludlow, 2011; Roberts et al., 2009). ....   | 139 |
| Table 5.15. Dose-determining parameters that were used for the Monte-Carlo simulations. ....   | 150 |
| Table 5.16. Modified input values used to compare their effects on the total effective dose.....   | 151 |
| Table 5.17. Equivalent dose $H_T$ ( $\mu\text{Sv}$ ) of individual organs/tissues and the total Effective dose ( <i>E</i> ) obtained from CBCT exams (using the NewTom <sup>®</sup> 5GXL).....   | 155 |
| Table 5.18. Equivalent dose $H_T$ ( $\mu\text{Sv}$ ) of individual organs/tissues and the total Effective dose ( <i>E</i> ) obtained from CBCT exams (using the CS 8100 <sup>®</sup> 3D). ....   | 155 |
| Table 5.19. Equivalent dose $H_T$ ( $\mu\text{Sv}$ ) of individual organs/tissues and the total Effective dose ( <i>E</i> ) obtained from panoramic exams (using the Sirona <sup>®</sup> XG3). ....  | 156 |
| Table 5.20. The equivalent dose ( $H_T$ ) of multiple organs/ tissues and total effective dose ( <i>E</i> ) obtained from TLD and PCXMC simulations of the NewTom <sup>®</sup> 5GXL exposures (FOV: 15 × 12 cm). ....  | 167 |

|  |     |
|--|-----|
| Table 5.21. The equivalent dose ( $H_T$ ) of multiple organs/ tissues and total effective dose ( $E$ ) obtained from TLD and PCXMC simulations of the NewTom <sup>®</sup> 5GXL exposures (FOV: 8 × 8 cm). .....    | 167 |
| Table 5.22. The equivalent dose ( $H_T$ ) of multiple organs/ tissues and total effective dose ( $E$ ) obtained from TLD and PCXMC simulations of the NewTom <sup>®</sup> 5GXL exposures (FOV: 8 × 8 cm (HiRes.)). | 168 |
| Table 5.23. Individual organ and total (net) PCXMC effective doses ( $E$ , in $\mu$ Sv) .....  | 169 |
| Table 5.24. The resultant PCXMC effective doses in $\mu$ Sv comparison when different input values were employed. ....   | 170 |
| Table 5.25. The contribution (%) of selected organs/tissues to the overall effective dose revealed from PCXMC simulations and TLDs. ....   | 176 |
| Table 6.1. Exposure information during the radiographic examinations with the shield in place. ....  | 195 |
| Table 6.2. Organ and total Effective doses ( $E$ ) captured with shields on. ....  | 198 |
| Table 6.3. A comparison between absorbed doses with/without using the shield - NewTom <sup>®</sup> 5GXL.   | 199 |
| Table 6.4. A comparison between absorbed doses with/without using the shield - CS <sup>®</sup> 8100 3D. ....   | 200 |
| Table 6.5. A comparison between absorbed doses with/without using the shield - Sirona <sup>®</sup> Orthophos XG3. ....   | 201 |
| Table 6.6. Exposure parameters with and without the shield. ....   | 214 |

## LIST OF FIGURES

|   |     |
|---|-----|
| Figure 1-1. Diagrammatic representation of the various facets of this research. ....  | 5   |
| Figure 2-1. A periapical radiograph showing two implants in the 36,37 region. Note the close proximity of the implant (lower part) to the apex of tooth #35. ....   | 37  |
| Figure 2-2. A panoramic radiograph acquired with a surgical guide in place for intended implant planning in the 36# area. Note the mild smile line exaggeration and chin cut due to positioning errors. ....            | 39  |
| Figure 2-3. CBCT scan. Reformatted panoramic view (top) and cross-sectional slices (bottom) were obtained. The measurement of the vertical dimension of a mandibular bone section (area of 36 #) was investigated. .... | 41  |
| Figure 3-1. Diagrammatic representation of the main research project. The current sub-study is highlighted. ....  | 65  |
| Figure 4-1. Diagrammatic representation of the main research project. The current sub-study is highlighted. ....  | 95  |
| Figure 4-2. Diagram showing the reference points and distances measured. ....   | 97  |
| Figure 4-3. CBCT (A), panoramic (B), and intraoral (C) machines. ....   | 100 |
| Figure 4-4. Virtual measurements done on CBCT volumes (A&B), Panoramic (C), and Periapical (D) radiographs. ....  | 101 |
| Figure 4-5. Demonstration of the curved distances (arc lengths) between jaw segments (A&B). ....  | 112 |

|   |     |
|---|-----|
| Figure 5-1. Diagrammatic representation of the main research project. The current sub-study is highlighted. ....  | 131 |
| Figure 5-2. Annealing of the TLD chips using the PTW® TLDO® annealing oven at Groote Schuur hospital, Cape Town (top and bottom). ....  | 140 |
| Figure 5-3. Calibration of the TLD-700 chips at Tygerberg Hospital, Cape Town (top and bottom). ....  | 141 |
| Figure 5-4. Read-out of the TLD chips using the REXON® UL-320 reader at Groote Schuur hospital, Cape Town (top & bottom). ....  | 142 |
| Figure 5-5. Preparation of the RANDO® phantom (exterior view). ....   | 143 |
| Figure 5-6. Preparation of the RANDO® phantom slabs (interior view). ....   | 144 |
| Figure 5-7. CBCT acquisition using NewTom® 5GXL at Groote Schuur hospital, Cape Town. ....  | 145 |
| Figure 5-8. CBCT acquisition using Carestream® 8100 3D at private practice, Cape Town (A&B).. ....  | 146 |
| Figure 5-9. Conventional panoramic acquisition using Sirona® Orthophos® XG3 at Tygerberg Hospital, Cape Town. ....  | 147 |
| Figure 5-10. Scouting x-ray image during the CBCT acquisition using the NewTom® 5GXL. ....  | 148 |
| Figure 5-11. A screenshot of the “user interface” of the PCXMC software. The field size at the rotation axis was calculated using the calculator shown. ....  | 149 |
| Figure 5-12. A screenshot of the Excel spreadsheet application provided with the PCXMC software allowing the simulation of large number projections at once (batch mode). ....  | 149 |
| Figure 5-13. The Z and Y reference coordinates for the direction of the central axis of the x-ray beam. Note that the ruler in the figure is only for explanation purposes and does not represent the actual scale. ....                      | 153 |
| Figure 5-14. Interactive field viewer (in the PCXMC) showing the primary beam direction and the covered anatomical region. ....   | 153 |
| Figure 5-15. Anteroposterior (top) and lateral cephalometric (bottom) radiographic views of the acquired CBCT volume (NewTom® 5GXL, FOV 15 × 12 cm, regular scan, and standard dose). ....  | 159 |
| Figure 5-16. Axial slice (top left), sagittal slice (top right), coronal slice (bottom left), and 3D view (bottom right) reconstructed from the acquired CBCT volume (NewTom® 5GXL, FOV 15 × 12 cm, regular scan, and standard dose). ....    | 160 |
| Figure 5-17. AP (top) and lateral cephalometric (bottom) radiographic views of the acquired CBCT volume (NewTom® 5GXL, FOV 8 × 8 cm, regular scan, and standard dose). ....   | 161 |
| Figure 5-18. Axial slice (top left), sagittal slice (top right), coronal slice (bottom left), and 3D view (bottom right) reconstructed from the acquired CBCT volume (NewTom® 5GXL, FOV 8 × 8 cm, regular scan, and standard dose). ....      | 162 |
| Figure 5-19. AP (top) and lateral cephalometric (bottom) radiographic views of the acquired CBCT volume (NewTom® 5GXL, FOV 8 × 8 cm (HiRes.), regular scan, and standard dose). ....  | 163 |
| Figure 5-20. Axial slice (top left), sagittal slice (top right), coronal slice (bottom left), and 3D view (bottom right) reconstructed from the acquired CBCT volume (NewTom® 5GXL, 8 × 8 cm (HiRes.), regular scan, and standard dose). .... | 164 |

|   |     |
|---|-----|
| Figure 5-21. Axial (top), coronal (bottom left), sagittal (bottom right) slices reconstructed from the acquired CBCT volume (CS <sup>®</sup> 8100 3D, 8 × 9 cm, Full jaw program, fast scan). .....   | 165 |
| Figure 5-22. 3D reconstructions (side and front views) from the acquired CBCT volume (CS 8100 <sup>®</sup> 3D, 8 × 9 cm, Full jaw program, fast scan). .....  | 165 |
| Figure 5-23. The resultant panoramic radiograph (using Sirona <sup>®</sup> XG3, 69 kVp, 15 mA, 13.9s).....  | 166 |
| Figure 6-1. Diagrammatic representation of the main research project. The current sub-study is highlighted. ....  | 192 |
| Figure 6-2. Diagram showing the architecture/design of the shield. ....   | 193 |
| Figure 6-3. During the phantom-head preparation, with the modified head shield attached.....  | 194 |
| Figure 6-4. During the CBCT acquisition (NewTom <sup>®</sup> 5GXL), with the modified head shield attached in place. ....   | 196 |
| Figure 6-5. During the CBCT acquisition (CS8100 <sup>®</sup> 3D), with the modified head shield attached in place .....   | 197 |
| Figure 6-6. During the panoramic acquisition, with the modified head shield attached in place. ....   | 197 |
| Figure 6-7. Anteroposterior (top) and lateral cephalometric (bottom) radiographic views of the CBCT volume with the attached modified shield (NewTom <sup>®</sup> 5GXL, FOV 15 × 12 cm, regular scan, and standard dose). ....  | 203 |
| Figure 6-8. Axial slice (top left), coronal slice (top right), sagittal slice (bottom left), and 3D view (bottom right), reconstructed from CBCT volume with the attached modified shield (NewTom <sup>®</sup> 5GXL, FOV 15 × 12 cm, regular scan, and standard dose).....  | 204 |
| Figure 6-9. Front view (top left), posterior view (top right), and right side (bottom) 3D models reconstructed using the NewTom <sup>®</sup> 5GXL (FOV: 15 × 12 cm) with the shield attached. ....  | 205 |
| Figure 6-10. 3D reconstruction with different filters (MIP and transparent bone) using the NewTom <sup>®</sup> 5GXL (FOV: 15 × 12 cm) with the shield attached. ....  | 206 |
| Figure 6-11. Axial slice series captured at various vertical levels of the head reconstructed from the CBCT volume, with the attached modified shield (NewTom <sup>®</sup> 5GXL, FOV 15 × 12 cm, regular scan, and standard dose).....  | 207 |
| Figure 6-12. Axial slices captured at the same vertical level (in the maxilla) with the shield attached (top) and without the shield (bottom) (using the NewTom <sup>®</sup> 5GXL, FOV 15 × 12 cm). When compared, both slices reveal no obvious alteration of the quality of the volume due to the lead shield (e.g. induced artefacts). ....  | 210 |
| Figure 6-13. Axial slices captured at the same vertical level (in the mandible) with the shield attached (top) and without the shield (bottom) (using the NewTom <sup>®</sup> 5GXL, FOV 15 × 12 cm). When compared, both slices reveal no obvious alteration of the quality of the volume due to the lead shield (e.g. induced artefacts). .... | 211 |
| Figure 6-14. Axial (top), coronal (bottom left), sagittal (bottom right) slices reconstructed from the CBCT volume with the shield in place (using the CS 8100 <sup>®</sup> 3D, 8 × 9 cm (Full jaw program), fast scan). There is no evidence of the shield structure nor artefacts on the rendered volume. ....                                | 212 |
| Figure 6-15. The resultant panoramic radiograph with the shield in place (the radiopaque structure in the upper third of the radiograph).....   | 212 |

## LIST OF CHARTS

|   |     |
|---|-----|
| Chart 3-1. The province of the dental practice of those surveyed. ....  | 69  |
| Chart 3-2. Distribution of the formal training received by participants. ....   | 70  |
| Chart 3-3. Radiographic modalities prescribed during the planning phase (A-E).....  | 71  |
| Chart 3-4. Factors influencing radiographic preference during the implant planning phase.....   | 75  |
| Chart 3-5. The radiographic modalities prescribed during and directly after surgery (A&B).....  | 76  |
| Chart 3-6. The radiographic modalities prescribed during the follow-up of A/symptomatic patients (A&B). ....                                    | 77  |
| Chart 3-7. Frequency of radiographic follow-up (after the delivery of the prosthesis).....  | 79  |
| Chart 5-1. (A-D) The contribution of various organs/tissues to the overall effective dose exposed using different CBCT and fields of view. .... | 156 |
| Chart 5-2. The contribution of various organs/tissues to the overall effective dose exposed during the panoramic examination. ....              | 158 |
| Chart 5-3. (A-C) The contribution of various organs/tissues to the overall effective dose revealed from PCXMC simulations. ....                 | 171 |
| Chart 7-1. Recommendation on dental implant imaging in SA.....  | 232 |

### Technical notes:

- This thesis complies with the recommended UWC thesis format (Font: Times New Roman, size: 12 pp, 1.5 space, 4×3×3×3 cm page margins).
- The thesis is divided into parts; each has its own chapters. This format was followed due to the presence of various sub-studies which contributed to the aim of this study.
- Tables, Figures, and Charts numbering system follow the part number (e.g. Figure 3-5 is Figure number 5 in Part number 3).



UNIVERSITY of the  
WESTERN CAPE

PART 1 | STUDY OVERVIEW

**CONTENTS AT A GLANCE**

- Chapter 1 | Introduction
- Chapter 2 | Aim, Objectives, and Rationale of the main study
- Chapter 3 | Materials and methods
  - 3.1 Expected outcomes: Establishment of recommendations
  - 3.2 Funding
  - 3.3 Ethics



UNIVERSITY of the  
WESTERN CAPE

**CHAPTER 1 | INTRODUCTION**

Dental implant therapy is an increasingly popular, highly successful dental treatment that aims to replace missing teeth (Moraschini et al., 2015; Tyndall & Brooks, 2000). Dental radiology is considered to be a core element for the assessment and planning of many phases of dental implant therapy (DIT) (Harris et al., 2002).

Although the panoramic and periapical radiographs remain popular radiographic techniques during several stages of dental implant therapy, development and integration of cone beam computed tomography (CBCT) into dental practice enhanced the diagnostic capabilities of dentists, and became an increasingly accepted modality during implant therapy (Tyndall et al., 2012; Benavides et al., 2012). Use of panoramic radiographs is popular in routine daily dental practice, as it offers advantages such as simplicity of procedure, availability, lower costs, and lower radiation dose compared to Computed Tomography (CT) or CBCT (Vazquez et al., 2008; Assaf & Gharbyah, 2014; Kim et al., 2011). Cone Beam Computed Tomography obviates deficiencies of two-dimensional modalities, including the ability to provide a three-dimensional view of the potential implant sites that is accurate and free of superimpositions (Benavides et al., 2012).

Despite the advantages offered by the CBCT examinations, concerns regarding the increased radiation exposure to patients have been raised; especially as the increasing popularity of CBCT has turned it into a routine procedure (Noffke et al., 2011; Li, 2013). The evaluation of the indications, advantages, and drawbacks of each radiographic modality is essential to achieve optimal treatment outcomes. For the purpose of implant therapy planning, there is a lack of a perfect, single radiographic examination (Tyndall et al., 2012).

Several stages of implant therapy need an appropriate imaging modality, which highlight the need to develop selection criteria that will ensure clinical efficiency, and, at the same time, save patients from unnecessary radiation (Tyndall et al., 2012).



Many radiographic and dental implant regulatory authorities/organisations have published guidelines/advisory recommendations for the geographic region of practice is (e.g. the American Academy of Oral and Maxillofacial Radiology, the European Association for Osseointegration, the European Commission, and the International Congress of Oral Implantologists). It is worth noting that most of the available recommendations are mainly advisory, consensus-based, and ascertained from clinical opinions or inconsistent published review reports (Tyndall et al., 2012; Ahmad & Chapokas, 2019; Harris et al., 2012; Bornstein et al., 2014; European Commission, 2004).

Each region of the world may vary in terms of practices, experiences, development, and socioeconomic status. The use of CBCT in South Africa (SA) was reported to be becoming increasingly popular, or even a routine procedure in some practices, and that it was being misused for screening purposes (Noffke et al., 2011). To the best of the author's knowledge, there is a lack of local imaging guidelines/protocols available for use during dental implant therapy in SA. In addition, no information was available which described the current radiographic prescription trends among South African dental clinicians.

### ***Project Development***

This research was developed in order to address the deficiencies described above in the South African context. In its entirety, the project consisted of five sub-studies which were designed to inform the various treatment aspects that influence the choice of radiographic modality during dental implant therapy. The findings of these investigations were further consolidated in order to suggest recommendations that aim at achieving “low-dose” imaging protocols in South Africa and in regional developing countries.

Each sub-study has its unique aims, methodologies, and research outputs and are, therefore, presented and discussed in separate parts with individual relevant chapters. A detailed methodology each sub-study is provided by the author intentionally in order

to allow reproducibility of the results by independent researchers, if necessary. For the sake of clarity, the various aspects of the study are tabulated (Table 1.1) and each sub-study is represented in Figure 1-1.

**Table 1.1. PhD study at a glance.**

| <b>Part</b> | <b>Project/sub-study title</b>  | <b>Study design</b>               | <b>Aim</b>   |
|-------------|---|-----------------------------------|--|
| <b>1</b>    | <b>Study overview</b>   | N/A                               | To introduce and provide an overview of the project.   |
| <b>2</b>    | <b>A review of recently published global guidelines and recommendations on imaging during implant therapy</b> | Narrative reviews                 | To review the recent international implant imaging protocols/guidelines.                                   |
|             | <b>Review of the radiographic modalities used during dental implant therapy: A narrative</b>                  | Narrative reviews                 | To review the most commonly used radiographic techniques during implant therapy.                           |
| <b>3</b>    | <b>Radiographic prescription trends among South African dentists during dental implant therapy</b>            | Survey (cross-sectional study)    | To report the current radiographic practices during dental implant therapy in SA.                          |
| <b>4</b>    | <b>The dimensional accuracy of various radiographic modalities used during implant therapy</b>                | In-vitro experimental study       | To assess the clinical accuracy of measurements obtained from different radiographic modalities.           |
| <b>5</b>    | <b>Radiation doses received by patients during dental implant therapy</b>                                     | In-vitro experimental study       | To calculate the radiation doses received by dental implant patients during the radiographic examinations. |
| <b>6</b>    | <b>Radiation protection</b>   | In-vitro experimental study       | To investigate the effect of a head and upper face shield designed by the author.                          |
| <b>7</b>    | <b>Discussion and conclusion</b>  |                                   |  |
|             | <b>Recommendations (Working Draft)</b>  | Consensus-based, clinical opinion |  |

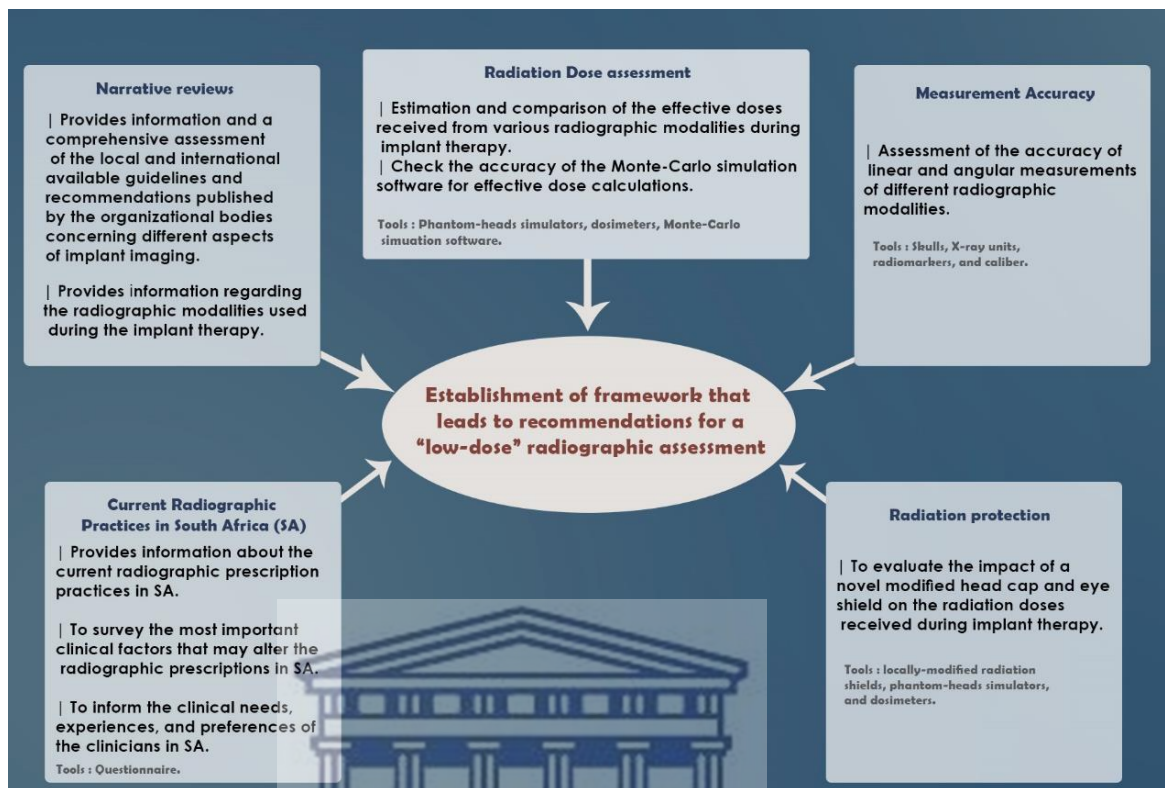


**Figure 1-1. Diagrammatic representation of the various facets of this research.**

**KEYWORDS:** implant, imaging, protocols, CBCT, low-dose, measurement accuracy, guidelines.

## CHAPTER 2 | AIM, OBJECTIVES, AND RATIONALE OF THE MAIN STUDY

### 2.1 AIM

To provide a framework that informs recommendations that aid in the development of a radiography protocol, in which patients receive the least amount of radiation exposure during dental implant therapy in the SA.

### 2.2 OBJECTIVES

1. To provide narrative reviews regarding recent imaging protocols worldwide and the most commonly used radiographic techniques for implant therapy.
2. To survey the current radiographic prescriptions during implant therapy in South African private, public, and academic dental institutions.
3. To assess the accuracy of linear and angular measurements of the different radiographic modalities that are used during implant therapy.
4. To calculate the radiation doses received during radiographic examinations with regard to implant therapy.
5. To investigate the impact of a novel design of a locally modified head cap shield on radiation dose reduction.

### 2.3 THE RATIONALE OF THE STUDY

1. The published national and international guidelines on implant therapy have the following shortcomings:
  - Lack of “evidence-based action-statements” (Bornstein et al., 2014; European Commission, 2004).
  - Recommendations /guidelines on CBCT use are at best “consensus-based or derived from a limited methodological approach” (Bornstein et al., 2014).

- There is ambiguity in published studies on the clinical efficacy of cross-sectional imaging (Tyndall et al., 2012; Bornstein et al., 2014).
2. The type and frequency of radiographs used in implant treatment vary and are dependent on professional judgment and the treatment phase, which change depending on the skill, competence, and experience of the clinician (Tyndall & Brooks, 2000; Tyndall et al., 2012; European Commission, 2004).
    - Standardization is required
  3. South Africa has no comprehensive implant imaging guidelines. Possible misuse of three-dimensional modalities has been reported (Noffke et al., 2011).
  4. Although limited guidelines regarding implant imaging protocols have been published worldwide, these guidelines are generic and the selection of the imaging modality depends on clinical judgment of the practitioner.
    - Radiographic practices vary among clinicians, which may lead to misuse of the radiographic modalities, especially the 3D ones. Consequently, resulting in hazardous exposure to patients. Moreover, dental x-ray units vary in their radiation output and the technology can be upgraded constantly.
    - Therefore, guidelines need to be reviewed frequently.
  5. This analysis evaluates various pieces of evidence required to suggest imaging recommendations. The findings and conclusions of this research project are aimed at contributing to the pool of evidence on implant imaging nationally and internationally. They can be utilised by local dental regulatory authorities and dental scientific societies in order to formulate local or regional guidelines.

## CHAPTER 3 | MATERIALS AND METHODS

This PhD study has five components (Figure 1-1) that are necessary in order to achieve the collective aim (Table 1.1). Detailed information regarding each sub-study is provided in the relevant parts.

### 3.1 EXPECTED OUTCOMES: ESTABLISHMENT OF RECOMMENDATIONS

The evidence obtained from various sub-studies include:

- Updated narrative reviews about the international/regional implant imaging guidelines and the most used radiographic techniques during implant therapy.
- A platform to inform the clinician's radiographic goals, share local clinicians' experiences, and report the current imaging prescription trends in South Africa.
- Information about the radiation doses and dimensional accuracy of various radiographic modalities used during implant therapy.
- Information about dose reduction effectiveness using a newly designed and locally modified head and eye shield.

Based on the findings of these investigations, conclusions are drawn and working draft recommendations/guidelines for South Africa are provided, that represent the informed clinical opinions of the investigator. The recommendations and/or evidence collected might be further explored/used during targeted workshops, conferences, and other academic meetings. Nevertheless, the findings of each piece of original research conducted can be used to enrich the available evidence pool, aimed at establishing local imaging guidelines by relevant authorities.

### 3.2 FUNDING

This research was funded by Senate Research funds, University of the Western Cape.

### 3.3 ETHICS

The research was submitted to the Senate Research Ethics Committee of the University of the Western Cape for approval, and permission was granted (BM19/1/20). All the information obtained during this study was kept confidential, and no personal identification of the patients (if any) or participants was disclosed. All the radiographs included in the study were obtained from the Faculty of Dentistry (UWC) with informed consents. All investigations were carried out according to the declaration of Helsinki and the Hippocratic Oath.

The researcher has no conflict of interest in any brands or products that were used during the study.





PART 2 | NARRATIVE REVIEWS

**CONTENTS AT A GLANCE**

|  |
|--|
| Chapter 1   Review of recently published global guidelines and recommendations on imaging during implant therapy |
| 1.1 Introduction   |
| 1.2 Recommendations by various organisational bodies   |
| 1.3 Conclusion   |
| 1.4 Limitations  |
| Chapter 2   Review of the radiographic modalities used during dental implant therapy: a narrative                |
| 2.1 Introduction   |
| 2.2 Current maxillofacial radiographic technologies  |
| 2.3 Phases of dental implant therapy where radiographic modalities are indicated                                 |
| 2.4 Emerging technologies  |
| 2.5 Discussion & conclusion  |



UNIVERSITY of the  
WESTERN CAPE



## CHAPTER 1 |

REVIEW OF RECENTLY PUBLISHED GLOBAL GUIDELINES  
AND RECOMMENDATIONS ON IMAGING DURING IMPLANT  
THERAPY

## ABSTRACT

Radiographic examination is an essential facet of dental implant therapy, and the success of this therapy depends on a suitable treatment based on adequate clinical and radiographic information. International organisational bodies have published guidelines on the use of radiographic imaging during implant therapy, but since the cone beam computed tomography modality became available, a need for the development of comprehensive imaging guidelines to limit the misuse of this modality became necessary. There is a lack of stringency regarding the recommendations and guidelines on radiographic imaging modalities used during implant therapy. This is due to variations in practice, experience, and socioeconomic factors. The most recent published global guidelines and recommendations and their relevance to dental implant therapy are described in this chapter.

**Keywords:** CBCT, dental implants, imaging guidelines, panoramic radiograph.

## LIST OF ABBREVIATIONS AND ACRONYMS

| Abbreviation | Description  |
|--------------|--|
| <b>AAOMR</b> | American Academy of Oral and Maxillofacial Radiology |
| <b>ACP</b>   | The American College of Prosthodontics               |
| <b>AO</b>    | Academy of Osseointegration                          |
| <b>CBCT</b>  | Cone beam computed tomography                        |
| <b>Ceph.</b> | Lateral cephalometric radiograph                     |
| <b>CT</b>    | Computed Tomography                                  |
| <b>CS</b>    | Cross-sectional                                      |
| <b>DGI</b>   | German Association of Oral Implantology              |
| <b>EAO</b>   | European Association for Osseointegration            |
| <b>EC</b>    | European Commission                                  |
| <b>ICOI</b>  | The International Congress of Oral Implantologists   |
| <b>OCC</b>   | Occlusal radiograph                                  |
| <b>PA</b>    | Periapical radiograph                                |
| <b>PAN</b>   | Panoramic radiograph                                 |
| <b>N/A</b>   | Not applicable                                       |

## 1.1 INTRODUCTION

The published materials guiding radiography in implant cases were obtained using an electronic search of several research databases, including MEDLINE (PubMed), EBSCOhost, ScienceDirect, and Wiley. The search included these keywords/research strings but not limited to [“dental implant” or “implant planning” or “planning phase” or “implant treatment” or “dental implant therapy”] and “guidelines” or “recommendations” or “position paper”] and [“cone beam computed tomography” or “CBCT” or “panoramic radiography” or “periapical radiography”]. Further, there was a direct exploration of the official websites of the related speciality bodies/organisations/societies for any position statements and/or recommendations/guidelines on implant imaging. Guidelines and recommendations on implant imaging published by affiliated organisational bodies/authorities and scientific societies were included. Selected systemic and narrative reviews were included based on the relevance of the contents. The main focus was to find recommendations on all types of radiographic examinations, but also guidelines concerning only single radiographic examinations (e.g. CBCT) were included (where applicable).

Currently, radiographic examination is deemed to be an indispensable aspect of dental implant therapy (Tyndall & Brooks, 2000; Harris et al., 2012; Dattatreya et al., 2016). The success of implant therapy depends largely on the quality and quantity of the pre-operative information obtained to establish a treatment plan, and thus appropriate imaging modalities are paramount during this initial phase of management (Tyndall et al., 2012; Tyndall & Brooks, 2000).

Several international organisational bodies, such as the American Academy of Oral and Maxillofacial Radiology, the European Association for Osseointegration, the European Commission, the International Congress of Oral Implantologists, and the American College of Prosthodontics, have released guidelines on implant imaging that are periodically reviewed and updated (Tyndall et al., 2012; Tyndall & Brooks, 2000; Harris et al., 2002; Harris et al., 2012; Ahmad & Chapokas, 2019; Benavides et al.,

2012; European Commission, 2012; European Commission, 2004). The introduction of the relatively recent cone beam computed tomography (CBCT) modality offers promising dental applications, particularly during implant therapy, while offering lower-dose radiographic acquisitions compared to computed tomography (CT scans) (Harris et al., 2012). The availability and relatively low price of the units and the higher diagnostic value have resulted in the increased use of this technology in dental practice (Harris et al., 2012). This has resulted in the need for the development of comprehensive imaging guidelines, in order to limit the misuse of the modality.

Guidelines enable the clinician to make informed choices regarding new technologies or techniques and to minimise bias in a health-related situation (Horner et al., 2015; Field & Lohr, 1992). The opinions of experts in the field and an evidence-based approach are necessary to establish credible guidelines, each of which may have advantages and disadvantages (Horner et al., 2015). The evidence-based approach is considered superior and uses a defined approach that is guided by a systematic review of the literature, along with grading and assessment of the available evidence (Grol & Grimshaw, 2003; Horner et al., 2015).

Published reports regarding the clinical efficiency of using cross-sectional modalities during implant planning provide ambiguous and inconclusive evidence (Tyndall et al., 2012; Jacobs et al., 1999; Schropp et al., 2001; Diniz et al., 2008; Frei et al., 2004; Vazquez et al., 2008; Schropp et al., 2011). A deficiency was noted with regard to evidence-based guidelines, and available imaging strategies are mainly ascertained from clinical opinions or published review reports that are not always consistent (European Commission, 2004; Bornstein et al., 2014; Horner et al., 2015; Ahmad & Chapokas, 2019).

The development of a coherent and thorough selection criterion for radiographic examinations during implant therapy is vital in order to reduce radiation hazards and at the same time achieve the treatment goals (Tyndall & Brooks, 2000; Tyndall et al.,

2012). In this review, the most important available published guidelines are highlighted (Table 2.1).

**Table 2.1. Selected relevant publications concerning implant imaging protocols and guidelines.**

| ORGANISATION/<br>REGULATORY BODIES                                  | AUTHOR/S                                       | Method   | NOTES                       |
|---|--|--|-----------------------------|
| <b>American Academy of Oral and Maxillofacial Radiology (AAOMR)</b> | (Tyndall & Brooks, 2000; Tyndall et al., 2012) | Consensus  |                             |
| <b>European Association for Osseointegration (EAO)</b>              | (Harris et al., 2002; Harris et al., 2012)     | Consensus  |                             |
| <b>European Commission (EC)</b>                                     | (European Commission, 2004)                    | Unspecified  |                             |
| <b>Academy of Osseointegration</b>                                  | (Academy of Osseointegration, 2010)            | Adopts EAO guidelines and SEDENTEXCT project (for imaging section) |                             |
| <b>Superior Health Council, Belgium – Report No 8705</b>            | (Superior Health Council, 2011)                | Experts opinions (working group)                                   | Advisory report for Belgium |
| <b>DGI – German Association of Oral Implantology</b>                | (Nitsche et al., 2011)                         | Systematic review, supplemented by consensus-based expert opinion  | Three-dimensional: CT, CBCT |
| <b>SEDENTEXCT project (European Commission)</b>                     | (European Commission, 2012)                    | Evidence   | Only CBCT                   |
| <b>The International Congress of Oral Implantologists (ICOI)</b>    | (Benavides et al., 2012)                       | Consensus  |                             |
| <b>International Team for Implantology</b>                          | (Bornstein et al., 2014)                       | Systematic review  | Only CBCT                   |

|   |                                |                             |                                  |
|---|--------------------------------|-----------------------------|----------------------------------|
| <b>The American College of Prosthodontics (ACP)</b>   | (Ahmad & Chapokas, 2019)       | Consensus                   |                                  |
| <b>The Korean Academy of Oral and Maxillofacial Radiology &amp; National Evidence-based Healthcare Collaborating Agency</b> | (Kim et al., 2020)             | Evidence, systematic review |                                  |
| N/A   | (Bornstein et al., 2017)       | Narrative review            | Only CBCT                        |
| N/A   | (Jacobs, Salmon et al., 2018)  | Narrative review            | Only CBCT                        |
| N/A   | (Horner & Shelley, 2016)       | Systematic review           |                                  |
| N/A   | (Jacobs, Vranckx et al., 2018) | Systematic review           | Only the post-operative phase    |
| N/A   | (Noffke et al., 2011)          | Expert opinion              | Recommendations for South Africa |



UNIVERSITY of the  
WESTERN CAPE

## 1.2 RECOMMENDATIONS BY VARIOUS ORGANISATIONAL BODIES

### 1.2.1 AMERICAN ACADEMY OF ORAL AND MAXILLOFACIAL RADIOLOGY (AAOMR) – 2000, 2012

Two-position papers were published in 2000 and 2012 by the American Academy of Oral and Maxillofacial Radiology (AAOMR) as advisory recommendations on implant therapy imaging (Tyndall et al., 2012; Tyndall & Brooks, 2000). In 2000, the AAOMR indicated that there was a deficiency in comprehensive dental implant imaging guidelines, which are crucial in assisting the clinician to select the most appropriate imaging modality to be used during various stages of implant therapy (Tyndall & Brooks, 2000). The AAOMR was also aware of the ambiguity of published evidence concerning the need for cross-sectional imaging during implant planning (Tyndall et al., 2012).

In 2000, the AAOMR assessed all the current modalities used at the time, which included intraoral, panoramic, cephalometric, tomographic, and computed tomography, but not CBCT – in order to provide direction on efficient implant imaging strategies (Tyndall & Brooks, 2000). The AAOMR stated that anatomical information of bone architecture may not adequately be acquired through 2-dimensional extra- and intraoral radiographic modalities, and that cross-sectional modalities such as conventional tomography were recommended for the evaluation of any potential implant site (Tyndall & Brooks, 2000).

The subcommittee of the American Academy of Oral and Maxillofacial Radiology (AAOMR) reviewed the current advances in radiographic modalities and evidence, and published an updated report in 2012 after the initial one published in 2000 (Tyndall et al., 2012). In this second position paper, the CBCT modality was included and their recommendation was that cross-sectional imaging be used and that the imaging method of choice was the CBCT for all potential implant sites (Tyndall et al., 2012).

Usually, the selection of a certain radiographic modality is a result of the professional judgment of the clinician, who then decides if the information yielded from the clinical

examination is insufficient or if further radiographic examinations are necessary to prepare a comprehensive treatment plan (Tyndall et al., 2012). These decisions vary among clinicians and depend on skill, clinical competence, experience, and knowledge (Tyndall et al., 2012).

The AAOMR subsequently made advisory recommendations for each implant therapy stage: the initial, pre-surgical, and post-operative phases. During the initial examination stage, the aim is to use radiographs to provide details about the patient's dental status, such as areas of missing teeth, pathology, and possible irregular anatomy (Tyndall et al., 2012). The Academy suggested that a panoramic radiograph supplemented with intraoral periapical x-rays is adequate for the initial assessment stage (Tyndall et al., 2012). Pre-surgical imaging is considered a pre-requisite for guided implant surgery procedures. During the pre-surgical stage of therapy, the radiographic assessment will help characterise the alveolar ridge at the candidate implant site, in terms of morphology, quantity, and quality of the bone (Tyndall et al., 2012). The academy recommends the use of the CBCT modality due to the satisfactory radiation exposure and decisive information it provides – which are vital for the success of the treatment. The Academy reaffirms that choosing to use CBCT should only be done if it is clinically justified, and when its use provides added evidence to improve the prosthetics, surgical procedure, and implant choice (Tyndall et al., 2012).

During the post-surgical stage, imaging is necessary to ensure the accurately planned placement of the implant (Tyndall et al., 2012). Images during the follow-up stages, which vary from 3-5 years, are indicated to assess the status of osteointegration status and to assess marginal bone height (Tyndall et al., 2012).

The various clinical stages of implant therapy, and the AAOMR 2012 recommendations, are presented in Table 2.2.



**Table 2.2. Clinical situations and the AAOMR recommendations 2012 (Tyndall et al., 2012).**

| TREATMENT STAGE                      | MODALITY ADVISED   | NOTES  |
|--------------------------------------|--|--|
| <b>Initial examination stage</b>     | <ul style="list-style-type: none"> <li>• Panoramic radiography.</li> <li>• Periapical radiographs (supplementary).</li> </ul>  | Cross-sectional imaging (e.g. CT, CBCT) is not indicated in the initial stage.   |
| <b>Pre-surgical stage</b>            | <ul style="list-style-type: none"> <li>• Cross-sectional imaging to be used in any candidate implant site.</li> <li>• CBCT is the best cross-sectional imaging modality to be chosen.</li> <li>• CBCT is recommended specifically in these clinical situations:               <ol style="list-style-type: none"> <li>1 - Bone augmentation and grafting are needed.</li> <li>2 - Evaluation of impacted dentition in the area of interest.</li> <li>3 - If there is a previous trauma in the area of interest.</li> <li>4 - Sinus augmentation.</li> <li>5 - Evaluation of ridges after bone grafting/ridge preservation procedure.</li> </ol> </li> </ul> | <ul style="list-style-type: none"> <li>• Although conventional tomography yields cross-sectional information, it has several drawbacks (technique sensitive and interpretation difficulties).</li> <li>• Appropriate selection of the exposure parameters and field of view (limited to the area of interest) to ensure minimum radiation exposure.</li> <li>• If CBCT is not available, CT scan to be considered, but “dose-sparing protocols must be used”.</li> </ul> |
| <b>Post-operative and follow-ups</b> |  |  |
| <b>Asymptomatic</b>                  | <ul style="list-style-type: none"> <li>• Periapical radiographs.</li> <li>• CBCT is not indicated for the periodic assessment of clinically asymptomatic implants.</li> </ul>  | <ul style="list-style-type: none"> <li>• Panoramic can be used in the case of extensive implant therapy.</li> <li>• Intraoral radiography is superior to assess asymptomatic implants, as the CBCT/CT modalities may show artefacts that hinder the proper assessment due to the metallic structure of the implant (beam-hardening artefacts).</li> </ul>  |
| <b>Symptomatic</b>                   | <ul style="list-style-type: none"> <li>• Post-operatively it is advised to use CBCT (preferably CBCT, but any cross-sectional imaging can also be used if CBCT is not available) in these <b>clinical situations</b>:               <ol style="list-style-type: none"> <li>1 - Mobility in the implant.</li> <li>2 - Impairment of the patient's sensation (particularly when the implant site is at a vicinity of vital structure).</li> </ol> </li> </ul>  | <ul style="list-style-type: none"> <li>• CBCT (preferably) or any cross-sectional modality to be considered when an implant needs to be retrieved.</li> </ul>  |

## 1.2.2 EUROPEAN ASSOCIATION FOR OSSEOINTEGRATION (EAO) – 2002, 2012

In 2002, following a consensus workshop organised by the European Association for Osseointegration in Dublin, a report that demonstrated the need for conducting a detailed clinical examination combined with conventional 2-dimensional radiographs as a standard approach, was published (Harris et al., 2002). Cross-sectional imaging was only to be considered in certain clinical situations and their recommendations (2002) are summarised in Table 2.3.

**Table 2.3. European Association for Osseointegration recommendations (Harris et al., 2002).**

| Clinical situation                  | Recommendations   |
|-------------------------------------|---|
| <b>Single-tooth implant sites</b>   | <ul style="list-style-type: none"> <li>• If the information revealed regarding the bony structure of the implant site (height, width) is adequate from a thorough dental and clinical examination and conventional 2-dimensional radiographs, cross-sectional radiography is not indicated.</li> <li>• Cross-sectional radiography may be indicated where proximity to neurovascular structures (particularly in the posterior mandible and in the maxillary central incisor area) and alveolar bone defects, are suspected.</li> </ul> |
| <b>Edentulous Maxilla</b>           | <ul style="list-style-type: none"> <li>• In most cases, a thorough clinical assessment of the implant sites, combined with conventional 2-dimensional radiographs, are adequate.</li> <li>• Cross-sectional imaging may be indicated in the case of deficiency in the bone volume and the need for bone grafting. Additionally, it can be indicated to improve the prosthetic outcome, and in the case of zygomatic implants.</li> </ul>  |
| <b>Partially edentulous maxilla</b> | <ul style="list-style-type: none"> <li>• A thorough clinical assessment of the implant sites, combined with conventional 2-dimensional radiographs, are the standard approach. Afterwards, deficiency in the information concerning the bone volume, anatomical positions of important adjacent structures, and information needed for prosthetic and restorative planning (particularly in the esthetic zone), may justify proceeding to cross-sectional imaging.</li> </ul>   |

|                                      |   |
|--------------------------------------|---|
| <b>Edentulous mandible</b>           | <ul style="list-style-type: none"> <li>• A thorough clinical assessment of the implant sites combined with conventional 2-dimensional radiographs are the standard approach. If the information gathered through the previous approach indicated unusual alveolar anatomy and severe deficiency of the bony structure, cross-sectional imaging is indicated.</li> </ul> |
| <b>Partially edentulous mandible</b> | <ul style="list-style-type: none"> <li>• A thorough clinical assessment of the implant sites, combined with conventional 2-dimensional radiographs, are the standard approach.</li> <li>• If the implant is to be placed close to the inferior dental canal, cross-sectional imaging is indicated.</li> </ul>   |

The EAO in 2012 stated that absence of guidelines of when and how Computed Tomography (CT) images should be used instead of conventional radiographic investigations, was of concern (Harris et al., 2012).

The recommendations released after the consensus workshop organised by the European Association for Osseointegration in 2011, were similar to those published in 2002, but included the CBCT modality with guidelines of its usage in implant dentistry (Harris et al., 2012). This report reaffirms that clinical examination combined with suitable conventional radiographs are adequate in the initial and treatment planning phase and can usually provide an overview about the density and basic structure of the alveolar bone, as well as any possible pathologies in the jaws. The advantages and disadvantages of each radiographic modality have been compared, and are summarised in Table 2.4.

**Table 2.4. Diagnostic properties of radiographic modalities (Harris et al., 2012).**

|                        | Periapical | Panorama | Lateral cep | CBCT    | CT  |
|------------------------|------------|----------|-------------|---------|-----|
| Dental pathology       | ++         | +        | -           | + / +++ | +   |
| Jawbone pathology      | +          | ++       | -           | +++     | +++ |
| Structure and density  | ++         | ++       | -           | + / +++ | +   |
| Bone shape and contour | -          | -        | - / +       | +++     | +++ |

|   |    |    |   |     |     |
|---|----|----|---|-----|-----|
| Anatomical boundaries   | +  | +  | - | +++ | +++ |
| <b>Measurements ACCURACY</b>                                      |    |    |   |     |     |
| Vertical dimension  | ++ | ++ | - | +++ | +++ |
| Horizontal dimension  | ++ | -  | - | +++ | +++ |
| Buccolingual direction  | -  | -  | - | +++ | +++ |
| <b>Key:</b>   |    |    |   |     |     |
| “-”: indicates poor value diagnostic value.                       |    |    |   |     |     |
| “+, ++: indicate intermediate ranges of useful diagnostic values. |    |    |   |     |     |
| “+++”: indicates the highest diagnostic value.                    |    |    |   |     |     |

The EAO advocates that cross-sectional modalities are not necessary for clinical situations where 2-dimensional modalities clearly show the anatomical boundaries, as well as necessary structural information of available bone (Harris et al., 2012). They suggest that patients with prosthetic considerations may be candidates for cross-sectional imaging, as this will enhance the outcome of the treatment (Harris et al., 2012). Other clinical situations that may require cross-sectional imaging include bone defects, maxillary sinus augmentation, intra-oral bone donor sites, the proximity of vital structures, special techniques such as zygomatic implants and osteogenic distraction, computer-assisted planning and placement, and where complications have arisen – e.g. nerve damage or post-operative infections (Harris et al., 2012). This report also emphasised that practitioners need to exercise interpretational caution when cross-sectional modalities are used, and therefore adequate safety margins should be applied "as a rule" in all situations (Harris et al., 2012). A possible error is the inaccurate transfer of information gathered from radiographic volumes into the actual surgical site (Harris et al., 2012).

During and after the surgery, the EAO recommends the use of conventional radiographs to confirm the optimum implant placement, and cross-sectional imaging is not indicated for follow-ups – unless postoperative complications exist (Harris et al., 2012). Harris et al. (2012) also reported that socioeconomic and availability factors be considered when cross-sectional imaging is requested.

---

### 1.2.3 EUROPEAN COMMISSION – 2004, 2012

The Directorate-General for Energy in the European Commission's report in 2004 (Radiation Protection No 136) provided guidance for dental and associated healthcare practitioners in terms of radiation protection measures during dental radiographic procedures (European Commission, 2004).

The authors of the report reaffirm the importance of radiological examination in dental implant therapy (European Commission, 2004). The phase of treatment and the number and location of the implant sites play a vital role in the selection of the appropriate imaging modality (European Commission, 2004). Recommended radiographic modalities during various treatment stages are documented in Table 2.5.

In 2012, The Directorate-General for Energy in the European Commission released a report (Radiation Protection No 172), which aimed to provide the medical and dental fraternity with scientific-based guidelines and recommendations regarding the safe use of CBCT (European Commission, 2012). This report describes the latest available information available at the time of publication concerning applications, advantages, and disadvantages regarding the use of CBCT (European Commission, 2012).

Central to the clinical assessment of a patient during the implant planning stage, is to determine the need for cross-sectional imaging – especially given that the decision to request cross-sectional imaging for a given patient is usually a matter of subjectivity (European Commission, 2012). The dimensional accuracy of an imaging modality is vital (particularly during dental implant therapy). Convincing evidence from published reports supports the role that CBCT provides with regard to dimensional accuracy and lower radiation dose (European Commission, 2012). When cross-sectional views are required during implant placement, the use of CBCT is indicated (European Commission, 2012). The use of CBCT with the adjustable field of view, is an advantage when only the field of interest can be imaged (European Commission, 2012).

**Table 2.5. European guidelines on radiation protection in dental radiology (Issue No 136) (European Commission, 2004).**

| # of implants                                   | Implant site                    | Recommended Radiographic modality   | Complicating scenarios  | Supplementary radiographs      |
|---|---------------------------------|---|---|--------------------------------|
| <b>PRE-OPERATIVE PLANNING</b>                   |                                 |   |   |                                |
| <b>Anterior regions</b>                         |                                 |   |   |                                |
| <b>One implant</b>                              | <b>Maxilla</b>                  | <b>PA (using paralleling techniques)</b>  | <ul style="list-style-type: none"> <li>• Irregular size of the incisive foramen</li> <li>• Considerable alveolar bone resorption</li> </ul> | Pan + Ceph                     |
|   | <b>Mandible</b>                 | <b>PA (using paralleling techniques)</b>  | <b>Exaggerated lingual fossa and buccal concavity</b>   | <b>Cross-sectional imaging</b> |
|   | <b>Premolar - molar regions</b> |   |   |                                |
|   | <b>Maxilla</b>                  | <b>PA + PAN</b>   | <ul style="list-style-type: none"> <li>• Close vicinity to the sinus floor</li> <li>• Considerable alveolar resorption</li> </ul>           | <b>Cross-sectional imaging</b> |
| <b>Mandible</b>                                 | <b>PA + PAN + OCC</b>           | <ul style="list-style-type: none"> <li>• Close vicinity to the neurovascular bundles</li> <li>• Considerable alveolar resorption</li> </ul> | <b>Cross-sectional imaging</b>  |                                |
| <b>Multiple implants</b>                        | <b>Cross-sectional imaging</b>  |   |   |                                |
| <b>During Surgery</b>                           |                                 |   |   |                                |
| PA  |                                 |   |   |                                |
| <b>Post-operative assessment</b>                |                                 |   |   |                                |
| <b>Healing phase</b>                            | PA, only if symptomatic         |   |   |                                |
| <b>12-month follow-up</b>                       | PA (parallel technique)         |   |   |                                |
| <b>Annual reviews to once every three years</b> | PA (parallel technique)         |   |   |                                |

Key| PAN: panoramic radiograph, PA: periapical radiograph, Ceph.: Lateral cephalometric radiograph, OCC: occlusal radiograph, Cross-sectional imaging includes CT and conventional tomography.

---

#### 1.2.4 ACADEMY OF OSSEOINTEGRATION (AO) – 2010

The AO published guidelines on the provision of dental implants and associated patient care in 2008. An update to this publication was published in 2010, with the addition of further information (Academy of Osseointegration, 2010).

The AO challenges the practitioners to review the SEDENTEX guidelines on CBCT. The indications of Computed Tomography (CT) for use during implant planning were adopted from E.A.O. guidelines in 2002 (Academy of Osseointegration, 2010).

The AO (Academy of Osseointegration, 2010) further recommends:

- Justification of each single CBCT examination is mandatory.
- The CBCT examinations have to add a new piece of information that was not acquired using conventional approaches.
- A thorough patient examination and review of the dental and medical history have to be performed prior to CBCT acquisitions. If the patient was referred for CBCT examination at another radiographic practice, the information gathered from clinical examination and patient history has to be provided for justification.
- Routine use of CBCT techniques is not recommended.
- The CBCT report is required, regardless of the provided field of view (FOV). The small FOV, up to the region of interest, is preferred for CBCT acquisitions.

---

#### 1.2.5 SUPERIOR HEALTH COUNCIL, BELGIUM – 2011

Multi-disciplinary experts in a working group organised by the Superior Health Council, Belgium, published an advisory report (N: 8705) on CBCT (Superior Health Council, 2011). The report distinguishes between low dose specifically manufactured CBCT devices for dental use and those that have dental exposure programmes, as the earlier provides lower radiation doses.

During implant planning and bone grafting procedures, the recommendation is to prescribe dental CBCT only in cases where the conventional two-dimensional imaging proved insufficient.

---

### 1.2.6 GERMAN ASSOCIATION OF ORAL IMPLANTOLOGY(DGI)- 2011

A systemic review which includes consensus statements and recommendations on the indication of 3D examinations during implant therapy, was published subsequent to the first DGI consensus conference held in 2010, Germany (Nitsche et al., 2011).

**This report concluded that:**

- The superiority of three-dimensional imaging in terms of the quality of surgical outcome and potential reduction of complications is not confirmed on human beings by randomised or controlled studies.
- Stress on practitioners concerning the yielded radiation doses – particularly for more radio-sensitive, younger patients.
- Adhering to the ALARA principle (as low as reasonably achievable), and reducing the field of view should be done.
- Cross-sectional (3D)\* views were found to be beneficial in providing a multi-dimensional and superimposition-free analysis of the region of interest, allowing for metric analysis, and helping in complicated surgical produces and bone grafting procedures.

\* 3D cross-sectional views include (CT and CBCT).

**Consensus-based recommendations:**

- 1- Imaging is mandatory prior to dental implant treatments in order to check the quality and quantity of the region of interest.
- 2- A review of the dental and clinical history followed by thorough clinical examination and cast analysis (if necessary) must be done before conventional radiographic examinations. If a marked abnormality or deviation from normal



values were found, a 3D examination may be indicated directly, so bypassing conventional imaging.

3- The indication for using cross-sectional imaging includes:

- Abnormal jaw anatomy (e.g. severe undercut, irregular architecture, insufficient bone volume, maxillary septations).
- Presence of pathologies noted on conventional radiographs.
- Uncertain proximity and ambiguous demarcation of vital anatomical structures (e.g. mandibular canal) if noted in conventional imaging modalities (2D).
- After bone augmentation of uncertain outcomes.
- Previous history of surgical intervention of the maxillary sinuses.
- Special treatment techniques (e.g. computer-guided surgery).
- Post-operative complications (e.g. alteration of sensation due to nerve injury, jeopardising roots).

---

### 1.2.7 INTERNATIONAL CONGRESS OF ORAL IMPLANTOLOGISTS (ICOI) – 2012

A consensus report (Benavides et al., 2012) was published with the support of the ICOI following a systematic review of the literature regarding the use of CBCT during implant therapy. The authors found a strong trend in support of the use of CBCT during the treatment planning in particular when alveolar ridge morphology needs to be assessed. In addition, CBCT was also utilized when computer-guided surgery is planned, and when the implant was to be placed in the vicinity of vital structures (Benavides et al., 2012). It was also highlighted that it was impossible to envisage which patients may or may not benefit from the additional radiographic information that a CBCT provides before the CBCT is performed (Benavides et al., 2012).

The ICOI further recommends that the CBCT procedure must be justified and the benefits of the examination must outweigh the possible risks – especially in instances where the conventional radiographic modalities failed to provide the needed

information for that particular clinical situation (Benavides et al., 2012). It was also emphasised that no CBCT examination should be performed without a prior thorough medical history and a detailed dental and clinical examination (Benavides et al., 2012). In the instance when the CBCT examination is justified, the operator was advised to choose the smallest applicable field of view that covers the region of interest (Benavides et al., 2012).

Compelling evidence for the use of CBCT is provided by the ICOI in clinical circumstances such as atypical alveolar bone anatomy, aesthetic zones, bone grafting cases, guided implant surgery, and instances of post-surgical complication – in particular infections, neural deficiency and sinonasal symptoms (Bornstein et al., 2014; Benavides et al., 2012).

---

### 1.2.8 INTERNATIONAL TEAM FOR IMPLANTOLOGY – 2014

A rigorous systematic review identified the available guidelines and indications of CBCT use during implant therapy (Bornstein et al., 2014). The analysis indicated a paucity of evidence-based guidelines (that are derived from rigorous systematic reviews), with the available guidelines mostly being consensus-based or retrieved from a limited review of literature containing ambiguous evidence (Bornstein et al., 2014). Although compelling evidence on the clinical benefit of cross-sectional imaging, in particular CBCT, was difficult to prove, indications of CBCT use include anatomic consideration, the need of extensive procedures (e.g. bone grafting), employing computer-guided surgeries, and post-operative complications (Bornstein et al., 2014).

Guidelines (The 5<sup>th</sup> consensus conference in Bern, in 2013) (International team for implantology, 2014):

- 1- The most updated imaging guidelines should be followed regarding CBCT examinations.

- 2- A comprehensive clinical examination is a prerequisite before prescribing the CBCT examination. If clinical examination and conventional imaging are not sufficient, CBCT is preferred over computed tomography (CT).
- 3- Radiographic guides (templates) are of benefit when used during CBCT acquisitions. Additionally, a limited field of view exposures (up to the region of interest) should be used, and personal radiation protection measures should be implemented.

### 1.2.9 THE AMERICAN COLLEGE OF PROSTHODONTICS (ACP) – 2016

A report by ACP (2016) stated that prior to any radiographic examination a thorough clinical assessment of the patient's oral cavity and previous medical and dental history must be performed (Ahmad & Chapokas, 2019). Though the college justifies the use of cross-sectional imaging during the planning phase, in particular, CBCT modality – the college reaffirms that the use of CBCT must be based on clinical evaluation and that the imaging should be confined only to the region of interest (Ahmad & Chapokas, 2019). These opinions are tabulated (Table 2.6).

**Table 2.6. Position statement of The American College of Prosthodontics (Ahmad & Chapokas, 2019).**

| Stage of treatment                   | Radiographic modality recommended   |
|--------------------------------------|---|
| <b>Initial examination</b>           | PAN +/-or PA<br><br>CBCT is not indicated   |
| <b>Pre-surgical site examination</b> | CBCT (or any other type of CS imaging, but CBCT is recommended).<br><br>- <b>The particular clinical situations for which CBCT is recommended include:</b><br><br>1- When implants need to be placed in the aesthetic zone, pterygoid plate, and zygomatic bone.<br><br>2- Bone grafting, sinus augmentation procedures needed. |

|  |  |
|--|--|
| <b>Post-operative and follow-ups (3 to 5 years and beyond)</b> | <p>-PAN +/-or PA</p> <p>CBCT is only indicated in the case of post-operative complications and when symptoms exist, as follows:</p> <ol style="list-style-type: none"> <li>1- Disturbance/loss of sensation.</li> <li>2- Antrum/nasal-related complications (e.g. infections).</li> <li>3- Site/bone infections.</li> <li>4- Pain, discomfort, and mobility of the fixture.</li> <li>5- Retrieval of the fixture.</li> </ol> |
|--|--|

Key| PAN: panoramic radiograph, PA: periapical radiograph, CBCT: cone beam computed tomography, CS: cross-sectional.

---

#### 1.2.10 AMERICAN ACADEMY OF PERIODONTOLOGY AND EUROPEAN FEDERATION OF PERIODONTOLOGY – 2018

A report (2018) was published after a consensus workshop that was held jointly by the American Academy of Periodontology and the European Federation of Periodontology on “the Classification of Periodontal and Peri-Implant Diseases and Conditions” (Berglundh et al., 2018). One of the recommendations was to acquire a “baseline” radiograph directly after the functional restoration is in place. Additional radiographs should be acquired after “a loading period” to act as a reference for bone level subsequent to bone remodelling (Berglundh et al., 2018).

---

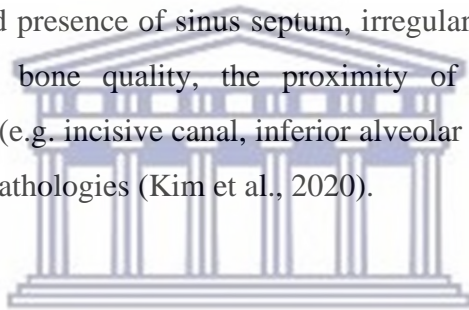
#### 1.2.11 THE KOREAN ACADEMY OF ORAL AND MAXILLOFACIAL RADIOLOGY & NATIONAL EVIDENCE-BASED HEALTHCARE COLLABORATING AGENCY – 2020

Joint research was conducted in South Korea (2020) between The Korean Academy of Oral and Maxillofacial Radiology and the National Evidence-based Healthcare Collaborating Agency to develop evidence-based guidelines on imaging during implant planning (Kim et al., 2020). A systematic review was conducted through the national

and international databases to analyse the available evidence considering the clinical efficiency, diagnostic benefits, and the potential hazards of radiographic modalities (Kim et al., 2020).

Panoramic radiographs are recommended in the initial examination in order to decide the need for succeeding cross-sectional imaging. If the collected information after the conventional imaging (i.e. panoramic and intraoral radiographs) proved insufficient or there was a clinical suspicion of abnormalities/pathologies in the jaw and maxillary sinus, the patient is then a candidate for cross-sectional imaging, with CBCT being the modality recommended (Kim et al., 2020).

Clinical situations that may benefit from cross-sectional imaging include proximate maxillary sinuses and presence of sinus septum, irregular alveolar ridge architecture, insufficient alveolar bone quality, the proximity of vital structures noted on conventional images (e.g. incisive canal, inferior alveolar canal, and mental foramen), and the presence of pathologies (Kim et al., 2020).



#### 1.2.12 UNAFFILIATED PUBLICATIONS (BY REGULATORY BODIES OR ORGANISATIONS)

Multiple publications were obtained that reviewed the available recommendations on implant imaging or the use of CBCT, in particular during the therapy.

The recommendations to use CBCT during implant planning is not unanimous in articles reviewed by Bornstein et al. (2017). It is mentioned (Bornstein et al., 2017) that some reports clearly recommend the use of CBCT for all pre-surgical planning cases (Drago & Carpentieri, 2011; Noffke et al., 2011; Tyndall et al., 2012), while other reports recommend practising a “selective approach” for CBCT utilisation (Benavides et al., 2012; Harris et al., 2012).

In South Africa, CBCT use was suggested as the radiographic examination of choice during implant planning for all cases (Noffke et al., 2011). This was recommended

since the usual candidate patients are of an older age range and the accurate spatial dimensional assessment offered by the modality may save the patient from any potential post-operative complications (e.g. nerve anaesthesia).

The use of CBCT during implant planning is justified according to Jacobs, Salmon, et al. (2018). CBCT is mentioned to exhibit a great potential to enhance surgical and prosthetic outcomes; nevertheless, strict dose optimisation measures should be followed (Jacobs, Salmon, et al., 2018).

Limited evidence was found in a systematic review to support the efficacy of using cross-sectional techniques for the planning of a single missing tooth (Horner & Shelley, 2016). Within the inconsistency noted in the existing guidelines on pre-implant imaging of a single tooth, it can be concluded that in simple cases, cross-sectional imaging may not be required (Horner & Shelley, 2016). Costs also influence the justification of the use of certain radiographic techniques (Horner & Shelley, 2016).

In a recent systematic review (Jacobs, Vranckx, et al., 2018), the role of CBCT compared with conventional examinations during the post-operative phase was assessed. Lack of compelling evidence for CBCT use, as a standard approach, was found when assessing the marginal bone in the peri-implant region – especially with the concurrence of artefacts that hinder accurate assessment of the surrounding tissues. Conversely, CBCT was found to be of value in post-operative pathologies (e.g. peri-implantitis).

### 1.3 CONCLUSION

Variations were found between the recommendations and guidelines of radiographic imaging modalities during implant therapy – particularly using three-dimensional images as a standard approach (e.g. CBCT). This is partially due to variations in practice, experience, and socioeconomic factors. Nevertheless, the organisations presented in this review agree that the use of three-dimensional radiographic modalities such as CT and CBCT should be clinically justified in all cases. The variations in clinical judgment among clinicians may account for inconsistencies in radiographic practices. These factors accentuate the need for rigorous guidelines and a standardised protocol. The researcher concludes that such a protocol should integrate the current regional practices, the socioeconomic factors, and the most recent evidence in the implant and radiography fields. These recommendations and guidelines should be updated periodically, in order to achieve ideal treatment approaches that will invariably result in optimal treatment management and clinical outcome.

### 1.4 LIMITATIONS

- Studies published in any language other than English were not included.
- Grey literature was not considered.

## CHAPTER 2 | REVIEW OF THE RADIOGRAPHIC MODALITIES USED DURING DENTAL IMPLANT THERAPY: A NARRATIVE

### Abstract

A significant radiographic development was the introduction of digital x-ray receptors that have replaced conventional films that are now commonly used in daily dental practice.

Dental implant therapy (DIT) is a sought after dental therapeutic intervention and together with dental radiography, plays an essential role in the success of the treatment of edentulous spaces. Dental radiographs taken in daily practice are conventional two-dimensional images and/or three-dimensional images. The choice of radiographic technique should be determined after a thorough clinical examination and consideration of the advantages, indications, and drawbacks. Digital three-dimensional modalities that have emerged over the last decade, have been incorporated into DIT with the assumption that treatment outcomes will be improved. These modalities are constantly being reassessed and improved, but research concerned with the assessment of all the variables such as dosages and dimensional accuracy of the emerging x-ray technologies, still needs to be carried out, in order to obtain evidence-based information that may influence future radiographic practices.

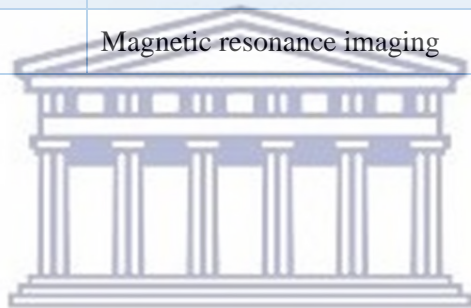
In this narrative, the author presents the most commonly utilised dental radiographic modalities currently used in DIT.

**Keywords:** CBCT, dental implant, panoramic radiograph, periapical radiograph.



## LIST OF ABBREVIATIONS AND ACRONYMS

| Abbreviation    | Description  |
|-----------------|--|
| <b>AAOMR</b>    | American Academy of Oral and Maxillofacial Radiology |
| <b>CBCT</b>     | Cone beam computed tomography                        |
| <b>CT</b>       | Computed Tomography                                  |
| <b>DIT</b>      | Dental implant treatment                             |
| <b><i>E</i></b> | Effective dose                                       |
| <b>HU</b>       | Hounsfield units                                     |
| <b>IPR</b>      | Intraoral periapical radiography                     |
| <b>MRI</b>      | Magnetic resonance imaging                           |



UNIVERSITY *of the*  
WESTERN CAPE

## 2.1 INTRODUCTION

Since its implementation in 1895 by Wilhelm Röntgen (Shah et al., 2014), medical radiology has undergone significant growth. A compelling advancement was the introduction of digital x-ray receptors that have largely replaced conventional films. These digital receptors were first introduced by Radiovisiography (RVG, France) in 1987 (Shah et al., 2014) and are now commonly used in daily dental practice.

The transition into digital imaging offers many advantages for clinicians, including the instant acquisition of dental radiographic images, interactive processing of the image characteristics (e.g. contrast), reduced clinical time, no darkrooms or processing procedures or chemistry needed, and reduced radiation dose to patients (Shah et al., 2014; Nair & Nair, 2007; Bansal, 2006; Jayachandran, 2017). Factors such as increased cost, reduced patient comfort (in the case of intra-oral solid-state sensors), and maintenance, are the most important drawbacks (Nair & Nair, 2007; Iannucci & Howerton, 2017).

Dental implant therapy (DIT) is a sought-after dental therapeutic intervention designed to replace missing teeth (Moraschini et al., 2015; Tyndall & Brooks, 2000). The number of new dental implant manufacturers increases each year, with millions of dental implants being placed and restored (Boyce & Klemons, 2015; Popelut et al., 2010). Dental radiography plays an essential role in implant therapy (Tyndall & Brooks, 2000; Nagarajan et al., 2014; Gupta et al., 2015), and various radiographic modalities have been incorporated into DIT – in the hope that treatment outcomes will be improved. The author presents the most commonly used dental radiographic modalities currently used in DIT.

## 2.2 CURRENT MAXILLOFACIAL RADIOGRAPHIC TECHNOLOGIES (TABLE 2.7)

Dental radiographs taken in daily practice are conventional two-dimensional (e.g. periapical, panoramic, cephalometric radiographs) and/or three-dimensional images (e.g. computed tomography (CT) and cone beam computed tomography (CBCT)).

**Table 2.7. Radiographic modalities used during implant therapy**

| Radiographic modality                |
|--------------------------------------|
| Intra-oral periapical radiographs    |
| Panoramic radiography                |
| Cephalometric radiography            |
| Computed tomography (CT)             |
| Cone beam computed tomography (CBCT) |
| Magnetic resonance imaging (MRI)     |

## 2.2.1 CONVENTIONAL TWO-DIMENSIONAL TECHNIQUES:

### 2.2.1.1 INTRAORAL PERIAPICAL RADIOGRAPHY

Intraoral periapical radiography (IPR) is a technique that depicts a limited number of teeth – revealing their position, outline, mesiodistal boundaries, and the periapical region (Gupta et al., 2014). This is one of the most popular modalities used in daily practice, especially for potential implant site assessment and the follow-up phase after the placement of the implant (Figure 2-1) (Deshpande & Bhargava, 2014; Tyndall et al., 2012).

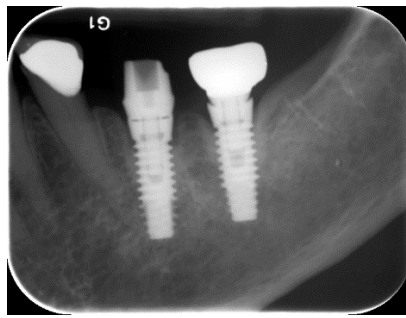


**Figure 2-1. A periapical radiograph showing two implants in the 36,37 region. Note the proximity of the implant (lower part) to the apex of tooth #35.**

Two techniques, the bisecting angle and parallel techniques, have been used to obtain IPR (Gupta et al., 2014; White & Pharoah, 2013). In the bisecting angle technique, which is based on Cieszynski's rule of isometry ("two triangles are equal when they share one complete side and have two equal angles" (White & Pharoah, 2013)), the central x-ray beam perpendicularly crosses an imaginary line that bisects the angle between the long axis of the tooth and the film (Gupta et al., 2014). Conversely, in the parallel technique, the x-ray beam crosses the teeth and the receptor at right angles (Gupta et al., 2014). The parallel technique is preferable to the bisecting angle in clinical practice, since it produces less image distortion and limits the x-ray beam to the area of interest (Gupta et al., 2014; White & Pharoah, 2013).

The IPR is an efficient tool to assess the periodontal status, periapical and interproximal bone, and the detection of periapical pathologies (Gupta et al., 2014). The indications, advantages, and disadvantages during dental implant therapy are summarised in Table 2.8.

Besides the immediate attainment of radiographic images, digital IPR may reduce the radiation dosage by 75-90% compared with analogue modalities (Agrawal et al., 2014). The received effective dose ( $E$ ) depends on the type of x-ray receptor and collimation used, for example, rectangular or rounded – with the rectangular collimation reducing the dose up to 5 fold (White & Pharoah, 2013). The estimated effective dose ( $E$ ) for a full mouth survey (18-20 radiographs) is 17  $\mu$ Sv (using a CCD sensor) (White & Pharoah, 2013).

---

#### 2.2.1.2 CEPHALOMETRIC RADIOGRAPHY

This lateral radiograph is a two-dimensional view that shows the antero-posterior aspect of the upper and lower jaws (Tyndall et al., 2012). Information about teeth position and inclination, the soft tissue profile of the patient, the architecture of the hard tissue, and the occlusal relationship between the jaws, is provided (Table 2.8) (Agrawal et al., 2014). The use of this modality during implant treatment is however limited

(Tyndall et al., 2012). Nevertheless, when the midline region is edentulous, the cephalometric radiograph can show a cross-sectional image allowing the assessment of the bucco-lingual and the vertical bone quantities of the anterior alveolar ridges (Tyndall et al., 2012). The estimated (*E*) is 2–6  $\mu\text{Sv}$  (White & Pharoah, 2013).

### 2.2.1.3 ORTHOPANTOMOGRAPHY OR PANORAMIC RADIOGRAPHY

Orthopantomography (Figure 2-2) – also referred to as panoramic radiography – is a technique that shows a panoramic view of the jaws, part of the maxillary sinuses, and the temporomandibular joints (White & Pharoah, 2013). Only the structures that lie inside a curved zone called the focal trough will be clearly represented on the radiograph (White & Pharoah, 2013). This modality is one of the most often used radiographs in dental practice, and, in particular, during implant therapy (Tyndall et al., 2012). It is used for the initial assessment of the implant site and the surrounding structures (Tyndall et al., 2012; Lingam et al., 2013). This radiographic modality is also commonly prescribed directly after the placement of several implants and during follow-up (Tyndall et al., 2012; Harris et al., 2012).



**Figure 2-2. A panoramic radiograph acquired with a surgical guide in place for intended implant planning in the 36# area. Note the mild smile line exaggeration and chin cut due to positioning errors.**

Panoramic radiography is technique-sensitive and decidedly influenced by the patient's head position, and sometimes can result in clinically significant magnification (15–22%) and image distortion (Gupta et al., 2015; Karjodkar, 2009). The magnification factor can be determined by dividing the physical diameter of an object by the radiographically measured one (Gupta et al., 2015; Lingam et al., 2013). The (*E*) ranges from 9–24  $\mu\text{Sv}$  (White & Pharoah, 2013).

Further information regarding the indications, advantages and drawbacks of the use of panoramic radiography during implant therapy is presented (Table 2.8).

---

## 2.2.2 THREE-DIMENSIONAL RADIOGRAPHIC TECHNIQUES

### 2.2.2.1 MAGNETIC RESONANCE IMAGING (MRI)

Magnetic resonance imaging (MRI) is a non-ionising radiographic modality that uses a magnetic field and radio waves to generate cross-sectional images (Nagarajan et al., 2014; Gray et al., 2003). Although cross-sectional imaging produced by this modality can be used during implant planning, its use is limited due to substantive costs, relatively long acquisition time, and interpretation challenges (Tyndall et al., 2012). Further advantages and disadvantages are illustrated in Table 2.8.

### 2.2.2.2 COMPUTED TOMOGRAPHY (CT)

Since its conception by Hounsfield (1972) (Hounsfield, 1973), CT technology underwent substantial development and is critical in the diagnostic processes essential in medicine and dentistry. The CT modality uses a fan-shaped x-ray beam with detectors that measure the intensity of the remaining beam to be used in mathematical algorithms for the reconstruction of cross-sectional images (White & Pharoah, 2013). This modality provides high-resolution, three-dimensional views of the anatomical structures – whereby both hard and soft tissue densities can be appreciated.

Reformatted CT slices in various planes can be generated as well as panoramic views (Nagarajan et al., 2014). Multiple generations of CT modality have evolved over the years, with specific developments in the x-ray emission and acquisition methodologies (Tyndall et al., 2012). The newer generations, use multiple detector arrays that receive fan-shaped x-ray beams (Tyndall et al., 2012). The volumes are reconstructed using mathematical formulae integrated within the manufacturer's software. Multiplanar slices and thickness can be reconstructed and presented from the main volume (Tyndall et al., 2012). Although the modality produces higher radiation doses (Tyndall et al., 2012), it offers an advantageous accurate three-dimensional assessment of the potential implant sites, including bone quality, which is vital for the success of DIT (Table 2.8) (Tyndall et al., 2012; Gupta et al., 2015; Seeram, 2009). The estimated (*E*) ranges from 280 to 1410  $\mu\text{Sv}$  (European Commission, 2012; Harris et al., 2012).

### 2.2.2.3 CONE BEAM COMPUTED TOMOGRAPHY (CBCT)

The CBCT technology uses a cone-shaped x-ray beam with an x-ray detector, flat-panel or image intensifier, to produce a three-dimensional volume using special reconstruction algorithms (Figure 2-3) (Tyndall et al., 2012).

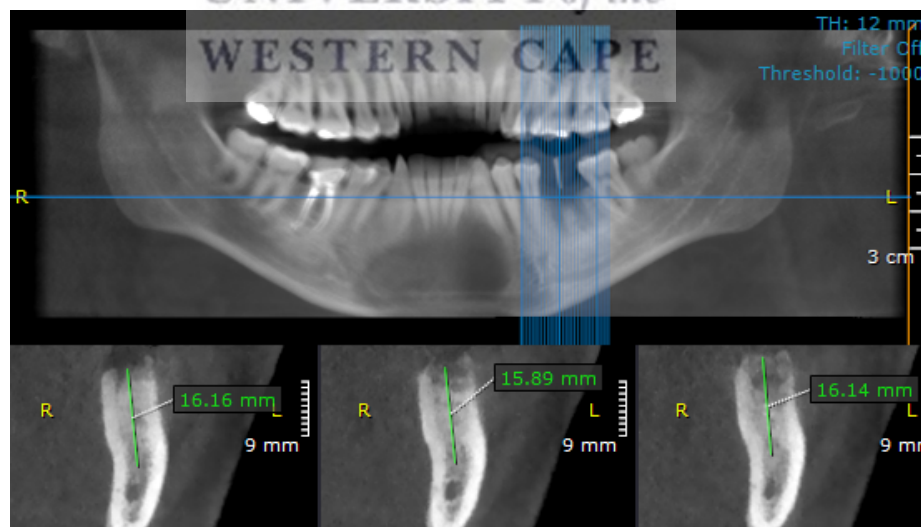


**Figure 2-3. CBCT scan. Reformatted panoramic view (top) and cross-sectional slices (bottom) were obtained. The measurement of the vertical dimension of a mandibular bone section (area of 36 #) was investigated.**

The technology's first commercial introduction for use in the maxillofacial area was in 1999, in Europe (Tyndall et al., 2012). There is an exponential growth in the use of CBCT during implant therapy (Jacobs, Salmon, et al., 2018). This broadens the scope of use of the radiographic modality from just diagnostic purposes to the pre-operative planning of dental implant treatments (Jacobs, Salmon, et al., 2018). The volumetric anatomical detail provided for the region of interest, e.g. the potential implant site, allows the clinician to accurately plan the surgical phase of dental implants with the opportunity to integrate it with guided surgical techniques (Jacobs, Salmon, et al., 2018). Compared to CT scans, the CBCT is more accessible for dental use, produces lower radiation doses, and the software is user-friendly and dentally-oriented (Tyndall et al., 2012). Although this modality offers many advantages during DIT (Table 2.8), it is vital to note that some of these advantages may vary among different CBCT machines (Jacobs, Salmon, et al., 2018). Variations in the resultant volume qualities and dose quantities of different machines and acquisition protocols, have been reported (Jacobs, Salmon, et al., 2018). The estimated (*E*) ranges from 19–1,073  $\mu\text{Sv}$  and is influenced by the field of view and individual units' dose parameters (Harris et al., 2012; White & Pharoah, 2013).





**Table 2.8. Indications, advantages, and disadvantages of radiographic modalities used in implant therapy consolidated by the author** (Tyndall et al., 2012; Harris et al., 2012; Nagarajan et al., 2014; Gupta et al., 2015; Agrawal et al., 2014; Manisundar et al., 2014; Lingam et al., 2013; Sahai, 2015; Gray et al., 2003; Fokas et al., 2018).

|                               | Indications  | Advantages   | Disadvantages   |
|-------------------------------|--|--|---|
| <b>Periapical radiographs</b> | <ul style="list-style-type: none"> <li>- Initial dental radiographic examination for implant-site assessment.</li> <li>- During and post-operative implant assessment.</li> <li>- Follow-up.</li> </ul>                            | <ul style="list-style-type: none"> <li>-Nominal geometrical distortion.</li> <li>-High spatial and contrast resolution.</li> <li>-Assessment of the vertical and mesiodistal boundaries of the ROI.</li> <li>-Economical and broadly available.</li> </ul> | <ul style="list-style-type: none"> <li>-Geometrical accuracy hinges on the experience of the operator and necessitates considerable compliance from the patients.</li> <li>-Wide edentulousness jaw segments may compromise the dimensions.</li> <li>-Lack of cross-sectional information.</li> <li>-The supporting bony structure quality and quantity may not be adequately assessed using periapical radiographs.</li> <li>- The relation with the vital structures in the vicinity may not be properly appreciated.</li> <li>-Limited field of view.</li> </ul>                           |
| <b>Panoramic Radiographs</b>  | <ul style="list-style-type: none"> <li>- Useful for initial implant site assessment.</li> <li>- Initial vertical bone height assessment.</li> <li>- During and post-operative implant assessment.</li> <li>- Follow-up.</li> </ul> | <ul style="list-style-type: none"> <li>- Widely available.</li> <li>- Broad coverage.</li> <li>- Cost-effectiveness.</li> <li>- Detection of any pathologies of the jaws and surrounding structures.</li> </ul>  | <ul style="list-style-type: none"> <li>- Possible distortion and inherent magnifications.</li> <li>- Challenges in the reproducibility of the radiographs.</li> <li>- Inferior in bone density and mineralisation assessment.</li> <li>- Lack of cross-sectional information.</li> <li>- Lower image resolution compared with intraoral periapical modalities.</li> <li>- Technique sensitive as minor patient positioning error can result in radiographic distortion and magnification.</li> <li>- Poor presentation of spatial relationships in-between structures of the jaws.</li> </ul> |

|   |  |   |   |
|---|--|---|---|
| <b>Lateral Cephalometric</b>                | <ul style="list-style-type: none"> <li>- DIT Planning of edentulous regions in the midline.</li> <li>- Assessment of dental arches' occlusal relationships.</li> </ul>                                 | <ul style="list-style-type: none"> <li>- Constant magnification ratios.</li> <li>- Availability of the modality and the ease of use.</li> <li>- Shows bone quantity and the angulation of the anterior dentoalveolar ridge.</li> <li>- Cross-sectional information at the mid-line area of the jaws and face.</li> </ul>  | <ul style="list-style-type: none"> <li>- The cross-sectional view is at the midline of the jaws.</li> <li>- Superimposition of the dental and bony structures from the opposite side of the jaw.</li> <li>- Not practical in terms of bone quality assessment.</li> <li>- Proper positioning is a prerequisite for distortion-free radiographs.</li> </ul>  |
| <b>Magnetic resonance imaging (MRI)</b>     | <ul style="list-style-type: none"> <li>- Despite its limited use, the MRI cross-sectional slices can be utilized during the implant planning phase.</li> </ul>   | <ul style="list-style-type: none"> <li>- Non-ionising radiation.</li> <li>- Appreciation of neurovascular structures.</li> <li>- Allows distinction between the oral mucosa/gingiva and the cortical bone of the alveolar bone.</li> <li>- High soft-tissue contrast.</li> <li>- Low incidence of image artefacts.</li> </ul>   | <ul style="list-style-type: none"> <li>- Prolonged acquisition time.</li> <li>- Cost-related factors.</li> <li>- Interpretation challenges.</li> <li>- Ferromagnetic metals' artefacts.</li> <li>- Poor bone mineral characterising.</li> <li>- Contra-indicated with a patient who has a cardiac pacemaker, surgical clips in situ, and a patient who had shrapnel wounds.</li> </ul>  |
| <b>Computed tomography (CT)</b>             | <ul style="list-style-type: none"> <li>- Implant planning.</li> <li>- Computer-guided surgery.</li> <li>- Sinus and ridge augmentation procedures.</li> <li>- Post-operative complications.</li> </ul> | <ul style="list-style-type: none"> <li>- Assessment of bone, quantitatively and qualitatively.</li> <li>- Undistorted reconstructed volumes.</li> <li>- High dimensional accuracy.</li> <li>- High soft and hard tissue contrast.</li> </ul>  | <ul style="list-style-type: none"> <li>- Higher radiation dose.</li> <li>- Not readily available.</li> <li>- Higher costs of the units and acquisitions.</li> <li>- Volume artefacts due to errors during the acquisition, patient movement, and metallic objects.</li> </ul>   |
| <b>Cone beam computed tomography (CBCT)</b> | <ul style="list-style-type: none"> <li>- Implant planning.</li> <li>- Computer-guided surgery.</li> <li>- Sinus and ridge augmentation procedures.</li> <li>- Post-operative complications.</li> </ul> | <ul style="list-style-type: none"> <li>- Easy to use and operate.</li> <li>- Allows limiting the field of view to depict only the region of interest.</li> <li>- High spatial resolution.</li> <li>- Cheaper than CT units.</li> <li>- Reduced radiation doses compared with CT in most cases.</li> <li>- Fast acquisitions (10-80 s).</li> <li>- Provides volumes with highly accurate and reliable dimensions.</li> <li>- Ability to merge the radiographic information with an optical scan of the patient or a model to create a surgical guide.</li> </ul> | <ul style="list-style-type: none"> <li>- Beam hardening artefacts, scattered radiation, and image noise.</li> <li>- Poor soft-tissue contrast.</li> <li>- The small variation in radiodensities is not adequately detected in the CBCT volumes.</li> <li>- Extra costs compared with conventional radiographic modalities.</li> <li>- Radiation doses are relatively higher than the conventional radiographic modalities.</li> </ul> |

### 2.3 PHASES OF DENTAL IMPLANT THERAPY WHERE RADIOGRAPHIC MODALITIES ARE INDICATED (TABLE 2.9)

The success of DIT depends on the quality and quantity of the information available of the implant-supporting structures, with dental radiography being a fundamental factor in its acquisition of this information (Tyndall & Brooks, 2000). These radiographs are necessary to assess the patient's craniofacial anatomy, bone quality and quantity, the anatomy of the potential implant site, detection of any possible pathologies, and identification of the boundaries and extents of vital structures in the surgical site (Nagarajan et al., 2014; Gupta et al., 2015; Karjodkar, 2009; Lingam et al., 2013). The selection of an appropriate radiographic modality is dependent on several factors, including the anatomical information needed, the adequacy of the information acquired from clinical examination, clinical judgment, the patient's clinical and aesthetic requirements, complications and risks assessment, and radiation dose considerations (Agrawal et al., 2014; Bornstein et al., 2014).

**Table 2.9. The radiographic indication of each treatment phase during dental implantology** (Nagarajan et al., 2014; Gupta et al., 2015).

| Treatment phase                             | Indication for a radiographic examination.  |
|---|---|
| <b>Pre-operative phase (planning phase)</b> | <ul style="list-style-type: none"> <li>- Assessment of bone quality and quantity.</li> <li>- Dimensional analysis and demarcation of vital structures in vicinity of the surgical site.</li> <li>- Analysis of prosthetic and surgical requirements.</li> </ul> |
| <b>Surgical phase</b>                       | <ul style="list-style-type: none"> <li>- To confirm the optimum insertion (location and alignment) of the fixture.</li> </ul>   |
| <b>Post-operative phase</b>                 | <ul style="list-style-type: none"> <li>- Assessment of healing process and osteointegration.</li> <li>- Maintenance of implant.</li> <li>- Detection of any post-operative changes in bony structure and implant surfaces.</li> </ul>                           |

---

### 2.3.1 RADIOGRAPHIC EXAMINATION: PLANNING PHASE

Comprehensive planning is required to optimise treatment results and to reduce potential complications. This phase allows the clinician to gather all necessary clinical information about the implant site prior to the surgery. Radiographs provide information that allows the clinician to visualise available bone dimensions, assess the osseous quality, demarcate anatomical boundaries, e.g. proximity of vital structures, determine the number of implants required, and evaluate prosthetic requirements (Nagarajan et al., 2014; Gupta et al., 2015).

Radiographic techniques, ranging from conventional to three-dimensional views, are used to assimilate this information (Tyndall & Brooks, 2000), but “a perfect imaging examination for dental-implant treatment planning does not exist” (Tyndall et al., 2012). The selection of a certain modality is usually subjective and dependent on the judgment of the clinician (Tyndall et al., 2012). Additionally, factors like the availability of a certain modality, costs, and radiation dose concerns, contribute to the type of radiograph selected (Gupta et al., 2015).

The intraoral periapical radiographs (IPR) are used to assess potential implant sites, detection of pathology, and identification of the vital anatomical structures in the vicinity of the surgical site (Nagarajan et al., 2014; Gupta et al., 2015). Even though periapical radiographs can be used as initial implant site radiographic examination, planning a surgical procedure based only on this view is risky, as geometrical accuracy is inconsistent and is influenced by operator skill and patient compliance (Tyndall et al., 2012). It is recommended to use radiographic markers for calibration of measurements, as it can enhance the accuracy of assessment of the vertical dimension (Tyndall et al., 2012).

Several reports highlight the usefulness of panoramic radiographs during DIT (Vazquez et al., 2008; Kim et al., 2011; Assaf & Gharbyah, 2014) and some clinicians prefer to prescribe only panoramic radiographs during DIT (Devlin & Yuan, 2013). Factors like simplicity, availability, lower costs, and lower radiation dose compared

with CT or CBCT, contributed to its popularity (Vazquez et al., 2008; Kim et al., 2011; Assaf & Gharbyah, 2014). Several studies have reported the common and dominant prescription of two-dimensional panoramic radiographs during implant therapy, compared to other radiographic modalities (Sakakura et al., 2003; Ramakrishnan et al., 2014; Alnahwi et al., 2017; Majid et al., 2014; Rabi et al., 2017). On the contrary, several reports (Pertl et al., 2013; Lindh et al., 1995; Riecke et al., 2015) do not recommend relying on panoramic radiographs alone for the assessment of vertical dimensions – as measurement inaccuracies have been noted. Malposition of the patient during panoramic radiography can have a substantial impact on the accuracy of implant planning, as the measurements on panoramic radiography might not be reliable (Riecke et al., 2015). Inconsistencies in the vertical and horizontal magnification factors in different jaw segments of the same panoramic radiograph were reported (Riecke et al., 2015; Gomez-Roman et al., 1999). It was also noted that distortion-free zones within the domain of the focal trough can be found only in certain points (Riecke et al., 2015).

The use of MRI during the implant planning phase is limited in daily dental practice due to cost issues, longer acquisition time, and interpretation complexities of these images (Tyndall et al., 2012). When MRI is used for implant planning, the T1-weighted sequences are advised (Gray et al., 2003). In this sequence, the cortical bone shows a low signal due to the deficiency of water and lipid protons, and appears black in contrast to the inside spongy bone, which appears bright since it contains fatty bone marrow (Gray et al., 2003). Moreover, in T1-weighted images, blood vessels and nerve bundles inside their canals have low signals and appear as dark areas within the bright surrounding bone marrow (Gray et al., 2003).

CBCT has gained popularity during the last decade, in particular for implant therapy (Deeb et al., 2017; Noffke et al., 2011; Jacobs, Salmon, et al., 2018). Compared to conventional CT scans, CBCT exposes the patient to lower radiation doses (Chau & Fung, 2009). In a relatively recent survey in the United States (2016), CBCT was commonly prescribed in the academic and private sectors, 49.6% and 59.1% respectively, during the implant planning phase (Carter et al., 2016). The CBCT

modality offers a valuable diagnostic tool for several dental procedures – including dental implants (Tyndall et al., 2012; Ganz, 2011). The multi-planar images are distortion- and superimposition-free and allow the clinician to accurately locate and measure the dimensions of the anatomical structures required for successful implant planning (Agrawal et al., 2014). Assessment of patient-specific and region-specific anatomy prior to surgical intervention should be performed to avoid harm to the structures that are near the implant site. Various complications such as cortical border perforation, sinus wall perforation, and injury to neural structures can be avoided – thus improving treatment outcome (Tyndall et al., 2012; Kraut, 1998; Hatcher et al., 2003).

In a relatively recent systemic review (Fokas et al., 2018) that summarised evidence on the accuracy of CBCT measurements, the authors concluded that the CBCT is highly accurate and reliable for linear measurements during implant planning. Although most of the included studies reported sub-millimetre differences (using CBCT), a wide range of over and underestimation was also reported, which lead to the implementation of a 2 mm safety margin (Fokas et al., 2018).

When computer-guided surgery is planned, a three-dimensional radiographic assessment is imperative (Flügge et al., 2017). Computer-guided planning allows a virtual simulation of the surgical and prosthetic stages using computer software (Colombo et al., 2017). This modality offers an interactive virtual implant planning, which adapts to the available bone dimensions, avoids vital anatomical structures, and provides a comprehensive overview of prosthetic and aesthetic requirements (Colombo et al., 2017; Grunder et al., 2005). Sometimes, extensive procedures like bone augmentation can be avoided, particularly when precise digital planning is performed (Colombo et al., 2017; Fortin et al., 2009).

### 2.3.1.1 ASSESSMENT OF BONE QUALITY

The bone density at the implant site is an important factor that influences the success of dental implant therapy (Wood et al., 2004; Drage et al., 2007; Lindh et al., 2004). At times, the terms ‘bone quality’ and ‘bone mineral density’ are used interchangeably, but ‘bone quality’ is a broader concept that encompasses the structure of the bone, such as alignment of the trabeculae, skeletal size, and matrix-related properties – in addition to mineral content (Sahai, 2015; Lindh et al., 2004).

The three-dimensional modalities such as CT and CBCT, construct virtual volume elements called “voxels”, that represent the assembly elements of the overall volume (Sahai, 2015; White & Pharoah, 2013). Each voxel is assigned a value referred to as an attenuation coefficient – consequent to the reconstruction processes (Mah et al., 2010; White & Pharoah, 2013). The Hounsfield units (HU) in CT modalities represent a standard scaling system for the linear attenuation coefficients that were previously reconstructed (Mah et al., 2010) and represent the density of a specific site in contrast with the density of air (–1,000 HU) and pure water (0 HU) (Cassetta et al., 2014). The value assigned to each voxel is a reflection of the density of the specific site – i.e. the degree of attenuation at that anatomical point (Sahai, 2015). The resultant densities on the multi-planar CT slices, presented in HU units, provide a reliable bone density assessment (Nagarajan et al., 2014; Lindh et al., 1996; Turkyilmaz et al., 2007; Aksoy et al., 2009). An example of different bone types and their corresponding Hounsfield units are tabulated in Table 2.10.

**Table 2.10. Estimated Hounsfield units for various bone types (Gupta et al., 2015).**

| Bone Quality Density | Hounsfield units (CT numbers) |
|----------------------|-------------------------------|
| <b>D1</b>            | 1250                          |
| <b>D2</b>            | 850–1250                      |
| <b>D3</b>            | 350–850                       |

|   |         |
|---|---------|
| <b>D4</b>   | 150–350 |
| <b>D5</b>   | < 150   |
| <ul style="list-style-type: none"> <li>• D1: dense cortical bone.</li> <li>• D2: porous cortical and coarse trabecular bone.</li> <li>• D3: porous cortical bone (thin) and fine trabecular bone.</li> <li>• D4: fine trabecular bone.</li> </ul> |         |

The grey values of the CBCT voxels are not absolute, as compared to the CT's HU values (Sahai, 2015; Cassetta et al., 2014; Arisan et al., 2013). These grey values are arbitrary and are predetermined by the manufacturers (Cassetta et al., 2014; Mah et al., 2010). A standard scaling system of the CBCT grey values is absent among the CBCT manufacturers, which further complicates the interpretation and comparison of grey values read from different CBCT units (Sahai, 2015; Mah et al., 2010). The exposure and unit parameters, in addition to modifications in the positioning of the object within the unit, may influence the grey values obtained (Nackaerts et al., 2011).

Some reports show an inconsistency between the CT's HU values and CBCT's grey values (Katsumata et al., 2007; Armstrong, 2006; Miles & Danforth, 2008; Nackaerts et al., 2011), while other reports (Naitoh et al., 2009; Nomura et al., 2010) suggest the contrary. Other authors reported the usefulness of using special conversion factors to convert the grey values into HU values (Reeves et al., 2012; Mah et al., 2010; Lagravère et al., 2006; Cassetta et al., 2014).

---

### 2.3.2 RADIOGRAPHIC EXAMINATIONS: SURGICAL PHASE (INTRA-OPERATIVE)

Radiographic evaluation during and directly after surgery is necessary to ensure the correct positioning and orientation of the fixture and to confirm the optimum prosthetic position (Nagarajan et al., 2014; Gupta et al., 2015).



Periapical, panoramic, and three-dimensional radiographs can be used during this phase, however, periapical radiographs are sufficient for this phase (Gupta et al., 2015; Harris et al., 2012). The use of three-dimensional radiographs, i.e. CBCT, directly after implant placement, is only justified in certain clinical scenarios according to the American Academy of Oral and Maxillofacial Radiology (AAOMR) – such as where the fixture is mobile or the patient has neurosensory alteration related to the procedure (Tyndall et al., 2012).

---

### 2.3.3 RADIOGRAPHIC EXAMINATIONS: RESTORATIVE PHASE

Procedures during this phase include the fabrication of a functional restoration on the implant. Intraoral periapical radiographs are commonly used to confirm the optimum mechanical integrity of various implant components (Wadhvani et al., 2012). In addition, intraoral radiographs help in the assessment of the status of osteointegration following the healing period, act as a baseline radiograph for future comparison, and to ensure the complete removal of excess cementation materials remaining in the peri-implant region, that lead to peri-implant complications (Wadhvani et al., 2012; Pauletto et al., 1999).

Digital periapical radiographs are considered to be superior to analogue ones in the detection of implant-abutment misfits (Oliveira et al., 2016). It is relevant, however, that the vertical angle of the x-ray beam can also affect the radiographic assessment of the fitting of implant components (Wadhvani et al., 2012; Begoña Ormaechea et al., 1999). The use of an x-ray film holder is recommended, since this would ensure that an orthogonal relation is attained in order to achieve an ideal parallel relationship with the implant axis and not the occlusal surfaces – as this may alter the angle between the film and the actual long axis of the implant (Wadhvani et al., 2012).

---

#### 2.3.4 RADIOGRAPHIC EXAMINATIONS: MAINTENANCE PHASE (POST-PROSTHETIC)

The maintenance phase of implant therapy begins from the time of the prosthetic restoration and continues throughout life, provided the implant remains in place (Nagarajan et al., 2014; Gupta et al., 2015). The radiographic evaluation consists mainly of the tracing of bone remodelling and osteointegration around the implant, assessment of bone loss, and overall status of the fixture and surrounding periodontium (Tyndall et al., 2012; Nagarajan et al., 2014).

The AAOMR advises taking periapical or panoramic radiographs in cases of extensive implant therapy and does not recommend the use of CBCT for periodic asymptomatic cases (Tyndall et al., 2012). Conventional periapical radiographs are considered superior to CBCT in the assessment of the peri-implant osseous structure, since the composition of the implant material may cause artefacts such as beam-hardening in the CBCT volumes, that may hinder optimal evaluation of the region of interest (Tyndall et al., 2012).

The European Association for Osseointegration advised that in the presence of post-implant therapy symptoms, including neurosensory deficiency and infections in the maxillary antrum – cross-sectional modalities such as the CBCT are justified (Harris et al., 2012). Nevertheless, in most cases, conventional modalities provide baseline information that is usually sufficient for the assessment (Harris et al., 2012).

During the first year post-implant restoration, a radiographic marginal bone loss of 0.9-1.6 mm around the implant and less than 0.2 mm in the following successive years is considered a marker of successful treatment (Cassetta et al., 2018; Albrektsson et al., 1986; Smith & Zarb, 1989). However, several factors may influence the radiographic perception of the marginal bone levels on a periapical radiograph – e.g. the angulation of the x-ray beam, film position, buccolingual position of the implant, and radiographic distortion that may occur in the interproximal buccal/lingual bony margins (Wadhvani et al., 2012; Cassetta et al., 2018; Sewerin, 1990). Optimum parallelism between the x-

ray receptor and the implant axis is necessary (Wadhvani et al., 2012; Cassetta et al., 2018). It is imperative to understand and appreciate the two-dimensional limitations of intraoral radiographs, as these images do not allow for the assessment of buccal and lingual bone structures adjacent to the implants (Wadhvani et al., 2012; Cassetta et al., 2018).

## 2.4 EMERGING TECHNOLOGIES

### GUIDED IMPLANT SURGERY

Guided implant surgery is a relatively modern approach that allows clinicians to virtually plan, and which simulates implant placement using virtual computer software (Flügge et al., 2017; Flügge et al., 2013). Thereafter, the virtual plan can be transferred to the patient's mouth using a surgical template that can be printed with the use of three-dimensional printers (Flügge et al., 2017; Flügge et al., 2013). The attainment of three-dimensional images i.e. CT or CBCT, is a crucial prerequisite to the commencement of virtual planning (Flügge et al., 2017; Flügge et al., 2013). The 3D volumes are then aligned with an intra-oral or a stone model surface scan. These scans present the teeth surface more accurately when compared to the CBCT or CT volumes, since these may have streak artefacts often caused by densely radiopaque materials (Plooij et al., 2011; Flügge et al., 2017).

Several reports confirm the effectiveness of computer-guided surgery to accurately plan and place dental implants (Shen et al., 2015; Filius et al., 2017; Platzer et al., 2012; Vercruyssen et al., 2014; Behneke et al., 2012) – but a precise transfer from the virtual software to the patient's mouth has to be maintained to ensure exact replication of the planned measurements (Flügge et al., 2017). Optimal alignment between radiographic volumes and intra-oral or model scans is mandatory in order to avoid any inherent inaccuracies in the surgical guide and planned surgery (Flügge et al., 2017).

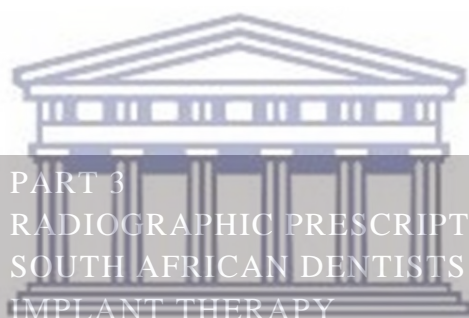
## 2.5 DISCUSSION & CONCLUSION

The choice of radiographic technique should be determined after a thorough clinical examination justifies the use of that particular modality, and with the advantages, indications, and drawbacks noted. Although three-dimensional modalities offer various advantages, the researcher also endeavoured to provide an informed gestalt of each modality.

Since the introduction of the CBCT modality into the various specialist fields of dentistry, it has become a widely used radiographic modality and the need to implement dose optimisation procedures in daily clinical practice has become obligatory.

Despite the relatively reduced radiation dosages from the CBCT compared with the CT scans, CBCT imaging yields greater radiation dosages when compared with conventional 2-dimensional radiographic modalities such as panoramic radiographs (Davies et al., 2012; Ludlow et al., 2003; Ludlow & Ivanovic, 2008). The radiation dose from CBCT examinations is one of the main concerns, since this has become a routine procedure in many regions (Noffke et al., 2011; Li, 2013).

The developments of the various aspects involved in different radiographic modalities are still ongoing. These include characteristics related to dose reduction and image quality improvements. It is imperative that research concerned with the assessment of all of these variables – such as dosages and dimensional accuracy of the emerging x-ray units – should be performed in order to provide evidence-based information that would direct decision-makers in their development of future radiographic practices.



PART 3  
RADIOGRAPHIC PRESCRIPTION TRENDS AMONG  
SOUTH AFRICAN DENTISTS DURING DENTAL  
IMPLANT THERAPY

UNIVERSITY of the  
WESTERN CAPE

**CONTENTS AT A GLANCE**

|  |
|--|
| Chapter 1   Introduction   |
| Chapter 2   Literature review                                    |
| 2.1 Dental implant radiographic prescription practices worldwide |
| 2.2 Radiographic prescriptions in Africa                         |
| Chapter 3   Aims and objectives                                  |
| Chapter 4   Materials and methods                                |
| 4.1 Tools and methods  |
| Chapter 5   Results  |
| Chapter 6   Discussion   |
| Chapter 7   Conclusion   |



UNIVERSITY of the  
WESTERN CAPE

**ABSTRACT**

**Aim:** To report the radiographic prescriptions commonly used in South Africa (SA) during implant therapy.

**Material and methods:** Electronic questionnaires were distributed during local dental conferences, through personal interviews, electronic channels (email lists) of several educational institutions, and dental and scientific societies in SA. Seventeen multiple-answer questions were formulated in order to investigate the radiographic prescriptions during various treatment phases and clinical scenarios.

**Results:** 142 dentists and dental specialists practising in various provinces in SA completed the electronic questionnaires. On average, during the implant planning phase, panoramic radiographs combined with cone beam computed tomography (PAN + CBCT) were the most preferred modality (39%), followed by CBCT (29%) as a single examination (ASE). Periapical radiographs, ASE, were most preferred during and directly after the surgery, 87% and 65%, respectively.

**Conclusion:** Panoramic radiographs combined with CBCT examinations were the most preferred examinations during dental implant planning. During, directly after the surgical placement of the implants, and during the follow-up of asymptomatic patients, the vast majority preferred periapical radiographs as single examinations. By contrast, CBCT, ASE, was preferred in the follow up of symptomatic patients. Factors related to the extra anatomical information and superior dimensional accuracy provided by three-dimensional volumes (e.g. CBCT volumes), were the most influencing factors on the radiographic prescriptions during implant planning.

**Keywords:** CBCT, Dental implant, radiographic trends, radiographical survey.

## LIST OF ABBREVIATIONS AND ACRONYMS

| Abbreviation   | Description   |
|----------------|---|
| <b>ASE</b>     | As a single examination   |
| <b>CBCT</b>    | Cone beam computed tomography   |
| <b>CT</b>      | Computed Tomography   |
| <b>GP</b>      | General practitioner  |
| <b>OMFR</b>    | Oral and Maxillofacial radiologist  |
| <b>OMFS</b>    | Oral and Maxillofacial surgeon  |
| <b>PA</b>      | Periapical radiograph   |
| <b>PAN</b>     | Panoramic radiograph  |
| <b>SA</b>      | South Africa  |
| <b>SADA</b>    | South African Dental Association  |
| <b>SASMFOS</b> | The South African Society of Maxillofacial and Oral Surgeons                  |
| <b>SASPIO</b>  | The South African Society for Periodontology, Implantology, and Oral Medicine |



UNIVERSITY *of the*  
WESTERN CAPE

**CHAPTER 1 | INTRODUCTION**

Radiographic assessment is considered vital during all dental implant treatment phases (Tyndall & Brooks, 2000; European Commission, 2004). The amount and the precision of information gathered during the planning phase from appropriate radiographic assessments, highly influences the success of the therapy (Tyndall & Brooks, 2000; Tyndall et al., 2012).

The radiographic examination is necessary to assess the patient's craniofacial and candidate implant site anatomy, bone quality and quantity, detection of possible pathologies, and identification of the boundaries and extents of vital structures in the surgical site (Tyndall & Brooks, 2000; Tyndall et al., 2012).

Panoramic radiography is a very common radiograph prescribed in daily practice (Tyndall et al., 2012). Multiple reports indicated the beneficial use of panoramic radiographs during implant therapy (Vazquez et al., 2008; Kim et al., 2011; Assaf & Gharbyah, 2014). Moreover, some practitioners prefer to prescribe panoramic as a single examination (Deylin & Yuan, 2013). Factors like the simplicity of the procedure, availability, lesser costs, and minor radiation dose generated compared with CT or CBCT, have motivated its popularity (Vazquez et al., 2008; Kim et al., 2011; Assaf & Gharbyah, 2014).

Cone beam computed tomography (CBCT) is an increasingly popular and promising imaging technique that has benefited multiple dental fields – including dental implantology. One of the chief advantages is the cross-sectional images generated for the regions of interest – while exposing the patient to lower radiation doses compared to computed tomography (CT scans) (Bornstein et al., 2017).

The evidence of the clinical efficiency of cross-sectional modalities used during implant planning, is inconclusive (Tyndall et al., 2012). Despite the scanty availability of rigorous dental implant imaging protocols in various regions around the world (including South Africa), regulatory bodies have published guidelines/advisory recommendations specific for particular geographical regions (e.g. the American



Academy of Oral and Maxillofacial Radiology, the European Association for Osseointegration, the European Commission, the International Congress of Oral Implantologists) (Tyndall et al., 2012; Harris et al., 2012; European Commission, 2012; European Commission, 2004; Benavides et al., 2012).

In South Africa, the use of CBCT has become popular or even a routine procedure in some practices for screening purposes (Noffke et al., 2011). The lack of local guidelines to use these modalities could lead to misuse, and consequently, the patient may be haphazardly exposed to higher radiation doses unnecessarily.

Each treatment phase during dental implant therapy necessitates appropriate imaging techniques to fulfil the treatment objectives. In this chapter, the imaging preferences and clinical opinions of clinicians who perform implant therapy in South Africa, have been reported.



## CHAPTER 2 | LITERATURE REVIEW

## 2.1 DENTAL IMPLANT RADIOGRAPHIC PRESCRIPTION PRACTICES WORLDWIDE

A survey was conducted in Brazil (Sakakura et al., 2003) to assess radiographic prescription trends during implant therapy. A questionnaire was provided to 69 practitioners investigating the modality of choice during pre-operative planning and follow-ups. The results showed that most participants prescribed panoramic radiographs as single examinations. The prescription patterns are shown in detail in Table (3.1).

The authors considered the factors that may alter the radiographic prescription during the treatment – e.g. cost factors, radiation exposure levels, and the area covered by the radiograph. Most participants chose the panoramic modality for wide anatomic coverage and cost purposes (Sakakura et al., 2003).

**Table 3.1. Summary of survey results** (Sakakura et al., 2003).

| PERCENTAGE | RADIOGRAPHIC MODALITY   |
|------------|---|
| 63.8%      | Panoramic radiographs (PAN) as a single examination.  |
| 28.9%      | Panoramic radiographs + Periapical radiographs (PA) and/or Conventional Tomography and/or Computed Tomography (CT). |
| 7.2%       | CT as a single examination.   |

Another survey was conducted in Brazil (2007) investigating the personal confidence level during the performance of measurements on radiographs during dental implant therapy (De Morais et al., 2007). The authors found that most interviewed participants were more confident about the accuracy of measurements estimated on CT during the pre-operative dental implant assessment, compared to panoramic radiographs.

A similar study was conducted in India (Ramakrishnan et al., 2014). Three hundred dentists were interviewed and asked about their radiographic prescriptions during implant site assessment. The results are presented in detail in Table (3.2).

**Table 3.2. Survey results (Ramakrishnan et al., 2014).**

| Percentage    | Radiographic modality                                      |
|---------------|--|
| <b>87.3%</b>  | Panoramic radiographs as a single examination.             |
| <b>4.6%</b>   | Panoramic radiographs (PAN) + Periapical radiographs (PA). |
| <b>4.3%</b>   | Panoramic radiographs (PAN) + CT.                          |
| <b>0.02%</b>  | CT as a single examination.                                |
| <b>0.066%</b> | Periapical radiograph (PA) as a single examination.        |
| <b>0%</b>     | Cone Beam Computed Tomography (CBCT).                      |

A study in Saudi Arabia in 2017 showed that during the pre-operative assessment of implant sites, most of the 120 dentists interviewed use panoramic radiography due to availability and broad coverage (Alnahwi et al., 2017). Details regarding the type of radiographs prescribed at each treatment stage are documented in Table (3.3).

**Table 3.3. Survey results (Alnahwi et al., 2017).**

|           | Pre-operative | During Surg. | Post-operative | Follow-up |
|-----------|---------------|--------------|----------------|-----------|
| PA (ASE)  | 4.2%          | 37%          | 27.1%          | 39.5%     |
| PAN + PA  | 18.5%         | 25.2%        | 44.9%          | 31.9%     |
| CT (ASE)  | 9.2%          | 12.6%        | 3.4%           | 2.5%      |
| PAN (ASE) | 13.4%         | 9.2%         | 16.1           | 21%       |

|               |       |      |      |      |
|---------------|-------|------|------|------|
| PAN + CT      | 19.3% | 5%   | 4.2% | 3.4% |
| PAN + CT + PA | 20.2% | 3.5% | 4.2% | 0.8% |

- ASE: as a single examination

In 2017, a study was conducted in Palestine to survey the current local radiographic prescription trends (Rabi et al., 2017). One hundred and fourteen dentists participated and the results showed that most of them (59%) preferred to prescribe panoramic radiographs for implant assessment – mainly due to availability (Table 3.4). The remaining participants preferred a combination of panoramic radiographs and computed tomography (CT).

**Table 3.4. Factors influencing radiographic prescriptions (Rabi et al., 2017).**

| FACTOR                       | PERCENTAGE |
|------------------------------|------------|
| Availability                 | 42.99%     |
| Availability + cost          | 17.53%     |
| Cost + measurement precision | 3.51%      |
| Cost + radiation dose        | 10.53%     |
| Measurement precision        | 25.44%     |

## 2.2 RADIOGRAPHIC PRESCRIPTIONS IN AFRICA

In Libya (Majid et al., 2014), a study was done to assess the current radiographic prescriptions during the pre-operative implant site assessment for 80 participants. Similar to the previous studies, most participants used panoramic radiographs for the assessment (Table 3.5), mainly for factors related to coverage and cost efficiency (Table 3.6).

**Table 3.5. Survey results of prescription trends (Majid et al., 2014).**

| <b>RADIOGRAPHIC MODALITY</b>                  | <b>PERCENTAGE</b> |
|---|-------------------|
| <b>PAN (ASE)</b>                              | 70%               |
| <b>PAN + PA</b>                               | 15%               |
| <b>CT with other conventional radiographs</b> | 8.75%             |
| <b>CT (ASE)</b>                               | 6.25%             |

**Table 3.6. Factors influencing radiographic prescriptions (Majid et al., 2014).**

| <b>Factor</b>                           | <b>Percentage</b> |
|---|-------------------|
| <b>Broad coverage of face and teeth</b> | 32.5%             |
| <b>Measurement accuracy</b>             | 17.5%             |
| <b>Cost</b>                             | 11.25%            |
| <b>Availability</b>                     | 10%               |
| <b>Radiation dose</b>                   | 2.5%              |

To the best of the author's knowledge, there are no published reports on radiographic prescription during dental implant therapy in South Africa (SA). Nevertheless, Noffke et al. (2011) mentioned that in SA the use of CBCT is becoming increasingly popular and in some instances, a routine procedure. The misuse of this modality includes its use for "non-specific screening purposes".

There is a paucity of literature regarding the current radiographic prescription trends among South African dentists. This requires investigation through multiple future surveys with representative samples. Such information may help decision-makers understand the specific needs of clinicians in SA, and to establish suitable imaging protocols for implant therapy.

## CHAPTER 3 | AIMS AND OBJECTIVES

### 3.1 AIM

To report the current radiographic practices during dental implant therapy in SA.

### 3.2 OBJECTIVES

- 1- Identify the current radiographic prescription trends of clinicians during implant therapy in SA.
- 2- Investigate the factors influencing radiographic prescriptions.
- 3- Report the clinical preferences, opinions, and experiences of academics and clinicians placing implants in SA.

### 3.3 RATIONALE

- 1- This study addresses the current radiographic prescription trends in several nationwide facilities in SA and highlights factors influencing radiographic prescriptions that are specific to the local working environment in SA.
- 2- Allows the local practitioners and academics to participate and share their experiences, thoughts, and clinical preferences for possible future guidelines to be established by organisational authorities in SA.
- 3- Highlights the value and increases the awareness of local practitioners concerning the establishment of implant imaging guidelines, that help save the patients from unnecessary exposure and at the same time ensures clinical efficiency.

## CHAPTER 4 | MATERIALS AND METHODS

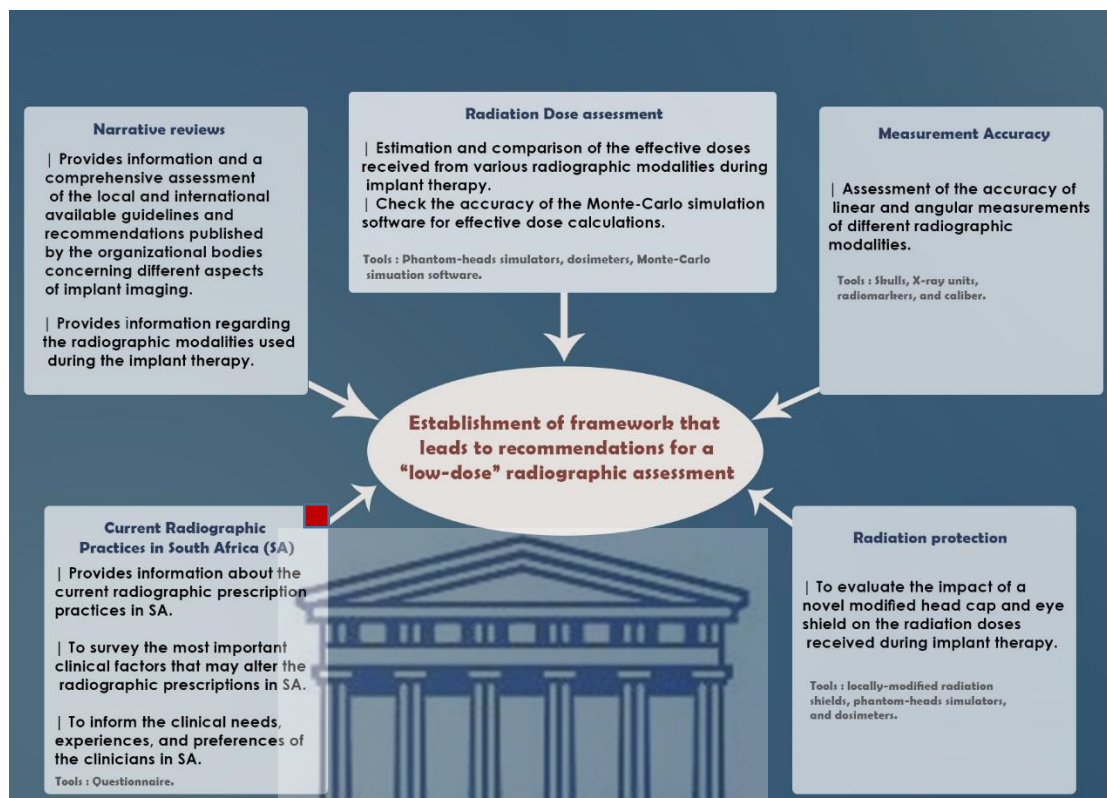


**Figure 3-1. Diagrammatic representation of the main research project. The current sub-study is highlighted.**

## 4.1 TOOLS AND METHODS

- Questionnaire (Q1/2018).
- Consent form: participation in the study (CF1/2018).
- Information sheet (INF1/2018).

### 4.1.1 OVERVIEW

Seventeen open-ended multiple-choice questions were delivered using an electronic questionnaire. An electronic information sheet (INF1/2018) was attached to the survey form and explained all the aspects of the research. A consent form (CF1/2018) was also embedded in the questionnaire and was collected electronically (as the participants

accepted to proceed and answer the questions). No names nor personal information was required or collected. The questionnaire was published online using Google<sup>®</sup> Forms<sup>®</sup>.

---

#### 4.1.2 SURVEY STRUCTURE

The questions were scenario-based, anonymous, and covered all the needed facets required to accomplish the aim of this study. Two questions were enabled for multiple answers. Information was collected mainly concerning the most used radiographic modalities, personal experiences, clinical preferences, and the possible factors that may influence radiographic prescriptions.

The radiographic modalities' preferences were assessed during different clinical situations, various anatomical regions, and covered all dental implant therapy phases (planning, intra-operative, and follow-up phases). The anatomical regions that were assessed during the planning phase included posterior mandible (unilateral, distal to first premolar region), anterior region of the maxilla/mandible (canine to canine region), posterior maxilla region (unilateral: distal to the first premolar), one jaw (mandible/maxilla) or both jaws (full mouth), and the mental foramen region (uni/bilateral).

The options of the radiographic modalities were: Periapical radiograph/s (PA) only, Panoramic radiograph (PAN) only, PAN + PA, PA + CBCT, PAN + CBCT, CBCT only, and no radiographs. Factors including cost, availability, radiation dose concerns, broad coverage, dimensional accuracy (3D volumes), additional anatomical information (3D volumes), and special procedures (e.g. 3D volumes for guided implant surgery) were inquired as motivating factors for the selection of radiographic examinations. For detailed information, please see the questionnaire ([Q1/2018](#)).

The level of formal training received (e.g. general dentist, postgraduate student, specialist) and the provinces where participants practice, were captured. Age and gender were not collected in the survey.



---

#### 4.1.3 INCLUSION CRITERIA

- 1- Practitioners/specialists/academics/senior residents at the departments of Periodontology, Oral maxillofacial surgery, Prosthodontics, and Oral and Maxillofacial Radiology, who are enrolled in implant therapy in dental schools in South Africa.
- 2- Specialists who perform implant therapy in private practice.
- 3- Private practitioners with dental implant experience of not less than three years.

---

#### 4.1.4 EXCLUSION CRITERIA

- 1- Dental facilities (private/public/academic) that do not offer dental implant therapies.

---

#### 4.1.5 SURVEY DISSEMINATION

- 1- Electronic mailing lists of the South African Dental Association (SADA), the South African Society for Periodontology, Implantology, and Oral Medicine (SASPIO), and the South African Society of Maxillofacial and Oral Surgeons (SASMFOs).
- 2- Personal survey/interviews of clinicians during conferences held in South Africa, including the ITI implant Congress (Cape Town, SA, July 2019) and the SADA congress (held in Durban, SA, September 2019).
- 3- Interviews/an online survey population by academics in the departments of periodontology, maxillofacial surgery, prosthodontics, oral and maxillofacial radiology, and the senior registrar at the University of the Witwatersrand, the University of Pretoria, and the University of the Western Cape.

The participants had the choice to be either interviewed or provided with an electronic survey link (Google<sup>®</sup> Forms<sup>®</sup>). A hard-copy format of the questionnaire was also offered, upon the participant's request. The interviewers (where applicable) were trained and calibrated to the format and questions of the questionnaire. The interviewers were available to answer any queries about the survey itself, but did not make suggestions or recommendations.

---

#### 4.1.6 SAMPLE SIZE AND SELECTION PROCESS:

The representative number of participants was advised by the statistician. The participants were selected according to the inclusion criteria (section 4.1.3).

#### 4.2 STATISTICAL OVERVIEW AND DATA ANALYSIS:

All data points were captured from multiple Google forms and exported to Excel<sup>®</sup> (Microsoft<sup>®</sup>, WA, USA) software for statistical analysis.



UNIVERSITY of the  
WESTERN CAPE

## CHAPTER 5 | RESULTS

One hundred and forty-two responses were captured and analysed (Table 3.7).

**Table 3.7. Distribution of the surveyees.**

| Survey platform       | Number of participants |
|-----------------------|------------------------|
| Conferences           | 40                     |
| Online population     | 71                     |
| Academic institutions | 31                     |
| <b>Total</b>          | <b>142</b>             |

The highest percentage of participants (Chart 3-1) were practising implantology in the Western Cape Province (excluding 47 participants that failed to capture their place of practice).

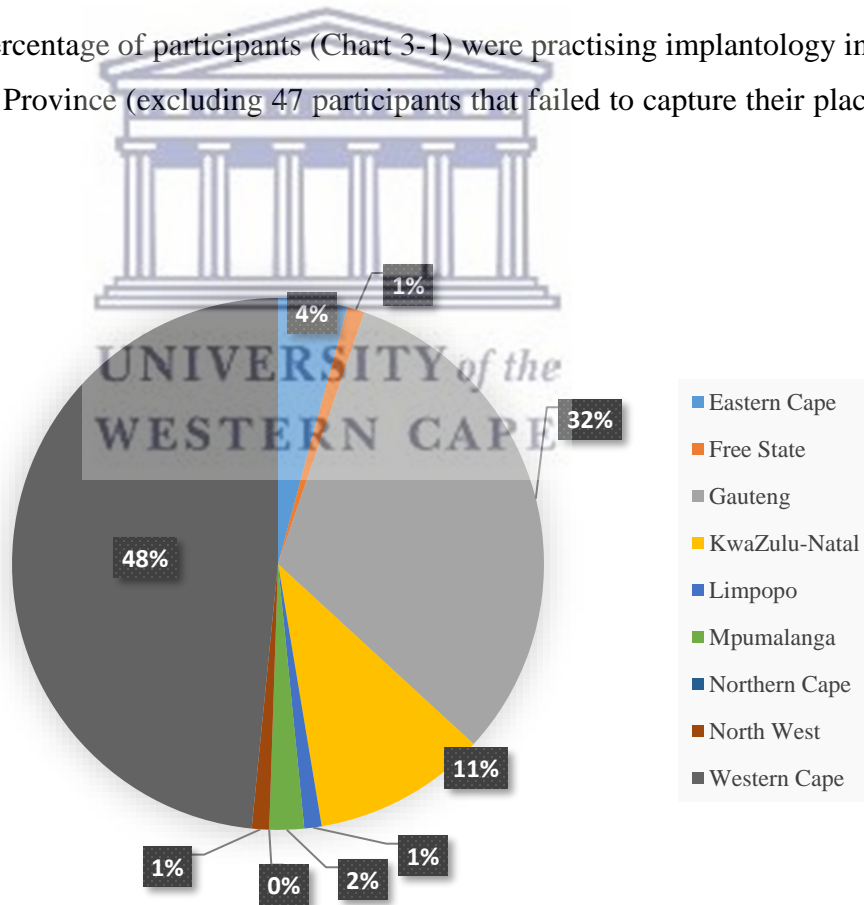


**Chart 3-1. The province of the dental practice of those surveyed.**

Sixty-three participants (44%) were general dentists with implant experience (3 years min.), followed by 28 periodontists (20%), 16 registrars (11%), 15 maxillofacial surgeons (11%), 12 prosthodontists (8%), and 8 maxillofacial radiologists (6%), further illustration in (Chart 3-2).

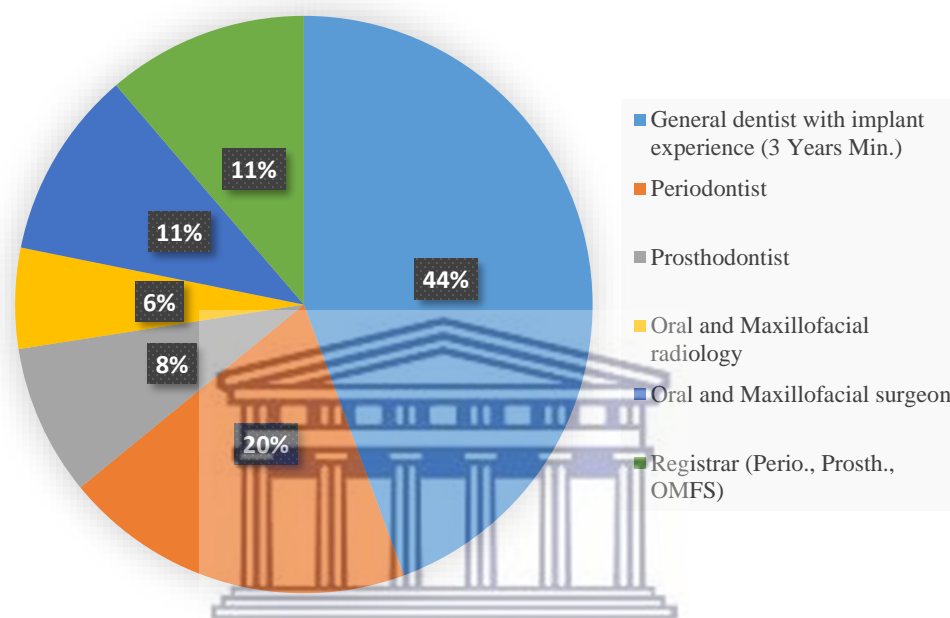


**Chart 3-2. Distribution of the formal training received by participants.**

On average, during the implant planning phase (for all anatomical regions in the jaws) the panoramic radiographs with cone beam computed tomography (PAN + CBCT) was the most preferred modality (39%), followed by CBCT (as a single examination) (29%), periapical radiograph (PA) with CBCT (19%), PAN + PA (8%), PAN only (2%), other (2%), and PA only (1%). Detailed radiographic preferences in various specific anatomical regions are depicted in Table 3.8 and Chart 3-3 (A-E).

**Table 3.8. Radiographic modalities preferred in various anatomical regions during the implant planning phase.**

| Modality         | Region 1 | Region 2 | Region 3 | Region 4 | Region 5 |
|------------------|----------|----------|----------|----------|----------|
| PA only          | 0        | 2        | 0        | 0        | 1        |
| PAN only         | 4        | 4        | 4        | 2        | 2        |
| PAN + PA only    | 10       | 10       | 12       | 14       | 10       |
| PA + CBCT        | 26       | 40       | 29       | 14       | 28       |
| Pan + CBCT       | 60       | 46       | 56       | 69       | 48       |
| CBCT only        | 39       | 38       | 38       | 40       | 50       |
| No Radiographs   | 0        | 1        | 0        | 0        | 0        |
| Other modalities | 3        | 1        | 3        | 3        | 3        |

- **Region 1: Posterior mandible (Unilateral, distal to first premolar region)**
- **Region 2: Anterior region of the Maxilla/Mandible (Canine to Canine region)**
- **Region 3: Posterior maxilla region (Unilateral: distal to the first premolar)**
- **Region 4: One jaw (Mandible/Maxilla) or both jaws (Full mouth)**
- **Region 5: Mental foramen region (Uni/bilateral).**
- **PA: Periapical radiograph, PAN: Panoramic radiograph, CBCT: Cone beam computed tomography.**

**A) Posterior mandible (Unilateral, distal to first premolar region)**

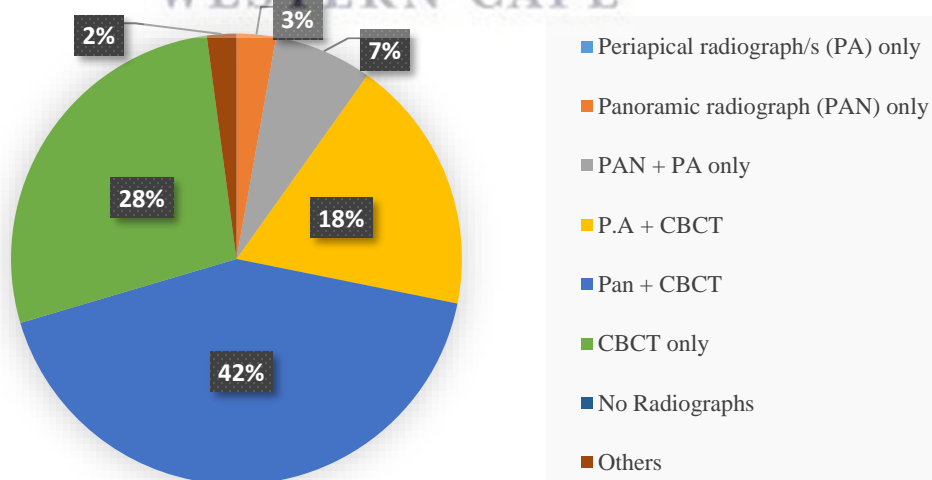
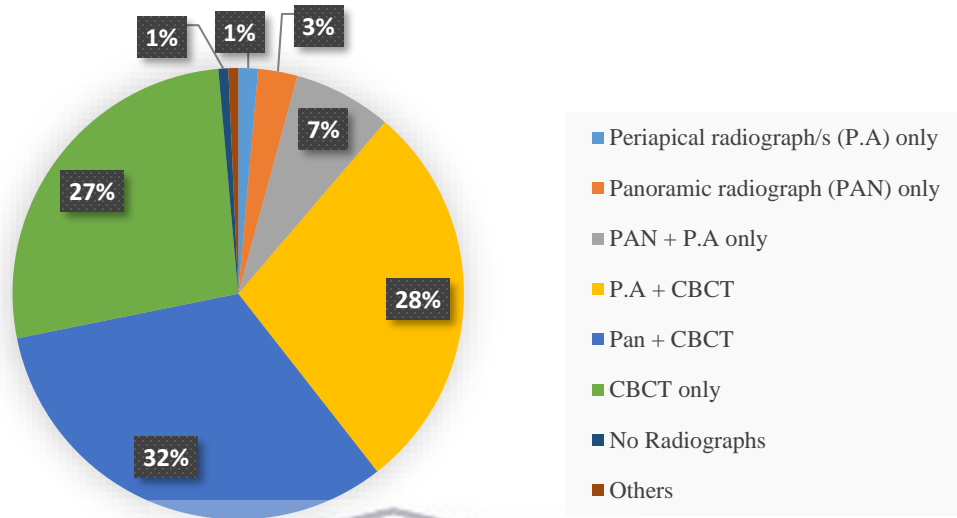


**Chart 3-3. Radiographic modalities prescribed during the planning phase (A-E).**

**B| Anterior region of the maxilla/mandible  
(Canine to Canine region)**



**C| Posterior maxilla region  
(Unilateral: distal to the first premolar)**

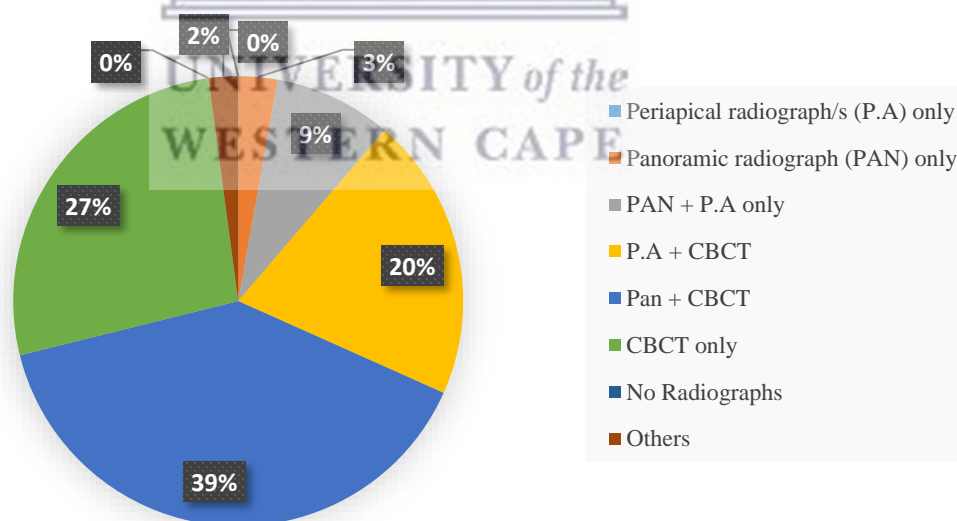
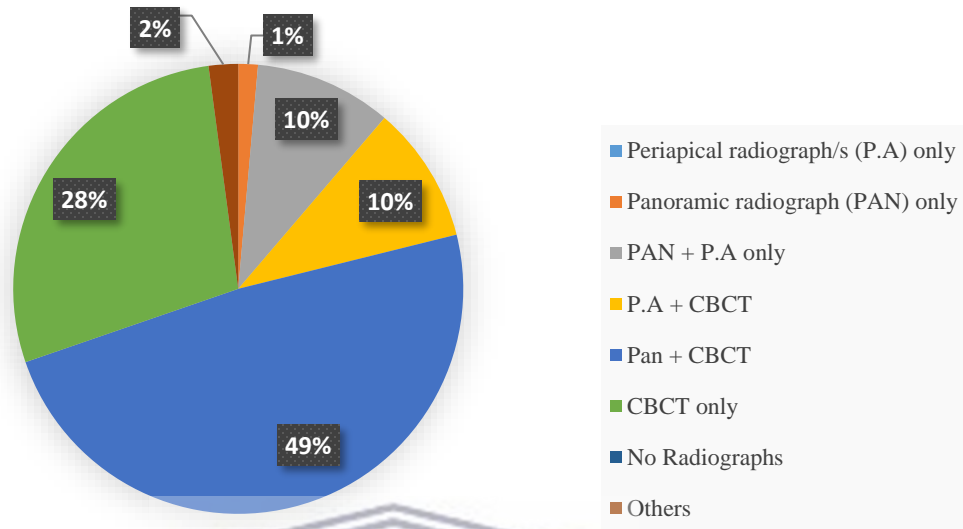


**Chart 3-3. (Cont.)**

**D| One jaw (Mandible/Maxilla) or both jaws (Full mouth)**



**E| Mental foramen region (Uni/bilateral)**

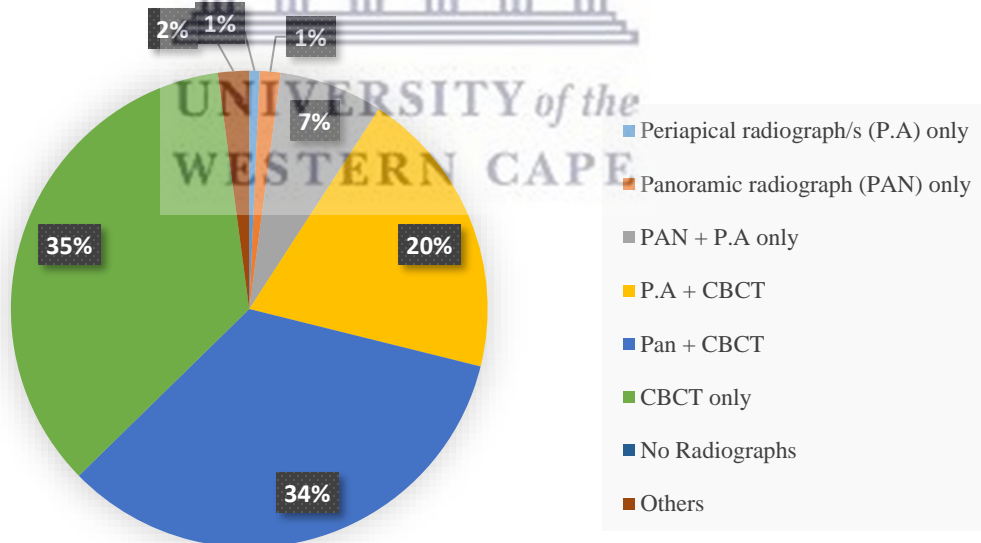


**Chart 3-3. (Cont.)**

Factors that mostly influenced selection of a certain radiographic modality/ies during the implant planning phase are shown in Table 3.9 and Chart 3-4. Generally, the influencing factor mostly selected was “Three-dimensional modalities provide more anatomical information necessary for the success of the therapy”, followed by “Better dimensional accuracy (if three-dimensional modalities, e.g. CBCT, were selected previously)”, followed by broad coverage of the designated anatomical area.

**Table 3.9. Factors that influence radiographic preference during the implant planning phase.**

| Factors (Multiple answers were allowed):  | Participants (n=142) |
|---|----------------------|
| Lower costs for the patients (if the conventional modalities PAN and/or PA were preferred previously)                                 | 12                   |
| Availability and ease of access of the radiographic modality (if the conventional modalities PAN and/or PA were preferred previously) | 18                   |
| Radiation dose concerns of three-dimensional modalities (if the conventional modalities PAN and/or PA were preferred previously)      | 7                    |
| Broad coverage of the designated anatomical area (If PAN and/or CBCT were preferred previously)                                       | 71                   |
| Better dimensional accuracy (if three-dimensional modalities, e.g. CBCT, were selected previously)                                    | 87                   |
| Three-dimensional modalities provide more anatomical information necessary for the success of the therapy                             | 110                  |
| Only three-dimensional modalities (e.g. CBCT), if guided implant surgery is considered  | 29                   |
| Other reasons   | 5                    |



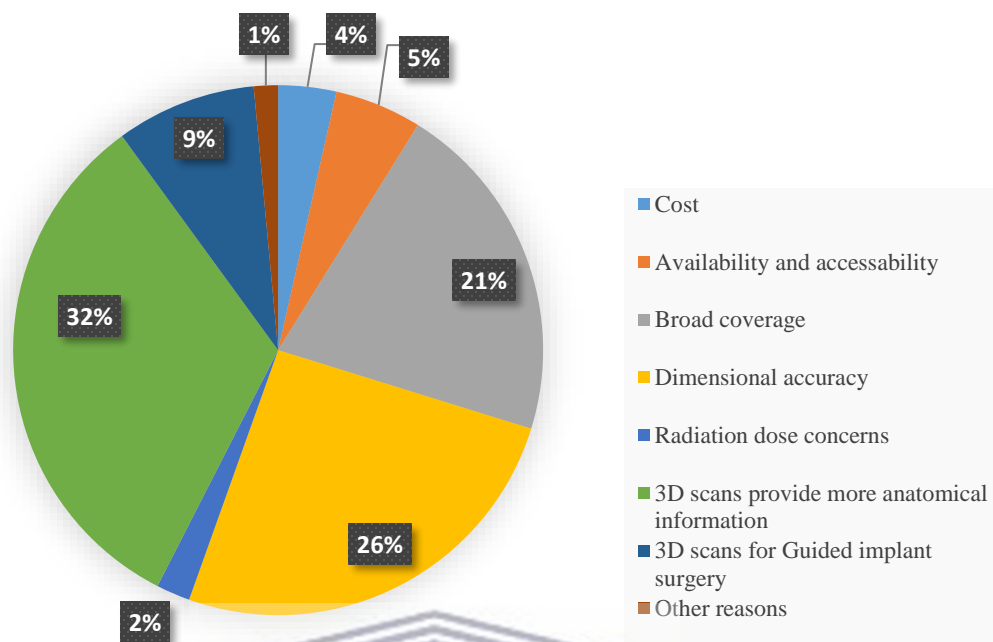


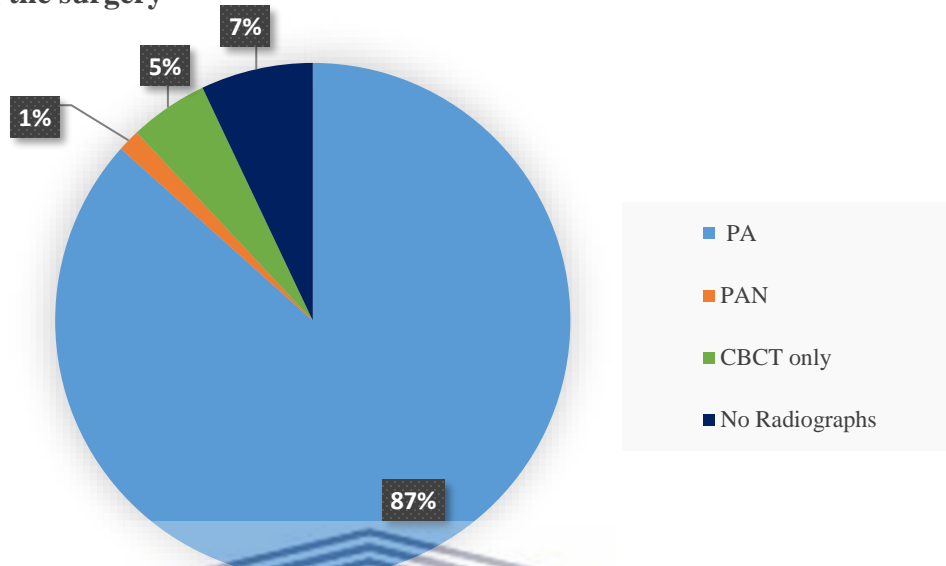
**Chart 3-4. Factors influencing radiographic preference during the implant planning phase.**

During and directly after surgery, periapical radiographs (as a single examination) were the most preferred (87% and 65%, respectively), and further details are documented in Table 3.10 and Chart 3-5 (A&B).

**Table 3.10. Radiographic modalities preferred during and directly after the surgery.**

| Modality              | During the implant surgery | Directly after the implant surgery |
|-----------------------|----------------------------|------------------------------------|
| Periapical radiograph | 123                        | 92                                 |
| Panoramic radiograph  | 2                          | 26                                 |
| CBCT only             | 7                          | 18                                 |
| No radiographs        | 10                         | 6                                  |

**A| During the surgery**



**B| Directly after the surgery**

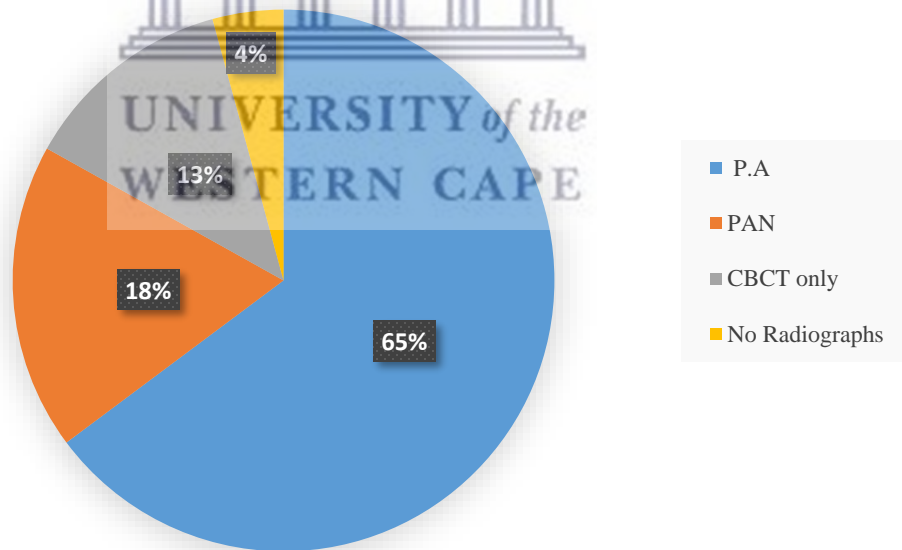


**Chart 3-5. The radiographic modalities prescribed during and directly after surgery (A&B).**

Periapical radiographs (as single examinations) were also the most preferred modality for the follow-up of asymptomatic patients (46%), while CBCT (a single examination) was the most selected examination in the case of any post-operative complications (32%); further details are tabulated (Table 3.11) and Chart 3-6 (A&B).

**Table 3.11. The radiographic modalities preferred during follow-ups for symptomatic and asymptomatic patients**

| Modality                          | Asymptomatic | Symptomatic |
|-----------------------------------|--------------|-------------|
| Periapical radiograph/s (PA) only | 66           | 11          |
| Panoramic radiograph (PAN) only   | 20           | 5           |
| PAN + PA only                     | 25           | 21          |
| PA + CBCT                         | 1            | 37          |
| Pan + CBCT                        | 8            | 17          |
| CBCT only                         | 12           | 46          |
| No Radiographs                    | 6            | 0           |
| Others                            | 4            | 5           |

**A) Follow-up  
(Asymptomatic patient)**

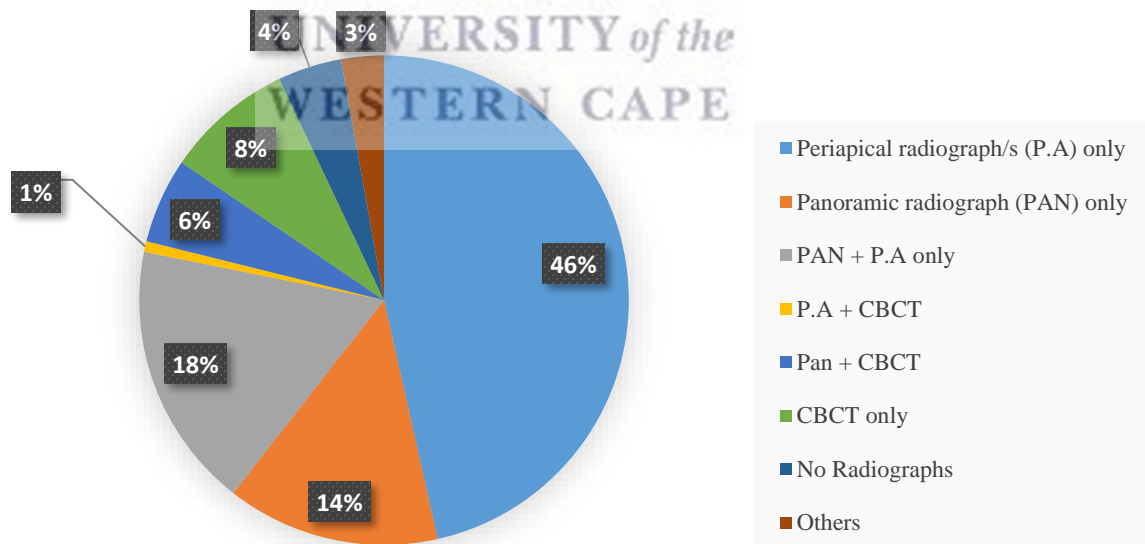


**Chart 3-6. The radiographic modalities prescribed during the follow-up of A/symptomatic patients (A&B).**

### B| Follow-up (Symptomatic patient)

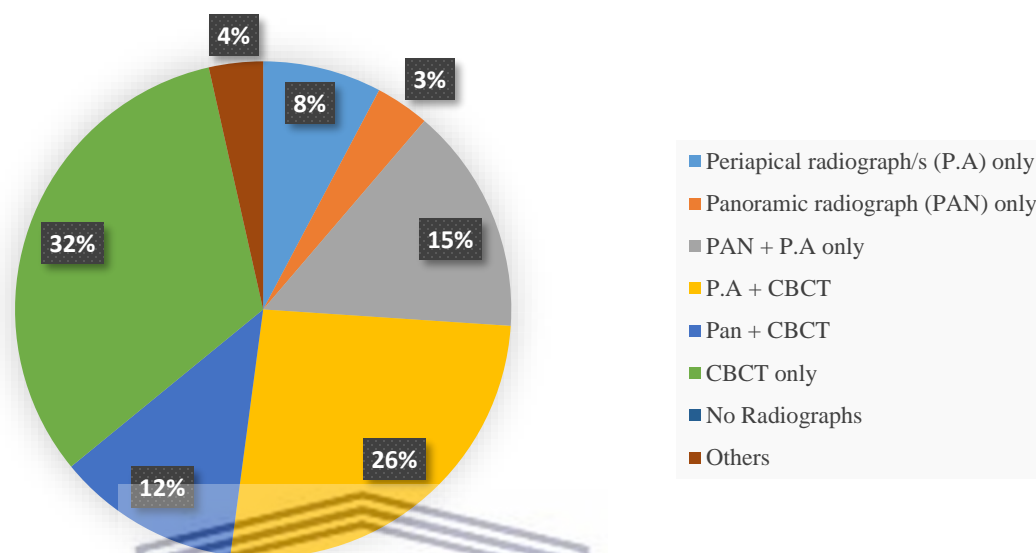


**Chart 3-6. (Cont.)**

Factors that mostly influenced radiographic preferences during the follow-up phase were “CBCT provides more information regardless of the limitations of possible beam radiographic artefacts caused by the implants”, followed by broad coverage, availability and ease of access and limitations of CBCT (beam hardening and scattering artefacts), and other reasons (Table 3.12).

**Table 3.12. Factors that influence the radiographic preference during follow-up.**

| Factors (Multiple answers were allowed):   | # Participants<br>(out of 142) |
|--|--------------------------------|
| Conventional radiographs (especially PA) are preferred, as the CBCT is of limited value if radiographic artefacts (caused by implants e.g. beam hardening and scattering) are evident in the volume. | 37                             |
| CBCT provides more information regardless of the limitations of possible beam radiographic artefacts caused by the implants  | 67                             |
| Availability and ease of access of the radiographic modality   | 37                             |
| Broad coverage of the designated anatomical area   | 40                             |
| Other reasons  | 8                              |

Most participants (56%) indicated that radiographic follow-up frequency (after the delivery of the prosthesis) was “After the first 6 months, 12 months, and then every year for a 10-year period” (Chart 3-7).

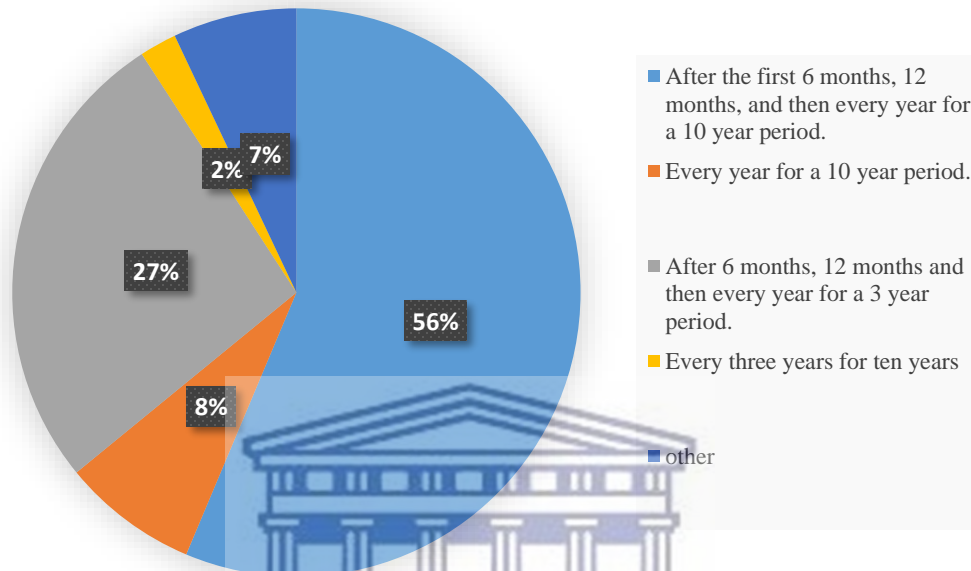


**Chart 3-7. Frequency of radiographic follow-up (after the delivery of the prosthesis).**

Comparisons between the level of formal training and the most frequently selected radiographic examination during various treatment phases, along with the motivating factors for their choice, are noted (Table 3.13, Table 3.14, and Table 3.15).

**Table 3.13. The most frequently selected radiographic examinations during planning phase by various dental specialities.**

| Region  |          | GP (63)        | Periodontists (28) | Prosthodontists (12) | OMFS (15)       | OMFR (8)    | Registrars (16)            |                 |
|---|----------|----------------|--------------------|----------------------|-----------------|-------------|----------------------------|-----------------|
| Planning phase  | Region 1 | <b>Overall</b> | PAN +CBCT (43%)    | CBCT (43%)           | PAN +CBCT (59%) | CBCT (46%)  | PAN +CBCT (62%)            | PAN +CBCT (56%) |
|   |          | <b>% CBCT*</b> | 51 (80.95%)        | 27 (96.42%)          | 10 (83.33%)     | 14 (93.33%) | 8 (100%)                   | 15 (93.75%)     |
|   | Region 2 | <b>Overall</b> | PA+CBCT (35%)      | CBCT (50%)           | PAN +CBCT (67%) | CBCT (53%)  | CBCT (38%)                 | PAN +CBCT (50%) |
|   |          | <b>% CBCT*</b> | 50 (79.36%)        | 26 (92.85%)          | 10 (83.33%)     | 14 (93.33%) | 8 (100%)                   | 16 (100%)       |
|   | Region 3 | <b>Overall</b> | PAN+CBCT (35%)     | CBCT (39%)           | PAN +CBCT (67%) | CBCT (60%)  | PAN +CBCT (50%)            | PAN +CBCT (63%) |
|   |          | <b>% CBCT*</b> | 49 (77.77%)        | 27 (96.42%)          | 10 (83.33%)     | 14 (93.33%) | 8 (100%)                   | 15 (93.75%)     |
|   | Region 4 | <b>Overall</b> | PAN+CBCT (52%)     | CBCT (53%)           | PAN +CBCT (67%) | CBCT (53%)  | PAN +CBCT (62%)            | PAN +CBCT (62%) |
|   |          | <b>% CBCT*</b> | 51 (80.95%)        | 26 (92,85%)          | 9 (75%)         | 14 (93.33%) | 8 (100%)                   | 15 (93.75%)     |
|   | Region 5 | <b>Overall</b> | PAN+CBCT (36%)     | CBCT (57%)           | PAN +CBCT (50%) | CBCT (67%)  | PAN+CBCT & CBCT only (50%) | PAN +CBCT (50%) |
|   |          | <b>% CBCT*</b> | 52 (82.53%)        | 26 (92,85%)          | 11 (91.66%)     | 14 (93.33%) | 8 (100%)                   | 15 (93.75%)     |
| Percentage of selections included CBCT (as a single examination or combined with other techniques) <ul style="list-style-type: none"> <li>• Region 1: Posterior mandible (Unilateral, distal to first premolar region)</li> <li>• Region 2: Anterior region of the Maxilla/Mandible (Canine to Canine region)</li> <li>• Region 3: Posterior maxilla region (Unilateral: distal to the first premolar)</li> <li>• Region 4: One jaw (Mandible/Maxilla) or both jaws (Full mouth)</li> <li>• Region 5: Mental foramen region (Uni/bilateral).</li> <li>• GP: General practitioners. OMFS, OMFR: Oral and Maxillofacial Surgeons and radiologists, respectively.</li> </ul> |          |                |                    |                      |                 |             |                            |                 |

**Table 3.14. The most frequently selected radiographic examinations during surgical and post-surgical phases by various dental specialities.**

| Phase                            | GP (63)        | Periodontists (28) | Prosthodontists (12) | OMFS (15)  | OMFR (8)   | Registrars (16) | GP (63)    |
|----------------------------------|----------------|--------------------|----------------------|------------|------------|-----------------|------------|
| During the surgery               | <b>Overall</b> | PA (90%)           | PA (96%)             | PA (83%)   | PA (67%)   | PA (75%)        | PA (81%)   |
|                                  | <b>% CBCT*</b> | 3 (4.76%)          | 1 (3.57%)            | 0          | 1 (6.66%)  | 1 (12.5%)       | 1 (6.25%)  |
| Directly after the surgery       | <b>Overall</b> | PA (70%)           | PA (64%)             | PA (50%)   | PA (40%)   | PA (62%)        | PA (81%)   |
|                                  | <b>% CBCT*</b> | 8 (12.69%)         | 6 (21.42%)           | 0          | 2 (13.33%) | 2 (25%)         | 0          |
| Follow-up (Asymptomatic patient) | <b>Overall</b> | PA (59%)           | PA (50%)             | PAN (25%)  | PAN (53%)  | PA (62%)        | PA (44%)   |
|                                  | <b>% CBCT*</b> | 8 (12.69%)         | 3 (10.71%)           | 2 (16.66%) | 2 (13.33%) | 1 (12.5%)       | 5 (31.25%) |

| Follow-up (symptomatic patient) | Overall | PA + CBCT (32%) | PA + CBCT and CBCT only (39%) | CBCT (41%) | CBCT (40%)  | CBCT (43%) | CBCT (50%) |
|---------------------------------|---------|-----------------|-------------------------------|------------|-------------|------------|------------|
|                                 | % CBCT* | 38 (60.31%)     | 23 (82.14%)                   | 9 (75%)    | 10 (66.66%) | 6 (75%)    | 14 (87.5%) |

\* Percentage of selections included CBCT (as a single examination or combined with other techniques)

**Table 3.15. The number of participants vs factors chosen by various dental specialities.**

| Motivating factor   | GP (% of 63) | Periodontists (% of 28) | Prosthodontists (% of 12) | OMFS (% of 15) | OMFR (% of 8) | Registrars (% of 16) |
|---|--------------|-------------------------|---------------------------|----------------|---------------|----------------------|
| Lower costs for the patients (if the conventional modalities PAN and/or PA were preferred previously)                                 | 10 (15.9%)   | 0 (0%)                  | 1 (8.3%)                  | 0 (0%)         | 0 (0%)        | 0 (0%)               |
| Availability and ease of access of the radiographic modality (if the conventional modalities PAN and/or PA were preferred previously) | 15 (23.8%)   | 0 (0%)                  | 0 (0%)                    | 2 (13.3%)      | 0 (0%)        | 2 (12.5%)            |
| Radiation dose concerns of three-dimensional modalities (if the conventional modalities PAN and/or PA were preferred previously)      | 2 (3.2%)     | 2 (7.1%)                | 0 (0%)                    | 1 (6.7%)       | 1 (12.5%)     | 1 (6.25%)            |
| Broad coverage of the designated anatomical area (If PAN and/or CBCT were preferred previously)                                       | 29 (46%)     | 12 (42.9%)              | 7 (58.3%)                 | 7 (46.7%)      | 6 (75%)       | 8 (50%)              |
| Better dimensional accuracy (if three-dimensional modalities, e.g. CBCT, were selected previously)                                    | 37 (58.7%)   | 13 (46.4%)              | 10 (83.3%)                | 11 (73.3%)     | 7 (87.5%)     | 8 (50%)              |
| Three-dimensional modalities provide more anatomical information necessary for the success of the therapy                             | 41 (65.1%)   | 24 (85.7%)              | 10 (83.3%)                | 13 (86.7%)     | 6 (75%)       | 14 (87.5%)           |
| Only three-dimensional modalities (e.g. CBCT) if guided implant surgery is considered   | 11 (17.5%)   | 4 (14.3%)               | 1 (8.3%)                  | 5 (33.3%)      | 5 (62.5%)     | 2 (12.5%)            |
| Other reasons   | 3 (4.8%)     | 0 (0%)                  | 1 (8.3%)                  | 1 (6.7%)       | 0 (0%)        | 0 (0%)               |

- Multiple answers were allowed.

## CHAPTER 6 | DISCUSSION

Although the preferred radiographic modalities were not consistent for all the anatomic regions investigated, the panoramic radiograph combined with the CBCT was the most chosen modality during implant planning. During implant planning in all regions of the jaws, the range of selections that contain CBCT (either in combination with other modalities or as a single examination) was 75 - 100% with an average of 91%. This provides compelling evidence that the CBCT examination is very popular and preferable during implant treatment planning. Slight variations between the most selected radiographic examinations during the therapy were noted between different dental specialities, and in different anatomical regions and treatment phases. During the implant planning phase, the OMFS and periodontists preferred CBCT (as a single examination) predominantly in all the anatomical regions, while prosthodontists and registrars predominantly selected panoramic radiograph combined with CBCT examination. General practitioners most often selected PAN + CBCT and PA + CBCT (in one region), while OMFR selections were a combination of PAN+CBCT and CBCT (as a single examination).

During and directly after surgery, most participants chose periapical radiographs (PA) as a single examination. During the follow-up of asymptomatic patients, most preferred examinations were PA only (Periodontists, GP, registrars, and OMFR) and PAN only (Prosthodontists and OMFS). By contrast, during the follow-up of symptomatic patients, the prosthodontists, OMFS, OMFR, and registrars agreed on CBCT (only) as the examination of the choice, while most GPs preferred a combination of PA and CBCT examinations. Moreover, PA and CBCT volumes and CBCT (as single examination) were preferred by periodontists (39%, 39%, respectively) during the follow-up of symptomatic patients. The range of selections that contain CBCT (either in combination with other modalities or as a single examination) was 0 - 25% with an average of 8.85% during and after the surgery, 10.71% -31.25% during the follow-up of asymptomatic patients (average of 16.19%), and 60.31% - 87.5% range with an average of 74.43% for symptomatic ones.



Most participants (56%) believe that the follow-up frequency should be after six months, 12 months and annually for 10 years.

For implant planning, most participants (in all specialities) indicated that the 3D examinations provide extra anatomical details that are paramount for the success of the therapy, in addition to the better dimensional accuracy provided with these techniques. Broad radiographic coverage of a certain radiographic modality, providing a wide field of view, was also a non-negligible factor in the selection of the radiographic modality during the therapy. Cost factors and radiation dose concerns were the least to affect the examination selection according to the participants. During follow-up of symptomatic patients, 47% of participants indicated that even within the possible radiographic artefacts caused by the structure of the dental implant (i.e. beam hardening artefact), CBCT still can provide more information needed to optimally assess the occurred complication. Nevertheless, 26% of participants indicated the opposite, with superior diagnostic value of conventional modalities advocated in these instances.

Three studies conducted in India by Singh et al. (2019), Shewale et al. (2017), and Mall and Pritam (2017) surveying the radiographic trends during implant planning for 160, 175, and 176 participants, respectively. The three studies reported that the majority prescribe panoramic radiographs as a single examination due to factors related to availability and broad coverage. Also, Singh et al. (2019) and Mall and Pritam (2017) reported that 8% and 5.3% (respectively) of the specialists prescribe Computed Tomography examinations (CT) as single examinations.

A survey was conducted in Italy (Di Murro et al., 2020) to assess the prescription trends of practitioners during the follow-up phase. Five hundred and sixteen clinicians participated, and of them, 84% indicated the use of intraoral periapical radiographs, 8.8% preferred panoramic radiographs, and 6.9% preferred CBCT.

Surveys conducted in Brazil (Sakakura et al., 2003) and India (Ramakrishnan et al., 2014) and Libya (Majid et al., 2014), of 69, 300, and 80 practitioners, respectively, showed that the panoramic radiographs (as a single examination) were the most

preferred modality for the surveyed clinicians during implant assessment. The effectiveness of the cost and broad coverage were the main influencing factors mentioned (Majid et al., 2014; Sakakura et al., 2003). In Palestine (2017), a study reported that the majority of 114 dentists preferred to prescribe panoramic radiographs mainly due to availability factors (Rabi et al., 2017). In a 2017 study in Saudi Arabia, most of the 120 dentists interviewed preferred panoramic radiography during various dental implant phases due to cost-effectiveness and coverage of the area of interest. During the pre-operative phase, the study reported that the combination of PAN, PA., and CT was the largest selected option (20.2%) (Alnahwi et al., 2017). In Turkey (2011), 383 dentists were surveyed with 166 indicating variable CBCT experience. The study reported that implant planning was the most common reason for CBCT prescriptions (Dölekoğlu et al., 2011).

Inconsistent radiographic prescriptions were found at the international level, which, in certain instances, was found to be independent of the social wealth and “dental health” levels (Horner et al., 2015). Multiple elements impacted the radiographic prescription. These include the information and treatment patterns inherited from educators (in all dental educational levels), as well as the economic strain of the clinician that may prefer a certain type of radiography (e.g. CBCT) to increase the profit range of treatment. In addition, the limited training and knowledge on CBCT use and interpretation by some clinicians also play a role (Horner et al., 2015).

## CHAPTER 7 | CONCLUSION

Within the limitations of this study, the panoramic radiograph combined with CBCT were the preferred examinations during dental implant planning among most surveyed practitioners in South Africa. During and directly after the surgical placement of implants, the vast majority preferred intraoral periapical radiographs as single examinations. Intraoral periapical radiographs (as single examinations) were also preferred for the follow-up of asymptomatic patients, while CBCT (as a single examination) was preferred in symptomatic patients. The factor which most influenced the radiographic prescription was the superior anatomical information provided by three-dimensional modalities (e.g. CBCT), followed by better dimensional accuracy. The most preferred radiographic follow-up frequency was after 6 and 12 months and then every year for a 10-year period.


### Limitations

The pandemic novel coronavirus (in South Africa) limited the ability to conduct the survey physically in various other SA provinces (other than the Western Cape), and online channels were used instead. This influenced the motivation, time, and the ability of several clinicians to participate.

### Acknowledgements:

The researcher would like to acknowledge the following for their valuable assistance/contributions/collaboration:

- 1- Dr Suvir Singh and the South African Society of Maxillo-Facial and Oral Surgeons.
- 2- Marilize van der Lind, Manager of Events and Public Relations, South African Dental Association.
- 3- Dr Suzette Stander, Dr Anthea Jeftha, and The South African Society for Periodontology.
- 4- Talya van Straaten, Training and Education Manager, Straumann Group SA (Pty).



PART 4  
DIMENSIONAL ACCURACY OF VARIOUS  
RADIOGRAPHIC MODALITIES USED DURING  
IMPLANT THERAPY

**CONTENTS AT A GLANCE**

|  |
|--|
| Chapter 1   Introduction                               |
| Chapter 2   Literature review                          |
| 2.1 Linear measurements accuracy: CBCT                 |
| 2.2 Linear measurement accuracy: Panoramic radiographs |
| Chapter 3   Aims and objectives                        |
| Chapter 4   Materials and methods                      |
| 4.1 Study design                                       |
| 4.2 Methodology  |
| Chapter 5   Results                                    |
| Chapter 6   Discussion                                 |
| Chapter 7   Conclusion                                 |



UNIVERSITY of the  
WESTERN CAPE

**ABSTRACT**

**Aim:** To assess the clinical accuracy of measurements obtained from different radiographic modalities.

**Materials and Methods:** Physical and virtual linear distances in three dimensions, were assessed in ten anatomical regions on six dried, edentulous human skulls. Metallic balls were used as radiographic markers in three radiographic modalities: cone beam computed tomography (CBCT), panoramic (PAN), and periapical radiographs (PA). The angular distances along the curved arches of both jaws (between the upper metallic balls) were measured using cords. Statistical analysis of the mean differences between physical measurements and the tested radiographic modalities was done using a one-way ANOVA ( $p$ -value < 0.05). The intra-class correlation coefficient (ICC) was used to analyse the level of consistency of observers.

**Results:** The overall mean difference between physical and radiographic (CBCT, PAN and PA) measurements for all the studied dimensions showed statistical significance. CBCT revealed the least discrepancy, with an overall submillimetre underestimation in maxilla (M.D = -0.638 mm, SD = 0.203) and overestimation in the mandible (M.D = 0.326 mm, SD = 0.23). The panoramic measurements showed overestimation in both the maxilla (M.D = 2.229 mm, SD = 0.856) and mandible (M.D = 3.832 mm, SD = 1.272). Periapical radiographs showed overall underestimation (M.D = -3.707 mm, SD = 1.31) in the maxilla and overestimation (M.D = 1.849 mm, SD = 0.875) in mandible.

**Conclusion:** Measurements obtained from the CBCT were the most accurate (i.e. submillimetre overall accuracy) when compared with panoramic and periapical radiographs. Although panoramic and periapical studies showed individual accurate readings (submillimetre), their overall measurement differences indicate an inferior dimensional accuracy compared with CBCT. The author confirms the precision of the CBCT modality and recommends it for implant planning purposes.

**KEYWORDS:** measurement accuracy, CBCT accuracy, panoramic accuracy, linear measurements, angular measurements.

## LIST OF ABBREVIATIONS AND ACRONYMS

| Abbreviation        | Description   |
|---------------------|---|
| <b>A-segment</b>    | Anterior segment.   |
| <b>CT</b>           | Computed tomography.  |
| <b>CBCT</b>         | Cone Beam Computed Tomography.  |
| <b>DH</b>           | Horizontal distance.  |
| <b>DLA</b>          | Distance lower anterior.  |
| <b>DLP</b>          | Distance lower posterior.   |
| <b>DUA</b>          | Distance upper anterior.  |
| <b>DUP</b>          | Distance upper posterior.   |
| <b>DV</b>           | Vertical distance.  |
| <b>ICC</b>          | Intra-class correlation coefficient                                     |
| <b>LHS</b>          | Left-hand side  |
| <b>M.D</b>          | Mean measurement difference.  |
| <b>M/C- segment</b> | M: mental foramen in the mandible.<br>C: canine segment in the maxilla. |
| <b>P- segment</b>   | Posterior segment.  |
| <b>PA</b>           | Periapical radiograph.  |
| <b>PAN</b>          | Panoramic radiograph.   |
| <b>RHS</b>          | Right-hand side.  |
| <b>SA</b>           | South Africa.   |
| <b>SD</b>           | Standard deviation.   |
| <b>TBH</b>          | Tygerberg Hospital.   |

**CHAPTER 1 | INTRODUCTION**

Dental radiology remains a core component in the diagnosis and planning of several dental therapies. In recent years, the development and integration of affordable cone beam computed tomography (CBCT) into dental practice introduced a new dimension to the diagnostic capabilities of dentists (Bornstein et al., 2017). Besides offering multi-planar images that are reconstructed with highly reproducible dimensions (Moshfeghi et al., 2012; Stratemann et al., 2008; Luangchana et al., 2015), it allows a three-dimensional perspective to surgical planning and the use of computer-aided surgical procedures (Flügge et al., 2017).

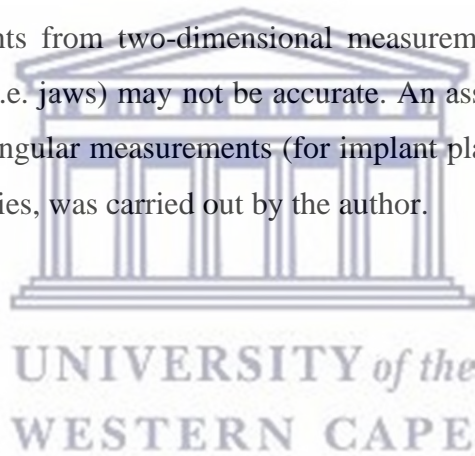
Despite all the advantages offered by three-dimensional modalities, conventional modalities like panoramic radiographs are still the most commonly used radiographs during various dental treatments – including dental implant therapy (Tyndall et al., 2012; Vazquez et al., 2008; Assaf & Gharbyah, 2014). Factors like simplicity, cost-effectiveness, lower radiation doses, and wide availability, contribute to this widespread of modality (Vazquez et al., 2008; Assaf & Gharbyah, 2014).

One of the most important requirements of a specific radiographic modality is the ability to provide accurate dimensions and reproducible measurements of the anatomical structures (Nagalaxmi et al., 2015; Özalp et al., 2018). Multiple reports have stated that during implant therapy, the tolerable measurement error obtained from different radiographic modalities need to be in the sub-millimetre range (Ganguly et al., 2011; Nikneshan et al., 2014).

To date, there is conflicting evidence concerning the optimum radiographic modality to use for implant planning purposes (particularly concerning the accuracy of measurements of various techniques) (Özalp et al., 2018). Some studies advocate the possibility of using 2-dimensional panoramic radiographs for implant planning (in non-complex cases) – particularly when used for vertical dimension assessment in the mandible (Assaf & Gharbyah, 2014; Özalp et al., 2018; Amarnath et al., 2015; Zarch

et al., 2011; Hu et al., 2012; Pertl et al., 2013; Kim et al., 2011; Vazquez et al., 2013). On the contrary, other authors (Bou Serhal et al., 2002; Correa et al., 2014; Bertram et al., 2018; Haghnegahdar & Bronoosh, 2013; Dudhia et al., 2011) found that using panoramic radiographs provided inaccurate dimensional readings which impose possible risks (especially if no magnification factors were considered).

The jaw arch architecture is curved, resembling a horse-shoe like conformation and does not lie in a single curved plane – but many. This must be considered during the planning of various procedures – especially with two-dimensional radiographic modalities. The practicality of applying angular measurements in certain anatomical regions is thus highlighted. The author hypothesises that the reproduction of virtually planned measurements from two-dimensional measurements into multidimensional physical structures (i.e. jaws) may not be accurate. An assessment of the accuracy of linear and physical angular measurements (for implant planning purposes) in various radiographic modalities, was carried out by the author.





**CHAPTER 2 | LITERATURE REVIEW****2.1 LINEAR MEASUREMENTS ACCURACY: CBCT**

The CBCT is considered one of the best currently available imaging modalities for the accurate assessment of the location, anatomy, and boundaries of the mental foramen (Aminoshariae et al., 2014).

The radiographic geometrical analysis was conducted on dry human skulls by Moshfeghi et al. (2012). The authors measured the physical distances between specific landmarks on the skulls using a calliper, and then compared them with measurements obtained from the corresponding CBCT volumes. They found that CBCT was very accurate (in the axial and coronal planes) and could precisely reproduce the linear measurements. The authors suggested the use of large voxel size during CBCT acquisitions, as the voxel size does not influence the measurement accuracy, while reducing the received radiation dose and accelerating the volume depiction time.

A study in Japan to compare the CBCT virtual measurements with their corresponding physical ones (Stratemann et al., 2008) found that CBCT showed highly accurate measurements when compared with the corresponding physical linear distances, revealing less than a 1% relative error.

Some studies reported slight underestimation in CBCT measurements compared with physical measurements (Baumgaertel et al., 2009; Luangchana et al., 2015). This underestimation from a clinical perspective is considered safer than overestimation in terms of the protection of vital anatomical structures during the surgical placement of implants in the vicinity (Luangchana et al., 2015).

The dimensions of 50 implant sites on CBCT and panoramic radiographs were investigated and compared with their corresponding physical measurements using six human dried skulls (Luangchana et al., 2015). The CBCT demonstrated accurate and reproducible vertical dimensions. The position of the head during radiography was found not to influence the accuracy of the measurements in CBCT. By contrast, in

panoramic examinations, accurate linear measurements were only obtained from correctly positioned patients.

## 2.2 LINEAR MEASUREMENT ACCURACY: PANORAMIC RADIOGRAPHS

The accuracy of measurements of the position of the mental foramen using panoramic radiography, and computed tomography (CT) was assessed (Bou Serhal et al., 2002). The corresponding physical measurements were compared in vivo during the implant surgery. Regarding the vertical dimension, the panoramic measurements were significantly different compared to perioperative measurements and computed tomography (CT). On the other hand, CT produced negligible submillimetre differences. An average of +0.6 mm (overestimation) of the distances in panoramic images and -0.3 mm in computed tomography mean errors were found. The negative mean error found in (CT) is argued to be due to the lack of magnification and superior control over the patient's position. The measurements' overestimation in panoramic radiographs suggested it was highly influenced by errors in the patient's positioning (Bou Serhal et al., 2002).

Zarch et al. (2011) assessed the vertical dimension measurements of the jaws on panoramic radiographs. Dried human skulls with metal markers were used and different head positions were assessed. The authors concluded that measurements done on panoramic radiographs were underestimated in 83% of the samples, with an only 8.5% overestimation, and 8.5% showed no difference. The study concluded that more reliable linear measurements were obtained in the posterior segment of the mandible.

In a relevant study (2012) done to assess the vertical and horizontal accuracy of the panoramic cross-sectional tomographs (Mehra & Pai, 2012), the measurements were found to be accurate in the horizontal and vertical dimensions. Hence, this can be considered a reliable modality for implant size estimation while considering the appropriate magnification factors.

In Austria (Pertl et al., 2013), a study investigated the accuracy of measurements obtained from panoramic, CT scan, and CBCT radiographs. The gold standard was physical anatomical measurements done on 10 human heads (cadaver). An inaccuracy of panoramic radiographs concerning the assessment of vertical distances (especially in the anterior regions compared to the posterior regions of the mandible) was reported. The authors also noted the accuracy of CT and CBCT measurements. The study confirmed the usefulness of using steel balls markers for the calibration of panoramic measurements.

Assessment of the accuracy of the vertical measurements in the posterior mandible regions using digital panoramic radiographs was done by Assaf and Gharbyah (2014). The study indicated a reliable vertical dimension assessment in the posterior mandibular segment, considering that the x-ray unit is calibrated and the manufacturer's software is used.

Investigation of the panoramic and CBCT accuracy of vertical and horizontal dimensions was conducted by Tang et al. (2017). Although there were inconsistent magnification rates on panoramic radiographs, the CBCT and panoramic measurements were significantly correlated.

## CHAPTER 3 | AIMS AND OBJECTIVES

### 3.1 AIM

To assess the clinical accuracy of measurements obtained from different radiographic modalities used for dental implant therapy.

### 3.2 OBJECTIVES

- 1- To measure the physical linear distances (width, length, and height) in-between designated reference points in the maxilla and mandible.
- 2- To measure the corresponding virtual distances on CBCT, periapical, and panoramic radiographs.
- 3- To compare each radiographic modality with its corresponding physical measurements.
- 4- To compare the accuracy of measurements obtained from three radiographic modalities.
- 5- To compare the physical linear and angular distances.

### 3.3 RATIONALE

- 1- As the measurement accuracy is an important clinical factor influencing the choice of a certain radiographic modality, the assessment of the dimensional accuracy of the x-ray units (at Tygerberg Hospital) becomes vital.
- 2- To provide evidence-based information on the dimensional accuracy of various radiographic techniques and machines.

## CHAPTER 4 | MATERIALS AND METHODS

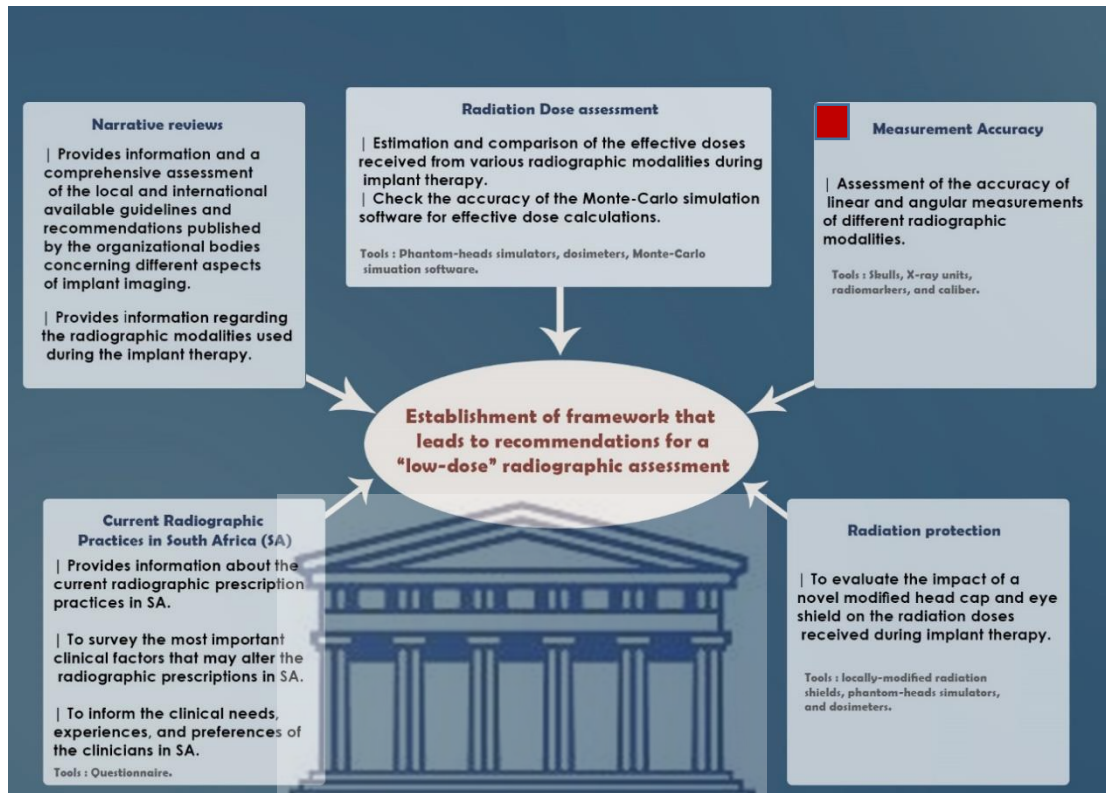


**Figure 4-1. Diagrammatic representation of the main research project. The current sub-study is highlighted.**

## 4.1 STUDY DESIGN

This study is experimental *in vitro* study.

## 4.2 METHODOLOGY

|              |  |
|--------------|--|
| <b>Tools</b> | <ul style="list-style-type: none"> <li>▪ Edentulous dried skull/s.</li> <li>▪ Panoramic x-ray unit (Sirona® Orthophos® XG3).</li> <li>▪ CBCT unit (NewTom® VGi).</li> <li>▪ Periapical radiographs (PSP: phosphor storage plates).</li> <li>▪ Digital calliper.</li> <li>▪ Radio-markers: (4.5 mm ball bearings).</li> </ul> |
|--------------|--|

---

#### 4.2.1 OVERVIEW

Six dried human skulls (gender and ethnicity neglected) were collected from the Division of Clinical Anatomy, Faculty of Medicine, Stellenbosch University (Cape Town, South Africa). The skulls were fully edentulous (with evident alveolar bone), adult-size, and with the calvarium cut off. Metallic bearing balls of known diameter (4.5 mm) were fixed directly on the mandibular and maxillary bone surfaces using a rigid, sticky wax. Five regions (segments) in each jaw were selected: A-segment (anterior), M/C- segment (M: mental foramen in the mandible and C: canine segment in the maxilla), and P- segment (posterior). In the mandible, each segment has three metallic ball markers placed in a triangular pattern (Y-ball- placed on the top of the alveolar ridge, and two parallel balls with one on the buccal (X-ball) and the other on the lingual/palatal surfaces (Z-ball)). In the maxilla, only two metallic balls (X and Y) were placed. X, Y, and Z balls were aligned on the same coronal (horizontal) level with the X and Z balls aligned at the same axial (vertical) level. The vertical distances (DV) between X and Y balls, as well as the horizontal distance (DH) between X and Z balls, were measured physically and compared with the corresponding virtual radiographic measurements. Additionally, alveolar arc lengths between Y balls (namely DLA: Distance lower anterior, DLP: Distance lower posterior, DUP: Distance upper posterior, and DUA: Distance upper anterior) in both arches were also measured (Figure 4-2).

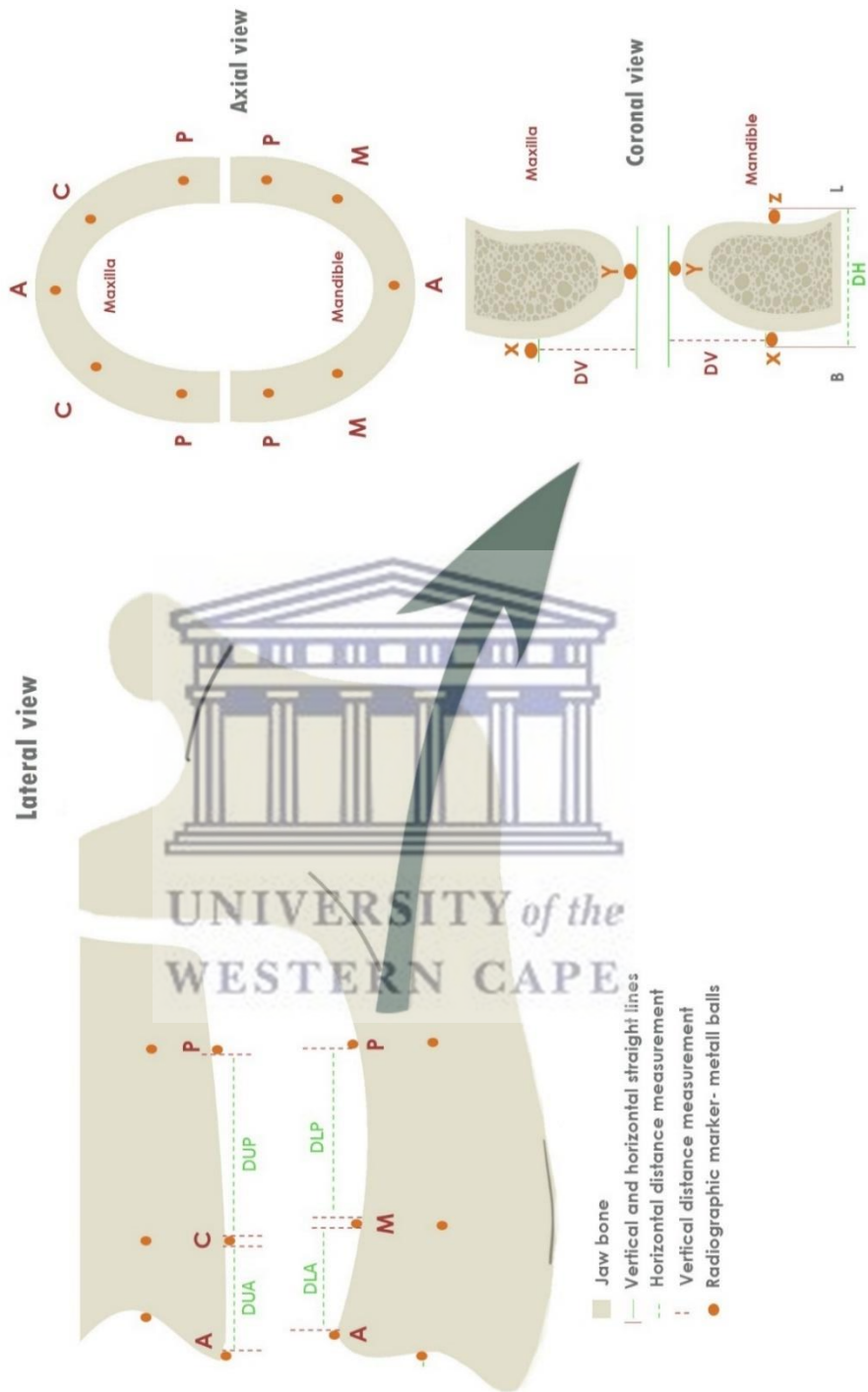


Figure 4-2. Diagram showing the reference points and distances measured.

---

#### 4.2.2 PHYSICAL MEASUREMENTS:

The physical measurements were conducted using a digital calliper (Mastercraft<sup>®</sup>, South Africa) with the following specifications: measure range 0-150 mm, resolution: 0,01 mm, accuracy: 0,03 mm, and repeatability: 0,01 mm. The calliper readings were reconfirmed manually using a ruler, prior to the analysis of every skull.

For panoramic and intraoral acquisitions, the mandibles were placed on a uniform table (rectangular wood 15 × 15 cm, fixed on a movable tripod). The mandibles were supported with uniformly-sized sponges placed under the mandibular angles (bilaterally), simulating an ideal radiographic position. The uniform level between the left and right sides of the mandible was ensured for each mandible using a combination square with a spirit level (ROSS<sup>®</sup>, Mitco<sup>®</sup>, China). During the analysis, a spirit level was placed on the uppermost surface of each Y- ball, establishing a levelled upper limit (tangent) for vertical measurements. The vertical distances (DV) between the level and the uppermost tangent of X balls were measured using the digital calliper (the calliper's inside jaws were used). The horizontal distances (DH) between the outermost borders of Y and Z balls were measured directly using the digital calliper's outside jaws.

The maxilla (with the attached skull base) was mounted upside down (to provide parallelism of Frankfort line with the floor, and was checked each time), and the distances were measured the same way as in the mandibles.

The alveolar arc lengths between segments in each jaw (i.e. A, C/M, and P) were measured (i.e. DLA, DLP, DUP, and DUA) between the outmost points on the mesial and distal surfaces of the balls and following the curvature of the arches by the digital calliper (i.e. shortest linear distance). For angular arc lengths measurement, thin nylon cords were fixed directly on the upper surface of the ridge between the Y balls (conforming to the anatomy of the bone) and then measured by the calliper's ruler. The resultant physical linear and angular alveolar arc lengths were then compared.



---

### 4.2.3 CONE BEAM COMPUTED TOMOGRAPHY (CBCT)

“Full mode” scans were done using the NewTom<sup>®</sup> VGi CBCT unit (QRLS, Verona, Italy). The ideal radiographic position was ensured with the aid of the unit’s positioning laser beams (Figure 4-3, A).

The virtual measurements were carried out using the manufacturer’s software (NNT<sup>®</sup>, 2.6.7). The cross-sectional slices were generated in both sagittal and coronal directions for each segment, and following the curvature. The slice’s thickness was 5 mm (and 0.3-0.5 mm each step) to ensure the depiction of the entire dimensions of the radiographic markers on the slices. Coronal (or oblique coronal) cross-sectional slices were used to measure DV and DH distances. The DV was attained by measuring the distance between two linear horizontal tangential lines that were drawn virtually on the X & Y balls’ uppermost surfaces (Figure 4-4, A). The horizontal distances (DH) were measured between two straight vertical tangential lines that were drawn virtually on the X (lateral surface) and Z balls (medial surface). The distances DLA, DLP, DUP, and DUA, were measured by generating cross-sectional images between the Y-balls on the ridge (Figure 4-4, B). Table 4.1 shows the technical specifications with the distances measured.

---

### 4.2.4 INTRAORAL RADIOGRAPHS’ MEASUREMENT\*

The periapical radiographs (PA) were taken using the parallel technique on the mounted skulls (maxilla and mandible) and with the aid of a film-holder to expose each jaw segment (Figure 4-3, C). Phosphor plates (PSPs) were used and scanned using a SOREDEX<sup>®</sup> DIGORA<sup>™</sup> Optime (Kavo/Soredex<sup>®</sup>, Helsinki, Finland) scanner (Table 4.1). The parallelism between the phosphor plates and the ridge axis was checked before each exposure, to ensure an ideal acquisition setting. The corresponding virtual measurements were carried out virtually using the manufacturer’s software (Digora<sup>®</sup>, version 36.6) (Figure 4-4, D).

#### 4.2.5 PANORAMIC RADIOGRAPHS (PAN)\*

The panoramic machine Sirona® Orthophos® XG 3 (Dentsply Sirona, Bernsheim, Germany) was used (Figure 4-3, B). The skulls were mounted with compliance to the ideal radiographic position (the midsagittal plane is centred, and a virtual line from the tragus (ear) to the eye canthus is parallel with the floor). The corresponding virtual measurements were carried out virtually using the manufacturer's software (Sirona®, version 36.6) (Figure 4-4, C). Table 4.1 shows the technical specifications with the distances measured.

*\*The Z metallic balls were removed from the lingual surfaces during the intraoral and panoramic radiographic acquisitions.*



**Figure 4-3. CBCT (A), panoramic (B), and intraoral (C) machines.**

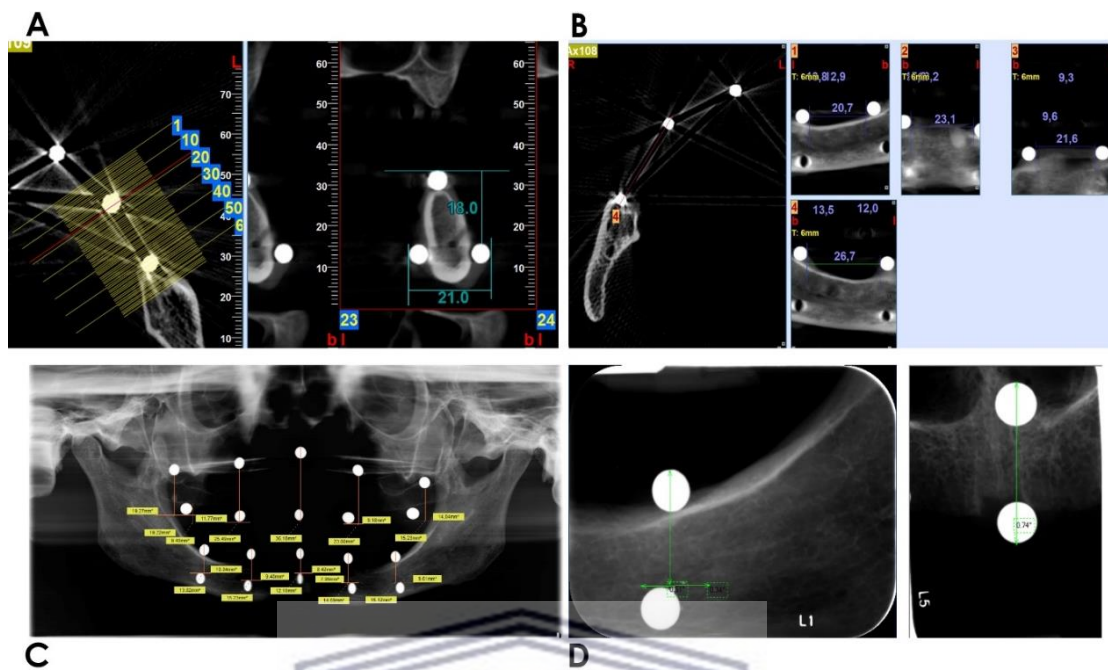


**Figure 4-4. Virtual measurements done on CBCT volumes (A&B), Panoramic (C), and Periapical (D) radiographs.**



**Table 4.1. Exposure parameters, x-ray unit's specification, and distances measured.**

|                      | Manufacturer   | Exposure Parameters                       | Specifications   | Distances measured                                  |
|----------------------|--|---|--|---|
| Periapical           | X-mind Intraoral x-ray.  | 70 kVp                                    | Pixel Size (selectable):30 $\mu\text{m}$ (Super Resolution) and 60 $\mu\text{m}$ (High Resolution), Resolution: 17 lp/mm.  | <b>Upper and lower jaw segments</b>                 |
|                      | SOREDEX <sup>®</sup> DIGORA <sup>™</sup> Optime (Phosphor plates using parallel technique) | 8 mA<br>0.25 S                            |  |   |
|                      | Desktop monitor  |   |  | DV  |
| Panoramic radiograph | Sirona <sup>®</sup> Orthophos XG3  | 62-64 kVp<br>6-8 8 mA                     | X-ray generator: 60-90 kV; 3-16 mA, Focal spot size: 0.5 mm, Sensor Digital CCD Sensor, Pixel size: 27 $\mu\text{m}$ , Focus-sensor distance: 530 mm   | <b>Panoramic view (Upper and lower jaw points)</b>  |
|                      | Desktop monitor  |   |  |   |
| CBCT                 | Newton <sup>®</sup> VGi  | “Full scan” mode<br>90-110 kVp<br>1-20 mA | X-ray Source :110 kV; 1-20 mA (pulsed mode), Focal spot: 0,3 mm, scan time: 18, X-ray Emission Time: 3.6s, Voxel size: 0.3 mm <sup>3</sup> , image pixels: 512x512 Pixels, Pixel depth: 16 bits. | <b>Cross-sectional (Upper and lower jaw points)</b> |
|                      | Barco <sup>®</sup> , Eonis 22" medical monitor.  |   |  |   |
|                      |  |   |  | DV<br>DH<br>DLA,<br>DLP,<br>DUP, and<br>DUA         |

### 4.3 DATA AND STATISTICAL ANALYSIS

A one-way ANOVA test was used to determine if there was a statistically significant difference between the physical and radiographic (CBCT, PAN, and PA) distances. Pairwise comparisons with Bonferroni correction were used to determine how large those differences were and also to determine where those differences were. If there were no statistically significant differences between the different modalities, then the two differences were deemed similar, as the  $p$ -value was greater than 0.05 and the confidence interval included zero. If the confidence interval included zero, this implied that at some stage the difference was zero and thus there was no difference in the estimation of the distance of the points between the physical point or any of the three modalities (CBCT, PAN, or PA). The mean measurement difference (M.D) was calculated in millimetres and using the following equation:

$$\text{M.D} = \text{mean radiographic measurements} - \text{mean physical measurements}$$

The intra-class correlation coefficient (ICC) was used to analyse the level of consistency of the results between the two observers. All the physical measurements were repeated a week after the primary analysis (except for the angular measurements) by the first and second observers. The first observer repeated all the measurements in all the radiographic modalities a week after the primary analysis. The second observer was requested (by the statistician) to repeat the measurements for only three skulls in each radiographic modality.

## CHAPTER 5 | RESULTS

The overall mean differences between physical measurements and the CBCT, PAN, and PA examinations for all the studied dimensions in maxilla and mandible, were statistically significant (Table 4.2). Nevertheless, the CBCT showed the least discrepancy with overall submillimetre underestimation in the maxilla (M.D = -0.638 mm, SD = 0.203) and submillimetre overestimation in the mandible (M.D = 0.326 mm, SD = 0.23). The panoramic measurements showed an overestimation in both the maxilla (M.D = 2.229 mm, SD = 0.856) and mandible (M.D = 3.832 mm, SD = 1.272). Periapical radiographs showed an overall underestimation (M.D = -3.707 mm, SD = 1.31) in the maxilla and overestimation (M.D = 1.849 mm, SD = 0.875) in mandible.

Individual anatomical segments (points) analysis showed no statistically significant difference using pairwise comparisons (with Bonferroni correction) between the studied radiographic modalities (i.e. CBCT vs physical readings, PAN vs physical readings, and PA vs physical readings). However, there was a statistically significant difference between the periapical and physical measurements in the distance vertical (DV) of point P in the right maxilla. The lack of statistical significance indicates similarity, and thus accuracy, between the modalities CBCT, PAN, and PA compared with the physical measurements.

In all 23 points (in maxilla and mandible), the smallest absolute difference was always between CBCT scans and the physical measurement, with the maximum absolute mean difference (M.D) being 2.047 mm (SD = 3.036) for the DV of point A (centre) of the mandible. The smallest absolute mean difference (M.D) between CBCT and the physical measurement was found in the distance horizontal (DH) of point M the right mandible, 0.127 mm (SD = 0.536). The statistical analysis is further demonstrated in Table 4.2 and Table 4.3.

*To provide clarity in the interpretation of Table 4.2, a reference to Figure 4-2 is advised.*

**Table 4.2. Statistical overview showing the mean and standard deviation (SD) of the measured distances in various modalities. The mean difference (mm) between the radiographic modality and the corresponding physical measurements with the standard deviation (SD), and the P-value is also tabulated.**

|                |          | Mean value (SD) |                           | CBCT vs. Physical        | Pan vs. Physical         | PA vs. Physical |        |         |        |
|----------------|----------|-----------------|---------------------------|--------------------------|--------------------------|-----------------|--------|---------|--------|
|                |          |                 |                           |                          |                          |                 |        |         |        |
| Mandible       | RHS      | Point p         | Physical                  | 15.02 (3.4)              | M.D                      | 1.18            | 4.87   | 2.252   |        |
|                |          |                 | CBCT                      | 16.2 (3.1)               | SD                       | -2.02           | -2.02  | 2.02    |        |
|                |          |                 | PAN                       | 19.89 (3.9)              | P.V                      | 1               | 0.154  | 1       |        |
|                |          |                 | PA                        | 17.27 (3.6)              |                          |                 |        |         |        |
|                |          | DH              | Physical                  | 18.59 (1.9)              | M.D                      | 0.362           |        |         |        |
|                |          |                 | CBCT                      | 18.95 (2.1)              | SD                       | -1.17           |        |         |        |
|                |          |                 |                           |                          | P.V                      | 0.764           |        |         |        |
|                |          | DLP             | Physical                  | 23.19 (3.9)              | M.D                      | -0.738          | 1.63   |         |        |
|                |          |                 | CBCT                      | 22.45 (3.8)              | SD                       | -2.21           | -2.21  |         |        |
|                |          |                 | PAN                       | 24.82 (3.7)              | P.V                      | 1               | 1      |         |        |
|                |          | Center          | Point M/C                 | Physical                 | 17.22 (4.2)              | M.D             | 1.582  | 6.692   | 2      |
|                |          |                 |                           | CBCT                     | 18.8 (4.4)               | SD              | -2.64  | -2.64   | -2.64  |
|                | PAN      |                 |                           | 23.91 (5.3)              | P.V                      | 1               | 0.118  | 1       |        |
|                | PA       |                 |                           | 19.22 (4.2)              |                          |                 |        |         |        |
|                | DH       |                 | Physical                  | 19.02 (0.9)              | M.D                      | 0.127           |        |         |        |
|                |          |                 | CBCT                      | 19.15 (0.9)              | SD                       | -0.538          |        |         |        |
|                |          |                 |                           |                          | P.V                      | 0.819           |        |         |        |
|                | DLA      |                 | Physical                  | 18.63 (3.8)              | M.D                      | -0.927          | 0.907  |         |        |
|                |          |                 | CBCT                      | 17.7 (3.8)               | SD                       | -2.3            | -2.3   |         |        |
|                |          |                 | PAN                       | 19.53 (4.4)              | P.V                      | 1               | 1      |         |        |
|                | Point A  |                 | DV                        | Physical                 | 16.05 (4.41)             | M.D             | 2.047  | 7.56    | 2.15   |
|                |          |                 |                           | CBCT                     | 18.1 (5.50)              | SD              | -3.036 | -3.036  | -3.036 |
|                |          | PAN             |                           | 23.61 (6.5)              | P.V                      | 1               | 0.13   | 1       |        |
|                |          | PA              |                           | 18.2 (4.27)              |                          |                 |        |         |        |
|                | DH       | Physical        | 21.44 (1.6)               | M.D                      | 0.31                     |                 |        |         |        |
|                |          | CBCT            | 21.75 (1.5)               | SD                       | -0.91                    |                 |        |         |        |
|                |          |                 |                           | P.V                      | 0.74                     |                 |        |         |        |
|                | LHS      | Point M/C       | Physical                  | 15.5 (3.4)               | M.D                      | 0.7             | 5.238  | 1.56    |        |
| CBCT           |          |                 | 16.2 (3.6)                | SD                       | -2.29                    | -2.29           | -2.29  |         |        |
| PAN            |          |                 | 20.74 (4.8)               | P.V                      | 1                        | 0.199           | 1      |         |        |
| PA             |          |                 | 17.06 (3.9)               |                          |                          |                 |        |         |        |
| DH             |          | Physical        | 19.46 (0.7)               | M.D                      | 0.242                    |                 |        |         |        |
|                |          | CBCT            | 19.7 (0.9)                | SD                       | -0.46                    |                 |        |         |        |
|                |          |                 |                           | P.V                      | 0.611                    |                 |        |         |        |
| DLA            |          | Physical        | 17.05 (4.2)               | M.D                      | -0.698                   | 1.31            |        |         |        |
|                |          | CBCT            | 16.35 (4.0)               | SD                       | -2.31                    | -2.31           |        |         |        |
|                |          | PAN             | 18.36 (3.8)               | P.V                      | 1                        | 1               |        |         |        |
| Point P        |          | DV              | Physical                  | 13.41 (2.92)             | M.D                      | 0.49            | 3.94   | 1.28    |        |
|                |          |                 | CBCT                      | 13.9 (2.68)              | SD                       | -1.83           | -1.83  | -1.83   |        |
|                | PAN      |                 | 17.35 (3.52)              | P.V                      | 1                        | 0.259           | 1      |         |        |
|                | PA       |                 | 14.68 (3.435)             |                          |                          |                 |        |         |        |
| DH             | Physical | 19.56 (2.2)     | M.D                       | 0.34                     |                          |                 |        |         |        |
|                | CBCT     | 19.9 (2.2)      | SD                        | -1.27                    |                          |                 |        |         |        |
|                |          |                 | P.V                       | 0.795                    |                          |                 |        |         |        |
| DLP            | Physical | 21.5 (5.1)      | M.D                       | -0.452                   | 2.33                     |                 |        |         |        |
|                | CBCT     | 21.1 (5.2)      | SD                        | -3.25                    | -3.25                    |                 |        |         |        |
|                | PAN      | 23.83 (6.5)     | P.V                       | 1                        | 1                        |                 |        |         |        |
| <b>Overall</b> |          |                 | <b>0.326*</b><br>(0.23)   | <b>3.832*</b><br>(1.272) | <b>1.849*</b><br>(0.875) |                 |        |         |        |
| Maxilla        | RHS      | Point p         | Physical                  | 17.67 (1.6)              | M.D                      | -0.671          | 1.155  | -3.786  |        |
|                |          |                 | CBCT                      | 17 (2.0)                 | SD                       | 1.07            | 1.07   | 1.07    |        |
|                |          |                 | PAN                       | 18.83 (2.4)              | P.V                      | 1               | 1      | 0.012*  |        |
|                |          |                 | PA                        | 13.89 (1.2)              |                          |                 |        |         |        |
|                |          | DUP             | Physical                  | 22.29 (3.3)              | M.D                      | .698            | 1.55   |         |        |
|                |          |                 | CBCT                      | 21.6 (3.2)               | SD                       | 1.99            | 1.99   |         |        |
|                |          |                 | PAN                       | 23.85 (3.8)              | P.V                      | 1               | 1      |         |        |
|                |          | Point M/C       | DV                        | Physical                 | 24.25 (4.1)              | M.D             | -0.15  | 3.97    | -4.57  |
|                |          |                 |                           | CBCT                     | 24.1 (3.9)               | SD              | 2.41   | 2.41    | 2.41   |
|                |          |                 |                           | PAN                      | 28.22 (4.8)              | P.V             | 1      | 0.689   | 0.436  |
|                |          |                 |                           | PA                       | 19.69 (3.8)              |                 |        |         |        |
|                |          | DUA             | Physical                  | 16.68 (3.9)              | M.D                      | -0.73           | 1.32   |         |        |
|                | CBCT     |                 | 15.95 (3.9)               | SD                       | 2.39                     | 2.39            |        |         |        |
|                | PAN      |                 | 18 (4.6)                  | P.V                      | 1                        | 1               |        |         |        |
|                | Point A  | DV              | Physical                  | 24.92 (2.5)              | M.D                      | 0.227           | 6.055  | -0.8357 |        |
|                |          |                 | CBCT                      | 25.15 (2.6)              | SD                       | 2.07            | 2.07   | 2.07    |        |
|                |          |                 | PAN                       | 30.97 (4.1)              | P.V                      | 1               | 0.05   | 1       |        |
|                |          |                 | PA                        | 24.09 (4.7)              |                          |                 |        |         |        |
|                | LHS      | Point M/C       | Physical                  | 21.34 (2.4)              | M.D                      | -0.293          | 3.801  | -3.775  |        |
|                |          |                 | CBCT                      | 21.05 (2.5)              | SD                       | 1.56            | 1.56   | 1.56    |        |
|                |          |                 | PAN                       | 25.15 (3.1)              | P.V                      | 1               | 0.147  | 0.153   |        |
|                |          |                 | PA                        | 17.57 (2.8)              |                          |                 |        |         |        |
|                |          | DUA             | Physical                  | 16.59 (3.9)              | M.D                      | -0.988          | 1.465  |         |        |
|                |          |                 | CBCT                      | 15.6 (3.7)               | SD                       | 2.313           | 2.313  |         |        |
|                |          |                 | PAN                       | 18.05 (4.3)              | P.V                      | 1               | 1      |         |        |
|                |          | Point P         | DV                        | Physical                 | 15.36 (3.2)              | M.D             | -1.807 | -0.777  | -5.578 |
|                |          |                 |                           | CBCT                     | 13.55 (3.1)              | SD              | 2.08   | 2.08    | 2.08   |
|                |          |                 |                           | PAN                      | 14.58 (3.7)              | P.V             | 1      | 1       | 0.086  |
| PA             |          |                 |                           | 9.78 (4.3)               |                          |                 |        |         |        |
| DUP            |          | Physical        | 21.73 (2.9)               | M.D                      | -0.633                   | 1.522           |        |         |        |
|                | CBCT     | 21.1 (2.7)      | SD                        | 1.895                    | 1.895                    |                 |        |         |        |
|                | PAN      | 23.26 (4.0)     | P.V                       | 1                        | 1                        |                 |        |         |        |
| <b>Overall</b> |          |                 | <b>-0.638*</b><br>(0.203) | <b>2.229*</b><br>(0.856) | <b>-3.707*</b><br>(1.31) |                 |        |         |        |

\*Statistically significant difference,  $p < 0.05$ , Negative values indicate underestimation while positive ones indicate overestimation

M.D: measurement discrepancy, SD: standard deviation, P.V:p-value ,RHS:right hand side, LHS: left hand side

**Table 4.3. An overview of the number of readings that showed differences attained by each radiographic modality, in both jaws.**

| Comparison  | PA (10 readings)        | Pan (18 readings)     | CBCT (23 readings)       |
|---|-------------------------|-----------------------|--------------------------|
| <b>Discrepancy over 1 mm limit</b><br>(Over or underestimation) | 9/10                    | 16/18                 | 4/23                     |
| <b>Detailed description of data</b>                             |                         |                       |                          |
| <b>Overestimation (&gt; 0 mm)</b>                               | <b>5/10</b>             | <b>17/18</b>          | <b>11/23</b>             |
| <b>Maxilla</b>  | 0                       | 8   R* [1.15-6.05 mm] | 1   M* (0.22 mm)         |
| <b>Mandible</b>   | 5   R* [1.27-2.52 mm]   | 9   R* [0.9-7.56 mm]  | 10   R* [0.31-2.04 mm]   |
| <b>Underestimation (&lt; 0 mm)</b>                              | <b>5/10</b>             | <b>1/18</b>           | <b>12/23</b>             |
| <b>Maxilla</b>  | 5   R* [-0.83 -5.57 mm] | 1   M* (-0.77)        | 8   R* [-0.15-(-1.8) mm] |
| <b>Mandible</b>   | 0                       | 0                     | 4   R* [-0.4-(-0.92) mm] |

R\*: Range, M\*: Maximum

The difference between the physical linear and angular measurements of the distances (alveolar arc lengths) DUP/DLP, DUA/DLA was also compared and documented in Table 4.4.

Thirty-six readings were obtained. Twenty-one readings of those showed over 1 mm difference between linear measurements and angular measurements (whether over or underestimating). Nevertheless, all the 21 readings showed negative values, which means that the angular measurements were more than the values of the linear ones. In other terms, the linear measurements underestimated angular distance. The other 15 readings were a combination of positive and negative differences – but all indicating submillimetre discrepancy.



**Table 4.4. Differences between physical linear and angular distances (linear – angular, mm).**

| Skull #   |          | Right side |         | Left side |         |
|---|----------|------------|---------|-----------|---------|
|   |          | DUP/DLP    | DUA/DLA | DUP/DLP   | DUA/DLA |
| 1   | Maxilla  | 0.36       | -5.04   | 0.95      | -2.42   |
|   | Mandible | 0.78       | -3.48   | -1.58     | -3.88   |
| 2   | Mandible | 0.25       | 0.84    | 0.04      | -1.81   |
| 3   | Mandible | -0.78      | -3.3    | -3.08     | -1.65   |
| 4   | Maxilla  | -1.58      | -0.44   | -3.09     | 0.9     |
|   | Mandible | -4.03      | 0.54    | -0.33     | -1.08   |
| 5   | Mandible | -2.61      | -2.55   | -0.05     | -4.64   |
| 6   | Maxilla  | 0.34       | -4.9    | -0.8      | -6.41   |
|   | Mandible | -4.01      | -2.8    | -2.08     | -0.24   |
| <ul style="list-style-type: none"> <li>- Positive values indicate that the linear measurements were bigger than angular ones and vice versa.</li> <li>- Values in color: &gt;1 or -1 mm difference (21 readings/36)</li> <li>- Values in Black: -1&gt;0&lt;1 difference (15 readings/36)</li> </ul> |          |            |         |           |         |

The intraclass correlation coefficient (ICC) test was used to assess inter- and intra-examiner reliability (Table 4.5). All the readings showed excellent inter-examiner reliability except the left side horizontal distance (DH) in M/C point, which showed poor reliability during CBCT assessment. Likewise, all the readings showed excellent intra-examiners reliability except the right-side P point (DUP/DLP), which showed moderate reliability during PAN measurements, and the left side DH point during physical and CBCT measurements, which showed good reliability.

Table 4.5. Inter-examiner and intra-examiner intraclass correlation coefficient.

|          | RIGHT SIDE |       |             |           |       |             | CENTER  |       | LEFT SIDE |       |             |         |       |             |       |
|----------|------------|-------|-------------|-----------|-------|-------------|---------|-------|-----------|-------|-------------|---------|-------|-------------|-------|
|          | POINT P    |       |             | Point M/C |       |             | POINT A |       | Point M/C |       |             | POINT P |       |             |       |
|          | DV         | DH    | DUP/<br>DLP | DV        | DH    | DUP/<br>DLP | DV      | DH    | DV        | DH    | DUP/<br>DLP | DV      | DH    | DUP/<br>DLP |       |
| Physical | A          | 0.937 | 0.992       | 0.968     | 0.996 | 0.92        | 0.988   | 0.992 | 0.91      | 0.988 | 0.81        | 0.994   | 0.926 | 0.983       | 0.994 |
|          | B          | 0.923 | 0.996       | 0.992     | 0.993 | 0.926       | 0.993   | 0.979 | 0.994     | 0.993 | 0.989       | 0.996   | 0.965 | 0.995       | 0.985 |
| CBCT     | A          | 0.994 | 0.988       | 0.993     | 0.997 | 0.917       | 0.997   | 0.998 | 0.977     | 0.994 | 0.778       | 0.998   | 0.993 | 0.99        | 0.996 |
|          | B          | 0.994 | 0.988       | 0.992     | 0.997 | 0.918       | 0.997   | 0.997 | 0.977     | 0.998 | 0.263       | 0.995   | 0.992 | 0.968       | 0.996 |
| PAN      | A          | 0.995 |             | 0.595     | 0.997 |             | 0.999   | 0.999 |           | 0.996 |             | 0.999   | 0.996 |             | 0.999 |
|          | B          | 0.987 |             | 0.998     | 0.996 |             | 0.997   | 0.998 |           | 0.992 |             | 0.997   | 0.999 |             | 0.999 |
| PA       | A          | 0.997 |             |           | 0.921 |             |         | 0.96  |           | 0.998 |             |         | 0.997 |             |       |
|          | B          | 0.994 |             |           | 0.996 |             |         | 0.998 |           | 0.999 |             |         | 0.998 |             |       |

A: Intra-examiner, B: Inter-examiner  
 | Values less than 0.5 are indicative of poor reliability (red), values between 0.5 and 0.75 indicate moderate reliability (green), values between 0.75 and 0.9 indicate good reliability, and values greater than 0.90 indicate excellent reliability.

## CHAPTER 6 | DISCUSSION

Although the overall statistical analysis shows statistical significance in the measurement differences for all modalities, only panoramic and periapical measurements (and not CBCT) are clinically significant. Variable ranges of measurement discrepancy were found in the different individual points/segments assessed in the maxilla and mandible.

The ability to get reliable data was noted to be dependent on the position of the skull during panoramic and periapical acquisitions. The current assessments were conducted with ideal radiographic positions and within simulated laboratory settings (as applicable) – which may not be the case in day-to-day clinical setting.

In a systematic review (Fokas et al., 2018) reported that several authors (Torres et al., 2012; Kobayashi et al., 2004) consider an error of less than one millimetre obtained from the radiographic analysis of CBCT volumes to be clinically negligible. The author of the current study acknowledges the negligible clinical relevance of these errors, but, surmises that it is reliant on the clinical context in which these data will be utilized. For instance, it may be influenced by the intended procedure, the vicinity of vital structures, and the quantity of remaining bone structure.

### ***Cone beam computed tomography***

Many reports confirmed the accuracy of measurements obtained from CBCT volumes conducted using different methodologies (e.g. in-vivo, ex-vivo, ridge mapping, sectioning) (Moshfeghi et al., 2012; Stratemann et al., 2008; Luangchana et al., 2015; Fokas et al., 2018; Ganguly et al., 2016; De Andrade et al., 2016).

Although indicating overall accuracy, some studies reported both slight underestimation (Sheikhi et al., 2015; Luangchana et al., 2015; Baumgaertel et al., 2009; Lascala et al., 2004) and overestimation (Al-Ekrish & Ekram, 2011; Luk et al., 2011; Kobayashi et al., 2004) in CBCT measurements compared to physical measurements – with most showing submillimetre error ranges (Fokas et al., 2018).

Hence, a safety distance of 2 mm is still recommended while planning procedures on CBCT (Fokas et al., 2018). Measurement underestimation from a clinical perspective is considered to be safer than overestimation in terms of safe-guarding vital structures during dental treatments in their vicinity (Luangchana et al., 2015).

In our study, we report that the overall mean distance differences for all the measured dimensions were -0.638 and 0.326 for the maxilla and mandible, respectively. Although these ranges are submillimetre and indicate overall superior accuracy, CBCT exceeded the submillimetre discrepancy range during the vertical distance (DV) in three mandibular sites [1.18 mm - 2.04 mm (overestimation)] and one in the maxilla (-1.8 mm (underestimation)).

The interradicular space was found to be underestimated on panoramic radiographs compared to CBCT (Tepedino et al., 2018). According to Beshtawi et al. (2020), non-statistically significant differences were found in the vertical and horizontal dimensions of the mental foramen position compared between digital and CBCT reformatted panoramic views. Nonetheless, significant discrepancies were found when comparing the vertical dimensions between the panoramic views (digital and CBCT) and the corresponding CBCT coronal views.

#### ***Factors affecting measurement accuracy of CBCT volumes***

##### ***- Metallic artefacts***

In the current study, the radiographic artefacts from the radio-markers (metallic balls) were minimal and did not affect the accuracy of the measurements; particularly that the references were the balls themselves and not the bone. Cremonini et al. (2011) reported that dental metallic artefacts did not affect the accuracy of linear measurements, but influenced the demarcation of the alveolar bone crest.

- *Head position*

Head position does not appear to impact the accuracy of acquired CBCT volumes (Adibi et al., 2017; El-Beialy et al., 2011), however, other factors are reported to affect the accuracy of measurements on CBCT volumes, including the exposure parameters used, CBCT artefact (e.g. beam hardening and motion artefacts), and the software used (Fokas et al., 2018).

During the physical measurements of the vertical distances, the sagittal tilt of the skull affected the perception of the vertical measurement limits, particularly that the two radiographic markers (i.e. X & Y) were not aligned on the exact horizontal level (on the same line, Figure 4-2). Subsequently, standardisation of the sagittal tilting of the skull was attempted to achieve an orthogonal position of the calliper, while measuring between the two radiographic markers.

With regards to virtual measurements on CBCT, the influence of non-ideal head position and/or sagittal tilting was mentioned (Mora et al., 2014). The inaccurate virtual orientation of the volume (especially sagittal tilt) may lead to an inaccurate perception of the reconstructed cross-sectional images, since this affects the height of subsequent cross-sections, and thus may lead to a discrepancy when these measurements are transferred to the patient's mouth (Mora et al., 2014).

***Angular vs linear measurements***

To the best of the author's knowledge, there is a paucity of published reports concerned with the clinical accuracy of panoramic/sagittal view measurements for the angular distances (arc length), between various segments of the jaws. Nevertheless, Kitai et al. (2013) found no significant differences ( $\pm 5\%$ ) between the arc length accuracy and the phantom measurements on the panoramic x-ray machines with tomosynthesis technology and in various head positions (except "at 12 mm forward position").

The author postulates that the transfer of the virtually planned linear measurements into a 3-dimensional physical structure that curves in two dimensions, maybe a source of

dimensional discrepancy when these measurements are physically reproduced (Figure 4-5). As the jaw bone curves, joining anterior and posterior regions of the maxilla and mandible, the alveolar bone has inconsistent vertical bone heights along its trajectory (Figure 4-5, B).

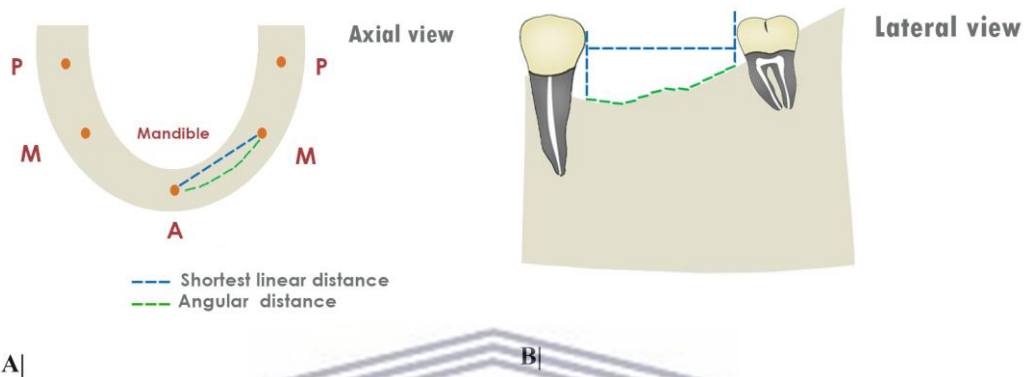


**Figure 4-5. Demonstration of the curved distances (arc lengths) between jaw segments (A&B).**

Interestingly, the inaccuracies of radiographic measurements from cross-sectional slices may occur from the erroneous transfer of those dimensions into the surgical setting (Harris et al., 2012).

Comparing the linear measurements of the arc length between different segments of the maxilla and the mandible between CBCT and panoramic radiographs to their corresponding physical ones, we demonstrated that CBCT underestimated all these measurements with a maximum submillimetre difference of -0.988 mm found in arch length (left side DUA distance). In panoramic radiographs, all the linear arch lengths were overestimated, with most being greater than the submillimetre difference [0.907 mm – 2.33 mm], while the highest difference was found in the left side DLP distance.

Comparing these arc lengths acquired in linear and angular fashions in the physical setting (using the cord), we demonstrated that 58% of the measurements crossed the 1 mm difference barrier and all of them were negative values (linear measurements underestimated the angular ones). The linear shortest distance between two points if

the surface was not orthogonal (in the vertical and horizontal levels), can be less than the distance measured directly on the alveolar surface – as was noted in this study (Figure 4-5). This could manifest clinically when performing freehand technique implant surgery, and using a cord/wire to reproduce the planned distance on the CBCT from an identified reference point to the drilling point. During implant planning, the clinician should also note that the cross-sectional slices generated from the CBCT volumes allow the measurement of bone heights represented on that exact slice, which may be inconsistent, along the reconstructed part of the jaw. These cross-sections are being reconstructed in specific thicknesses and steps, which must also be appreciated during virtual planning and physical transfer to the patient's mouth.

### *Panoramic radiographs*

Panoramic radiographs are a commonly prescribed radiograph in dental practices, as they offer various advantages (Shah et al., 2014; Tyndall et al., 2012). Disadvantages include magnification and inherent distortion (Shah et al., 2014; Tyndall et al., 2012). While multiple papers confirm the reliability of measurements taken on panoramic radiographs, particularly in the posterior segments (Assaf & Gharbyah, 2014; Özalp et al., 2018; Amarnath et al., 2015; Hu et al., 2012; Pertl et al., 2013; Kayal, 2016; Kim et al., 2011; Vazquez et al., 2013; Zarch et al., 2011), opposing evidence was also reported (Bou Serhal et al., 2002; Correa et al., 2014; Bertram et al., 2018; Haghnegahdar & Bronoosh, 2013; Dudhia et al., 2011).

In this study, the overall mean distance differences for all the measured dimensions were 2.229 and 3.832 mm for maxilla and mandible, respectively. The maximum mean difference was found in the vertical distance DV in mandibular point A, with an overestimation of 7.56 mm. Of 18 panoramic readings, the mean difference was over 1 mm in 16 locations in maxilla and mandible, was overestimated (>0 mm) in 17 readings [1.15 – 7.56 mm], and underestimated (>0 mm) in one reading (-0.77 mm).

The influence of the magnification ratios due to off-axis angle (negative angle) of the incident x-ray beam in panoramic radiography is more prominent in the maxillary jaw compared to the mandibular jaw, as the former will be exposed to a more angulated x-ray beam compared to the mandible (Yassaei et al., 2010).

### *Periapical radiographs*

Compared to periapical radiographs for which only vertical distances (DV) were analysed, the overall mean distance differences were -3.707 and 1.849 mm for maxilla and mandible, respectively. In PA, mandibular values showed less mean difference compared to the maxilla (1.89 mm); however, it is still not clinically tolerable. The author noted that in the maxilla, even conducted with simulated ideal settings, distortion can be easily encountered due to anatomical challenges counteracting the ideal parallelism between the axis of the alveolar ridge and the x-ray receptor. In the mandible, without any muscular interference it was easier to achieve such parallelism, which manifested with fewer mean differences (individual and overall) compared to the maxillary counterparts. The standardisation in panoramic and periapical techniques is challenging, and may account for the inconsistency of measurements. Though PA radiographs displayed accurate individual dimensions in various anatomical locations, the inconsistency of the results is also apparent. Precise reproduction of the anatomical structures cannot be guaranteed in all the clinical settings – mainly due to anatomical limitations, as noted during this assessment.



## CHAPTER 7 | CONCLUSION

CBCT showed a submillimetre overall accuracy when compared with the panoramic and periapical radiographs. The panoramic modality showed more precision in the maxillary arch compared to lower arch – with the highest discrepancy in the anterior region. Mandibular periapical measurements showed greater accuracy than the maxillary, but, the mean difference was still clinically intolerable. Although panoramic and periapical studies showed individual accurate readings, the overall difference indicates inferior dimensional accuracy when compared with CBCT. Although CBCT was superior in the linear measurement of arc length in the jaws (compared to PAN), linear-fashioned acquisition of arc lengths on radiographic and physical settings may vary from the angular physical counterparts, and this necessitates attention when reproducing these radiographic measurements into the patient mouth. In this analysis, the author confirms the superior dimensional stability of the CBCT modality, and hence this can be recommended for implant planning.

### Limitations

Angular measurements were not repeated (for inter- and intra- observers' agreement analysis).

### Acknowledgements

The researcher would like to acknowledge the following for their valuable contributions:

- Dr K.J. Baatjes, Head: Division of Clinical Anatomy, Faculty of Medicine and Health Sciences, Stellenbosch University.
- Dr Mandi Alblas, Division of Clinical Anatomy, Faculty of Medicine and Health Sciences, Stellenbosch University.
- Dr Faheema Kimmie-Dhansay, for statistical analysis.



PART 5  
RADIATION DOSES RECEIVED BY PATIENTS  
DURING DENTAL IMPLANT THERAPY

**CONTENTS AT A GLANCE**

|                                    |
|------------------------------------|
| Chapter 1   Introduction           |
| Chapter 2   Literature review      |
| 2.1 Absorbed and equivalent doses  |
| 2.2 Effective dose                 |
| Chapter 3   Aims and objectives    |
| Chapter 4   Materials and methods  |
| 4.1 Study phases                   |
| 4.2 Data analysis                  |
| Chapter 5   Results                |
| 5.1 Phase I: TLDS received doses   |
| 5.2 Phase II: Computer simulations |
| Chapter 6   Discussion             |
| Chapter 7   Conclusion             |

UNIVERSITY of the  
WESTERN CAPE



UNIVERSITY of the  
WESTERN CAPE

## ABSTRACT

**Aim:** To report the effective doses of multiple radiographic modalities used during implant planning, and to compare them to those generated by a computer-simulation software.

**Materials and Methods:** Twenty-four thermoluminescent chips (TLD-700) were used to capture the absorbed doses of twenty-four anatomical sites in the head and neck region using an anthropomorphic phantom during CBCT and panoramic examinations. A panoramic x-ray machine (Sirona<sup>®</sup> Orthophos<sup>®</sup> XG3) and two CBCT x-ray machines, i.e. NewTom<sup>®</sup> 5GXL (field of view selected 15×12, 8×8, and 8 × 8 cm (HiRes.)) and Carestream<sup>®</sup> 8100 3D, were used. The equivalent and effective doses retrieved from NewTom<sup>®</sup> 5GXL examinations were compared to their counterparts simulated on the Monte-Carlo based dose simulation software (PCXMC).

**Results:** The resultant effective doses (*E*) ranged from [75.3 μSv – 194.1 μSv] during exposures performed using the NewTom<sup>®</sup> 5GXL with various fields of view selected (15×12 and 8×8) and exposure protocols (standard vs. high resolution). The corresponding PCXMC simulation ranged from [79.12 μSv – 173.46 μSv]. The CS 8100<sup>®</sup> 3D (8×9 cm) exposure resulted in an effective dose of 101.8 μSv, while the panoramic examination using Sirona<sup>®</sup> Orthophos<sup>®</sup> XG3 revealed an effective dose of 21.1 μSv.

**Conclusion:** The effective doses revealed from CBCT and panoramic examinations were within the acceptable ranges of a dental CBCT and panoramic exposure values. Limiting the field of view and choosing the low exposure protocols, efficiently reduced the effective doses. Comparable PCXMC effective doses to their counterparts retrieved using the TLDs. Accurate x-ray exposure characterizing parameters is key to obtaining accurate computer simulations.

**Keywords:** CBCT, low-dose, effective dose, radiation, PCXMC.

## LIST OF ABBREVIATIONS AND ACRONYMS

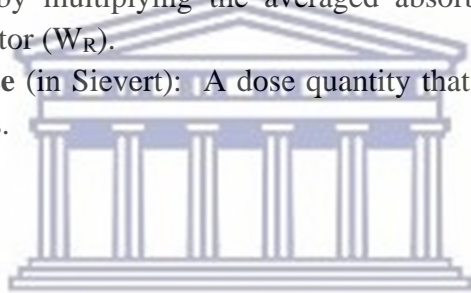
| Abbreviation         | Description   |
|----------------------|---|
| °C                   | Degrees Celsius   |
| µm                   | Micrometre  |
| µSv                  | Micro Sieverts  |
| Å                    | Ångström  |
| AP                   | Anteroposterior skull view                              |
| CT                   | Computed tomography                                     |
| CBCT                 | Cone beam computed tomography                           |
| cm                   | Centimetre  |
| Co                   | Cobalt  |
| CS                   | Carestream®   |
| <i>D</i>             | Average absorbed dose                                   |
| DAP                  | Dose area product                                       |
| <i>E</i>             | Effective dose  |
| <i>f</i>             | The fraction of tissue irradiated                       |
| FOV                  | Field of view   |
| Gy                   | Gray  |
| H x D x W            | Height x Depth x Width                                  |
| <i>H<sub>T</sub></i> | The equivalent dose                                     |
| ICRP                 | The International Commission on Radiological Protection |
| keV                  | Kilo-electronvolt                                       |
| kV                   | Kilovolt  |
| kVp                  | Kilo-voltage peak                                       |
| Lat.                 | Lateral skull view                                      |
| LiF                  | Lithium fluoride  |
| mAs                  | Milliamperere-second                                    |
| Mg                   | Magnesium   |
| mm                   | Millimetre  |
| MOSFET               | Metal oxide semiconductor field-effect                  |
| s                    | Second  |
| SA                   | South Africa  |
| SI                   | The International System of Units                       |
| Sv                   | Sieverts  |
| TBH                  | Tygerberg Hospital                                      |

|                         |                             |
|-------------------------|-----------------------------|
| <b>Ti</b>               | Titanium                    |
| <b>TLD</b>              | Thermoluminescent dosimeter |
| <b>TS</b>               | Technical specifications    |
| <b><math>W_R</math></b> | Radiation weighting factor  |
| <b><math>W_T</math></b> | Tissue weighting factors    |

---

### RELEVANT DEFINITIONS (WHITE & PHAROAH, 2013):

- **Absorbed dose** (in Gray): The amount of absorbed energy by various ionizing radiation per unit mass.
- **Equivalent dose** (in Sievert): A dose quantity that considers the various types of radiation by multiplying the averaged absorbed doses by the radiation weighting factor ( $W_R$ ).
- **Effective dose** (in Sievert): A dose quantity that is used to estimate risks in human beings.



UNIVERSITY *of the*  
WESTERN CAPE

**CHAPTER 1 | INTRODUCTION**

Currently, cone beam computed tomography is a very popular procedure that has benefited multiple dental specialities. The number of CBCT machines offered commercially is increasing, offering models with different specifications and output qualities (Pauwels et al., 2012). Different CBCT devices with variable exposure parameters (e.g. kVp, mAs), fields of view, and filtration, may result in a wide spectrum of radiation outputs and image qualities (Pauwels et al., 2012).

*Effective dose (E)* is a numerical value that allows the risk estimation of possible biological detriments when human tissues are being radiated (Shin et al., 2014; McCollough & Schueler, 2000). The effective dose allows the risk estimation (i.e. stochastic effects), not only for partial-body irradiation, but also for the equivalent whole-body dose (McCollough & Schueler, 2000). This value can be obtained through experimental methods, e.g. radiation dosimeters such as thermoluminescent dosimeter (TLD) embedded in the anthropomorphic phantoms. In addition, non-laborious methods including mathematical calculations based on specific conversion factors (previously derived from previous experimental approaches), and the use of Monte Carlo simulation software can be utilised (Kim et al., 2018; Batista, 2016).

CBCT was found to yield lower doses compared to CT acquisitions (Ludlow, 2011). Moreover, different CBCT devices and acquisition protocols/exposure parameters (of the same machine) may expose the patient to variable doses (Ludlow, 2011; Pauwels et al., 2012).

Although offering fewer diagnostic advantages compared with CBCT, panoramic radiographs expose the patients to lower radiation dose (3-7 times) compared with CBCT acquisitions (Tsiklakis et al., 2005; Granlund et al., 2016). Due to their anatomic location, the thyroid and salivary gland are included in the exposure domain of the primary x-ray beam, putting them at risk during panoramic and periapical examinations (Granlund et al., 2016). During the panoramic and full-mouth periapical examinations,

the salivary glands and the oral mucosa received the highest dosages (Granlund et al., 2016).

The estimation of the radiation doses yielded from various radiographic modalities would help clinicians optimally weigh the benefits and risks of each radiographic examination. The findings of this study provide evidence to clinicians regarding the estimated doses that could be received by patients during various radiographic examinations. A comparison between the simulated effective doses using Monte-Carlo simulation software and the conventional dosimetry methods (i.e. thermoluminescent dosimeters) was also conducted.



## CHAPTER 2 | LITERATURE REVIEW

### 2.1 ABSORBED AND EQUIVALENT DOSES

The absorbed dose is the primary-dose physical quantity representing the amount of energy that is absorbed by a tissue per unit mass (European Commission, 2012). The International System of Units (SI) unit used for this quantity is Gray (Joule per kg). While this quantity forms the bases of the calculation of other radiation dose quantities (like equivalent dose), on its own, it does not indicate the biological damage of certain radiation (European Commission, 2012). Once radiation weighting factors are applied to these absorbed doses the Equivalent doses ( $H_T$ ) can be retrieved (European Commission, 2012). These radiation weighting factors are meant to indicate the variant biological effectiveness of different kinds of radiation (e.g. gamma, alpha, and x-ray radiation). The equivalent doses are more indicative of individual organ radiation risk than the absorbed doses and are represented by the unit Sievert (Sv). Interestingly, the equivalent and the absorbed doses for x-ray radiation is numerically the same as the tissue weighting factor for the x-ray is one (European Commission, 2012).

### 2.2 EFFECTIVE DOSE

#### 2.2.1 OVERVIEW

The effective dose ( $E$ ) is an acceptable approach to evaluate the biological risk of certain examinations (Pauwels et al., 2012). This value considers the radiation type, the received doses by individual organs, and the corresponding tissue-weighting factor that is based on the radio-sensitivity of that tissue/organ (Shin et al., 2014; White & Pharoah, 2013). These weighting factors are related to the radio-sensitivity of that specific tissue and demonstrate the relative contribution of that organ to the entire possible detriment (Obed et al., 2015).

The International Commission on Radiological Protection (ICRP) published multiple, periodically updated recommendations on the tissue weighting factors ( $W_T$ ) to be used



during the calculation of effective dose – i.e. ICRP 26 (in 1977), ICRP 60 (in 1991), and the latest ICRP 103 (in 2007) (Obed et al., 2015). In 2007, the ICRP recommendations (ICRP 103) consider the brain as “independently weighted tissue” for the effective dose calculation with the addition of salivary gland  $W_T$ , moreover, the oral mucosa was added to the “remainder tissues” (Schilling & Geibel, 2013). The latest ICRP (103) weighting factors are listed in Table 5.1.

**Table 5.1. Tissue weighting factor (ICRP 103 in 2007) (SCENIHR, 2012).**

| Tissue /organ   | Tissue weighting factor ( $W_T$ ) for each mentioned tissue/organ | The Total of Tissue weighting factor $\Sigma (W_T)$ |
|---|---|---|
| Bone marrow, Breast, Stomach, Colon, and Lungs.   | 0.12  | 0.60  |
| Remaining tissues: Adrenals, extra-thoracic region, gall bladder, heart, kidneys, lymphatic nodes, muscle, oral mucosa, pancreas, prostate, small intestine, spleen, thymus, and uterus/cervix. | -   | 0.12  |
| Gonads  | 0.08  | 0.08  |
| The thyroid gland, Bladder, Liver, and Oesophagus.  | 0.04  | 0.16  |
| Skin, Brain, Salivary glands, and Bone surface.   | 0.01  | 0.04  |
|   | <b>Total</b>  | <b>1.0</b>  |

The effective dose can be calculated using the following equation (Obed et al., 2015):  $E = \sum W_T \times H_T$ , (Where  $W_T$ : tissue weighting factor and  $H_T$  the equivalent dose of that each tissue/organ).

Although this calculation is not specific for any individual person, the numerical value of the effective dose estimates the risk of the occurrence of a stochastic effect (Kim et al., 2018; McCollough & Schueler, 2000). This is particularly due to multiple factors that influence the radiation risk among individuals, including the gender and age of the patient when exposed (SCENIHR, 2012). It is feasible to use the effective dose quantity to report the accumulative amount of radiation received by a given patient during a period of time (Obed et al., 2015; Wall et al., 1988).

---

### 2.2.2 CALCULATION OF THE EFFECTIVE DOSAGES ( $E$ )

Estimating the effective doses of different radiographic examinations can be done indirectly, as it is unreasonable to be carried out in the clinical setting (Aliasgharzadeh et al., 2015). The process of effective dose ( $E$ ) calculation commences with the capture of the absorbed dose of each organ/tissue, post radiographic examination (McCollough & Schueler, 2000).

While it requires considerable time and effort, an anthropomorphic phantom simulator that accommodates radiation dosimeters (e.g. a Thermoluminescent dosimeter) is an experimental method used to record individual absorbed organ doses (Batista, 2016; Shin et al., 2014; Lee et al., 2016).

Absorbed organ doses and effective doses can also be estimated by a simpler method using special software based on Monte Carlo simulations of photon interactions with the human tissues (Kim et al., 2018; McCollough & Schueler, 2000; Batista, 2016).

Panoramic and CBCT modalities have unique beam geometry in addition to the rotational movement of the x-ray generating gantry. This may impose certain challenges and uncertainties when using Monte-Carlo based computer software for ( $E$ ) estimation compared to the virtual simulation of conventional radiographic modalities (Batista, 2016; Lee et al., 2016).

The Radiation and Nuclear Safety Authority in Finland developed a Monte Carlo-based software called PCXMC (Batista, 2016). This software is used to estimate the received

organ and effective doses using the ICRP 103 (2007) weighting tissue factors. An upgrade was attached to the software, and simulation modules for rotational-based radiography techniques were added (Batista, 2016). This supplemental program estimates doses in the x-ray units that have a centre of rotation where the axis of the incident beam crosses this centre from multiple angles (Kim et al., 2018).

This software can be efficiently used to estimate ( $E$ ) from CBCT examinations, instead of conventional methods (Kim et al., 2018). Lee et al. (2016) compared the estimated ( $E$ ) obtained from thermoluminescent dosimeters (TLD) and computer-based Monte Carlo (PCXMC) software during panoramic examinations. By contrast, they found that the simulation software overestimated the doses obtained from the TLD detectors by 9.55% to 51.24%. They added that the accuracy of the estimation obtained was highly influenced by “input values for dose-determining factors” (Lee et al., 2016).

Koivisto et al. (2012) compared ( $E$ ) obtained using metal oxide semiconductor field-effect transistor (MOSFET) dosimeters (embedded in an anthropomorphic RANDO phantom) with PCXMC simulations. The results showed relatively comparable effective doses (MOSFET ( $E$ ): 153  $\mu$ Sv vs PCXMC ( $E$ ): 136  $\mu$ Sv).

Further details regarding the most recent reports comparing or using the Monte-Carlo simulation program (i.e. PCXMC) are further listed in Table 5.2.

**Table 5.2. Published reports on the use of Monte-Carlo software for  $E$  calculations.**

| Authors            | Instrument  | Software         | Comments /conclusion  |
|--------------------|---|------------------|---|
| (Kim et al., 2018) | <ul style="list-style-type: none"> <li>TLD-thermoluminescent dosimeters.</li> <li>CBCT: The Alphard VEGA (Asahi)</li> </ul> | PCXMC20 Rotation | “The use of PCXMC software could be an alternative to the TLD measurement method for effective dose estimation in |

|                                |   |  |   |
|--------------------------------|---|--|---|
|                                | Roentgen Ind. Co.,<br>Kyoto CBCT Japan).  |  | CBCT with large and medium FOVs”  |
| <b>(Lee et al., 2016)</b>      | <ul style="list-style-type: none"> <li>• TLD-thermoluminescent dosimeters.</li> <li>• Panoramic x-ray unit: OP-100 (Instrumentarium Dental, Tuusula, Finland).</li> </ul> | PCXMC20 Rotation (STUK, Helsinki, Finland) | “The effective dose calculated with PCXMC was generally higher than the dose measured by using TLD” |
| <b>(Koivisto et al., 2012)</b> | <ul style="list-style-type: none"> <li>• Anthropomorphic phantom+ MOSFET.</li> <li>• CBCT: Promax 3D (Planmeca, Helsinki, Finland)</li> </ul>                             | PCXMC v. 2.0 software                      | “MOSFET dosimeters placed in a head phantom gave results similar to Monte Carlo simulation”         |
| <b>(Aps &amp; Scott, 2014)</b> | <ul style="list-style-type: none"> <li>• Conventional bitewing radiographs.</li> <li>• Oblique lateral radiographs.</li> </ul>  | PCXMC v. 2.0 software                      | No comparison   |
| <b>(Yeh &amp; Chen, 2018)</b>  | CBCT: i- CAT <sup>®</sup> (Imaging Sciences International Inc., PA, U.S.A.)   | PCXMC 2.0 Rotation                         | No comparison   |

Mathematical calculations based on certain exposure characterizing quantities (e.g. dose area product (DAP), Air kerma) and using conversion factors is another simpler method that can be used for the estimation of  $E$  (Batista, 2016; Walker & van der Putten, 2012; Lee et al., 2016). These conversion factors are based on previously collected dose values (using detectors e.g. an ion chamber). Relevant reported effective doses are tabulated in Table 5.3 and Table 5.4.

**Table 5.3. Reported (*E*) for selected CBCT machines.**

| Model                        | Manufacturer                                | FOV (cm)                          | kVp          | mAs                             | Effective dose ( $\mu$ Sv)               | Reference                 |
|------------------------------|---|-----------------------------------|--------------|---------------------------------|--|---------------------------|
| <b>NewTom VGi</b>            | CEFLA s.c.<br>(Imola, Italy)                | 15×15                             | 110          | 7.8                             | <b>97</b>                                | (Ludlow et al., 2015)     |
|                              |   | 15 ×15                            |              | 8.8                             | <b>194</b>                               | (Pauwels et al., 2012)    |
|                              |   | 12 × 15                           |              | 6.2                             | <b>103</b>                               | (Ludlow et al., 2015)     |
|                              |   | 6×6<br>(Posterior) <sup>+</sup>   |              | 70.1                            | <b>140</b>                               | (Ludlow et al., 2015)     |
|                              |   | 6×6<br>(Anterior) <sup>+</sup>    |              | 65                              | <b>131</b>                               | (Ludlow et al., 2015)     |
|                              |   | 6×6 <sup>++</sup>                 |              | 42.1,<br>29                     | <b>191, 130</b>                          | (Ludlow et al., 2015)     |
|                              |   | 8×8 <sup>++</sup>                 | 6.3,<br>38.7 | <b>61, 206</b>                  | (Ludlow et al., 2015)                    |                           |
| <b>NewTom VG</b>             |   | 10 × 15                           |              | 10.4                            | <b>83</b>                                | (Pauwels et al., 2012)    |
| <b>NewTom 3G</b>             |   | 19 × 19                           |              | 8.1                             | <b>68</b>                                | (Ludlow & Ivanovic, 2008) |
| <b>NewTom 5G</b>             |   | 6×6                               |              | 72                              | <b>172</b>                               | (Kadesjö et al., 2018)    |
| <b>Galileos Comfort Plus</b> | Dentsply Sirona<br>(Bensheim,<br>Germany)   | 8.5 × 15 <sup>+</sup>             | 98           | 8, 10,<br>12,<br>20, 25,<br>30  | <b>27, 34, 41<br/>84, 103,<br/>122</b>   | (Ludlow et al., 2015)     |
| <b>Orthophos XG</b>          |   | 5×5.5<br>(Anterior) <sup>+</sup>  | 85           | 36, 51,<br>66,72,<br>86,<br>101 | <b>21, 30,<br/>39,45, 53,<br/>60</b>     | (Ludlow et al., 2015)     |
|                              |   | 5×5.5<br>(Posterior) <sup>+</sup> |              |                                 | <b>25, 36, 47,<br/>58, 70, 81</b>        |                           |
| <b>Orthophos XG</b>          |   | 8 × 8 <sup>++</sup>               | 85           | 36, 51,<br>66,72,<br>86,<br>101 | <b>48, 67, 91,<br/>117, 144,<br/>166</b> | (Ludlow et al., 2015)     |
| <b>Galileos Comfort</b>      |   | 15×15                             | 85           | 21, 42                          | <b>70, 128</b>                           | (Ludlow & Ivanovic, 2008) |
| <b>Galileos Comfort</b>      |   | 15×15                             | 85           | 21, 42                          | <b>51, 95</b>                            | (Rotke et al., 2013)      |
| <b>The Alphard VEGA</b>      | Asahi Roentgen<br>Ind. Co.(Kyoto,<br>Japan) | 10.2 ×10.2<br>cm                  | 80           | 136                             | <b>187</b>                               | (Kim et al., 2018)        |

|                         |                                 |                               |    |                         |                               |                            |
|-------------------------|---------------------------------|-------------------------------|----|-------------------------|-------------------------------|----------------------------|
| <b>3D Accuitomo 170</b> | J. MORITA Corp. (Osaka, Japan)  | 10×10                         | 90 | 45, 79, 87.5, 154       | <b>132, 232, 257, 453</b>     | (Ludlow et al., 2015)      |
| <b>3D Accuitomo 170</b> |                                 | 10×14                         | 90 | 45, 79, 87.5, 154       | <b>138, 242, 269, 473</b>     | (Ludlow et al., 2015)      |
| <b>3D Accuitomo 170</b> |                                 | 4×4 (Anterior) <sup>+</sup>   | 90 | 87.5                    | <b>32</b>                     | (Theodorakou et al., 2012) |
| <b>CS 9300</b>          | Carestream Dental (Atlanta, GA) | 10 × 10                       | 90 | 25                      | <b>76</b>                     | (Ludlow et al., 2015)      |
| <b>CS 9300</b>          |                                 | 11 × 17                       | 90 | 25.6, 51.5              | <b>101, 204</b>               | (Ludlow et al., 2015)      |
| <b>CS 9300</b>          |                                 | 13.5 × 17                     | 90 | 45.2                    | <b>184</b>                    | (Ludlow et al., 2015)      |
| <b>CS 9300</b>          |                                 | 5×5 (Anterior) <sup>++</sup>  | 84 | 60, 100                 | <b>66, 127</b>                | (Ludlow et al., 2015)      |
| <b>CS 9300</b>          |                                 | 5×5 (Posterior) <sup>++</sup> |    |                         | <b>48, 81</b>                 | (Ludlow et al., 2015)      |
| <b>CS 9000</b>          |                                 | 4×5 (Anterior) <sup>+</sup>   | 70 | 107                     | <b>5</b>                      | (Ludlow et al., 2015)      |
| <b>CS 9000</b>          |                                 | 4×5 (Posterior) <sup>+</sup>  | 70 | 107                     | <b>10</b>                     | (Ludlow et al., 2015)      |
| <b>CS 9000</b>          |                                 | 4×5 (Anterior) <sup>++</sup>  | 70 | 107                     | <b>38</b>                     | (Ludlow et al., 2015)      |
| <b>CS 9000</b>          |                                 | 4×5 (Posterior) <sup>++</sup> | 70 | 107                     | <b>22</b>                     | (Ludlow et al., 2015)      |
| <b>ProMax Mid</b>       | Planmeca (Helsinki, Finland)    | 16 × 16                       | 90 | 108, 127, 145, 271, 325 | <b>95, 112, 128, 223, 283</b> | (Ludlow et al., 2015)      |
| <b>ProMax 3D*</b>       |                                 | 4×5 (Anterior) <sup>+</sup>   | 84 | 120                     | <b>10</b>                     | (Al-Okshi et al., 2013)    |
| <b>ProMax 3D*</b>       |                                 | 5×8 <sup>+</sup>              | 84 | 192                     | <b>131</b>                    | (Qu et al., 2010)          |
| <b>ProMax 3D</b>        |                                 | 8×8 <sup>++</sup>             | 84 | 19.6, 169               | <b>28, 122</b>                | (Pauwels et al., 2012)     |
| <b>ProMax 3D*</b>       |                                 | 5×8 <sup>++</sup>             | 84 | 192                     | <b>171</b>                    | (Qu et al., 2010)          |

|                      |  |                                |     |      |            |                               |
|----------------------|--|--------------------------------|-----|------|------------|-------------------------------|
| <b>ProMax3D</b>      |  | 4×5                            | 90  | 109  | <b>88</b>  | (Kadesjö et al., 2018)        |
| <b>DCT PRO</b>       | VATECH<br>(Seoul,<br>Korea)                  | 10 × 16                        | 90  | 105  | <b>249</b> | (Qu, Li, Zhang, et al., 2012) |
| <b>Picasso Trio</b>  |  | 7×12 <sup>++</sup>             | 85  | 91   | <b>81</b>  | (Pauwels et al., 2012)        |
| <b>PaX-Uni3D</b>     |  | 5×5<br>(Anterior) <sup>+</sup> | 85  | 120  | <b>44</b>  | (Pauwels et al., 2012)        |
| <b>i-CAT Classic</b> | Imaging Sciences International LLC (PA, USA) | 13 × 16                        | 120 | 18.5 | <b>69</b>  | (Ludlow & Ivanovic, 2008)     |

<sup>+</sup> FOV including the maxilla, <sup>++</sup> FOV including the mandible, \* additional filtration was added

**Table 5.4. Reported (*E*) for selected panoramic x-ray machines.**

| Model                      | Brand   | kVp | mAs (mA×s)        | Effective dose (µSv) | Reference                  |
|----------------------------|---|-----|-------------------|----------------------|----------------------------|
| <b>Orthophos XG 5</b>      | Dentsply Sirona<br>(Bensheim,<br>Germany)       | 69  | 211.5 (15 × 14.1) | <b>27.1</b>          | (Chinem et al., 2016)      |
| <b>Orthophos XG</b>        |   | 64  | 112.8 (8 × 14.1)  | <b>14.2</b>          | (Ludlow et al., 2008)      |
| <b>Orthophos XG</b>        |   | 64  | 112               | <b>13</b>            | (Qiang et al., 2019)       |
| <b>Orthophos DS</b>        |   | 70  | 140 (10×14)       | <b>10</b>            | (Silva et al., 2008)       |
| <b>Orthophos XGplus DS</b> |   | 69  | 211.5 (15×14.1)   | <b>50</b>            | (Carrafiello et al., 2010) |
| <b>ProMax</b>              | Planmeca<br>(Helsinki,<br>Finland)              | 68  | 208 (13×16)       | <b>24.3</b>          | Ludlow et al., 2008)       |
| <b>ProMax</b>              |   | 70  | 160 (10×16)       | <b>37.8</b>          | (Lee et al., 2013)         |
| <b>ProMax</b>              |   | 62  | 42                | <b>4.1</b>           | (Kadesjö et al., 2018)     |
| <b>ProlineXC</b>           |   | 70  | 216 (12×18)       | <b>27.6</b>          | (Lee et al., 2013)         |
| <b>OP-100</b>              | Instrumentarium Dental<br>(Tuusula,<br>Finland) | 73  | 176 (10 × 17.6)   | <b>7.153</b>         | (Lee et al., 2016)         |
| <b>Kodak 9000 3D</b>       | Carestream Dental (Atlanta, GA)                 | 70  | 143 (10 × 14.3)   | <b>14.7</b>          | (Ludlow, 2009)             |

## CHAPTER 3 | AIMS AND OBJECTIVES

### 3.1 AIM

To determine the radiation doses received by patients undergoing radiographic examinations for dental implant treatments.

### 3.2 OBJECTIVES

- 1- To capture the received absorbed organ doses using an anthropomorphic phantom-head simulator and TLDs for two CBCT and one panoramic x-ray machine.
- 2- To capture the absorbed organ doses received during different exposure protocols and fields of view.
- 3- To calculate the equivalent dose received from each radiographic modality and field of view.
- 4- To calculate and compare the effective dose received from each radiographic modality and field of view.
- 5- To obtain and compare the corresponding simulated effective doses obtained using Monte-Carlo software.

### 3.3 RATIONALE

- 1- The provided comprehensive radiation dose charts by the author (whether tested during this investigation or the ones reported in the literature) aim to alert clinicians to the level of risks arising during various radiographic examinations used in implant therapy.
- 2- Confirming the clinical efficacy of using simpler, accessible, and cost-effective Monte-Carlo software for radiation dose assessment can help to ameliorate the radiation protection measures in several facilities that cannot employ the traditional methods (which require time, effort, and need sophisticated machinery).



## CHAPTER 4 | MATERIALS AND METHODS

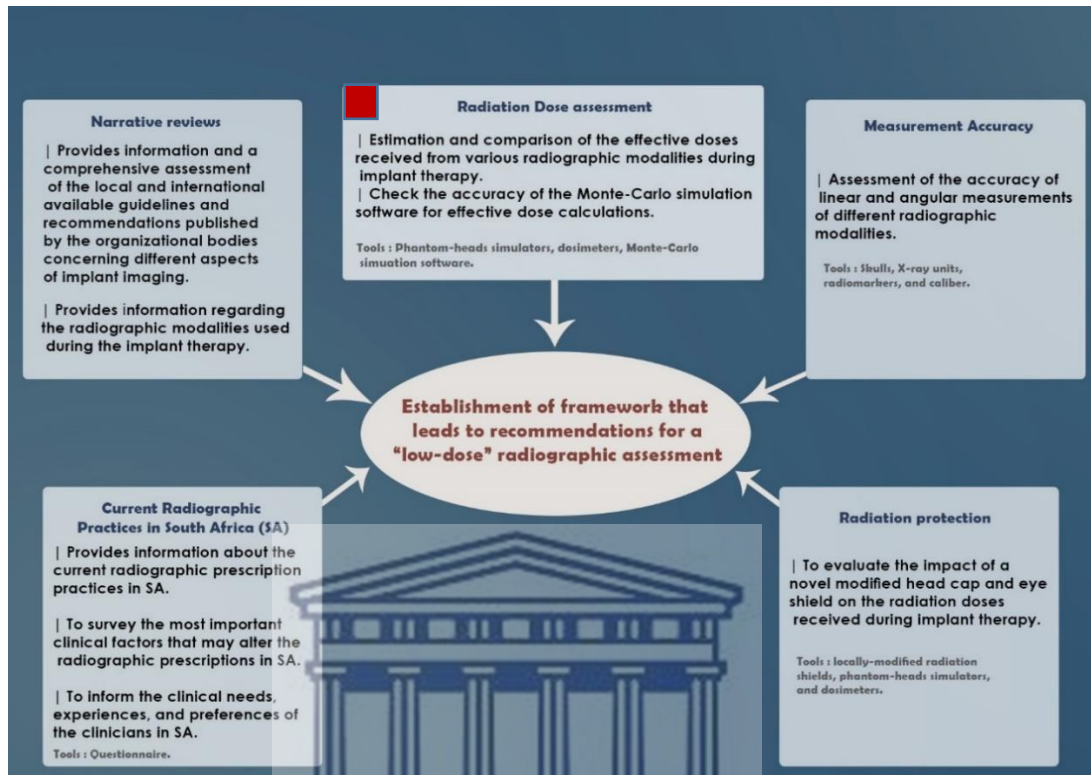


Figure 5-1. Diagrammatic representation of the main research project. The current sub-study is highlighted.

## 4.1 STUDY PHASES

This analysis was conducted in two phases:

- The first phase was laboratory-based to measure the radiation doses using an anthropomorphic phantom (with embedded TLD chips).
- The second phase was conducted virtually to estimate the radiation doses using Monte-Carlo simulation computer software (for the same experimental settings tested in phase 1).

Both phases were executed via collaboration with the Medical Physics Department, Faculty of Health Sciences, Stellenbosch University, SA.

|                 |                                    |
|-----------------|------------------------------------|
| Research design | Experimental <i>in vitro</i> study |
|-----------------|------------------------------------|

#### 4.1.1 PHASE I: TLD DOSES

In this phase, the individual organ absorbed doses were recorded using an average adult-size, female RANDO<sup>®</sup> phantom head (Alderson Research Laboratories, Stamford, CT). Thermoluminescent dosimeter-700 (TLD-700) chips (Thermo Electron Cor., Oakwood Village, OH, USA) were used to capture the absorbed organ doses at different selected anatomical sites in the head and neck. The technical specifications of these TLDs are listed (Table 5.5).

|              |  |
|--------------|--|
| <b>Tools</b> | <ul style="list-style-type: none"> <li>- <b>Simulation phantom-heads (RANDO<sup>®</sup>).</b></li> <li>- <b>Thermoluminescent dosimeters (TLD-700).</b></li> <li>- <b>TLD reader (REXON<sup>®</sup> UL-320)</b></li> <li>- <b>PTW<sup>®</sup> FREIBURG TLDO<sup>®</sup> annealing oven.</b></li> <li>- <b>PTW<sup>®</sup> NOMEX<sup>®</sup> Dosimeter</b></li> </ul> |
|--------------|--|

##### 4.1.1.1 PREPARATION OF THE THERMOLUMINESCENT CHIPS

The chips were annealed before each radiation exposure and following the annealing protocols implemented at the Medical Physics Department, Groote Schuur Hospital (Cape Town, South Africa). The TLD chips were annealed using the PTW<sup>®</sup> FREIBURG TLDO<sup>®</sup> annealing oven (Freiburg, Germany), the technical specifications (TS) of the oven are shown in Table 5.6. The annealing protocol steps were as follows (Figure 5-2):

- Annealed for 1 hour at 400 °C.
- At 100 °C for two hours.
- Finally, the chips were cooled to ambient temperature.

The calibration of the TLDs was done using a conventional x-ray tube (Figure 5-3) against a calibrated PTW<sup>®</sup> NOMEX<sup>®</sup> Dosimeter connected to NOMEX<sup>®</sup> Multimeter<sup>®</sup> (TS are shown in Table 5.7). A total dose of 200 mGy was delivered to the chips over two x-ray pulses, each had a 110 kVp, 320 mAs, 2 seconds exposure time, and a 50 mGy/s dose rate (Figure 5-3). The chips were read-out (Figure 5-4) on the same day

using the REXON® UL-320 TLD reader (Ohio, USA), and unique calibration profiles (files) were created for each TLD chip to serve the subsequent readings (TS of the reader are in detail, in Table 5.8). The exposed TLD chips (during the primary analysis) were read on the same reader on either the same day or early the next day after each exposure. The nitrogen gas levels of the TLD reader were monitored at all times in order to ensure quality readings. No discoloured or damaged chips were used.

#### 4.1.1.2 PHANTOM HEAD PREPARATION:

The phantom head that was used contained eleven slabs, each with a 2.5 cm thickness (Figure 5-5). Twenty-four sites were selected to capture various organs absorbed doses at different regions in the head and neck (Figure 5-6) adopted from (Ludlow, 2011). One pre-calibrated TLD-700 chip was inserted into each of the 24-sites (Table 5.9). The chips' vertical level inside their sockets (in each slab) was sometimes modified using the manufacturer socket plugs of various heights (same surrounding tissue density) to accurately correspond to the spatial location of designated organ/tissue, since some tissues/organs can be located at different vertical levels in the same slab. The identification of each chip socket on the slab was done after careful analysis of each slab, and spatial location of the designated organ/tissue by two oral and maxillofacial radiologists and the medical physicist.

**Table 5.5. Technical specifications of the TLD-700 chips.**

| Specifications            | Value                                      |
|---------------------------|--|
| <b>Measurement Ranges</b> | 10 pGy to 10Gy                             |
| <b>Emission Spectra</b>   | 3500 to 6000Å (4000 maximum)               |
| <b>Energy Response</b>    | 1.25 keV/60Co                              |
| <b>Material</b>           | Lithium Fluoride (7 Li isotope) LiF:Mg, Ti |
| <b>Sensitivity</b>        | 1.0 at 60Co relative to LiF                |
| <b>Dimensions</b>         | 3.2 × 3.2 × 0.89 mm                        |

**Table 5.6. Technical specifications of the annealing oven.**

| Specifications               | Value                             |
|------------------------------|-----------------------------------|
| <b>Model/brand</b>           | PTW <sup>®</sup> - TLDO           |
| <b>Temperature (Highest)</b> | Max 400 °C                        |
| <b>Capacity (one cycle)</b>  | 360 elements (in standard trays)  |
| <b>Insulation</b>            | Ceramic fiber                     |
| <b>Chamber size</b>          | 10 mm × 16.5 mm × 15.5 mm (H×D×W) |

**Table 5.7. Technical specifications of the dose-measuring device.**

| Specifications           | Value   |
|--------------------------|---|
| <b>Model/brand</b>       | NOMEX <sup>®</sup> Multimeter <sup>®</sup>                          |
| <b>Air kerma rate</b>    | 40 nGy/s ... 460 mGy/s  |
| <b>Air kerma</b>         | 40 nGy ... 4.6 kGy  |
| <b>Resolution</b>        | 0.4 nGy/s   |
| <b>Energy dependence</b> | ≤± 5%   |
| <b>kV R/F</b>            | (40 ... 150) kV, ± 1.5 % or ± 1 kV (typically ± 0.75 % or ± 0.5 kV) |
| <b>Dose per pulse</b>    | 50 nGy ... 500 Gy, ± 3.5 % (typically ± 1.5 %)                      |

**Table 5.8. Technical specifications of the TLD chips' reader.**

| Specifications                     | Value  |
|------------------------------------|--|
| <b>Model/brand</b>                 | REXON <sup>®</sup> UL-320  |
| <b>Cycle Time</b>                  | Variable: 0 to 3 min.  |
| <b>Test Light:</b>                 | Stable LED reference light   |
| <b>Dosimeter Heating System:</b>   | <ul style="list-style-type: none"> <li>• Direct contact heating with linear Time/Temp. profile (TTP). Temperature set-point resolution: 1C Range: RT to 450 °C</li> <li>• Temperature control: ten points</li> <li>• Accuracy: +/- 4 °C</li> </ul> |
| <b>Reported TLD Data:</b>          | <ul style="list-style-type: none"> <li>• TL Digitization (digital glow-curve) period resolution: 100 ms</li> <li>• TL signal data: integrated TL signal</li> <li>• Temperature reporting resolution, 1 °C</li> </ul>                               |
| <b>Programmable Heating Cycle:</b> | User-controlled, up to 10-node programmable temperature cycle  |

**Table 5.9. TLDs' location in the phantom-head** (adopted from (Ludlow, 2011)).

| Site number | Anatomical site                     | Slab level | TLD number |
|-------------|-------------------------------------|------------|------------|
| 1           | Calvarium (anterior)                | 3          | 1          |
| 2           | Calvarium (left side)               | 3          | 2          |
| 3           | Calvarium (posterior)               | 3          | 3          |
| 4           | Midbrain region                     | 3          | 4          |
| 5           | Pituitary gland                     | 4          | 5          |
| 6           | Orbit (right side)                  | 3          | 6          |
| 7           | Orbit (left side)                   | 3          | 7          |
| 8           | Eye lens (right side)               | 4          | 8          |
| 9           | Eye lens (left side)                | 4          | 9          |
| 10          | Cheek (left side)                   | 6          | 10         |
| 11          | Parotid gland (right side)          | 7          | 11         |
| 12          | Parotid gland (left side)           | 7          | 12         |
| 13          | Ramus (right side)                  | 7          | 13         |
| 14          | Ramus (left side)                   | 7          | 14         |
| 15          | Center C spine                      | 6          | 15         |
| 16          | Back of the neck (right side)       | 8          | 16         |
| 17          | Mandibular body region (right side) | 8          | 17         |
| 18          | Mandibular body region (left side)  | 8          | 18         |
| 19          | Submandibular gland (right side)    | 8          | 19         |
| 20          | Submandibular gland (left side)     | 8          | 20         |
| 21          | Centre sublingual gland             | 8          | 21         |
| 22          | Thyroid gland (midline)             | 10         | 22         |
| 23          | Thyroid gland surface (left side)   | 10         | 23         |
| 24          | Oesophageal tube                    | 11         | 24         |

#### 4.1.1.3 RADIOGRAPHIC EXAMINATIONS

The doses delivered from x-ray exposures using two CBCT and one panoramic x-ray machines were captured in this analysis. The x-ray machines used are:

- 1- NewTom<sup>®</sup> 5GXL CBCT unit (CEFLA s.c., Imola, Italy). TS are found in Table 5.10. Three fields of view/scan modes were tested ( $15 \times 12$  cm,  $8 \times 8$  cm, and  $8 \times$

8 cm (HiRes)), (Figure 5-7). The exposure parameters including the kVp and mAs were automatically set based on the scouting exposures executed prior to the primary acquisition.

- 2- Carestream<sup>®</sup> 8100 3D CBCT unit (Carestream Dental, Atlanta, GA, USA), and further TS are found in Table 5.11. One field of view  $8 \times 9$  cm was tested (Figure 5-8).
- 3- Sirona<sup>®</sup> Orthophos XG3 (Figure 5-9) panoramic x-ray unit (Dentsply Sirona, Bernsheim, Germany), and further TS are found in Table 5.12.

The information regarding exposures during the radiographic acquisitions using the three radiographic modalities is found in Table 5.13. The phantom was stabilised on a medical trolley, and an ideal radiographic position was achieved with the aid of positioning laser light (where available). Only the NewTom<sup>®</sup> 5GXL executed scouting exams before the primary acquisitions (Figure 5-10). The x-ray exposures were repeated five times during CBCT acquisitions and ten times during digital panoramic examination to ensure the attainment of a good signal by the TLDs. Three unexposed TLD chips were used for background radiation for each examination.

**Table 5.10. Technical specifications of the first CBCT unit used.**

| Parameter                               | Description   |
|---|---|
| <b>Brand/model</b>                      | NewTom <sup>®</sup> 5GXL  |
| <b>X-ray source</b>                     | High-frequency generator, a rotating-anode X-ray tube               |
| <b>Focal spot</b>                       | 0.3 mm  |
| <b>Exposure Control</b>                 | SafeBeam <sup>™</sup> to reduce exposure according to patient build |
| <b>Sensor</b>                           | Amorphous silicon flat panel  |
| <b>Greyscale</b>                        | 16-bit  |
| <b>3D scan time</b>                     | 18 - 36s  |
| <b>3D emission time</b>                 | 0.9s - 9.0s (single scan)   |
| <b>Selectable voxel size (Standard)</b> | 200 - 300 $\mu\text{m}$   |
| <b>Selectable voxel size (HiRes)</b>    | 100 - 150 $\mu\text{m}$   |

**Table 5.11. Technical specifications of the second CBCT unit used.**

| Parameter                 | Description   |
|---------------------------|---|
| <b>Brand/model</b>        | Carestream® 8100 3D   |
| <b>Tube voltage</b>       | 60 - 90 kV  |
| <b>Tube current</b>       | 2 - 15 mA   |
| <b>Tube focal spot</b>    | 0.7 mm  |
| <b>Field of View</b>      | 4 × 4 / 5 × 5 / 8 × 5 / 8 × 8 / 8 × 9 cm                                  |
| <b>Radiological exams</b> | Full, upper or lower jaw - Full, upper or lower molar - Occlusion – Teeth |
| <b>Grayscale</b>          | 16384 -14 bits  |
| <b>Voxel size (µm)</b>    | 75 µm minimum   |
| <b>Exposure time</b>      | 7 to 15 sec   |

**Table 5.12. Technical specifications of the panoramic x-ray machine used.**

| Parameter                    | Description             |
|------------------------------|-------------------------|
| <b>Brand/model</b>           | Sirona® Orthophos® XG 3 |
| <b>X-ray generator</b>       | 60-90 kV; 3-16 mA       |
| <b>Focal spot size</b>       | 0.5 mm                  |
| <b>Total filtration</b>      | > 2.5 mm Al             |
| <b>Sensor</b>                | Digital CCD line sensor |
| <b>Active sensor area</b>    | 138 x 6.48 mm           |
| <b>Pixel size</b>            | 27 µm                   |
| <b>Focus-sensor distance</b> | 530 mm                  |

**Table 5.13. Exposure information during the radiographic examinations.**

|                            | NewTom® 5GXL          |                     |                  | CS® 8100 3D   | Orthophos® XG 3  |
|----------------------------|-----------------------|---------------------|------------------|---|--|
|                            | FOV / MODE            |                     |                  | FOV / MODE  | FOV / MODE   |
|                            | 15 × 12<br>(Standard) | 8 × 8<br>(Standard) | 8 × 8<br>(HiRes) | 8×9   | -  |
| <b>Scan mode / program</b> | Regular (18s)         | Regular (18s)       | Regular (20s)    | <ul style="list-style-type: none"> <li>Adult (medium-sized) patient.</li> <li>Full jaw (both upper and lower jaw) program.</li> <li>Fast scan.</li> </ul> | <ul style="list-style-type: none"> <li>P1 program.</li> <li>Adult (medium-sized) patient.</li> </ul> |
| <b>kVp</b>                 | 110                   | 110                 | 110              | 90  | 69   |
| <b>mAs</b>                 | 37.50                 | 45.78               | 113.39           | 22.4 (3.20 mA X 7 s)  | 208.95 (15 mA x 13.9s)   |
| <b>Exposure time (s)</b>   | 3.6                   | 3.6                 | 5.4              | 7   | 13.9   |
| <b>Air Kerma (mGy)</b>     | 5                     | 5.84                | 12.81            | -   | -  |
| <b>DAP (mGy.cm2)</b>       | 1120.05               | 520.64              | 1141.25          | 512   | 101  |
| <b>Voxel size (µm)</b>     | 250                   | 200                 | 125              | 300   | -  |
| <b>Scout images</b>        | 2                     | 2                   | 2                | 0   | -  |

#### 4.1.1.4 EQUIVALENT AND EFFECTIVE DOSE MEASUREMENTS:

The average background dose was obtained and subtracted from each irradiated TLD chip reading. The captured absorbed doses from the TLD chips were divided by 5 (CBCT acquisitions) or 10 (panoramic) to get the absorbed dose per scan for each site. The individual absorbed doses retrieved from various TLDs representing a tissue or an organ (Table 5.14), were averaged and used to calculate the equivalent dose ( $H_T$ ).

Using the averaged organ dose, the following equation ( $H_T$ ) was used:  $H_T = W_R \times \Sigma D \times f$ , where  $W_R$  (radiation weighting factor) is one for the x-ray,  $D$ : average absorbed dose,  $f$ : the fraction of tissue irradiated. The fractions of the tissue irradiated mentioned by (Ludlow, 2011; Roberts et al., 2009) were adapted by the author to the field of view used in this sub-study (Table 5.14). The resultant equivalent doses (micro Sieverts ( $\mu\text{Sv}$ )) were used for the following effective dose calculations.



The equivalent dose for the bone surface was calculated by multiplying the equivalent dose of bone marrow by a correction factor (Bone: muscle attenuation ratio), which was 2.4 for 110 kVp, 4.09 for 69 kVp, and 3.23 for 90 kVp (calculated using the following equation:  $-0.0618 \times 2/3 \text{ kVp} + 6.9406$ , (National Bureau of Standards, 1964; Ludlow, 2011)).

The effective dose ( $E$ ) was then calculated via the following equation:  $E = \sum W_T \times H_T$  Where  $H_T$ : the equivalent dose, and  $W_T$ : the tissue-weighting factor. The tissue-weighting factors (ICRP 2007) were used (Table 5.1). From the remainder tissues, only the lymphatic nodes, muscles, extra-thoracic airway, and oral mucosa were considered.

**Table 5.14. The fractions of tissue irradiated adapted by the author to measure FOV relevant to the study (Ludlow, 2011; Roberts et al., 2009).**

| Organ / Tissue         | Fraction of irradiated tissue (%) |               | TLD ID       |
|------------------------|-----------------------------------|---------------|--------------|
|                        | Field of view (cm × cm)           |               |              |
|                        | 15 × 12                           | 8×8, 8×9, PAN |              |
| <b>Bone marrow</b>     |                                   | <b>16.5</b>   | <b>10,00</b> |
|                        | Mandible                          | 1,3           | 1,3          |
|                        | Calvaria                          | 11,8          | 5,3          |
|                        | Cervical spine                    | 3,4           | 3,4          |
| <b>Thyroid</b>         | <b>100</b>                        | <b>100</b>    | 22, 23       |
| <b>Esophagus</b>       | <b>10</b>                         | <b>10</b>     | 24           |
| <b>Skin</b>            | <b>5</b>                          | <b>4</b>      | 8, 9, 10, 16 |
| <b>Bone surface</b>    |                                   | <b>16.5</b>   | <b>10,00</b> |
|                        | Mandible                          | 1,3           | 1,3          |
|                        | Calvaria                          | 11,8          | 5,3          |
|                        | Cervical spine                    | 3,4           | 3,4          |
| <b>Salivary Glands</b> |                                   | <b>100</b>    | <b>100</b>   |
|                        | Parotid                           | 100           | 100          |
|                        | Submandibular                     | 100           | 100          |
|                        | Sub-lingual                       | 100           | 100          |
| <b>Brain</b>           | <b>100</b>                        | <b>60</b>     | 4, 5         |
| <b>Remainder</b>       | Lymphatic nodes                   | 5             | 5            |
|                        | Muscle                            | 5             | 5            |
|                        | Extra-thoracic airway             | 100           | 100          |
|                        | Oral mucosa                       | 100           | 100          |

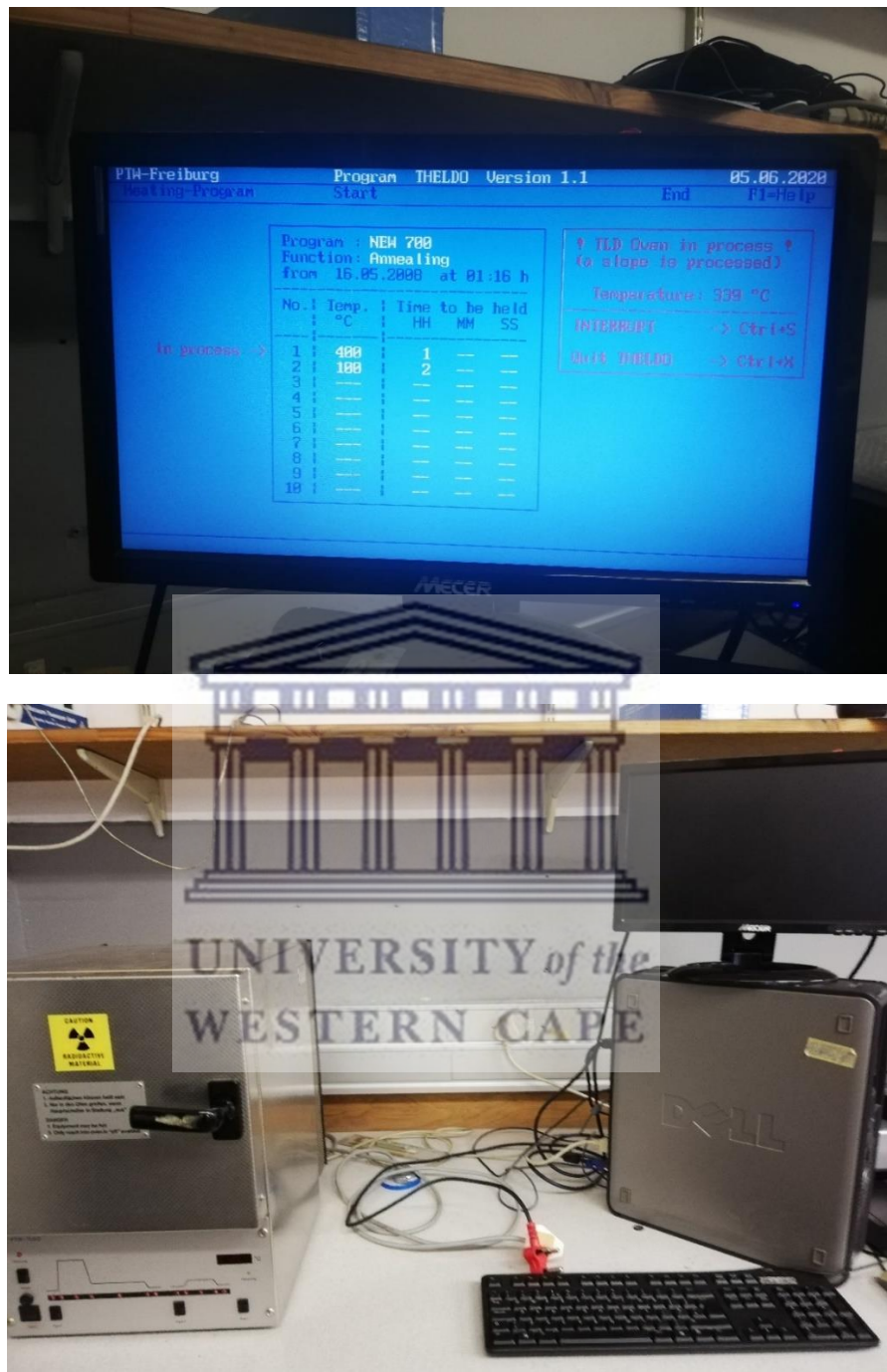


**Figure 5-2. Annealing of the TLDO chips using the PTW® TLDO® annealing oven at Groote Schuur hospital, Cape Town (top and bottom).**

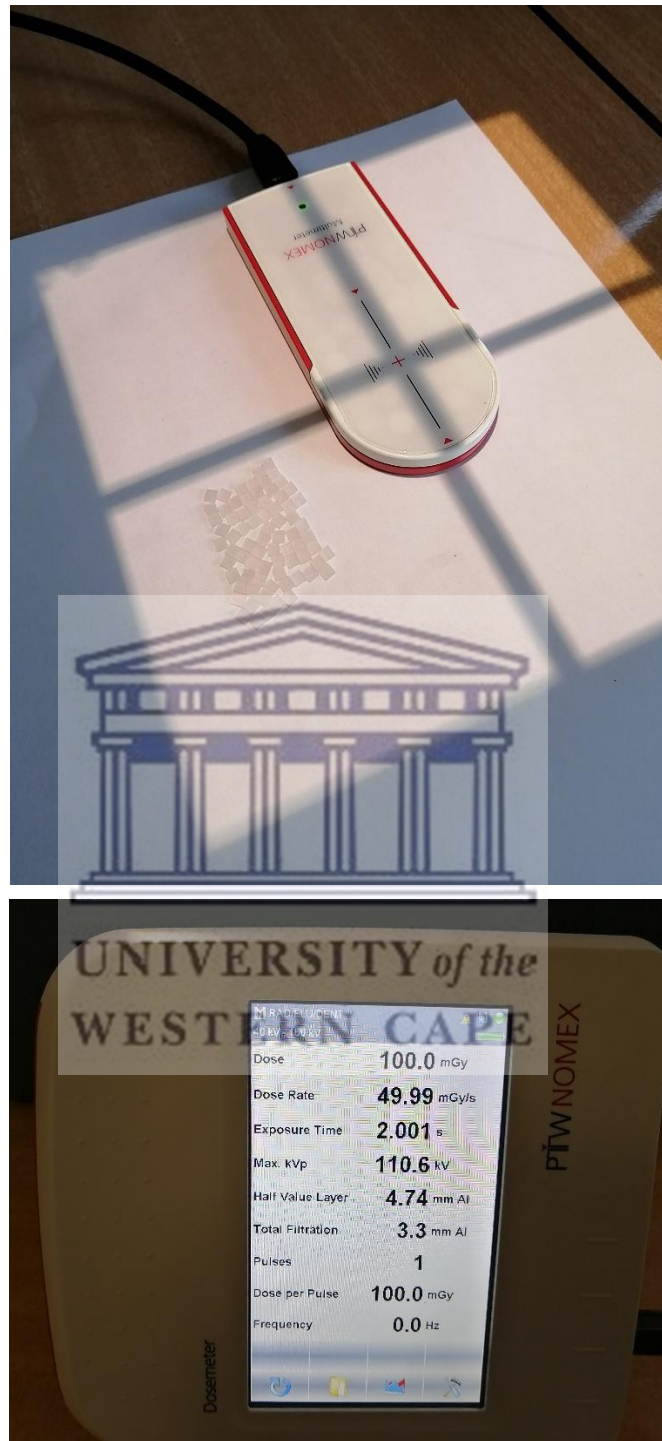


**Figure 5-3. Calibration of the TLD-700 chips at Tygerberg Hospital, Cape Town (top and bottom).**

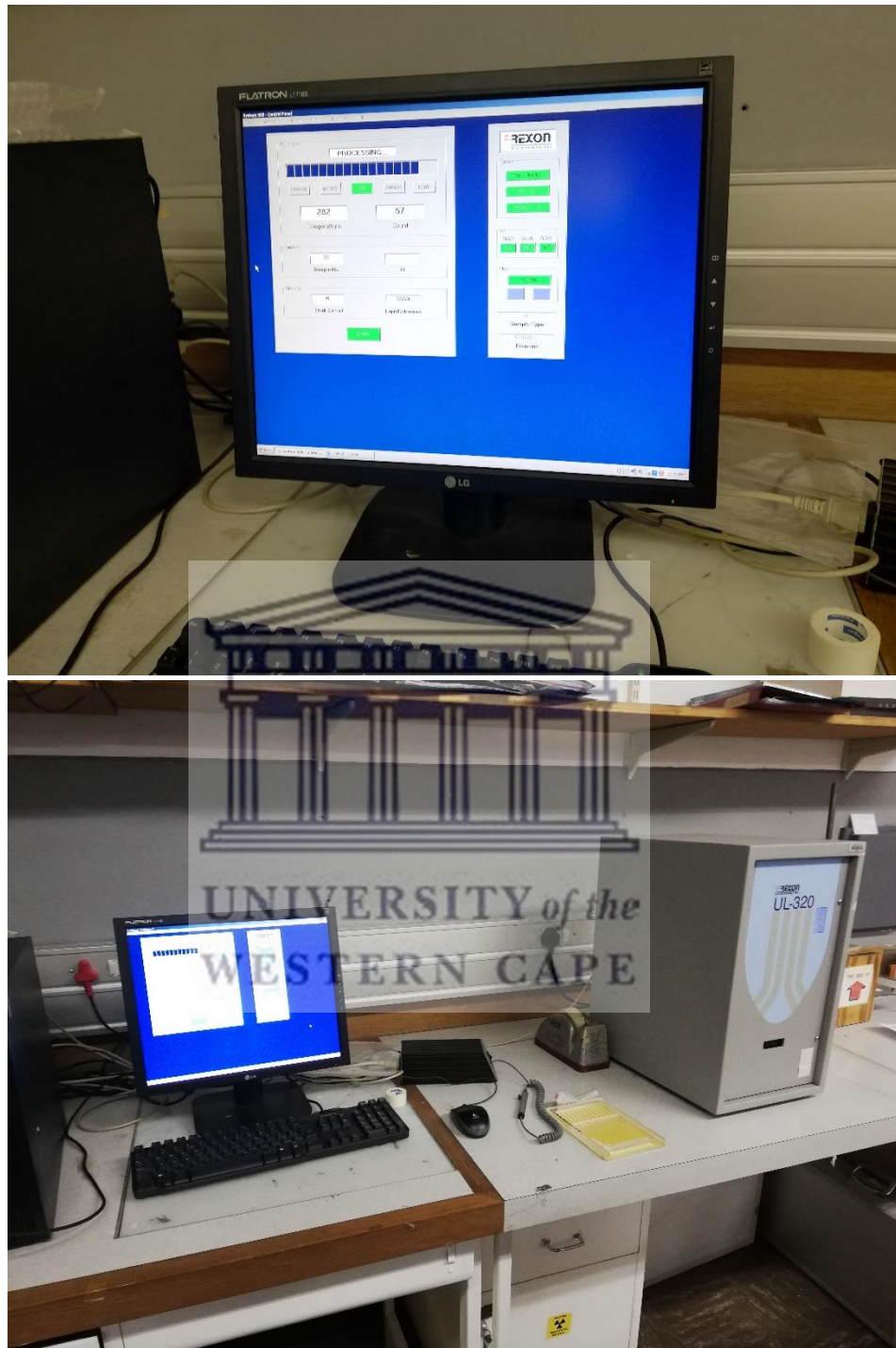


Figure 5-4. Read-out of the TLD chips using the REXON® UL-320 reader at Groote Schuur hospital, Cape Town (top & bottom).



**Figure 5-5. Preparation of the RANDO® phantom (exterior view).**

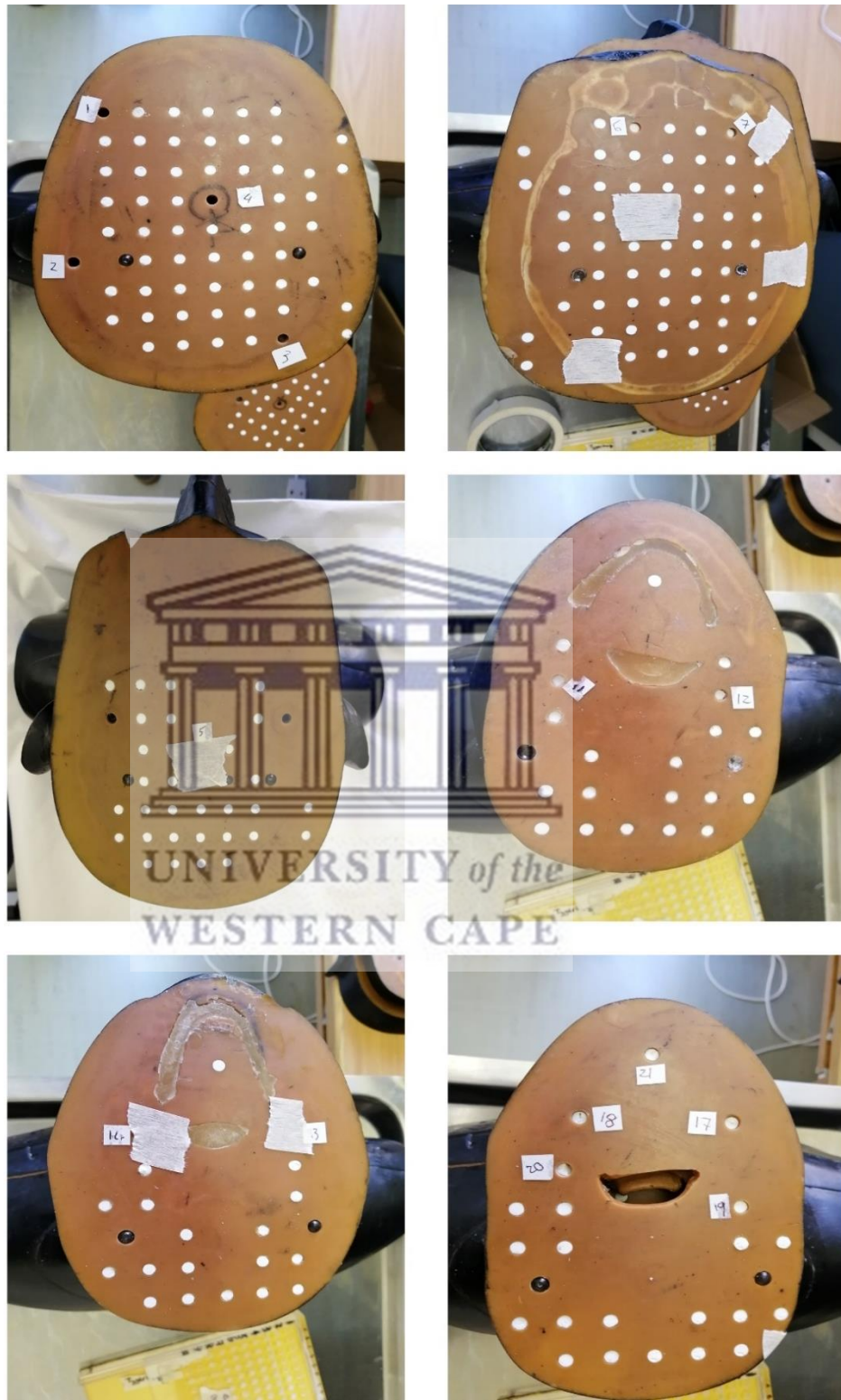


Figure 5-6. Preparation of the RANDO® phantom slabs (interior view).



**Figure 5-7. CBCT acquisition using NewTom® 5GXL at Groote Schuur hospital, Cape Town.**



**Figure 5-8. CBCT acquisition using Carestream® 8100 3D at private practice, Cape Town (A&B).**





**Figure 5-9. Conventional panoramic acquisition using Sirona® Orthophos® XG3 at Tygerberg Hospital, Cape Town.**



**Figure 5-10. Scouting x-ray image during the CBCT acquisition using the NewTom® 5GXL.**

#### 4.1.2 PHASE II: MONTE CARLO BASED SOFTWARE.

PCXMC20Rotation (Radiation and Nuclear Safety Authority, Helsinki, Finland) was used to conduct the virtual calculations of the received doses during CBCT examinations. This software simulates several tissue interactions to incident virtual x-ray beams by which predicting the received organs doses (Lee et al., 2016). The software also executes equations to calculate the effective doses using the ICRP 103 (2007) and ICRP60 weighting tissue factors.

The software can be utilized using the user-friendly graphical interface (Figure 5-11) or the supplementary Excel® application “batch mode” (Figure 5-12). The latter is linked with the main software and allows for the batch simulation of a large number of projections at once (each can be with different input values). For the NewTom® 5GXL received doses simulation, the batch mode was used simulating a bulky number of projection angles executed in each rotational acquisition.

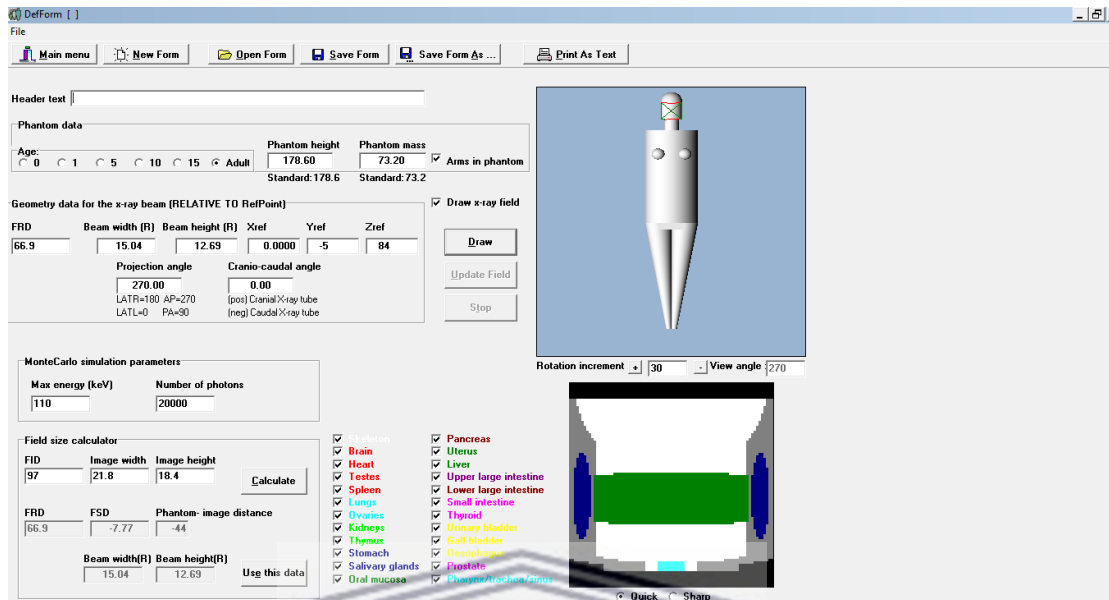


Figure 5-11. A screenshot of the “user interface” of the PCXMC software. The field size at the rotation axis was calculated using the calculator shown.

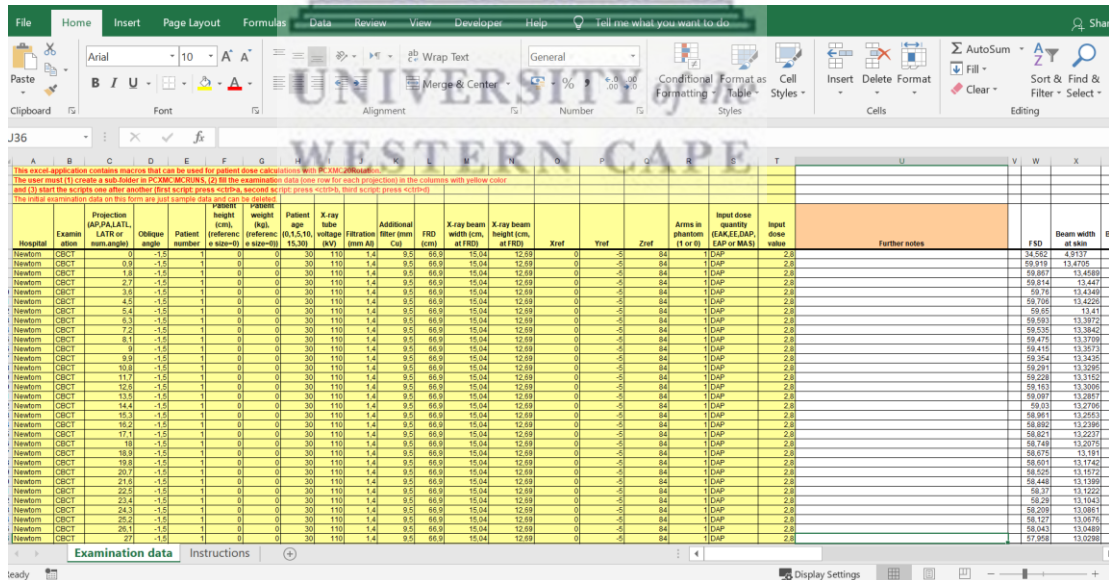


Figure 5-12. A screenshot of the Excel spreadsheet application provided with the PCXMC software allowing the simulation of large number projections at once (batch mode).

Several values were inserted into the software to commence the simulations. These input values used are further detailed in Table 5.15. The input information was acquired from the manufacturer's manual and the local authorized supplier of the x-ray machine.

**Table 5.15. Dose-determining parameters that were used for the Monte-Carlo simulations.**

| Parameter  | NewTom® 5GXL   |                             |                               |
|--|--|-----------------------------|-------------------------------|
|  | 15 × 12<br>(Standard)  | 8 × 8<br>(Standard)         | 8 × 8<br>(HiRes)              |
| Patient's age  | 30   |                             |                               |
| X-ray voltage (kVp)  | 110  |                             |                               |
| Filtration   | 1.4 mm Al (Inherent filtration) + 9.5 mm Al (Supplementary filtration) |                             |                               |
| Number of projection angles  | 400  | 400                         | 360                           |
| Number of photons  | 20000  |                             |                               |
| The oblique angle of the central ray (°)                           | -1.5   | -1.5                        | -1.5                          |
| The focus-to-reference point distance (FRD) in cm                  | 66.9   |                             |                               |
| The x-ray beam size at the reference point (width × height, in cm) | 15,04 × 12,69  | 8,14 × 8,28                 | 8,14 × 8,28                   |
| The reference points on the X-, Y-, and Z-axes                     | (0, -5, 84)  | (0, -5, 84)                 | (0, -5, 84)                   |
| Dose Area Product (DAP) reading (mGy.cm <sup>2</sup> )             | 1120.05 (2.8 per projection)   | 520,64 (1.3 per projection) | 1141.25 (3.17 per projection) |

The x-ray beam size (height and width) at the reference point (the centre of the rotational axis of the x-ray unit) for each field of view was calculated using the field size calculator provided by the software (Figure 5-11) and based on the following parameters:

- Focus-reference point distance (FRD): the distance between the focal spot of the x-ray tube and the reference point (the centre of the rotational axis). For comparison sake, the effective doses using a  $\pm 2$  cm difference of the primary used FRD value were simulated (with all other input values remained constant). Changing the FRD values will change the beam size at the reference point,

which was recalculated on the software's field size calculator and using the new values (Table 5.16).

- Focus-image receptor distance: the distance between the focal spot of the x-ray tube and the sensor.
- X-ray beam height and width at the receptor.

Different input dose quantities can be employed for the simulation including Air Kerma, Dose-area product (DAP), Current-time product (mAs). For this analysis, the machine's DAP reading was used as an input dose quantity. The x-ray machine's DAP output was indicated "passed" in the latest periodic quality control test report conducted by the local company responsible for the Quality Assurance (QA's) and acceptance tests. The DAP reading of each examination was divided by the number of projections (i.e. DAP/400 or 360). A variation of  $\pm 20\%$  of the machine DAP readings of each examination was also tested to investigate their impacts on the resultant effective doses while all other factors remained constant (Table 5.16).

**Table 5.16. Modified input values used to compare their effects on the total effective dose**

|   | Y, Z coordinates             |                              |                               |
|---|------------------------------|------------------------------|-------------------------------|
|   | -2                           | Primary value                | +2                            |
| <b>Reference points Y-axes</b>                        | -3                           | -5                           | -7                            |
| <b>Reference points Z-axes</b>                        | 82                           | 84                           | 86                            |
| <b>Dose Area Product (DAP, in mGy.cm<sup>2</sup>)</b> |                              |                              |                               |
|   | -20%                         | Primary value                | +20%                          |
| <b>DAP</b>  | 896.04 (2.24 per projection) | 1120.05 (2.8 per projection) | 1344.06 (3.36 per projection) |
| <b>Focus-reference point distance (FRD, in cm)</b>    |                              |                              |                               |
|   | -2 cm                        | Primary value                | +2 cm                         |
| <b>FRD (beam size width x height):</b>                | 64.9 (14.59 x 12.31)         | 66.9 (15.04 x 12.69)         | 68.9 (15.48 x 13.07)          |

The projection angles represent the angles where the x-ray beams project to the phantom during the rotation of the gantry (Tapiovaara & Siiskonen, 2008). The rotational radiographic techniques expose the patients from different angles (projection angles), and so the number of these projections in a full rotation angle of the machine is a required piece of information. The NewTom<sup>®</sup> 5GXL CBCT manufacturer's software shows the number of projections in the 360° rotation angle (Table 5.15).

The *X*, *Y*, *Z* reference points are arbitrarily-defined and represent the directional coordinates of the central axis of the x-ray beam projecting to the phantom (Tapiovaara & Siiskonen, 2008). The software coordinates have their origins set at the centre of the bottom trunk of the virtual phantom, where the positive values of the *X*, *Y*, *Z*-axes are directed to the left, back, and upwards, respectively (Tapiovaara & Siiskonen, 2008), further illustration is in Figure 5-13. According to the product's user guide "Choosing any point along the intended beam centre-line will give the same calculation results" (Tapiovaara & Siiskonen, 2008). The values were arbitrarily chosen by the investigator and mapped by the software interactive viewer that simulates the virtual phantom and the position of the projected radiation field (Figure 5-14). This was also conducted with reference to the actual exposed anatomical region demarcated on the previously-acquired CBCT scouting views. For comparison (Table 5.16), an additional value of  $\pm 2$  of the input values of *Y* and *Z* was also simulated (with all other factors being constant).

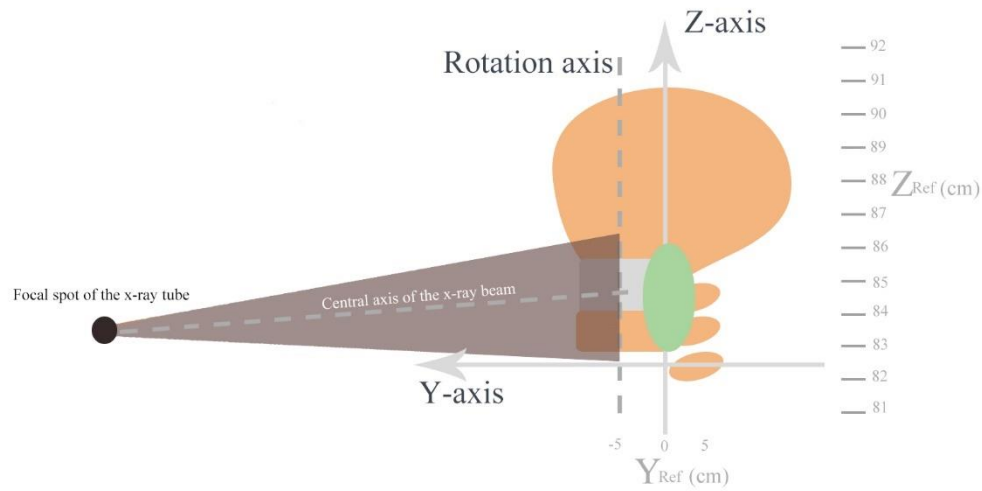


**Figure 5-13.** The Z and Y reference coordinates for the direction of the central axis of the x-ray beam. Note that the ruler in the figure is only for explanation purposes and does not represent the actual scale.

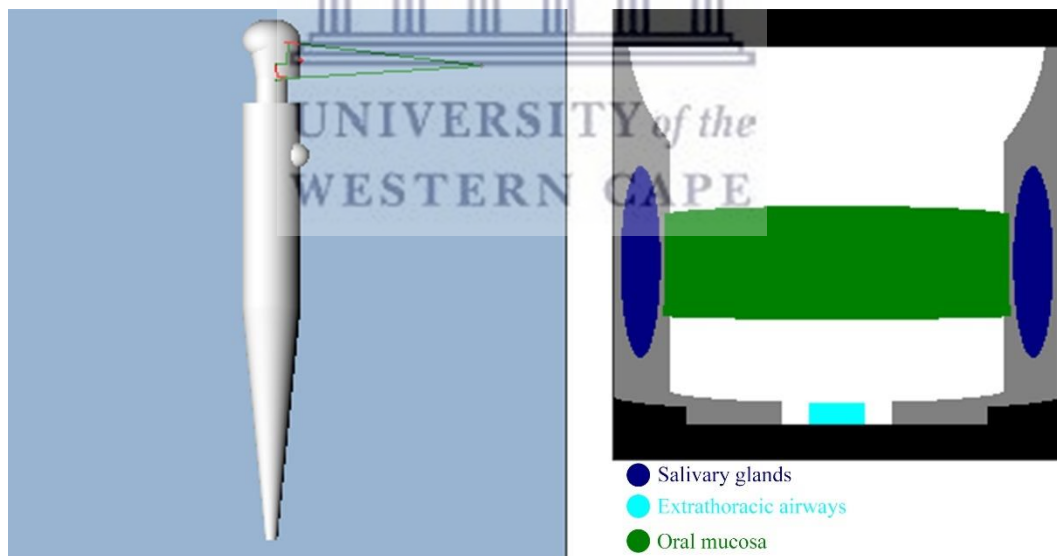


**Figure 5-14.** Interactive field viewer (in the PCXMC) showing the primary beam direction and the covered anatomical region.

The software in the batch mode (Excel<sup>®</sup> application) calculates the effective doses including those organs that are outside the main radiation domain and include adrenals, breasts, colon, gall bladder, heart, liver, kidneys, lungs, ovaries, pancreas, prostate, skeleton, spleen, stomach, testicles, thymus, urinary bladder, and uterus. As these organs/tissues were deemed to receive no dose (particularly when shielding aprons are used), the effective doses excluding the absorbed doses of these organs were calculated separately to facilitate the comparison with their counterparts obtained from the TLDs. In the excel sheet macros (application), the anode angle is set by default at “16” degrees which was modified to “15”, and the second filtration atomic number was of the Copper (Cu) element which was also changed to Aluminum (Al) with the atomic number “13”.

The NewTom<sup>®</sup> 5GXL executes two obligatory scouting views. Hence, their doses need to be considered in addition to the primary exposure dose; particularly if it would be compared with the TLDs doses that captured the scouting and the primary acquisitions together. The scouting views executed by the CBCT machine are anteroposterior (AP) and lateral skull views (Lat.). The available exposure parameters during these two exposures were the kVp and mAs, while the Air kerma and DAP readings are assigned n/a in the software (most probably due to the extremely low exposure outputs for these exposures). The averages of mAs (over five exposures) for the first scouting view (Lat.) were 0,05778, 0,05391, and 0,09504 and the second scouting view (AP) were 0,12798, 0,17739, and 0,288 for the fields of view  $15 \times 12$ ,  $8 \times 8$ , and  $8 \times 8$  (HiRes), respectively. The PCXMC (main software and not the rotational module) was used to simulate the doses of these scouting views. The software alerts the users to possible inconsistent accuracy when choosing a current-time product (mAs) as dose input quantity. Nevertheless, it was used to simulate these scouting images due to the absence of DAP readings, and the originally extremely low radiation output of such scouting exposures.

## 4.2 DATA ANALYSIS

All data were captured in Excel<sup>®</sup> (Microsoft<sup>®</sup>, WA, USA). The mathematical equations were implemented in the software for the equivalent and effective dose calculations.



## CHAPTER 5 | RESULTS

## 5.1 PHASE I: TLD RECEIVED DOSES

The calculations of Equivalent dose ( $H_T$ ) based on the average organ doses for various x-ray machines are depicted in Tables 5-17, 5-18, and 5-19. A total effective dose of 75.3, 124, 194.1 microsieverts were obtained from CBCT exams using the NewTom<sup>®</sup> 5GXL with various FOV ( $8 \times 8$ ,  $15 \times 12$ ,  $8 \times 8_{(\text{HiRes})}$ ), respectively (Table 5.17). The total effective dose revealed from the CBCT exams using the CS 8100<sup>®</sup> 3D was 101.8  $\mu\text{Sv}$  (Table 5.18), while the panoramic examination was 21.1  $\mu\text{Sv}$  using the Sirona<sup>®</sup> Orthophos XG3 (Table 5.19).

**Table 5.17. Equivalent dose  $H_T$  ( $\mu\text{Sv}$ ) of individual organs/tissues and the total Effective dose ( $E$ ) obtained from CBCT exams (using the NewTom<sup>®</sup> 5GXL).**

|  | Equivalent dose $H_T$ (in $\mu\text{Sv}$ ) |                                      |  |
|--|--|--------------------------------------|--|
|  | Field of view (FOV)                        |                                      |  |
|  | $8 \times 8$                               | $15 \times 12$                       | $8 \times 8_{(\text{HiRes.})}$         |
| <b>Bone marrow</b>                           | 25.3                                       | 96.6                                 | 57.3                                   |
| <b>Thyroid</b>                               | 300  | 560                                  | 1180                                   |
| <b>Oesophagus</b>                            | 16   | 28                                   | 68                                     |
| <b>Skin</b>                                  | 32.8                                       | 125                                  | 75.6                                   |
| <b>Bone surface</b>                          | 60.6                                       | 231.9                                | 137.5                                  |
| <b>Salivary Glands</b>                       | 2233.3                                     | 2546.7                               | 5106.7                                 |
| <b>Brain</b>                                 | 240  | 1640                                 | 372                                    |
| <b>Remainder</b>                             | 283.1                                      | 362.7                                | 669.9                                  |
| <b>Total Effective dose (<math>E</math>)</b> | <b>75.3 <math>\mu\text{Sv}</math></b>      | <b>124 <math>\mu\text{Sv}</math></b> | <b>194.1 <math>\mu\text{Sv}</math></b> |

**Table 5.18. Equivalent dose  $H_T$  ( $\mu\text{Sv}$ ) of individual organs/tissues and the total Effective dose ( $E$ ) obtained from CBCT exams (using the CS 8100<sup>®</sup> 3D).**

|                     | Equivalent dose $H_T$ (in $\mu\text{Sv}$ ) |
|---------------------|--|
|                     | $8 \times 9 \text{ cm}$ (FOV)              |
| <b>Bone marrow</b>  | 35.14                                      |
| <b>Thyroid</b>      | 340  |
| <b>Oesophagus</b>   | 16   |
| <b>Skin</b>         | 35.6                                       |
| <b>Bone surface</b> | 83.6                                       |

|                                 |                                 |
|---------------------------------|---------------------------------|
| <b>Salivary Glands</b>          | 2926.7                          |
| <b>Brain</b>                    | 204                             |
| <b>Remainder</b>                | 421.1                           |
| <b>Total Effective dose (E)</b> | <b>101.8 <math>\mu</math>Sv</b> |

**Table 5.19. Equivalent dose  $H_T$  ( $\mu$ Sv) of individual organs/tissues and the total Effective dose ( $E$ ) obtained from panoramic exams (using the Sirona® XG3).**

| Equivalent dose $H_T$ (in $\mu$ Sv) |                                |
|-------------------------------------|--------------------------------|
| <b>Bone marrow</b>                  | 7.3                            |
| <b>Thyroid</b>                      | 60                             |
| <b>Oesophagus</b>                   | 2                              |
| <b>Skin</b>                         | 5                              |
| <b>Bone surface</b>                 | 29.7                           |
| <b>Salivary Glands</b>              | 560                            |
| <b>Brain</b>                        | 12                             |
| <b>Remainder</b>                    | 98                             |
| <b>Total Effective dose (E)</b>     | <b>21.1 <math>\mu</math>Sv</b> |

The overall contribution for each organ /tissue included in the effective dose calculation for CBCT exposures is shown in Chart 5-1 (A-D), and conventional panoramic radiograph in Chart 5-2.

A) CBCT| NewTom® 5GXL| FOV: 15×12 cm

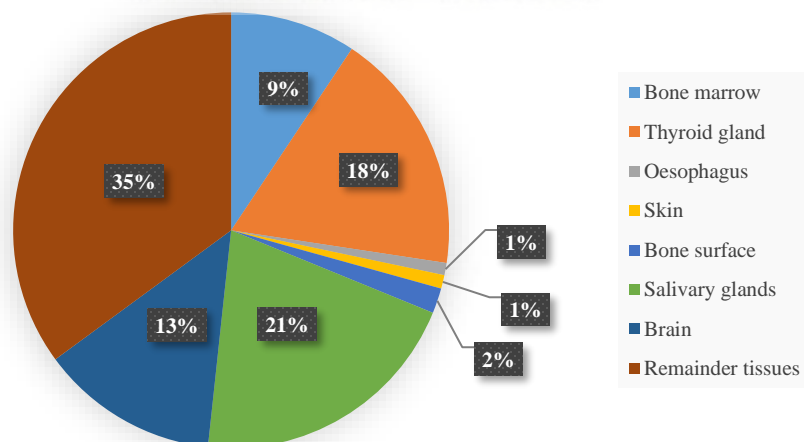
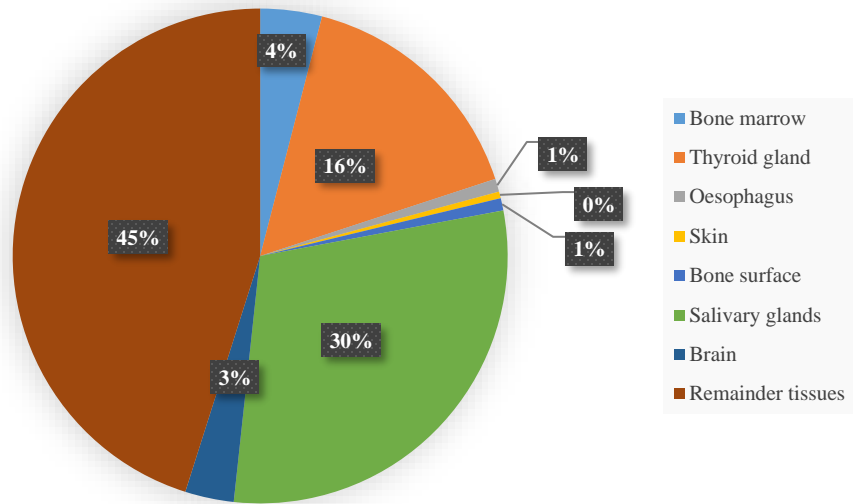


**Chart 5-1. (A-D) The contribution of various organs/tissues to the overall effective dose exposed using different CBCT and fields of view.**

B) CBCT| NewTom® 5GXL| FOV: 8×8 cm



C) CBCT| NewTom® 5GXL| FOV: 8×8 cm (HiRes)

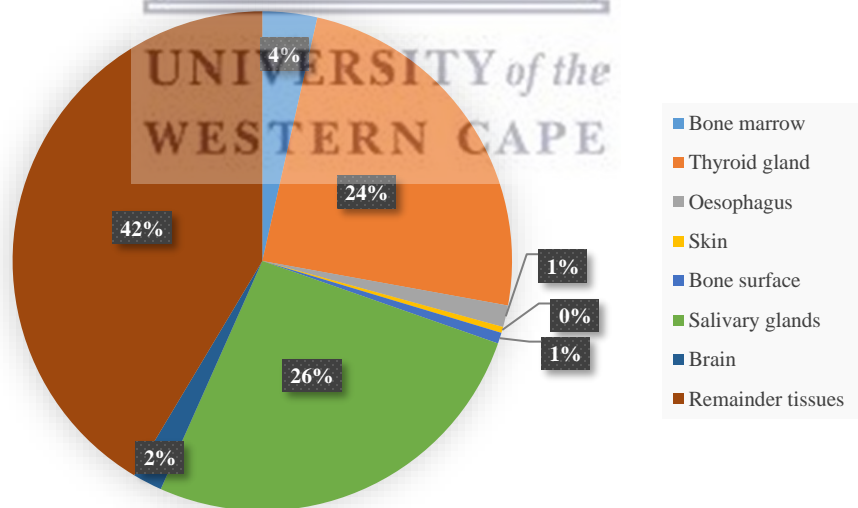


Chart 5-1. (Cont.)

D) CBCT| CS® 8100 3D | FOV: 8×9 cm

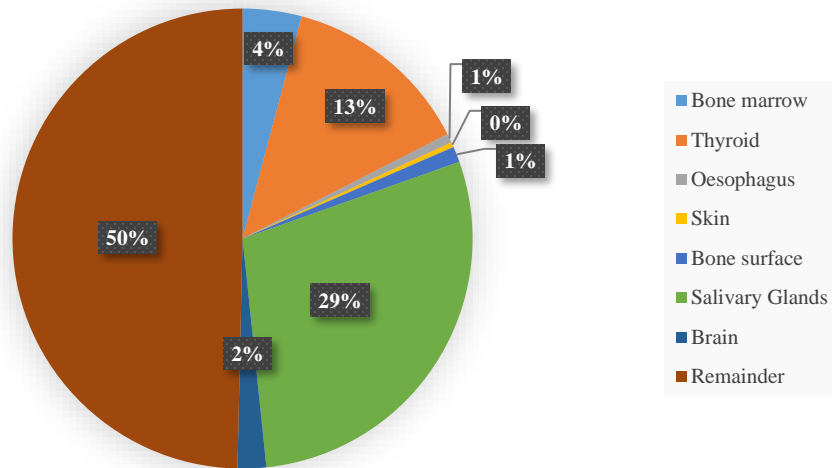


Chart 5-1. (Cont.)

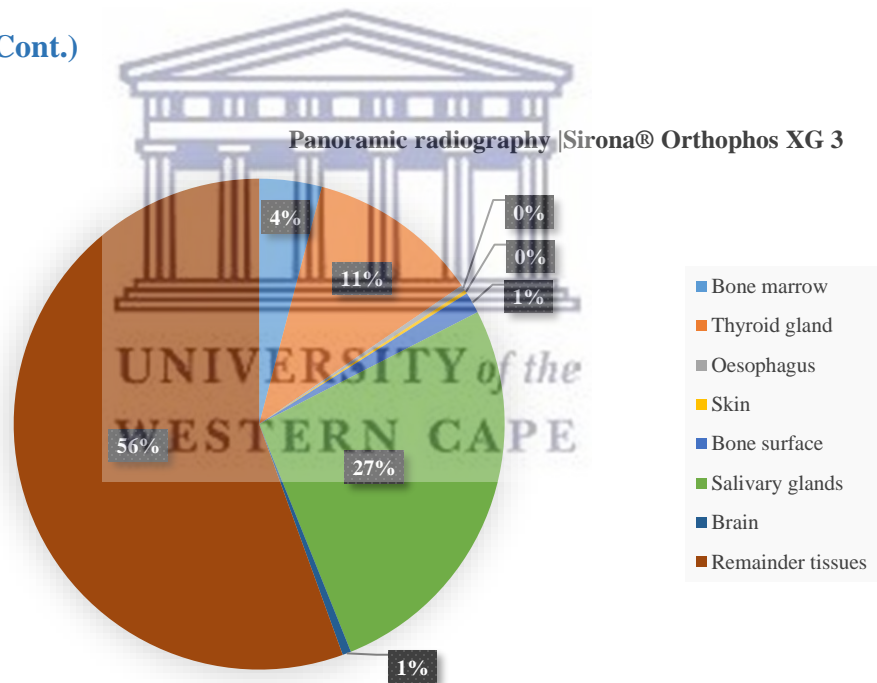
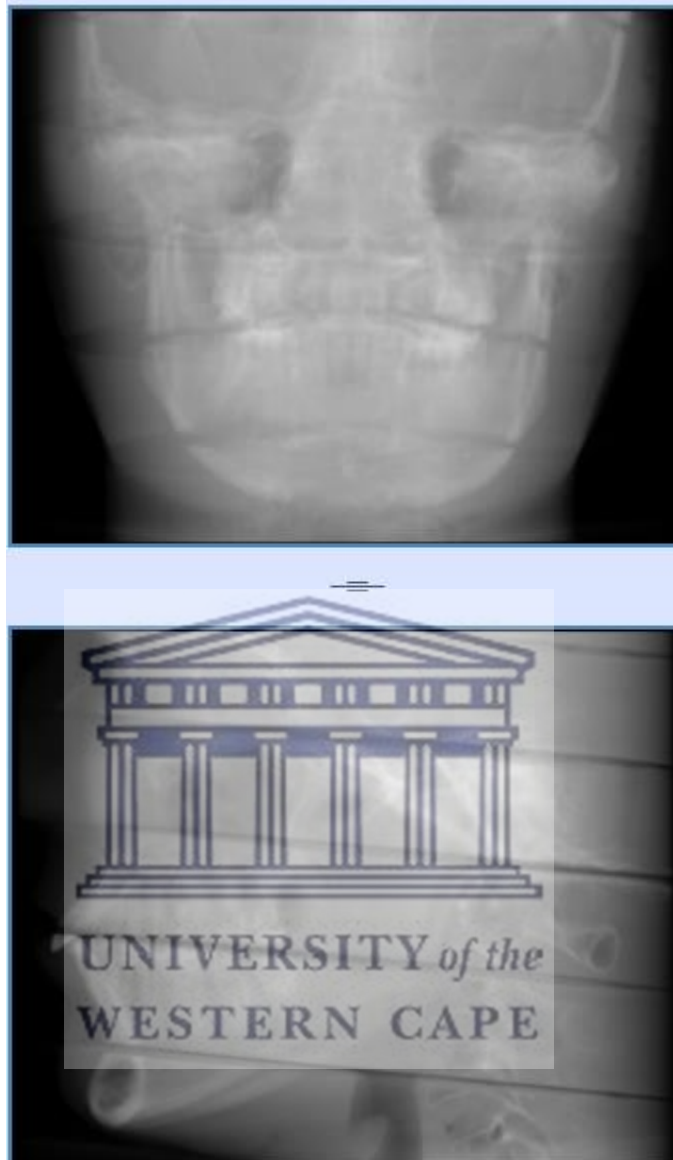
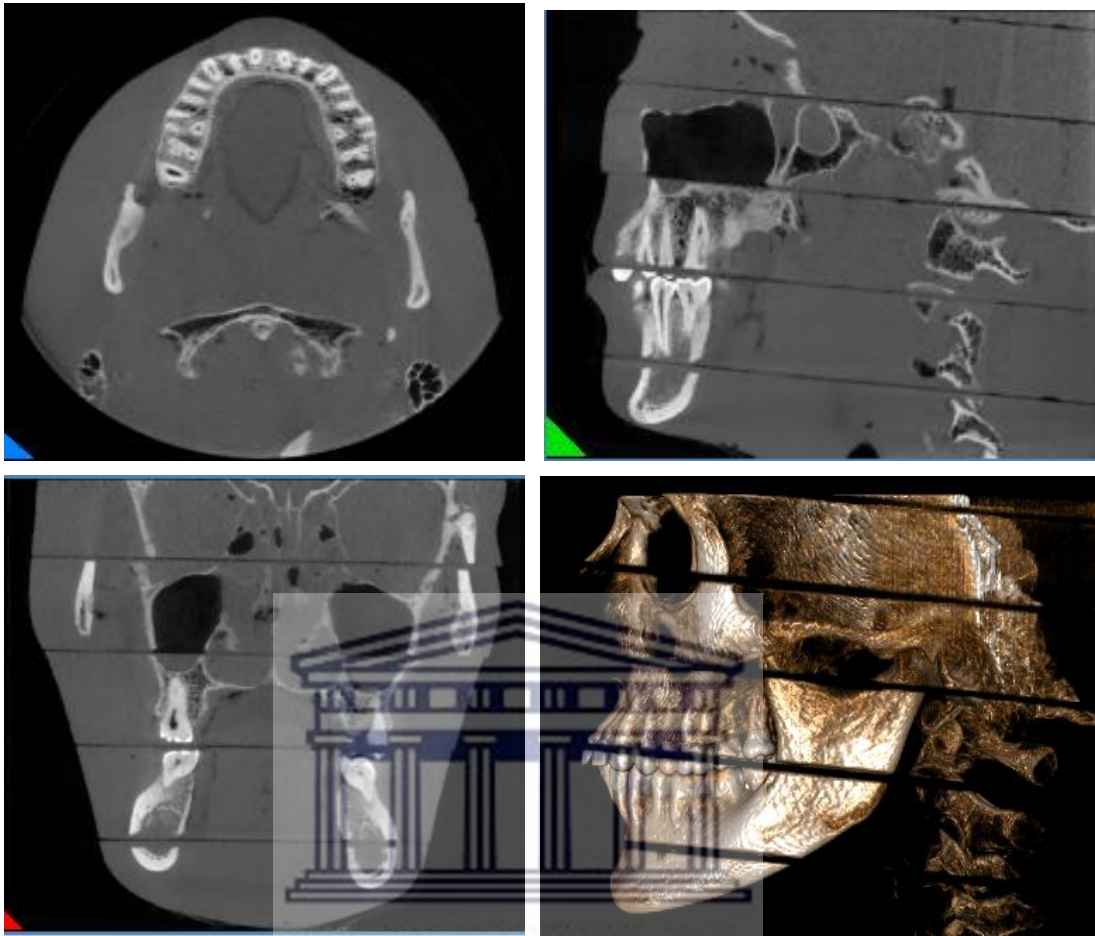


Chart 5-2. The contribution of various organs/tissues to the overall effective dose exposed during the panoramic examination.

The reconstructed CBCT volumes using the NewTom® 5GXL are illustrated in Figure 5-15 – Figure 5-20. Figure 5-21 and Figure 5-22 show the resultant reconstructed views on the CS® 8100 3D. Moreover, the acquired panoramic view is demonstrated in Figure 5-23.



**Figure 5-15.** Anteroposterior (top) and lateral cephalometric (bottom) radiographic views of the acquired CBCT volume (NewTom® 5GXL, FOV 15 × 12 cm, regular scan, and standard dose).



**Figure 5-16.** Axial slice (top left), sagittal slice (top right), coronal slice (bottom left), and 3D view (bottom right) reconstructed from the acquired CBCT volume (NewTom® 5GXL, FOV 15 × 12 cm, regular scan, and standard dose).

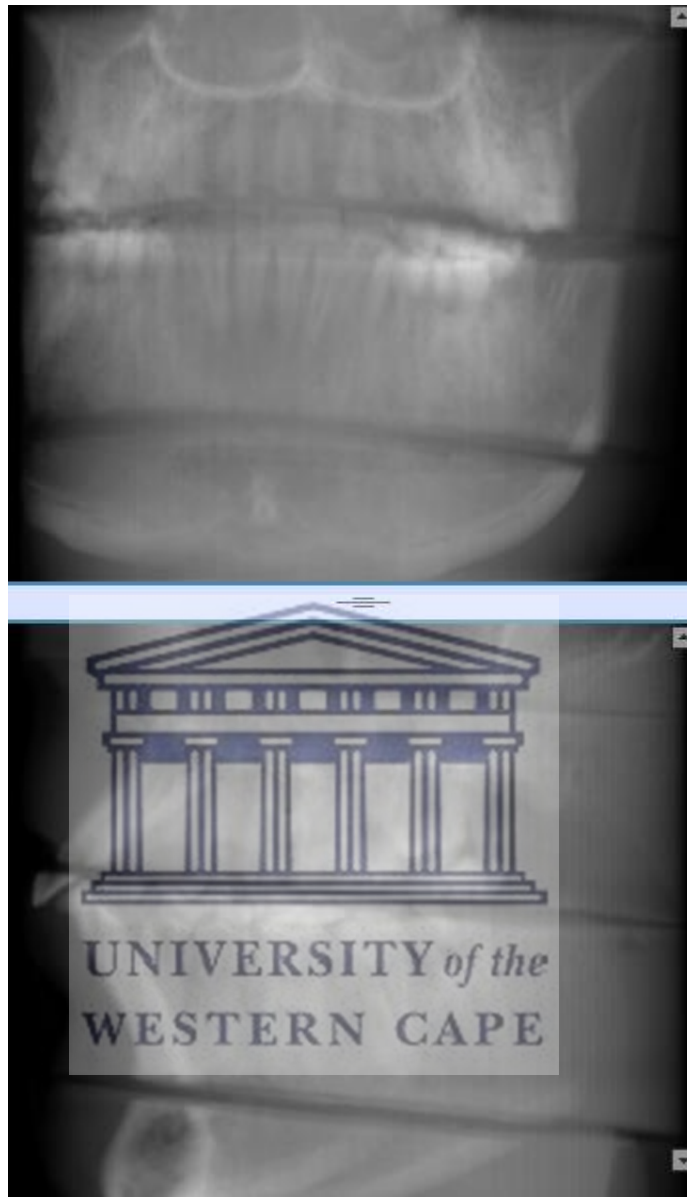


**Figure 5-17.** AP (top) and lateral cephalometric (bottom) radiographic views of the acquired CBCT volume (NewTom® 5GXL, FOV 8 × 8 cm, regular scan, and standard dose).

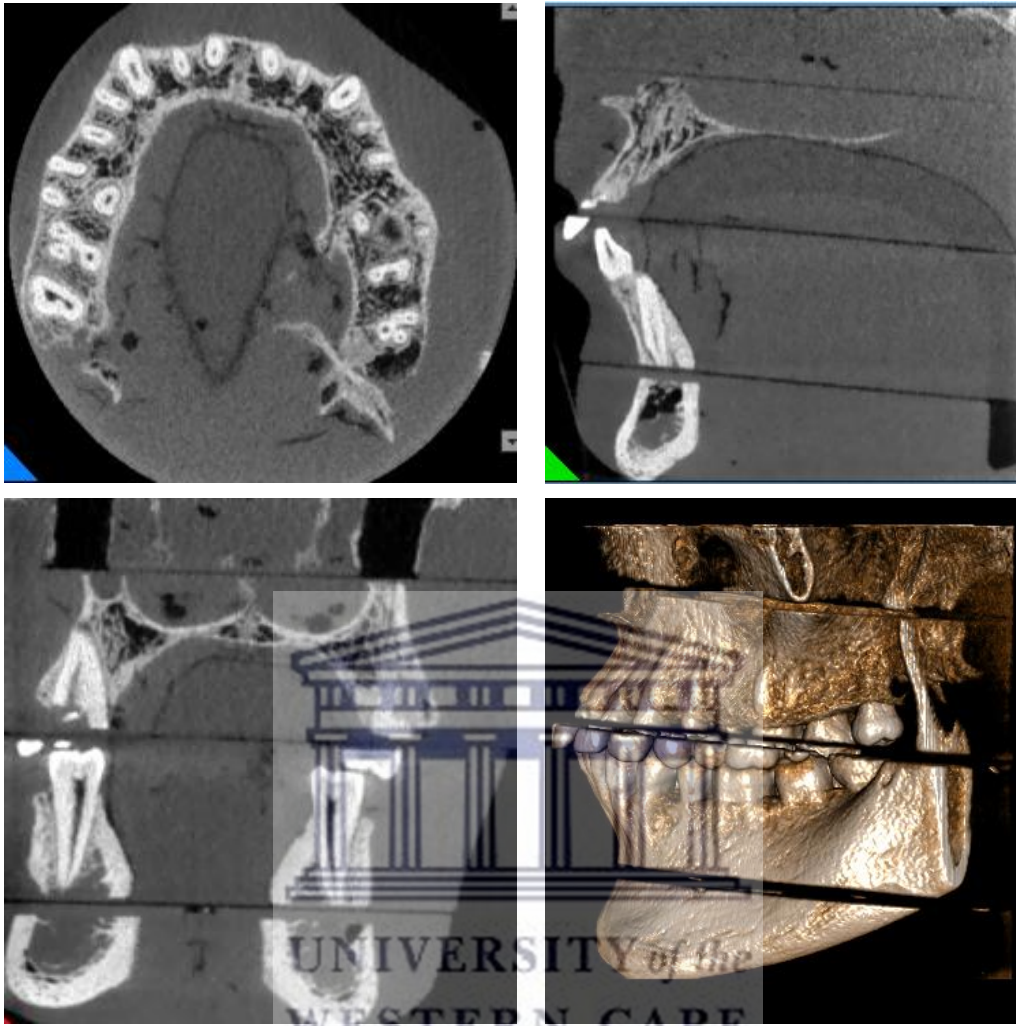


**Figure 5-18.** Axial slice (top left), sagittal slice (top right), coronal slice (bottom left), and 3D view (bottom right) reconstructed from the acquired CBCT volume (NewTom® 5GXL, FOV 8 × 8 cm, regular scan, and standard dose).



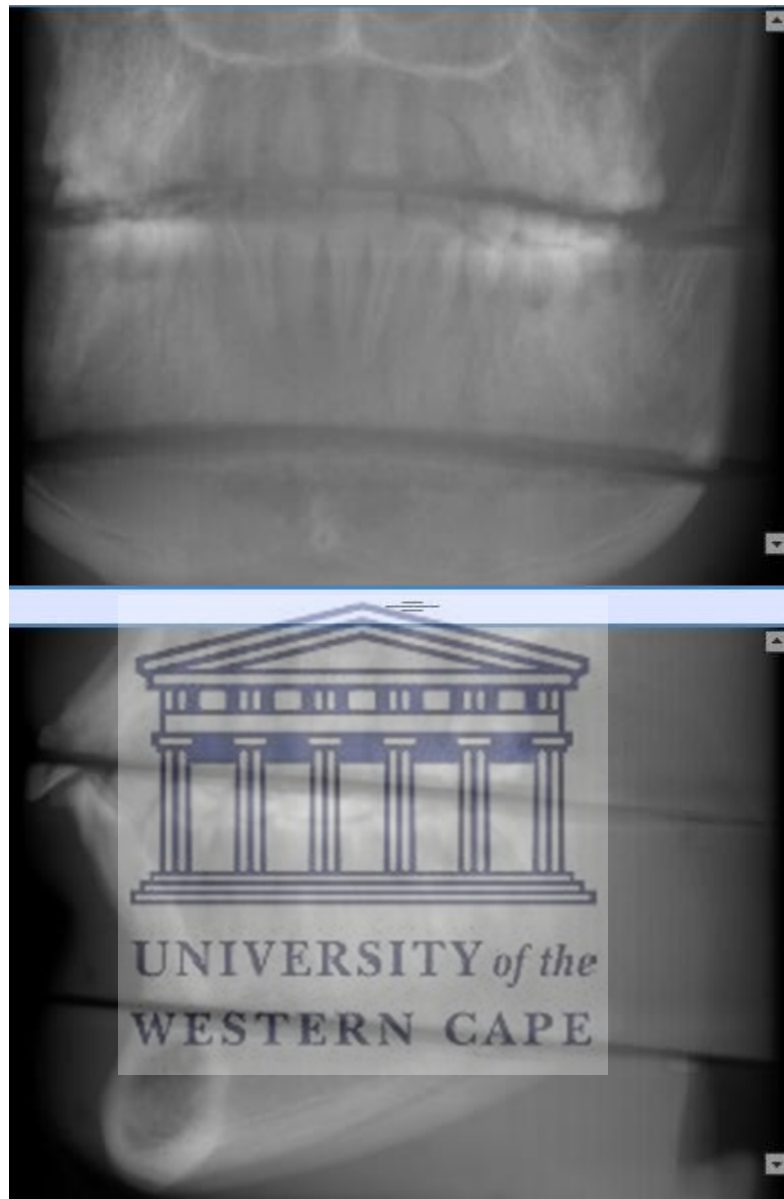


**Figure 5-19.** AP (top) and lateral cephalometric (bottom) radiographic views of the acquired CBCT volume (NewTom® 5GXL, FOV 8 × 8 cm (HiRes.), regular scan, and standard dose).

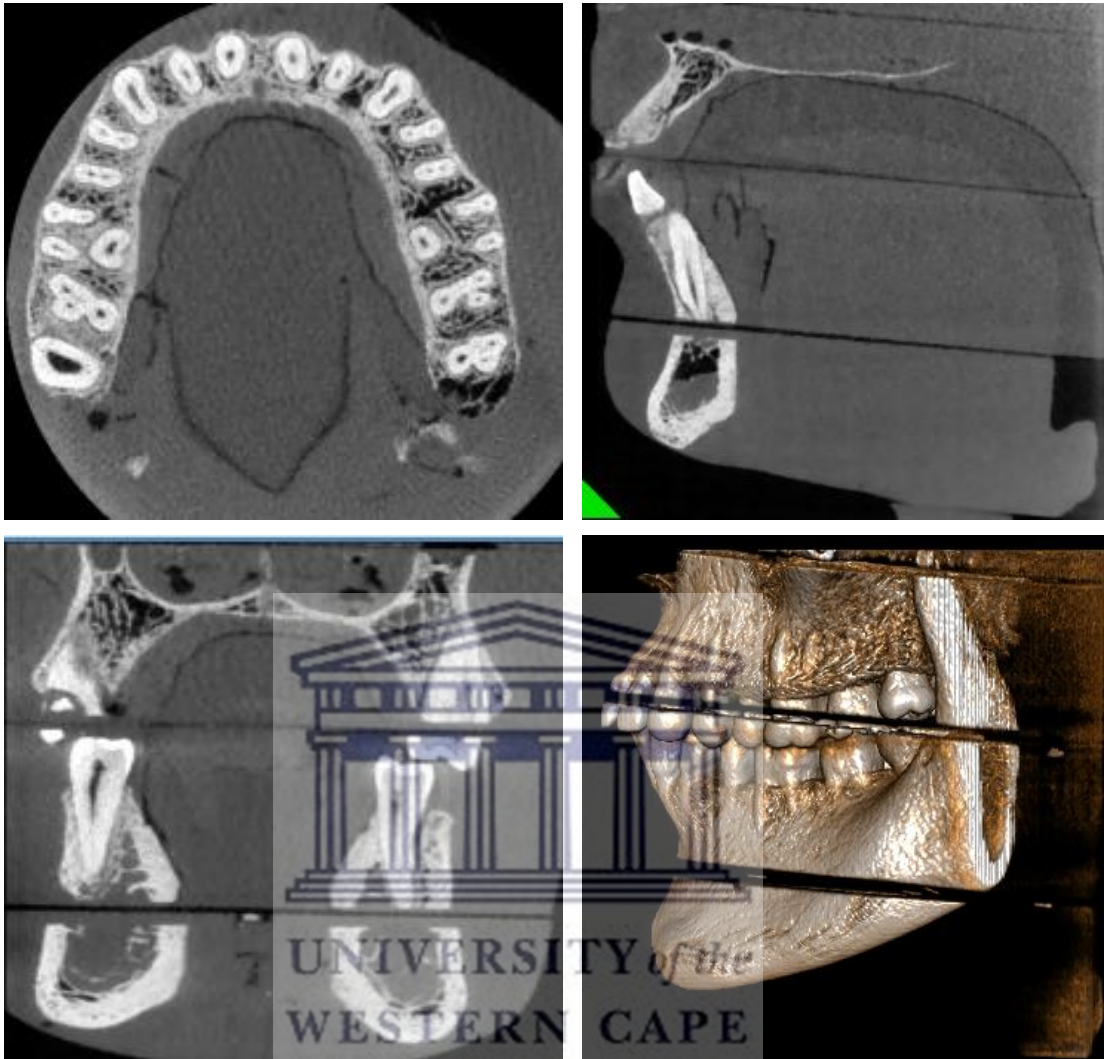


**Figure 5-20.** Axial slice (top left), sagittal slice (top right), coronal slice (bottom left), and 3D view (bottom right) reconstructed from the acquired CBCT volume (NewTom® 5GXL, 8 × 8 cm (HiRes.), regular scan, and standard dose).

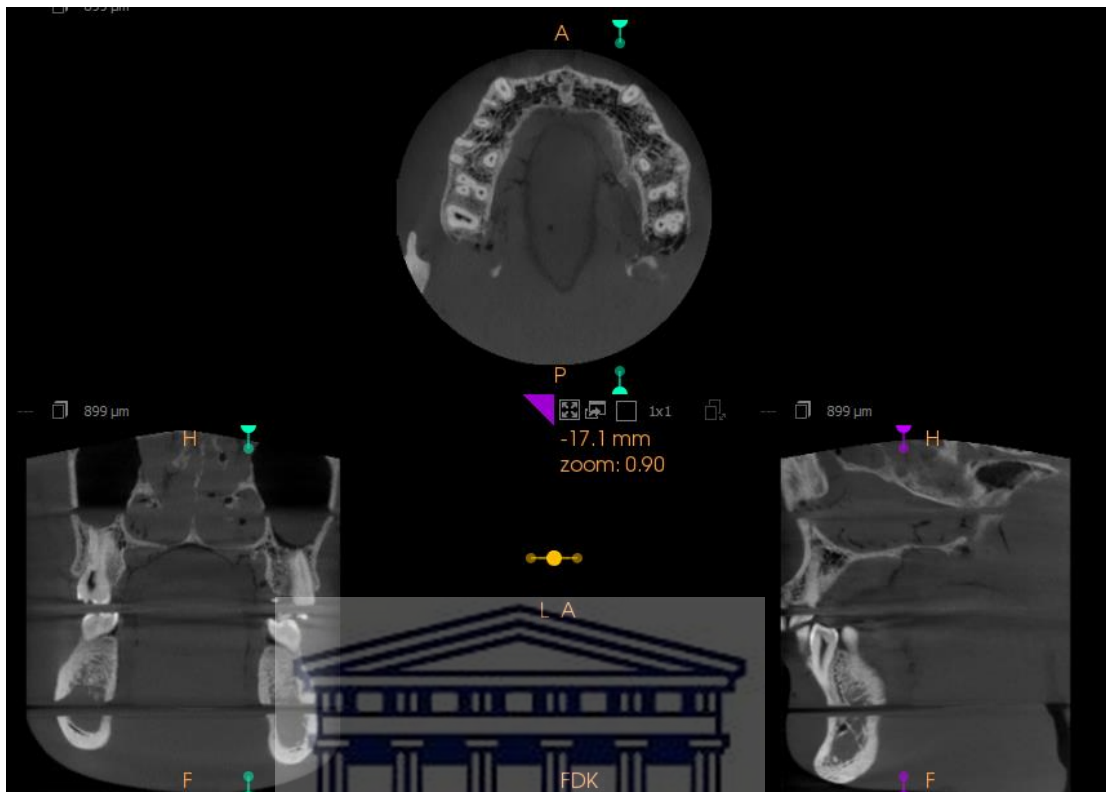


**Figure 5-21.** Axial (top), coronal (bottom left), sagittal (bottom right) slices reconstructed from the acquired CBCT volume (CS<sup>®</sup> 8100 3D, 8 × 9 cm, Full jaw program, fast scan).

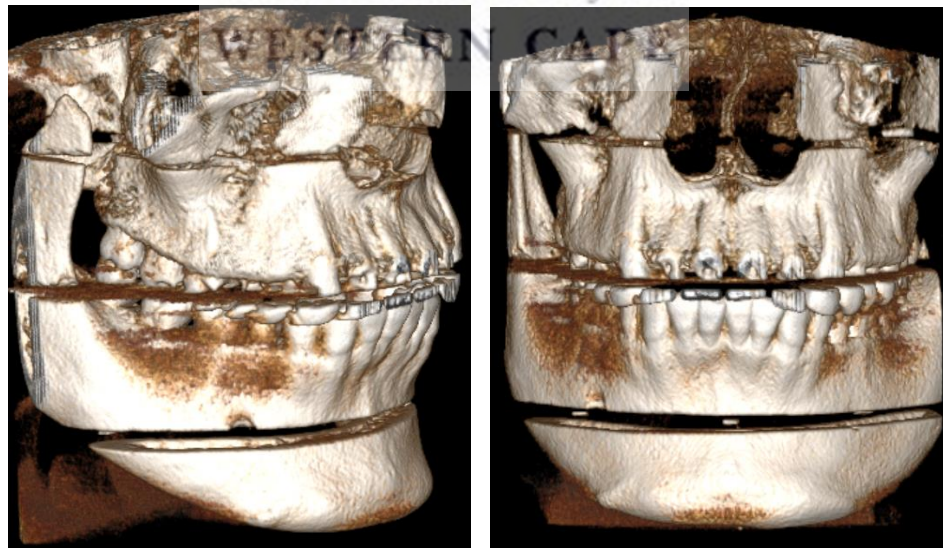


**Figure 5-22.** 3D reconstructions (side and front views) from the acquired CBCT volume (CS 8100<sup>®</sup> 3D, 8 × 9 cm, Full jaw program, fast scan).



**Figure 5-23. The resultant panoramic radiograph (using Sirona® XG3, 69 kVp, 15 mA, 13.9s).**



## 5.2 PHASE II: COMPUTER SIMULATIONS

The computer simulations conducted using the PCXMC software and according to the input values reported earlier in Table 5.15, showed very close total effective doses to their counterparts attained from the TLDs (Table 5.20, Table 5.21, and Table 5.22).

**Table 5.20. The equivalent dose ( $H_T$ ) of multiple organs/ tissues and total effective dose ( $E$ ) obtained from TLD and PCXMC simulations of the NewTom® 5GXL exposures (FOV: 15 × 12 cm).**

|                              | Equivalent dose $H_T$ (in $\mu\text{Sv}$ ) |            |             |              |
|------------------------------|--|------------|-------------|--------------|
|                              | FOV: 15 × 12 cm                            |            |             |              |
|                              | PCXMC                                      | TLD        | Difference* | %            |
| <b>Bone marrow</b>           | 37.70                                      | 96.62      | -58.93      | -60.99       |
| <b>Thyroid</b>               | 288.48                                     | 560.00     | -271.52     | -48.49       |
| <b>Oesophagus</b>            | 1.36                                       | 28.00      | -26.64      | -95.14       |
| <b>Skin</b>                  | 10.00                                      | 125.00     | -115.00     | -92.00       |
| <b>Bone surface</b>          | 90.47                                      | 231.89     | -141.42     | -60.99       |
| <b>Salivary Glands</b>       | 3702.99                                    | 2546.67    | 1156.32     | 45.41        |
| <b>Brain</b>                 | 1167.16                                    | 1640.00    | -472.84     | -28.83       |
| <b>Remainder tissues</b>     | 452.38                                     | 362.75     | 89.63       | 24.71        |
| <b>Effective dose (E) †</b>  | <b>120.1</b>                               |            |             |              |
| <b>Effective dose (E) ††</b> | <b>120.6</b>                               | <b>124</b> | <b>-3.4</b> | <b>-2.74</b> |

\*Difference:  $H_T$  (PCXMC) –  $H_T$  (TLD). Negative values indicate underestimation of the TLD values by the PCXMC. %Diff. =  $H_T$  (PCXMC) –  $H_T$  (TLD) /  $H_T$  (TLD) × 100%  
†without scouting views. ††: with scouting views included

**Table 5.21. The equivalent dose ( $H_T$ ) of multiple organs/ tissues and total effective dose ( $E$ ) obtained from TLD and PCXMC simulations of the NewTom® 5GXL exposures (FOV: 8 × 8 cm).**

|                     | Equivalent dose $H_T$ (in $\mu\text{Sv}$ ) |        |             |        |
|---------------------|--|--------|-------------|--------|
|                     | FOV: 8 × 8 cm                              |        |             |        |
|                     | PCXMC                                      | TLD    | Difference* | %      |
| <b>Bone marrow</b>  | 14.16                                      | 25.27  | -11.10      | -43.94 |
| <b>Thyroid</b>      | 130.42                                     | 300.00 | -169.58     | -56.53 |
| <b>Oesophagus</b>   | 0.60                                       | 16.00  | -15.40      | -96.26 |
| <b>Skin</b>         | 3.24                                       | 32.80  | -29.56      | -90.11 |
| <b>Bone surface</b> | 33.99                                      | 60.64  | -26.64      | -43.94 |

|   |              |             |             |             |
|---|--------------|-------------|-------------|-------------|
| <b>Salivary Glands</b>  | 2140.89      | 2233.33     | -92.44      | -4.14       |
| <b>Brain</b>  | 268.09       | 240.0       | 28.09       | 11.70       |
| <b>Remainder tissues</b>  | 395.95       | 283.08      | 112.87      | 39.87       |
| <b>Effective dose (E) †</b>   | <b>78.9</b>  |             |             |             |
| <b>Effective dose (E) ††</b>  | <b>79.12</b> | <b>75.3</b> | <b>3.82</b> | <b>5.07</b> |
| * <b>Difference:</b> $H_T(\text{PCXMC}) - H_T(\text{TLD})$ . Negative values indicate underestimation of the TLD values by the PCXMC. % <b>Diff.</b> = $H_T(\text{PCXMC}) - H_T(\text{TLD}) / H_T(\text{TLD}) \times 100\%$<br>† <b>without scouting views.</b> ††: <b>with scouting views included</b> |              |             |             |             |

**Table 5.22. The equivalent dose ( $H_T$ ) of multiple organs/ tissues and total effective dose ( $E$ ) obtained from TLD and PCXMC simulations of the NewTom® 5GXL exposures (FOV:  $8 \times 8$  cm (HiRes.)).**

|   | Equivalent dose $H_T$ (in $\mu\text{Sv}$ ) |              |               |               |
|---|--|--------------|---------------|---------------|
|   | FOV: $8 \times 8$ cm (HiRes.)              |              |               |               |
|   | PCXMC                                      | TLD          | Difference*   | %             |
| <b>Bone marrow</b>  | 31.08                                      | 57.31        | -26.23        | -45.77        |
| <b>Thyroid</b>  | 285.04                                     | 1180.00      | -894.96       | -75.84        |
| <b>Oesophagus</b>   | 1.31                                       | 68.00        | -66.69        | -98.07        |
| <b>Skin</b>   | 7.13                                       | 75.60        | -68.47        | -90.57        |
| <b>Bone surface</b>   | 74.59                                      | 137.55       | -62.96        | -45.77        |
| <b>Salivary Glands</b>  | 4701.84                                    | 5106.67      | -404.82       | -7.93         |
| <b>Brain</b>  | 588.48                                     | 372.00       | 216.48        | 58.19         |
| <b>Remainder tissues</b>  | 868.27                                     | 669.99       | 198.28        | 29.59         |
| <b>Effective dose (E) †</b>   | <b>173.1</b>                               |              |               |               |
| <b>Effective dose (E) ††</b>  | <b>173.46</b>                              | <b>194.1</b> | <b>-20.64</b> | <b>-10.63</b> |
| * <b>Difference:</b> $H_T(\text{PCXMC}) - H_T(\text{TLD})$ . Negative values indicate underestimation of the TLD values by the PCXMC. % <b>Diff.</b> = $H_T(\text{PCXMC}) - H_T(\text{TLD}) / H_T(\text{TLD}) \times 100\%$<br>† <b>without scouting views.</b> ††: <b>with scouting views included</b> |  |              |               |               |

The resultant PCXMC simulations of the scouting views were all below one micro Sievert. When the TLD values were considered as the reference, the PCXMC underestimated it by  $-3.4 \mu\text{Sv}$  ( $-2.74\%$  of the  $E_{(\text{TLD})}$ ) during the  $15 \times 12$  cm FOV acquisition, overestimated it by  $3.82 \mu\text{Sv}$  ( $5.07\%$  of the  $E_{(\text{TLD})}$ ) during the  $8 \times 8$  cm FOV exam, and underestimated it by  $-20.64 \mu\text{Sv}$  ( $-10.63\%$  of the  $E_{(\text{TLD})}$ ) during the  $8 \times 8$  cm (HiRes.) acquisition.

The individual organ effective dose was also captured and shown in detail in Table 5.23. The overall contribution for each organ/tissue included in the PCXMC effective dose calculations is shown in Chart 5-3 (A-C).

**Table 5.23. Individual organ and total (net) PCXMC effective doses ( $E$ , in  $\mu\text{Sv}$ )**

|   | Effective organ dose ( $E$ , in $\mu\text{Sv}$ ) |               |               |
|---|--|---------------|---------------|
|   | Field of view (FOV)                              |               |               |
|   | 8×8  | 15×12         | 8×8 (HiRes.)  |
| <b>Bone marrow</b>                              | 1.70   | 4.52          | 3.73          |
| <b>Thyroid</b>                                  | 5.22   | 11.54         | 11.40         |
| <b>Oesophagus</b>                               | 0.02   | 0.05          | 0.05          |
| <b>Skin</b>                                     | 0.03   | 0.10          | 0.07          |
| <b>Bone surface</b>                             | 0.34   | 0.90          | 0.75          |
| <b>Salivary Glands</b>                          | 21.41  | 37.03         | 47.02         |
| <b>Brain</b>                                    | 2.68   | 11.67         | 5.88          |
| <b>Remainder</b>                                | 47.51  | 54.29         | 104.19        |
| <b>Total Effective dose (<math>E</math>) †</b>  | <b>78.9</b>                                      | <b>120.10</b> | <b>173.1</b>  |
| <b>Total Effective dose (<math>E</math>) ††</b> | <b>79.12</b>                                     | <b>120.6</b>  | <b>173.46</b> |

†without scouting views. ††: with scouting views included

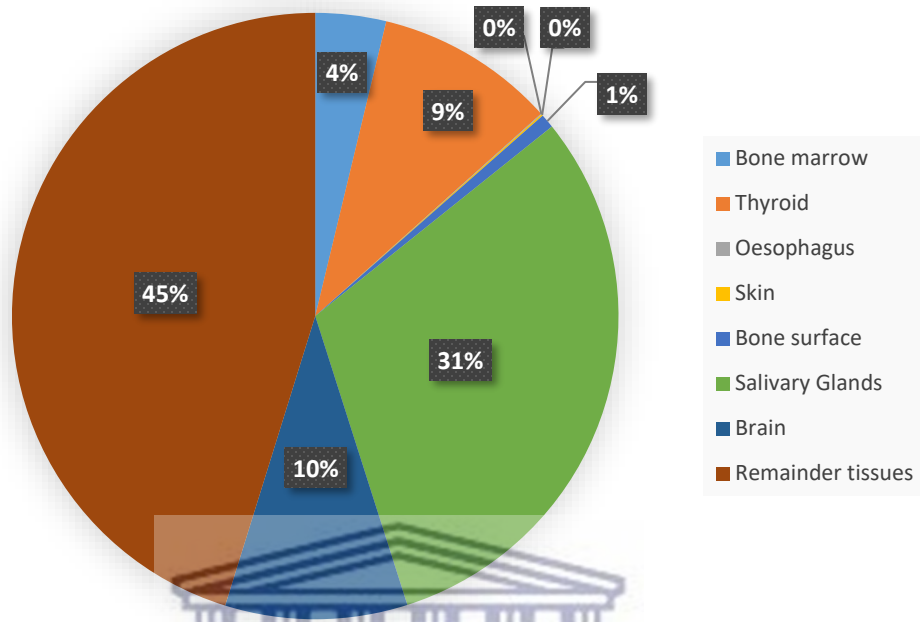
The total effective dose resulted using the primary input values (Table 5.15) was used for comparisons when modifying the Y & Z reference coordinates and FRD by  $\pm 2$  and the DAP reading by  $\pm 20\%$  (each tested separately while the other factors remained constant as the primary analysis). The net effective doses of these modified input values are shown in Table 5.24.

**Table 5.24. The resultant PCXMC effective doses in  $\mu\text{Sv}$  comparison when different input values were employed.**

| Y, Z coordinates   |                                 |                                 |                                  |
|--|---------------------------------|---------------------------------|----------------------------------|
|  | 2 points less                   | Primary value*                  | 2 points more                    |
| Reference points Y-axes  | -3                              | -5                              | -7                               |
| Effective dose $E$<br>(Difference, %)  | 127.41 (7.31,<br>6.09%)         | 120.1                           | 110.50 (-9.6, -7.99%)            |
| Reference points Z-axes  | 82                              | 84                              | 86                               |
| Effective dose $E$<br>(Difference, %)  | 127.61 (7.51,<br>6.26%)         | 120.1                           | 112.13 (-7.97, -6.64%)           |
| Dose Area Product (DAP, in mGy.cm <sup>2</sup> )   |                                 |                                 |                                  |
|  | -20%                            | Primary value*                  | +20%                             |
| DAP  | 896.04 (2.24 per<br>projection) | 1120.05 (2.8 per<br>projection) | 1344.06 (3.36 per<br>projection) |
| Effective dose $E$<br>(Difference, %)  | 96.20 (-23.9, -<br>19.90%)      | 120.1                           | 144.3 (24.2, 20.15%)             |
| Focus-reference point distance (FRD, in cm)  |                                 |                                 |                                  |
|  | -2 cm                           | Primary value*                  | +2 cm                            |
| FRD (beam size: width<br>× height):  | 64.9<br>(14.59 × 12.31)         | 66.9<br>(15.04 × 12.69)         | 68.9<br>(15.48 × 13.07)          |
| Effective dose $E$<br>(Difference, %)  | 123.28 (3.18,<br>2.65%)         | 120.1                           | 117.08 (-3.02, -2.52%)           |
| * The $E_{(\text{PCXMC})}$ (using primary value) is the total effective dose excluding the scouting views.<br><b>Difference:</b> $E_{(\text{PCXMC})}$ (using modified input value) – $E_{(\text{PCXMC})}$ (using primary input values)<br><b>%Diff.</b> = Difference / $E_{(\text{PCXMC})}$ (using primary input value) × 100% |                                 |                                 |                                  |



A| NewTom® 5GXL (FOV :15 X 12)



B| NewTom® 5GXL (FOV :8 X 8)

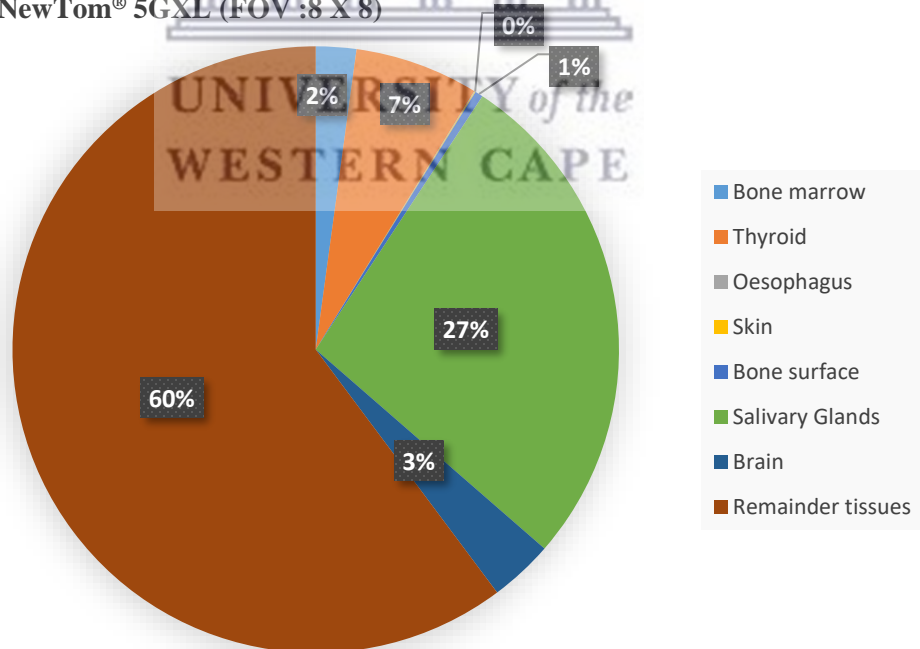


Chart 5-3. (A-C) The contribution of various organs/tissues to the overall effective dose revealed from PCXMC simulations.

C| NewTom® 5GXL (FOV :8 X 8 HiRes.)

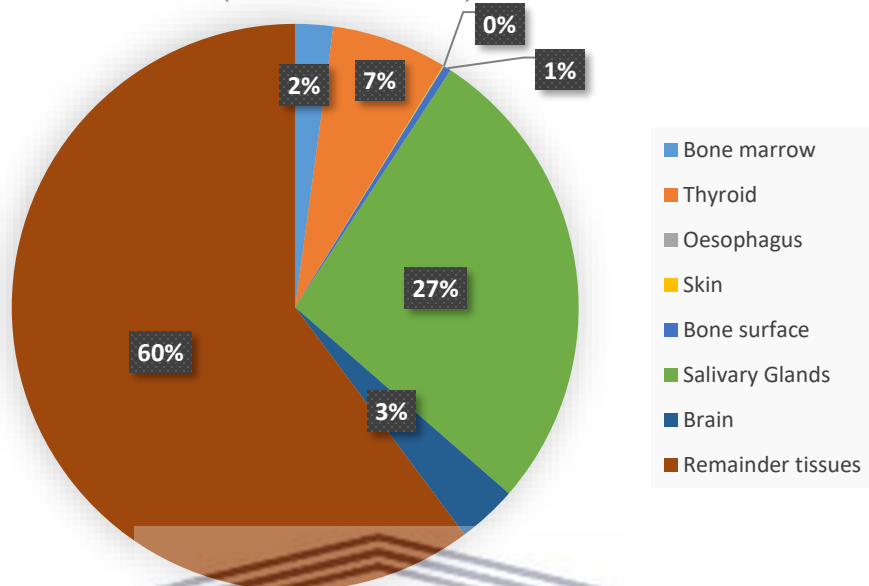


Chart 5-3. (Cont.)



UNIVERSITY of the  
WESTERN CAPE

## CHAPTER 6 | DISCUSSION

Multiple factors must be considered when interpreting the doses yielded from a CBCT acquisition. In particular, the resultant image quality, the chosen field of view, exposure parameters, and the diagnostic goal intended from an individual exposure.

When comparing doses reported from various published sources, it is imperative to consider that possible variation in these values could exist. These variations could be contributed by dissimilarities in the construction material of the phantom (since they can be made of human tissues or stimulatory material of the same densities), the soft tissue architecture, the size of the phantom head, and the variable location of the TLDs used during the exposures (Qu et al., 2010). Moreover, as the absorbed dose is an average dose, Pauwels et al., (2012) suggested that the dosimeters (i.e. TLDs) should be of greater numbers and cover multiple locations for the same organ to achieve as accurate values as possible. The authors also indicated that published doses analysed using different numbers of TLD chips must be compared with “caution” particularly if the quantity of TLDs used was smaller. A deviation by 18-28% can be encountered when a limited quantity of TLD chips are used for the estimation of organ /tissue absorbed dose (Pauwels et al., 2012). Increased filtration and kVp of the primary beam were found to decrease the possibility of the absorption of low energy x-ray and thus decrease the doses (Ludlow, 2011).

### ***Thermoluminescent dosimetry***

In all the radiographic acquisitions in this investigation (CBCT and panoramic radiograph), the remaining tissues (mainly the oral mucosa and extra-thoracic airway) ranging from 35-56%, followed by the salivary glands (ranging from 21-30%) were the major contributors to the total effective doses Chart 5-1 (A-D) and Chart 5-2. In the field of view of 15×12 cm (using the NewTom® 5GXL), the third most contributing effective organ dose to the overall effective dose was the thyroid gland by 18% and followed by the brain by 13%. These organ effective doses were reduced in the smaller FOV (8×8cm) on the same machine with the thyroid contributed by 16% and the brain

by only 3%. By contrast, using the same FOV (8×8cm) but with HiRes exposure mode, increased the thyroid contribution to 24%, where the brain dose was reduced to 2%. In 8×9 cm (FOV) using the CS<sup>®</sup> 8100 3D, the thyroid gland effective dose contribution was 13% and the brain 2%. During the panoramic examination, the thyroid contributed 11% of the total effective dose, and the brain by only 1%.

For implant planning purposes and while significantly reducing the dose, reducing the exposure parameters (e.g. scanning time, mA, rotation degree (360 or 180)) was shown not to significantly alter the diagnostic quality (Dawood et al., 2012), one exception being, if, higher quality data is needed for computer-guided surgeries (and 3D model reconstruction).

The investigator presumed that the resultant total effective doses of the CBCT and panoramic examinations studied were within the acceptable ranges of dental radiographic machines doses (Table 5.3 and Table 5.4).

While the image quality is highly influenced by the voxel size and radiation dose (e.g. the smaller the chosen voxel size is, the higher the resultant quality and dose), the identification of the diagnostic object of acquisition should be done on an individual basis. The diagnostic benefits versus the imposed risks must be considered, while attempting to maintain as low a radiation level as possible (Waltrick et al., 2013).

Using the NewTom<sup>®</sup> 5G (FOV: 8 × 8 cm, mAs: 6.76), (Nikneshan et al., 2016) found the individual organ effective doses of the thyroid, red bone marrow, and the salivary glands to be 15, 2247, 295 μSv, respectively; compared to 12, 3, 22.3 μSv, respectively, found in this study (using NewTom<sup>®</sup> 5GXL, FOV: 8 × 8 cm).

#### ***Computer simulations: PCMXC***

The use of PCXMC software offers a convenient and possibly efficient alternative method to the conventional TLD dosimetry (Kim et al., 2018). In conventional medical radiology, several reports found promising and reliable results when PCMXC

simulations were used (Bai et al., 2013; Khelassi-Toutaoui et al., 2008; Aps & Scott, 2014).

In the current investigation, it was found that the PCXMC underestimated the total TLD effective doses by 2.74 – 10.63% (of the  $E_{(TLD)}$ ) for various FOV tested. Comparison with results from the literature should be done with consideration of the various experimental settings (e.g. x-ray machines used, FOV), percentage difference calculations (based on PCMXC or TLD value), and the input values used. Nevertheless, Kim et al., (2018) found that the PCXMC effective doses were comparable but slightly underestimating the TLDs doses by 16-18% during CBCT Monte-Carlo simulations for different fields of view. Similar results were also found between PCMXC and doses captured using MOSFET dosimeters during CBCT exams (136 and 153  $\mu\text{Sv}$ , respectively) by Koivisto et al., (2012).

During the  $15 \times 12$  cm (FOV) virtual dose simulation, the PCXMC resultant equivalent doses ( $H_T$ ) were underestimating their TLDs counterparts of the bone marrow, thyroid, oesophagus, skin, and brain (Table 5.20) while overestimating the salivary glands and remainder tissues [ $H_T$  difference range: 26.6  $\mu\text{Sv}$  - 1156.3  $\mu\text{Sv}$ ]. The most notable ( $H_T$ ) differences were -95.14% and -92% (of the  $H_{T(TLD)}$ ), which were obtained from the oesophagus and skin, respectively. A possible reason for the severe oesophagus  $H_T$  (PCMXC) underestimation is the variations between the actual location of the dosimeter capturing the absorbed dose of the oesophagus and the PCXMC's location in the model under the shoulder line (Koivisto et al., 2012).

For  $8 \times 8$  cm (FOV) exposure simulation, the PCMXC and TLD equivalent doses ( $H_T$ ) of the salivary glands were very close (diff. -4.14% (of the  $H_{T(TLD)}$ )) compared with 45.41% difference found during  $15 \times 12$  cm (FOV) simulation. Yet, the oesophagus and skin showed -96.26% and -90.11% (of the  $H_{T(TLD)}$ ) differences, respectively. A comparable finding of high PCXMC underestimation of individual organ effective dose (compared to MOSFET dosimeters) of the oesophagus was also reported by Koivisto et al., (2012) during “8×8 cm” CBCT exam ( $E$ : 2.9 mSv (MOSFET) & 0.4 mSv

(PCXMC), Diff. :600 %). The absolute  $H_T$  differences in the current analysis (PCXMC vs. TLDs) ranged from 11.10 to 169,58 and the difference ranged from 4.14% – 96.62%. In the  $8 \times 8$  cm (HiRes.) exposure simulations, a significant underestimation of the oesophagus TLD equivalent dose (-98.07 %) was noted. Moreover, the absolute  $H_T$  differences (PCXMC vs. TLDs) ranged from 26.23  $\mu$ Sv to 894.96  $\mu$ Sv and the percentages of difference ranged from 7.93 % - 98.07 %.

Multiple factors contribute to the variation between the virtual and the physically acquired doses. These factors are related to variations in the methodology of the organ/tissue dose measurement, variations between the physical phantom and the virtual stimulatory model, the limited number of dosimeters to represent relatively large tissues, and variations in the fractions of each tissue irradiated used in the  $E$  calculation in each method (Koivisto et al., 2012).

Similar to results obtained from the TLDs, the remainder tissues followed by the salivary glands contributed the most to the PCXMC total effective dose ( $E$ ) in all the field of views tested (Table 5.25 and Chart 5-3 (A-C)). In addition, PCXMC underestimated the TLD individual effective dose of the thyroid regardless of the field size.

**Table 5.25. The contribution (%) of selected organs/tissues to the overall effective dose revealed from PCXMC simulations and TLDs.**

|                          | NewTom® 5GXL        |     |       |     |              |     |
|--------------------------|---------------------|-----|-------|-----|--------------|-----|
|                          | Fields of view (cm) |     |       |     |              |     |
|                          | 15×12               |     | 8×8   |     | 8×8 (HiRes.) |     |
|                          | PCXMC               | TLD | PCXMC | TLD | PCXMC        | TLD |
| <b>Thyroid</b>           | 9%                  | 18% | 7%    | 16% | 7%           | 24% |
| <b>Salivary Glands</b>   | 31%                 | 21% | 27%   | 30% | 27%          | 26% |
| <b>Brain</b>             | 10%                 | 13% | 3%    | 3%  | 3%           | 2%  |
| <b>Remainder tissues</b> | 45%                 | 35% | 60%   | 45% | 60%          | 42% |

For the simulation of panoramic radiography (although not conducted in the current study), multiple challenges have been reported. These include input values influenced

by the complicated machine geometry (as it entails tomography and scanography), the fluctuating location of the rotation axis during the examination, and the uncertain resultant beam size at the rotation axis (Lee et al., 2016). During panoramic radiography, higher effective doses (9.55% - 51.24%) were obtained from PCXMC simulations when compared with TLDs counterparts (Lee et al., 2016).

### ***The impact of different input values on PCXMC simulations***

A study (Aps & Scott, 2014) assessing the effects of various beam characterizing input values on the PCXMC's results (e.g. horizontal angulation of the beam, focus to skin distance (FSD), exposure time, and collimation) during bitewings and oblique lateral radiography. This study found a significant influence of these factors on the resultant effective doses. In the current PCXMC study, a rotational radiographic modality (CBCT) was investigated, and hence, an exact comparison to our findings might not be accurate; Nonetheless, variations in the DAP readings predominantly impacted the ( $E$ ) values in this study.

Changing the  $Y_{(ref)}$  coordinate by subtracting “2” from the absolute numerical value resulted in an increase of the total effective dose measured in PCXMC using primary input values by 7.31  $\mu\text{Sv}$  (6.09% of  $E_{(primary\ PCXMC)}$ ). When adding “2”, the opposite ensued (the  $E$  difference was -9,6  $\mu\text{Sv}$ , -7.99%). The  $Z_{(ref)}$  coordinate showed comparable findings to  $Y_{(ref)}$  modified coordinates by overestimating the primary  $E_{(PCXMC)}$  value by 6.26% when the “2” was subtracted, and underestimating it by -6.64% when the “2” was added. The overall absolute effective dose difference range [6.09% - 7.99%] is not substantial when  $\pm 2$  of the primary  $Y_{(ref)}$ ,  $Z_{(ref)}$  identified coordinates were used. In comparison to our study, changing the Z reference point from 83 to 82 and 87 cm showed an effective dose difference by  $\pm 25\%$  compared to the MOSFET readings (Koivisto et al., 2012). The authors (Lee et al., 2016) indicated that achieving reliable software readings are highly dependent on the input values. Y and Z reference coordinates influenced the effective dose during PCXMC simulations of panoramic examination (where the Y is the highest). By contrast, changing FRD alone showed

limited effect (Lee et al., 2016). Similarly, modifying the primary FRD value by  $\pm 2$  cm in this study did not reveal a significant  $E$  difference when compared with the primary  $E_{(PCXMC)}$  [2.52 - 2.65%]. It is worth noting that adding 2 cm to the FRD resulted in a lower effective dose (-2.52%). Changing the DAP reading by  $\pm 20\%$  impacted the primary  $E_{(PCXMC)}$  by 20.15% when 20% was added and -19.9% when 20% of the DAP reading was subtracted. Further investigations of the factors which dictated the software outputs were not investigated, as this was not an objective of this sub-study.





**CHAPTER 7 | CONCLUSION**

According to our findings, the effective doses ( $E$ ) received for the NewTom<sup>®</sup> 5GXL exposures depended on the field of view selected ( $15 \times 12$  and  $8 \times 8$ ), the exposure protocols (Standard vs. high resolution), and ranged from [ $75.3 \mu\text{Sv} - 194.1 \mu\text{Sv}$ ]. We concluded that limiting the beam size and choosing the “low-dose” exposure protocol, markedly reduces the effective doses. The effective dose obtained from the CS 8100<sup>®</sup> 3D ( $8 \times 9$  cm) was  $101.8 \mu\text{Sv}$ , while panoramic examination using Sirona<sup>®</sup> Orthophos XG3 resulted in an effective dose of  $21.1 \mu\text{Sv}$ .

Comparison of the radiation doses reported in the current investigation to similar published studies – which might be conducted with different clinical and experimental settings- should be conducted with caution. The doses should be interpreted with attention to the exposure factors used, the diagnostic objective, and the output quality required for a certain examination to achieve the best treatment outcomes.

The primary results of the virtual dose simulations are promising. Although the individual equivalent doses showed a greater range of variability with the TLDs (as considered as a gold standard), the total effective doses were similar. Changing the input values i.e. Z & Y coordinates, focus to reference distance (FRD), and dose-area product (DAP) are able to influence the total effective doses, with the latter being the most influential factor. Hence, proper identification of each value is a fundamental importance in order to obtain comparable and reliable results.

**Disclaimer**

The investigator declares that there is no conflict of interest and there is no relevant financial nor non-financial competing interest in any of the products/items used.

## Acknowledgements

- 1- All the staff members at the Medical Physics Department, Groote Schuur Hospital, Cape Town.
- 2- Dr Christian Traunchet, Division of Medical Physics, Faculty of Health Sciences, Stellenbosch University.
- 3- All the staff members at the department of Radiology, Groote Schuur Hospital, Cape Town, especial thanks to Ms. Nazlea Behardien-Peters.
- 4- Gendent SA, especially Mrs Gillian Swart, for her generous assistance.
- 5- AXIM – Africa X-Ray Industrial and Medical (Pty) Ltd, especially Ghrizinda van Zyl (Dental Sales Executive), to supply us with required technical specifications.



UNIVERSITY *of the*  
WESTERN CAPE



PART 6  
RADIATION PROTECTION

**CONTENTS AT A GLANCE**

|                                   |                   |
|-----------------------------------|-------------------|
| Chapter 1   Introduction          | UNIVERSITY of the |
| Chapter 2   Literature review     | WESTERN CAPE      |
| 2.1 Biological risks              |                   |
| 2.2 Radiation protection measures |                   |
| Chapter 3   Aims and objectives   |                   |
| Chapter 4   Materials and methods |                   |
| 4.1 Methodology                   |                   |
| Chapter 5   Results               |                   |
| Chapter 6   Discussion            |                   |
| Chapter 7   Conclusion            |                   |



UNIVERSITY of the  
WESTERN CAPE

**ABSTRACT**

**Aim:** To investigate the effectiveness of dose reduction of a novel head and face shield (designed by the author) during various radiographic examinations taken during implant planning.

**Materials and Methods:** An anthropomorphic phantom head with 24 TLD-700 chips was used to record the absorbed doses in 24 anatomical sites. A locally designed and modified shield was placed on the phantom, and multiple radiographic examinations were recorded including two CBCT exams ( $15 \times 12$  and  $8 \times 9$  cm FOV) and a panoramic examination. Absorbed and effective doses obtained from this analysis were captured and compared with doses attained without the shield.

**Results:** A reduction of the absorbed doses, ranging from 0.36 mGy (20.9%) to 2.4 mGy (81.3%) was observed when the shield was used during the  $15 \times 12$  cm CBCT exam. Using the same FOV, the overall effective dose was reduced by 4.94% (6.12  $\mu$ Sv). When the  $8 \times 9$  cm FOV was captured, inconsistent differences of the absorbed doses were recorded, with the overall effective dose higher by -2.3  $\mu$ Sv (-2.25%). During panoramic examinations, the absorbed doses of the tissues covered by the shield were often 0 mGy, with and without the shield and the overall effective dose was higher by 0.7  $\mu$ Sv (-3.31%).

**Conclusion:** A substantial dose reduction was achieved using the novel shield design for various critical organs/tissues, including the eye lens and the brain. This suggests the beneficial use of the shield for the field of view of  $15 \times 12$  cm. There was limited to no effect on the absorbed doses using the shield in  $8 \times 9$  cm field of view and during panoramic examinations. No effects were noted on the images' quality (i.e. artefacts) in the region of interest during all the radiographic exams performed.

**Keywords:** dosimetry, effective dose, protection shield.

## LIST OF ABBREVIATIONS AND ACRONYMS

| Abbreviation                | Description                            |
|-----------------------------|--|
| <b>(S)</b>                  | Shielded                               |
| <b>(US)</b>                 | Unshielded                             |
| <b>µm</b>                   | Micrometre                             |
| <b>µSv</b>                  | Micro Sieverts                         |
| <b>CT</b>                   | Computed tomography                    |
| <b>CBCT</b>                 | Cone beam computed tomography          |
| <b>cm</b>                   | Centimetre                             |
| <b>CS</b>                   | Carestream®                            |
| <b>DAP</b>                  | Dose area product                      |
| <b><i>E</i></b>             | Effective dose                         |
| <b>FOV</b>                  | Field of view                          |
| <b><i>H<sub>T</sub></i></b> | The equivalent dose                    |
| <b>kVp</b>                  | Kilo-voltage peak                      |
| <b>mAs</b>                  | Milliamperere-second                   |
| <b>MGy</b>                  | Milligray                              |
| <b>MOSFET</b>               | Metal oxide semiconductor field-effect |
| <b>SA</b>                   | South Africa                           |
| <b>TBH</b>                  | Tygerberg Hospital                     |
| <b>TG</b>                   | Thyroid gland                          |
| <b>TLD</b>                  | Thermoluminescent dosimeter            |

**CHAPTER 1 | INTRODUCTION**

Despite the reduced doses of CBCT acquisitions compared to the medical CT scans, these acquisitions still yield greater radiation doses compared to the conventional radiographic modalities – e.g. panoramic radiographs (Davies et al., 2012; Ludlow et al., 2003; Ludlow & Ivanovic, 2008).

The radiation dose yielded from CBCT examinations is considered a major concern worldwide, especially given that it has become, in some instances, a popular or even routine procedure (Li, 2013; Noffke et al., 2011).

The interaction of ionising radiation with biological human tissue can induce two risk types i.e. stochastic (e.g. malignancies, inheritable mutations) and tissue reactions (previously known as deterministic effects, e.g. eye cataract, xerostomia) (Harris et al., 2012). Fortunately, these deterministic effects are very unlikely to take place during dental exposures. Unfortunately, stochastic effects may occur at any level of radiation exposure (Harris et al., 2012; White & Pharoah, 2013).

There is no agreement on the threshold of safe radiation dose, as any dose has the potential to induce stochastic effects (Halboub et al., 2015; Abbott, 2000). For this reason, clinicians have an ethical responsibility to reduce the radiation exposure to the minimum, while justifying each radiographic acquisition with strict employment of the ALARA (as low as reasonably achievable) principles (Abbott, 2000).

Brain, oesophagus, and salivary glands are mentioned as organs with possible risk for cancer development (Attaia et al., 2020). In addition, the eye is highly sensitive to radiation, and various detrimental effects, such as cataracts which can arise after exposures to doses ranging from 0.5 to 2 Gy in adults and almost half this range in young children (Mukundan et al., 2007). Fortunately, dental radiology yields dose far lower than these detrimental ranges, nonetheless, every effort should be made to protect these organs, which might unnecessarily be exposed during radiographic examinations.

In this chapter, a novel shield designed and developed by the author which encloses the orbits and the upper part of the head was tested for its ability to reduce radiation dose. The effect of using such a shield on absorbed doses of various anatomically sensitive sites was tested using different fields of view and radiographic modalities – i.e. CBCT and panoramic radiography. Moreover, the radiographic images obtained were analysed for any possible radiographic artefacts (e.g. metallic artefact) which would have interfered with the analysis of the region of interest intended for implant planning.



## CHAPTER 2 | LITERATURE REVIEW

## 2.1 BIOLOGICAL RISKS

The deterministic effects (or tissue reaction) can lead to cellular death and alterations in the structure and functions of organelles inside the cell (Harris et al., 2012; White & Pharoah, 2013). This type of radiation effect is dose-dependent, with the severity of the impact increases with the dose delivered (Harris et al., 2012; White & Pharoah, 2013). Examples of deterministic effects include xerostomia, cellular death, osteoradionecrosis, eye cataract, effects on fetal development, and erythema on the skin (Harris et al., 2012; White & Pharoah, 2013).

Stochastic effects are caused by an irreparable defect in the genetic deposition of a cell, which leads to the formation of cancers or heritable mutation (White & Pharoah, 2013). Unlike the deterministic effects, these effects have no minimum dose limits to be induced, but the risk of its occurrence is proportional to the dose delivered (Harris et al., 2012; Lin, 2010).

The estimation of relative biological damage/risk (e.g. stochastic effects) after exposure to radiation can be presented numerically by the effective dose value ( $E$ , in Sieverts) (European Commission, 2012; Harris et al., 2012; White & Pharoah, 2013). This value determines the possible biological risk to the equivalent whole-body dose (European Commission, 2012). Several factors are considered during the calculation of this value and include the type of radiation, the organs radiated, the doses delivered, and the radio-sensitivity of each tissue (using a unique tissue-weight factor) (Harris et al., 2012; Shin et al., 2014). Although this value does not necessarily reflect the radiation risk of individual patients (since variation in age, gender, and genetic radiation sensitivity play an influential role), it is considered a reliable measure to compare various radiographic modalities and exposure protocols (Kim et al., 2018).

Fortunately, the doses that dental units operate in are far too small to induce deterministic effects, but not stochastic effects (Harris et al., 2012; White & Pharoah,



2013). Typically, a person is already exposed to average background radiation of 2.4 mSv (Harris et al., 2012) - 3.1 mSv (White & Pharoah, 2013) per year, particularly from radon gas and terrestrial and space radiation. Medical exposure averages about 3 mSv per year, with dental exposure contributing as little as 0.26% (0.007 mSv) (White & Pharoah, 2013).

---

### 2.1.1 CANCER RISK FORMATION

The data acquired on cancer formation induced by radiation were mainly attained from the survivors of the Japanese atomic bomb (main source) and from groups introduced to radiation due to medical, environmental and occupational reasons (Little et al., 2009).

Biological harm begins after the creation of hydroxyl radicals subsequent to ionising the cellular water atoms by x-ray radiation. These radicals might engage with the deoxyribonucleic acid (DNA) of the cell resulting in impairments in its strands or bases. On the other hand, the x-ray radiation can act instantly on the DNA (direct ionisation) (Lin, 2010). While most post-radiation cellular injuries are counteracted by the cellular reparative mechanisms, an incompetent repair can result in mutation in the cellular DNA, gene fusion, and chromosomal translocation, thus inducing cancer (Brenner & Hall, 2007). The effects of these cellular damages (i.e. cancers) can manifest from 5, 10 and 20 or more years after the radiation exposure (Berrington De González et al., 2009; Amis et al., 2007).

Radiation doses higher than 100 millisieverts provides compelling evidence of increasing the risk of cancer development (Lin, 2010; Council, 2006; Tubiana et al., 2009), while being contentious in the dose ranges of 10 to 100 millisieverts (Lin, 2010). Although there is a lack of “direct epidemiological data” indicating the increased risk of cancer development at doses less than 10 millisieverts (due to statistical insufficiency); this does not signify the lack of risk (Verdun et al., 2008).

### 2.1.1.1 THE LINEAR NO-THRESHOLD (LNT)

LNT is a model used by radiation protection authorities to evaluate the risks of low dose radiation exposures based on risk levels established using a high level of radiation doses (Tharmalingam et al., 2019). The excess cancer risk is then proportional to the delivered dose, including low and high dose exposures according to the LNT theory (Lin, 2010). Though controversial, due to the absence of any other theory which proves the risk of low dose radiation, the LNT is nevertheless, even in the absence of any actual data to support it, widely used (by extrapolation) (Lin, 2010).

While in this model (LNT) every exposure, including minute doses, are deemed detrimental (i.e. no safe dose), research in modern radiation and molecular biology indicates opposing evidence on the accurate risk estimation using LNT on the health effects of low-dose radiation (Tharmalingam et al., 2019). According to Tharmalingam et al. (2019), the evidence provided on cancer formation due to low radiation doses is minuscule.

Spreading panic in respect of cancer formation due to diagnostic radiation based on disputable hypotheses is “unethical” and “unjust”. Particularly, since this is not based on any scientific background, and that cancer formation risk is clinically negligible (if it occurs) based on established carcinogenesis dose thresholds (Tubiana et al., 2009).

Albeit the controversy in the literature regarding the carcinogenic threshold of low dose exposures, the “risk of excess cancer mortality” due to single diagnostic imaging is not proven (Lin, 2010).

## 2.2 RADIATION PROTECTION MEASURES

A bismuth-impregnated latex on a foam pad was used as an eye shield in a study by Mukundan et al. (2007). The authors (2007) assessed the effect of this shield on dose reduction during CT, using a metal oxide semiconductor field-effect transistor (MOSFET). The shield covered the outer side of the orbits and reduced the absorbed

dose to the orbits from 46 to 28 mGy and 29 to 21 mGy to the eye lens. Moreover, radiographic artefacts induced by the shield were not found to degrade the diagnostic quality of the region of interest.

McLaughlin and Mooney (2004) assessed the effect of a commercially available eye and thyroid shield on dose reduction during CT scans *in vivo* (on 40 patients). The mean absorbed dose reduction was from 6 to 4.9 mGy to the eye and from 16.4 to 7.1 mGy to the thyroid gland.

In the same way, bismuth-based eye and thyroid shields were used (14×3.5×0.32 cm and 15×8.5×0.48 cm) during CT scans on phantoms (Lee et al., 2010). The absorbed dose to the eye was 16.91 mGy without the shield and was reduced to 12.44 mGy with the shield on, while the absorbed dose to the thyroid was 17.81 mGy and was reduced to 13.69 mGy.

The effective dose is influenced by the doses received by the thyroid glands (TG), though it is minimal compared with salivary glands and the brain. Proper positioning of the patient during CBCT acquisitions should expose the TG to only scattered radiation, and hence reduce the dose received (Hidalgo et al., 2015).

Hidalgo et al. (2015) examined the effect of a TG shield during CBCT acquisitions using a pediatric anthropomorphic phantom head. The researchers also assessed the effect of different shield designs on the doses received by the TG. It was found that those shields significantly reduced the received dose compared to without shielding. No significant difference was evident between various shield designs. A similar conclusion concerning effective dose reduction using the TG shield, were reported by Tsiklakis et al. (2005).

Qu, G Li, et al. (2012) tested the impact of thyroid shields on the individual average tissue-absorbed dose and the overall effective dose. The doses were tested in the following scenarios:

- No shield.

- One shield placed loosely anterior to the neck,
- Two shields placed loosely anterior and posterior to the neck,
- One shield tightly fitted anterior to the neck.
- Two shields tightly fitted anterior and posterior to the neck.

The results showed that the examination where the shields were tightly placed (one or two shields) revealed the most significant dose reduction. The loosely-fitted thyroid shields resulted in comparable doses received without the shield.



## CHAPTER 3 | AIMS AND OBJECTIVES

### 3.1 AIM

To investigate the dose reduction effect of a novel design of modified head shield which can be used during CBCT and panoramic radiographic examination.

### 3.2 OBJECTIVES

- 1- To capture the absorbed organ doses received with the shield in place using different CBCT units (with different fields of view) and a panoramic x-ray machine.
- 2- To compare the absorbed doses with the shield, with counterparts without a shield.
- 3- To obtain and compare the effective doses between the radiographic acquisitions with and without shields.
- 4- To evaluate the effect of the shield on the quality of the rendered radiographic images.

### 3.3 RATIONALE

- 1- To the best of the author's knowledge, it is thought that such an exact shield design has not been reported in the literature.
- 2- The impact of this modified shield on the radiation doses received during the radiographic examinations performed during implant therapy will be of significant benefit if it proved efficient:
  - It may protect the patients from unnecessary radiation, particularly those who undergo radiographic acquisition where exposure to the orbit and cranium is unavoidable.
  - It can be manufactured/fabricated at reasonable costs when compared to other measures.

## CHAPTER 4 | MATERIALS AND METHODS

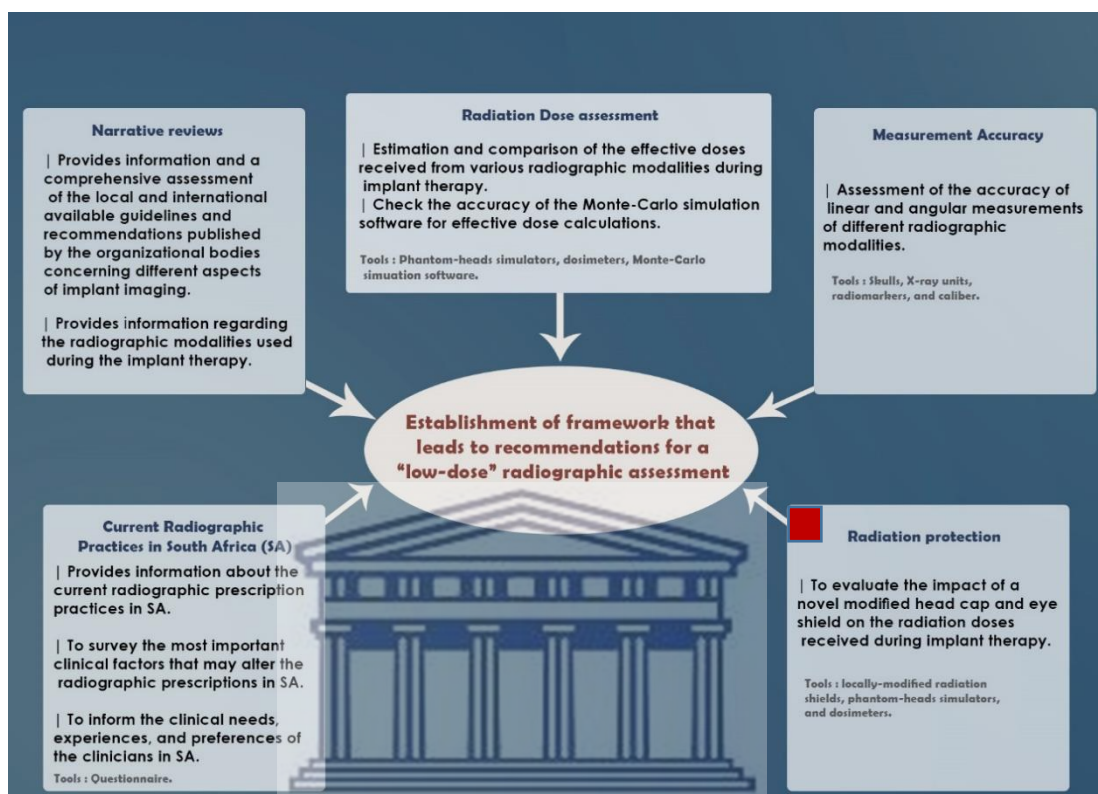


Figure 6-1. Diagrammatic representation of the main research project. The current sub-study is highlighted.

## 4.1 METHODOLOGY:

**Tools**

- Anthropomorphic phantom-heads.
- Thermoluminescent dosimeters (TLD-700).
- The modified head shield

#### 4.1.1 MODIFIED HEAD AND EYE SHIELD: NOVEL DESIGN

A 0.35 mm leaded surgical head cap (Radshield, South Africa) was modified to accommodate a locally fabricated eye mask (Figure 6-2). A 0.5 mm thickness lead sheet was cut in an eye mask outline, covering the orbits and a wide periorbital region.

The lead sheet of the eye mask is fairly flexible and adjustable to patient-specific anatomy. The sheet is laminated by multiple layers of plastic material covering its borders to provide comfort and remove sharp edges. The sheet was then embedded into the eye mask and tailored. VELCRO sheets were also stitched on the right and left sides of the eye mask and the counterpart head cap in an oblique pattern, in order to be adjustable.

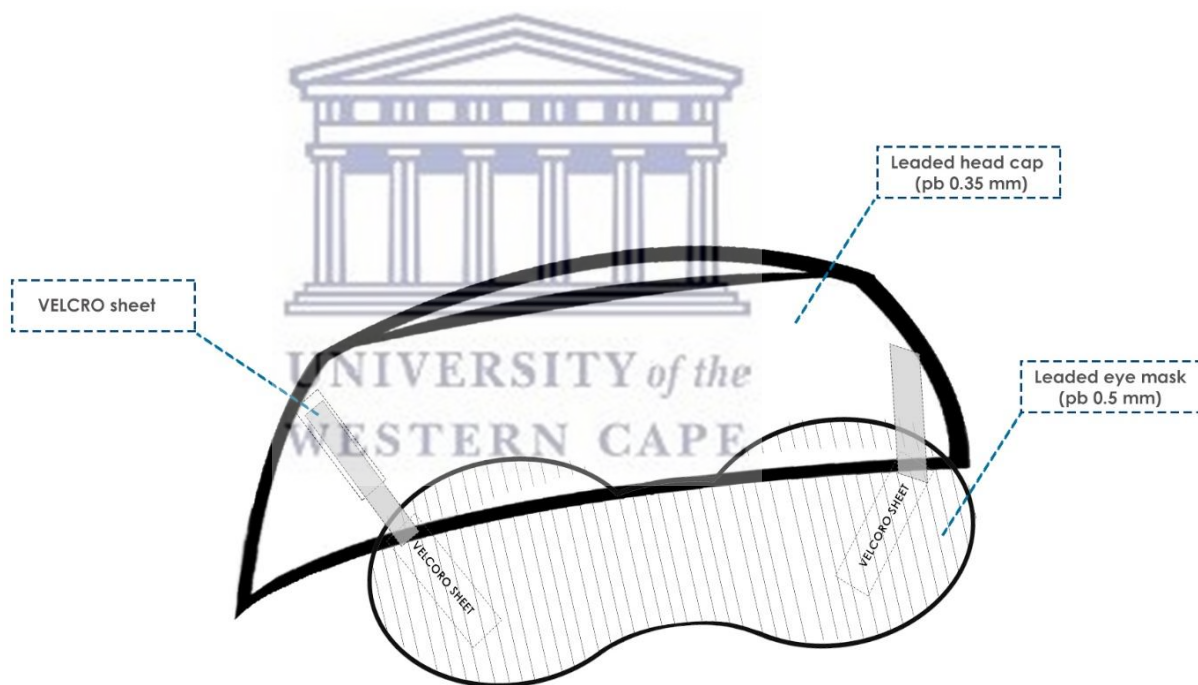


**Figure 6-2. Diagram showing the architecture/design of the shield.**

#### 4.1.2 PHANTOM HEAD PREPARATION

The exact procedures mentioned in sections 4.1.1.1 and 4.1.1.2 were reproduced in the analysis regarding TLD chips and phantom head slab preparation (Part 5, Chapter 4). The phantom heads were readied for any subsequent exposures after proper attachment of the modified shield (Figure 6-3).



**Figure 6-3. During the phantom-head preparation, with the modified head shield attached.**



### 4.1.3 RADIATION EXAMINATION

X-ray examinations using two CBCT and one panoramic x-ray machines were performed (Figure 6-4, Figure 6-5, and Figure 6-6). The x-ray machines with the exposure parameters used and the fields of view tested during this investigation are tabulated in Table 6.1. The same procedures mentioned in section 4.1.1.3 (in Part 5, Chapter 4) were followed. The x-ray exposures were repeated five times during CBCT and ten times during conventional panoramic acquisitions.

**Table 6.1. Exposure information during the radiographic examinations with the shield in place.**

|                                 | NewTom® 5GXL                       | CS 8100® 3D   | Orthophos® XG 3  |
|---------------------------------|------------------------------------|---|--|
|                                 | FOV (cm)                           | FOV (cm)  | FOV (cm)   |
|                                 | 15×12                              | 8×9   | -  |
| <b>Scan mode/program</b>        | Regular scan (18s), Standard dose. | <ul style="list-style-type: none"> <li>• Adult (medium-sized) patient.</li> <li>• Full jaw (both upper and lower jaw) program.</li> <li>• Fast scan.</li> </ul> | <ul style="list-style-type: none"> <li>• P1 program.</li> <li>• Adult (medium-sized) patient.</li> </ul> |
| <b>kVp</b>                      | 110                                | 90  | 69   |
| <b>mAs</b>                      | 45.79                              | 22.4 (3.20 mA × 7 s)  | 208.95 (15 mA × 13.9 s)  |
| <b>Exposure time (s)</b>        | 3.6                                | 7   | 13.9   |
| <b>Air Kerma (mGy)</b>          | 5.85                               | -   | -  |
| <b>DAP (mGy.cm<sup>2</sup>)</b> | 1311.25                            | 512   | 101  |
| <b>Voxel size (µm)</b>          | 250                                | 300   | -  |
| <b>Scout images</b>             | 2                                  | 0   | -  |

### 4.1.4 EFFECTIVE DOSE MEASUREMENT

The exact procedures mentioned in section 4.1.1.4 (in Part 5, Chapter 4) were once again followed in order to calculate the equivalent and effective doses, with the shield attached. The difference percentage of absorbed dose between the shielded (S) and unshielded (US) was calculated using the following formula: **% Difference = (US – S) / US × 100**



**Figure 6-4. During the CBCT acquisition (NewTom® 5GXL), with the modified head shield attached in place.**



**Figure 6-5.** During the CBCT acquisition (CS8100® 3D), with the modified head shield attached in place



**Figure 6-6.** During the panoramic acquisition, with the modified head shield attached in place.

## CHAPTER 5 | RESULTS

The overall and individual organ/tissue effective doses are reported in detail (Table 6.2).

**Table 6.2. Organ and total Effective doses (*E*) captured with shields on.**

|  | Effective organ dose ( <i>E</i> , in $\mu\text{Sv}$ ) |               |                |
|--|---|---------------|----------------|
|  | NewTom® 5GXL  | CS® 8100 3D   | Orthophos® XG3 |
|  | 15×12 cm (FOV)  | 8×9 cm (FOV)  | -              |
| <b>Bone marrow</b>                     | 7.58  | 4.40          | 0.88           |
| <b>Thyroid</b>                         | 20.80   | 14.40         | 2.80           |
| <b>Oesophagus</b>                      | 1.28  | 0.64          | 0.00           |
| <b>Skin</b>                            | 0.70  | 0.44          | 0.05           |
| <b>Bone surface</b>                    | 1.52  | 1.17          | 0.30           |
| <b>Salivary Glands</b>                 | 29.20   | 30.40         | 5.80           |
| <b>Brain</b>                           | 11.20   | 1.80          | 0.12           |
| <b>Remainder</b>                       | 45.61   | 50.86         | 11.85          |
| <b>Total Effective dose (<i>E</i>)</b> | <b>117.88</b>   | <b>104.11</b> | <b>21.80</b>   |

The absorbed doses of each chip in the 24 anatomical sites were captured and compared with their counterparts where the modified head shield is in place. Only nine anatomical sites (including the brain region, part of the pituitary gland, and orbit region) were expected to be influenced by the overlaying shield (site numbers 1-9, presented in red in Table 6.3, Table 6.4, and Table 6.5).

During the CBCT acquisitions using the NewTom® 5XL (FOV: 15×12 cm), the difference between the doses without shield (US) and with the shield (S) for the nine sites of interest showed a maximum dose difference of 2.4 mGy (left eye lens) and a minimum of 0.36 mGy (pituitary gland). This constitutes a dose difference of 20.9-81.3 % of the doses captured without shields for the same sites (Table 6.3). The overall effective dose (*E*) was reduced by 6.12 ( $\mu\text{Sv}$ ) (4.94%) using the shield.

**Table 6.3. A comparison between absorbed doses with/without using the shield - NewTom® 5GXL.**

| Site number                              | Anatomical site                     | TLD number | Without shield (mGy) | With shield (mGy) | Difference (mGy)* | Difference (%) † |
|--|-------------------------------------|------------|----------------------|-------------------|-------------------|------------------|
| 1  | Calvarium (anterior)                | 1          | 1.76                 | 0.36              | 1.4               | 79.5             |
| 2  | Calvarium (left side)               | 2          | 1.68                 | 1.08              | 0.6               | 35.7             |
| 3  | Calvarium (posterior)               | 3          | 1.2                  | 0.56              | 0.64              | 53.3             |
| 4  | Midbrain region                     | 4          | 1.56                 | 0.88              | 0.68              | 43.6             |
| 5  | Pituitary gland                     | 5          | 1.72                 | 1.36              | 0.36              | 20.9             |
| 6  | Orbit (right side)                  | 6          | 1.52                 | 0.56              | 0.96              | 63.2             |
| 7  | Orbit (left side)                   | 7          | 1.8                  | 0.44              | 1.36              | 75.6             |
| 8  | Eye lens (right side)               | 8          | 2.92                 | 0.56              | 2.36              | 80.8             |
| 9  | Eye lens (left side)                | 9          | 3                    | 0.56              | 2.44              | 81.3             |
| 10                                       | Cheek (left side)                   | 10         | 3.2                  | 3.72              | -0.52             | -16.3            |
| 11                                       | Parotid gland (right side)          | 11         | 2.4                  | 2.92              | -0.52             | -21.7            |
| 12                                       | Parotid gland (left side)           | 12         | 2.32                 | 2.88              | -0.56             | -24.1            |
| 13                                       | Ramus (right side)                  | 13         | 2.16                 | 2.36              | -0.2              | -9.3             |
| 14                                       | Ramus (left side)                   | 14         | 2.32                 | 2.2               | 0.12              | 5.2              |
| 15                                       | Center C spine                      | 15         | 2.24                 | 2.32              | -0.08             | -3.6             |
| 16                                       | Back of the neck (right side)       | 16         | 0.88                 | 0.72              | 0.16              | 18.2             |
| 17                                       | Mandibular body region (right side) | 17         | 2.6                  | 2.64              | -0.04             | -1.5             |
| 18                                       | Mandibular body region (left side)  | 18         | 2.52                 | 2.64              | -0.12             | -4.8             |
| 19                                       | Submandibular gland (right side)    | 19         | 2.84                 | 2.64              | 0.2               | 7.0              |
| 20                                       | Submandibular gland (left side)     | 20         | 2.28                 | 2.68              | -0.4              | -17.5            |
| 21                                       | Centre sublingual gland             | 21         | 2.72                 | 3.2               | -0.48             | -17.6            |
| 22                                       | Thyroid gland (midline)             | 22         | 0.6                  | 0.6               | 0                 | 0.0              |
| 23                                       | Thyroid gland surface (left side)   | 23         | 0.52                 | 0.44              | 0.08              | 15.4             |
| 24                                       | Oesophageal tube                    | 24         | 0.28                 | 0.32              | -0.04             | -14.3            |
| Overall Effective dose ( <i>E</i> , μSv) |                                     |            | 124                  | 117.88            | 6.12              | 4.94             |

\* Represents the difference between the dose (without shield) – (dose with shield). Positive values represent a reduction of the dose using the shield and vice versa. % Difference =  $(US - S) / US \times 100$ .

† The dose difference percentage (of the dose without shield).

-Anatomical sites presented in red font colour are the organs/tissues covered by the overlaying shield.

Although the TLD readings of the nine sites were minimal, even without the shield using CS<sup>®</sup> 8100 3D (FOV: 8×9 cm), the readings showed variable values with two of these sites receiving more doses compared to their counterparts without shields (sites 1 and 6 by -0.04 mGy and -0.12 mGy, respectively). The maximum reduction was in the calvarium (left) and orbit (left) regions, with the difference being 50% lower of the dose without the shield (Table 6.4). The difference between the overall effective dose (*E*) was -2.3 (μSv) (-2.25%) using the shield, which indicates that the effective dose was higher by 2.3 μSv when the shield was in place (Table 6.4).

**Table 6.4. A comparison between absorbed doses with/without using the shield - CS<sup>®</sup> 8100 3D.**

| Site number | Anatomical site                     | TLD number | Without shield (mGy) | With shield (mGy) | Difference (mGy)* | Difference (%) † |
|-------------|-------------------------------------|------------|----------------------|-------------------|-------------------|------------------|
| 1           | Calvarium (anterior)                | 1          | 0.08                 | 0.12              | -0.04             | -50              |
| 2           | Calvarium (left side)               | 2          | 0.08                 | 0.04              | 0.04              | 50               |
| 3           | Calvarium (posterior)               | 3          | 0.04                 | 0.04              | 0                 | 0                |
| 4           | Midbrain region                     | 4          | 0.24                 | 0.2               | 0.04              | 16.7             |
| 5           | Pituitary gland                     | 5          | 0.44                 | 0.4               | 0.04              | 9.1              |
| 6           | Orbit (right side)                  | 6          | 0.16                 | 0.28              | -0.12             | -75              |
| 7           | Orbit (left side)                   | 7          | 0.16                 | 0.08              | 0.08              | 50               |
| 8           | Eye lens (right side)               | 8          | 0.2                  | 0.2               | 0                 | 0                |
| 9           | Eye lens (left side)                | 9          | 0.2                  | 0.2               | 0                 | 0                |
| 10          | Cheek (left side)                   | 10         | 1.32                 | 2.08              | -0.76             | -57.6            |
| 11          | Parotid gland (right side)          | 11         | 3.16                 | 3.68              | -0.52             | -16.5            |
| 12          | Parotid gland (left side)           | 12         | 2.8                  | 2.4               | 0.4               | 14.3             |
| 13          | Ramus (right side)                  | 13         | 3.04                 | 3.04              | 0                 | 0                |
| 14          | Ramus (left side)                   | 14         | 2.72                 | 3                 | -0.28             | -10.3            |
| 15          | Center C spine                      | 15         | 1.8                  | 1.92              | -0.12             | -6.7             |
| 16          | Back of the neck (right side)       | 16         | 1.84                 | 1.92              | -0.08             | -4.3             |
| 17          | Mandibular body region (right side) | 17         | 3.44                 | 3.48              | -0.04             | -1.2             |
| 18          | Mandibular body region (left side)  | 18         | 3.32                 | 3.12              | 0.2               | 6                |

|  |                                   |    |              |              |             |              |
|--|-----------------------------------|----|--------------|--------------|-------------|--------------|
| 19   | Submandibular gland (right side)  | 19 | 2.92         | 2.72         | 0.2         | 6.8          |
| 20   | Submandibular gland (left side)   | 20 | 3.64         | 3.04         | 0.6         | 16.5         |
| 21   | Centre sublingual gland           | 21 | 2.52         | 3.2          | -0.68       | -27          |
| 22   | Thyroid gland (midline)           | 22 | 0.44         | 0.44         | 0           | 0            |
| 23   | Thyroid gland surface (left side) | 23 | 0.24         | 0.28         | -0.04       | -16.7        |
| 24   | Oesophageal tube                  | 24 | 0.16         | 0.16         | 0           | 0            |
| <b>Overall Effective dose (<math>E</math>, <math>\mu\text{Sv}</math>)</b>  |                                   |    | <b>101.8</b> | <b>104.1</b> | <b>-2.3</b> | <b>-2.25</b> |
| * Represents the difference between the dose (without shield) – (dose with shield). Positive values represent a reduction of the dose using the shield and vice versa. |                                   |    |              |              |             |              |
| † The dose difference percentage (of the dose without shield).   |                                   |    |              |              |             |              |

During the panoramic examination, the doses of the nine sites were 0 mGy with and without the shield. An exception was the pituitary gland which showed 0.04 mGy with and without the shield (the difference is 0 mGy, 0%), and the left side eye lens which was 0.02 mGy without shield and the shield was able to reduce the dose to 0 mGy (100 % dose difference). The difference between the overall effective dose ( $E$ ) was -0.7 ( $\mu\text{Sv}$ ) (-3.31%) using the shield, which indicates that the effective dose was higher by 0.7  $\mu\text{Sv}$  using the shield (Table 6.5).

**Table 6.5. A comparison between absorbed doses with/without using the shield - Sirona® Orthophos XG3.**

| Site number | Anatomical site       | TLD number | Without shield (mGy) | With shield (mGy) | Difference (mGy)* | Difference (%) † |
|-------------|-----------------------|------------|----------------------|-------------------|-------------------|------------------|
| 1           | Calvarium (anterior)  | 1          | 0                    | 0                 | 0                 | 0                |
| 2           | Calvarium (left side) | 2          | 0                    | 0                 | 0                 | 0                |
| 3           | Calvarium (posterior) | 3          | 0                    | 0                 | 0                 | 0                |
| 4           | Midbrain region       | 4          | 0                    | 0                 | 0                 | 0                |
| 5           | Pituitary gland       | 5          | 0.04                 | 0.04              | 0                 | 0                |
| 6           | Orbit (right side)    | 6          | 0                    | 0                 | 0                 | 0                |
| 7           | Orbit (left side)     | 7          | 0                    | 0                 | 0                 | 0                |
| 8           | Eye lens (right side) | 8          | 0                    | 0                 | 0                 | 0                |
| 9           | Eye lens (left side)  | 9          | 0.02                 | 0                 | 0.02              | 100              |

|   |                                     |    |      |      |       |       |
|---|-------------------------------------|----|------|------|-------|-------|
| 10  | Cheek (left side)                   | 10 | 0    | 0.02 | -0.02 | -100  |
| 11  | Parotid gland (right side)          | 11 | 0.64 | 0.8  | -0.16 | -25   |
| 12  | Parotid gland (left side)           | 12 | 0.7  | 0.82 | -0.12 | -17.1 |
| 13  | Ramus (right side)                  | 13 | 1.08 | 1.24 | -0.16 | -14.8 |
| 14  | Ramus (left side)                   | 14 | 1.52 | 1.38 | 0.14  | 9.2   |
| 15  | Center C spine                      | 15 | 0.32 | 0.34 | -0.02 | -6.3  |
| 16  | Back of the neck (right side)       | 16 | 0.48 | 0.5  | -0.02 | -4.2  |
| 17  | Mandibular body region (right side) | 17 | 0.44 | 0.34 | 0.1   | 22.7  |
| 18  | Mandibular body region (left side)  | 18 | 0.32 | 0.26 | 0.06  | 18.8  |
| 19  | Submandibular gland (right side)    | 19 | 0.78 | 0.78 | 0     | 0     |
| 20  | Submandibular gland (left side)     | 20 | 0.8  | 0.76 | 0.04  | 5     |
| 21  | Centre sublingual gland             | 21 | 0.22 | 0.16 | 0.06  | 27.3  |
| 22  | Thyroid gland (midline)             | 22 | 0.08 | 0.1  | -0.02 | -25   |
| 23  | Thyroid gland surface (left side)   | 23 | 0.04 | 0.04 | 0     | 0     |
| 24  | Oesophageal tube                    | 24 | 0.02 | 0    | 0.02  | 100   |
| <b>Over all Effective dose (E, <math>\mu</math>Sv)</b>  |                                     |    | 21.1 | 21.8 | -0.7  | -3.31 |
| * Represent the difference between the dose (without shield) - (dose with shield). Positive values represent a reduction of the dose using the shield and vice versa. % Difference = $(US - S) / US \times 100$ . |                                     |    |      |      |       |       |
| † The dose difference percentage (of the dose without shield).  |                                     |    |      |      |       |       |

The CBCT volume reconstructed using the NewTom<sup>®</sup> 5GXL are illustrated in Figure 6-7, Figure 6-8, Figure 6-9, and Figure 6-10. A series of axial slices captured at different vertical levels covering the upper part of the head region is represented in Figure 6-11. No effects (i.e. artefacts) on the adjacent anatomical region other than the anatomical area covered by the shield were noted. A comparison between axial slices captured at the same levels in the maxilla and mandible is further illustrated in Figure 6-12 and Figure 6-13. The resultant CBCT volume using the CS<sup>®</sup>8100 3D showed no effects of the shield on the rendered field of view (Figure 6-14). The resultant panoramic view is also illustrated in Figure 6-15.





**Figure 6-7.** Anteroposterior (top) and lateral cephalometric (bottom) radiographic views of the CBCT volume with the attached modified shield (NewTom® 5GXL, FOV 15 × 12 cm, regular scan, and standard dose).

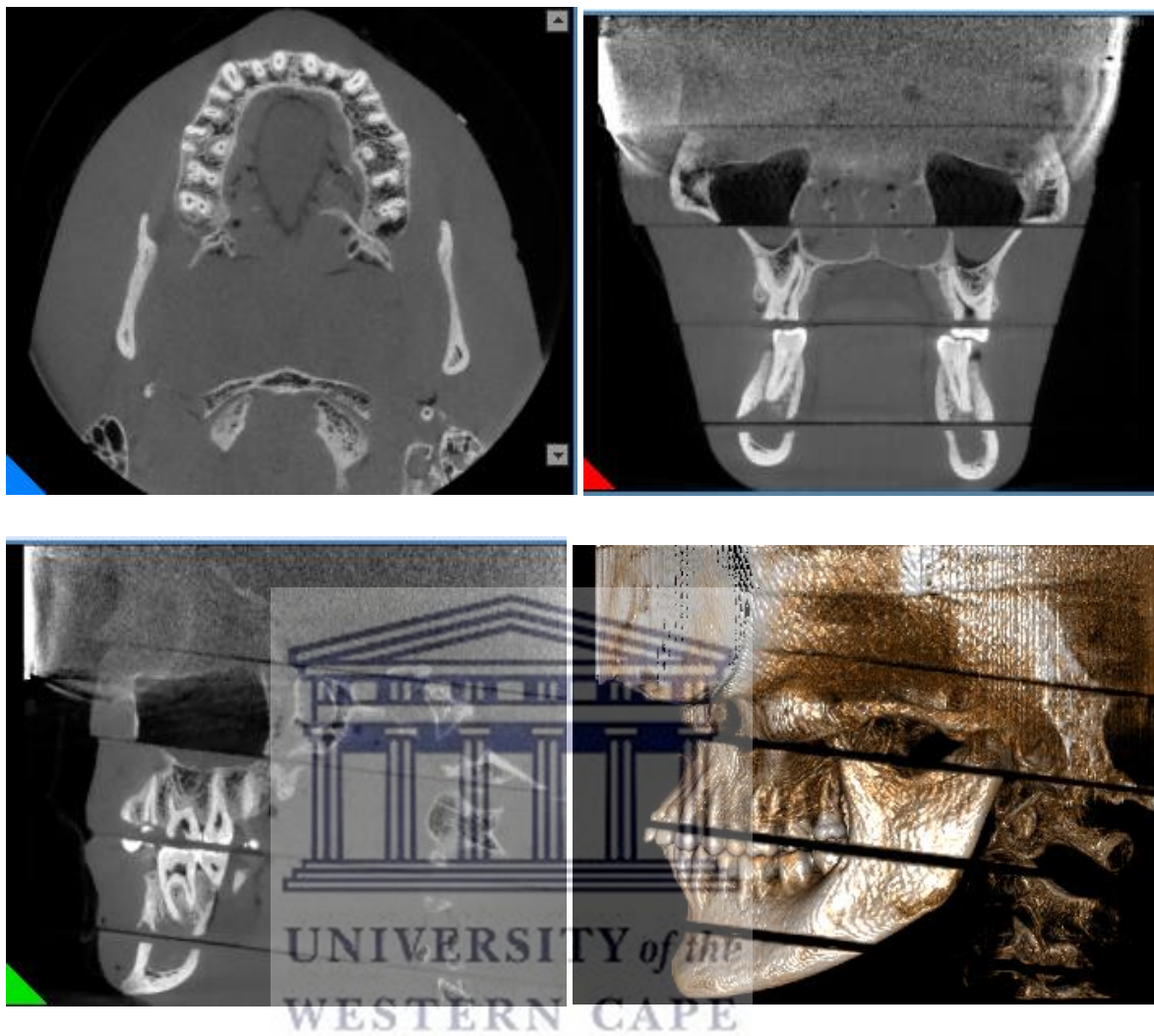


**Figure 6-8.** Axial slice (top left), coronal slice (top right), sagittal slice (bottom left), and 3D view (bottom right), reconstructed from CBCT volume with the attached modified shield (NewTom® 5GXL, FOV 15 × 12 cm, regular scan, and standard dose).

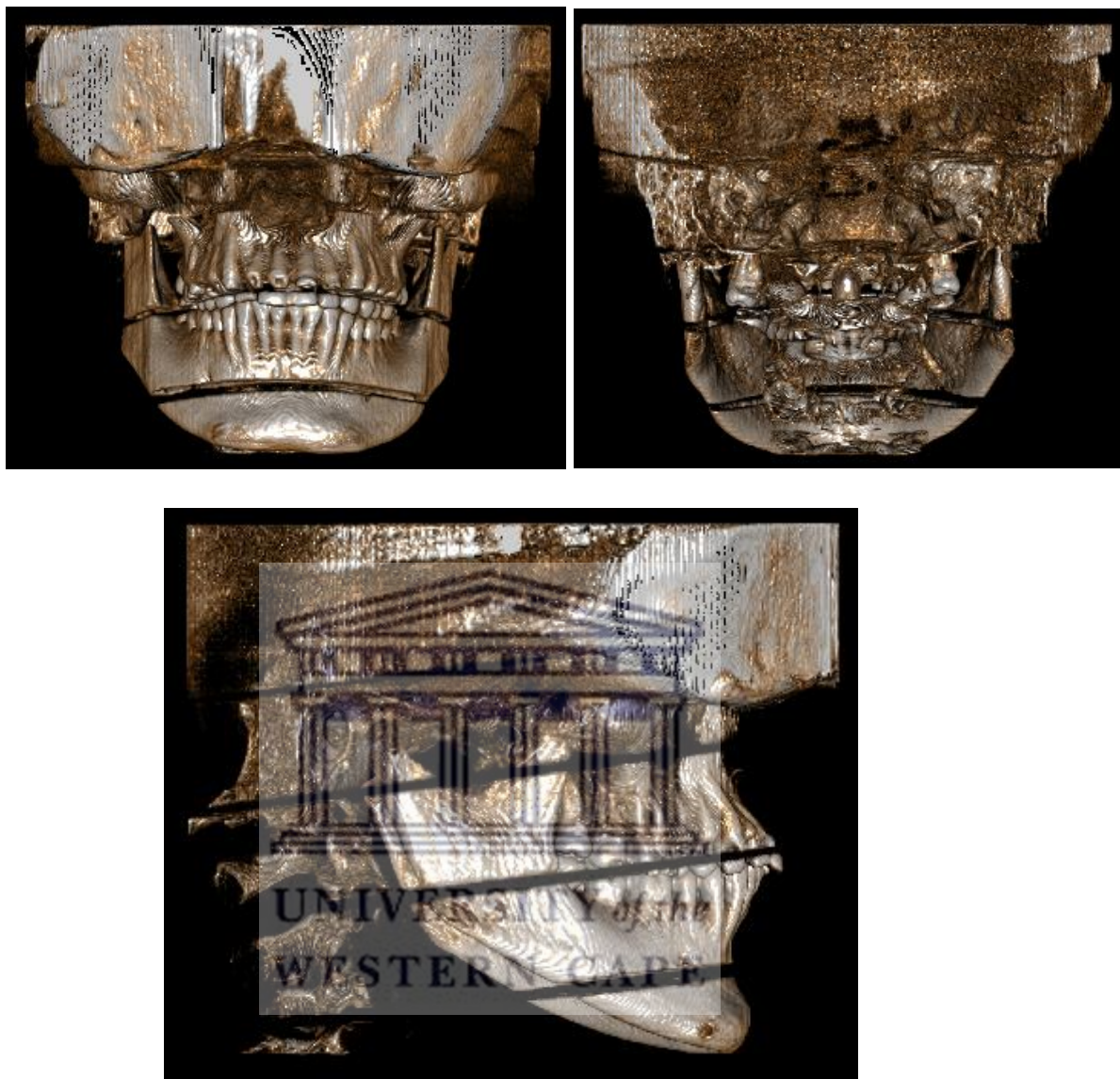


**Figure 6-9.** Front view (top left), posterior view (top right), and right side (bottom) 3D models reconstructed using the NewTom® 5GXL (FOV: 15 × 12 cm) with the shield attached.



**Figure 6-10. 3D reconstruction with different filters (MIP and transparent bone) using the NewTom® 5GXL (FOV: 15 × 12 cm) with the shield attached.**

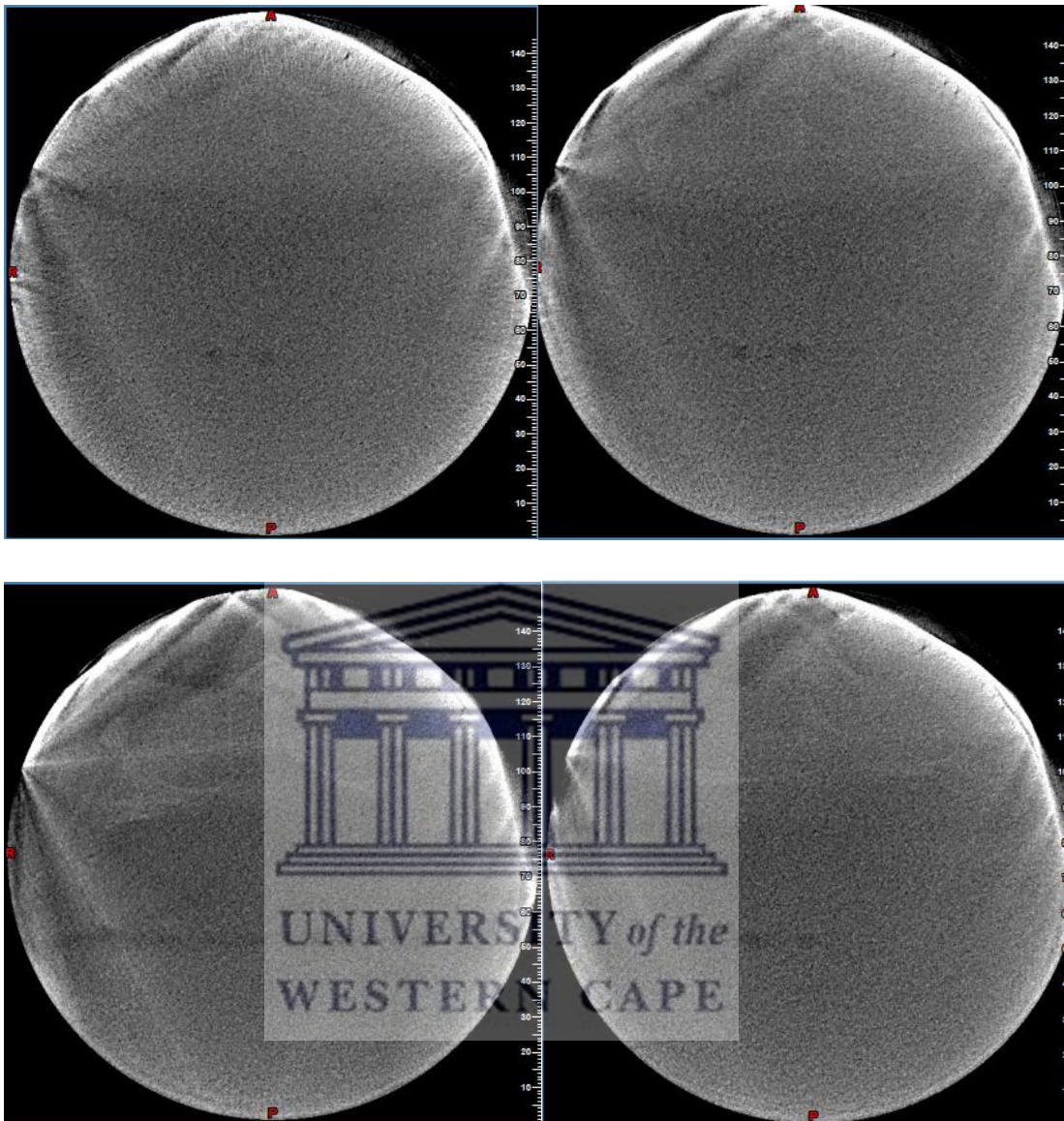


**Figure 6-11.** Axial slice series captured at various vertical levels of the head reconstructed from the CBCT volume, with the attached modified shield (NewTom® 5GXL, FOV 15 × 12 cm, regular scan, and standard dose).

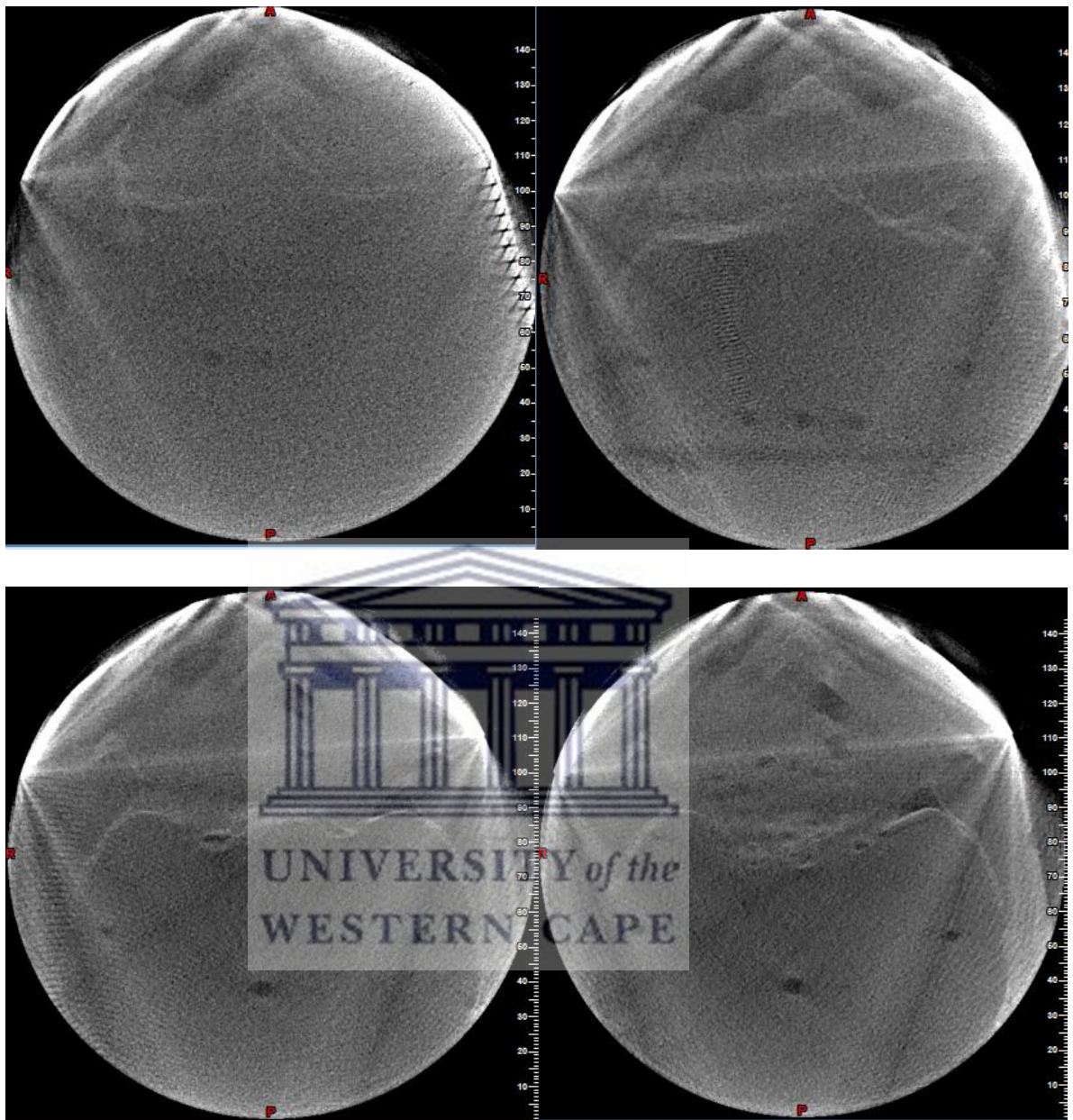


Figure 6-11 (Cont.)

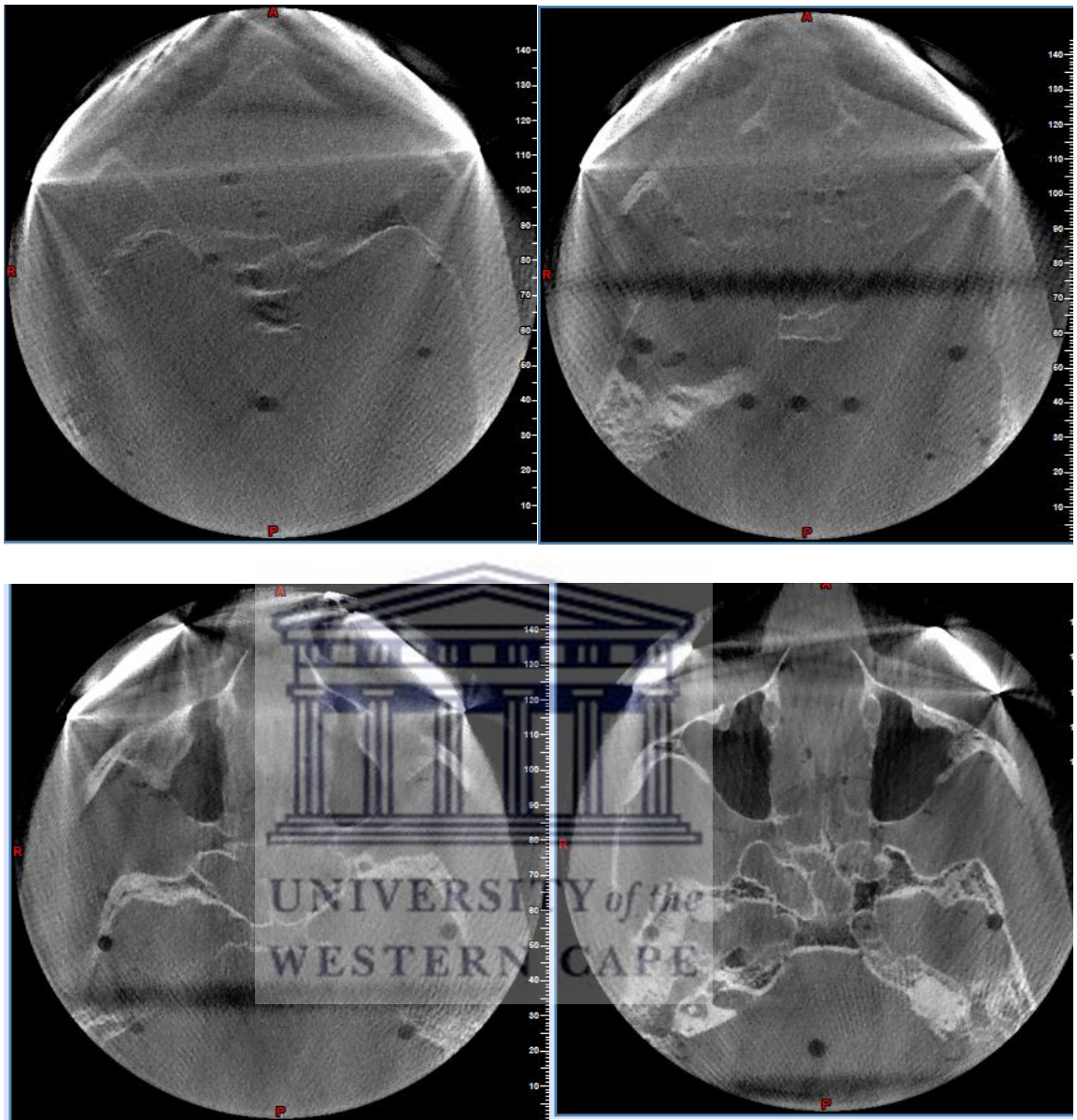
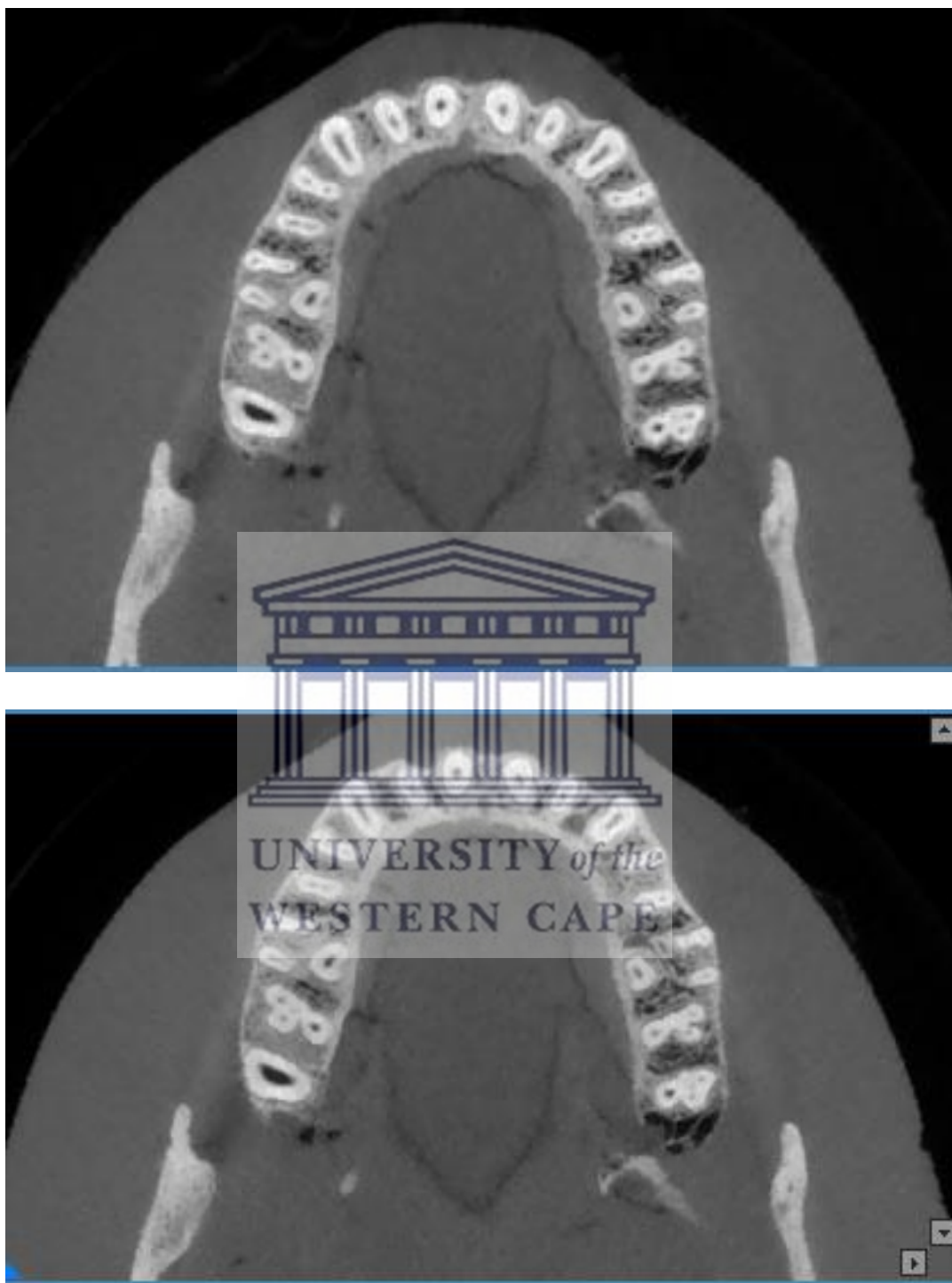
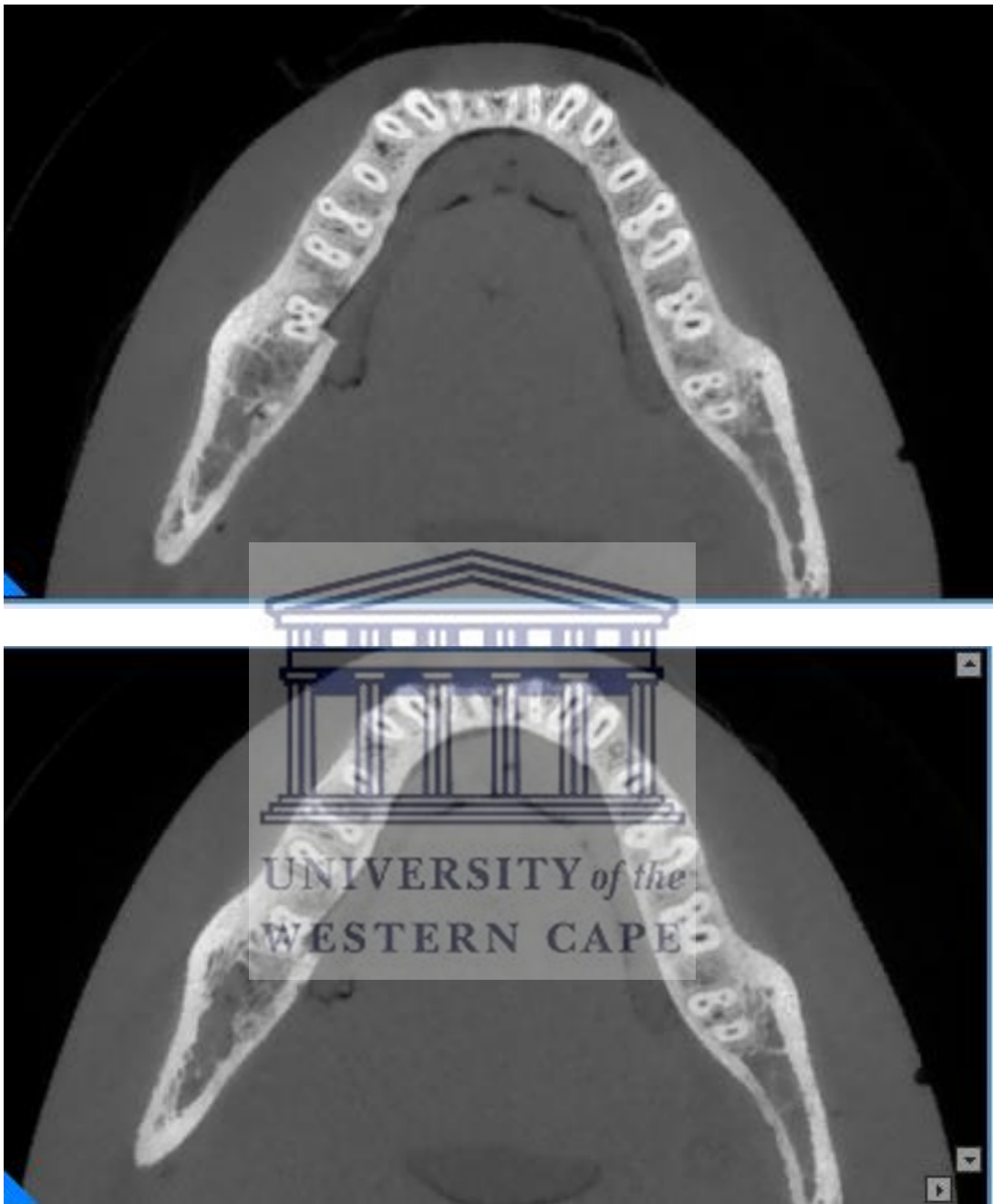


Figure 6-11 (Cont.)



**Figure 6-12.** Axial slices captured at the same vertical level (in the maxilla) with the shield attached (top) and without the shield (bottom) (using the NewTom<sup>®</sup> 5GXL, FOV 15 × 12 cm). When compared, both slices reveal no obvious alteration of the quality of the volume due to the lead shield (e.g. induced artefacts).





**Figure 6-13.** Axial slices captured at the same vertical level (in the mandible) with the shield attached (top) and without the shield (bottom) (using the NewTom<sup>®</sup> 5GXL, FOV 15 × 12 cm). When compared, both slices reveal no obvious alteration of the quality of the volume due to the lead shield (e.g. induced artefacts).

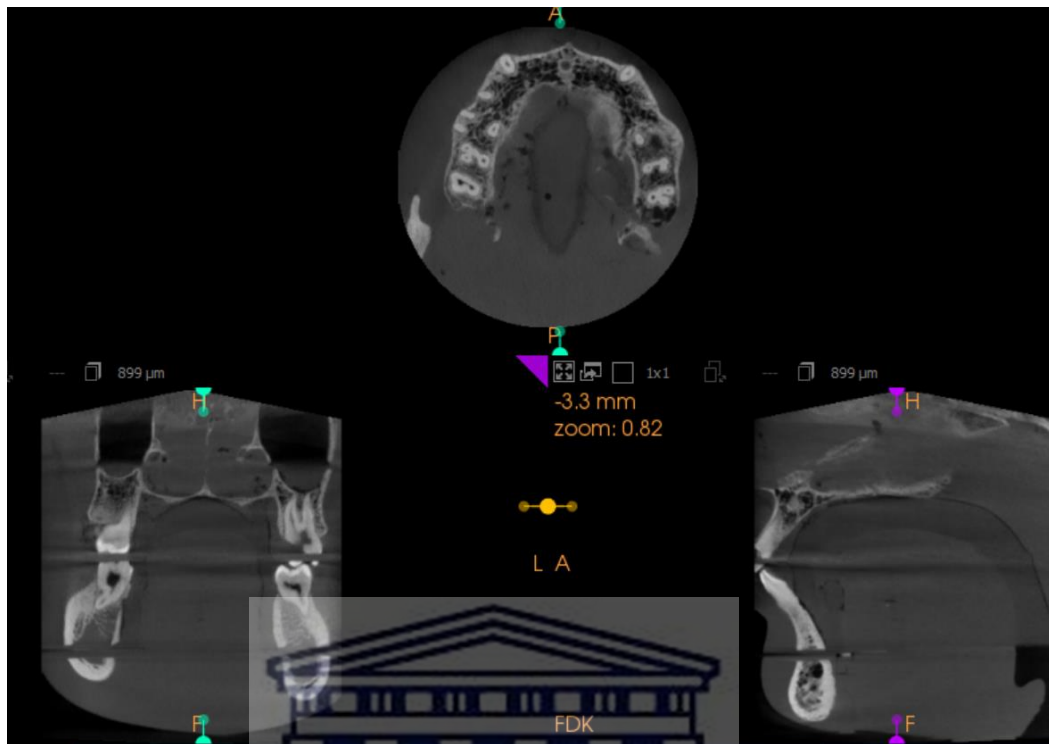


**Figure 6-14.** Axial (top), coronal (bottom left), sagittal (bottom right) slices reconstructed from the CBCT volume with the shield in place (using the CS 8100® 3D, 8 × 9 cm (Full jaw program), fast scan). There is no evidence of the shield structure nor artefacts on the rendered volume.

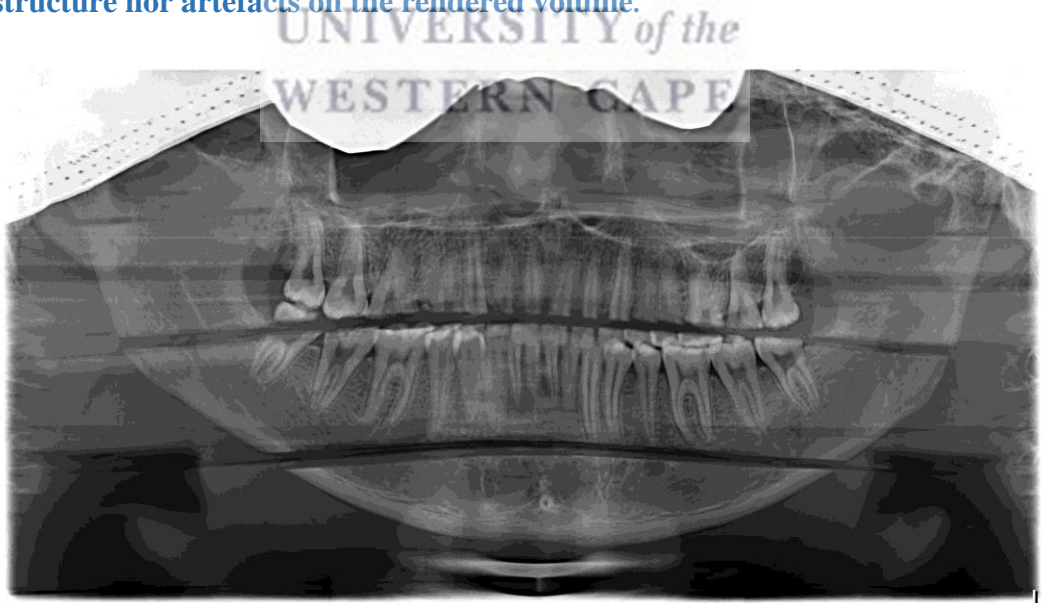


**Figure 6-15.** The resultant panoramic radiograph with the shield in place (the radiopaque structure in the upper third of the radiograph).

## CHAPTER 6 | DISCUSSION

The shield was carefully designed after contemplative scouting of the available literature relevant to the available protective solutions during CT and CBCT examinations. The challenge was to design a combined shield for the head and the upper third of the face (and not limited to the orbits) and adjustable. The shield's design also meant to cover optimally the organs within the cranial cavity from all projection angles (and not only from one entrance point), including the zone between the eye shield and the head cap. This is particularly vital as the x-ray beams in rotational radiographic modalities (including the CBCT and panoramic radiography) would approach and expose the same anatomical site from different angles and different travelling distances along their way to the x-ray receptor. This modified shield design aimed at offering an easily accessible solution that can be manufactured locally at affordable costs.

In a  $15 \times 12$  cm field of view exposure (using the NewTom<sup>®</sup> 5GXL), the shield could considerably reduce the absorbed doses in various vital and sensitive structures, saving them from unavoidable exposure. Hence, using the shield would be of clinical significance if the patient is referred for a comparable FOV CBCT exam where the cranial cavity region including the orbits is not the interest of the radiographic examination. Nevertheless, the automatic exposure parameters (defined automatically based on the attenuation values acquired from scouting views) were noted to be set higher compared to the counterpart examination performed without the shield (Table 6.6). The author speculates that this is due to the attenuation values returned from the shield that prompt the increase of exposure parameters to boost up the penetration power of the primary x-ray beam; such an effect is also mentioned in the literature (Pauwels et al., 2019). Consequently, this is presumed to be the reason why the overall effective dose was not substantially reduced using the shield. In this situation, placing the shields after the scouting views and prior to the main acquisition would overcome this issue, although further investigations should be executed to confirm this.

**Table 6.6. Exposure parameters with and without the shield.**

| Exposure parameter              | Without shield (FOV 15×12 cm) | With shield (FOV 15×12 cm) |
|---------------------------------|-------------------------------|----------------------------|
| <b>DAP (mGy.cm<sup>2</sup>)</b> | 1120.05                       | 1311.25                    |
| <b>Air Kerma (mGy)</b>          | 5.00                          | 5.85                       |
| <b>mAs</b>                      | 37.5                          | 45.79                      |
| <b>First scout view mA</b>      | 6.66                          | 6.42                       |
| <b>Second scout view mA</b>     | 14.22                         | 19.8                       |

A high level of radiographic noise was noted in the superior facial third in the reconstructed 3D volumes. This was mainly due to under-sampling in these sites as only a minuscule fragment of x-ray beams managed to penetrate the regions enclosed by the shield. For this reason, some ghost-like presentation of the bony structures of the orbital sockets were noted at the inferior axial levels covered by the shield (Figure 6-11). It was mentioned that a lead sheet with (0.5 mm) thickness can attenuate 94% of the photons at 60 keV (Pauwels et al., 2019). In our study, the shield was constructed with 0.35 mm lead for the head cap and 0.5 mm for the eye mask and exposure performed at 110 kVp; hence, increasing the thickness of the lead layer of the cap should be further investigated in the future.

It is worth noting that the shield did not induce radiographic artefacts including scattering and beam hardening effects on the adjacent anatomical regions and region of interest (Figure 6-12 and Figure 6-13).

Dose reduction measures should be implemented, particularly given that the risk imparted from radiation is “cumulative” (Qu et al., 2010). Every effort should be made to reduce the received dose to the minimum, particularly for the young patients who are more vulnerable to be affected from x-ray radiation (Qu, Li, Zhang, et al., 2012).

Qu et al., (2010) stated that the operator of the CBCT machine should be knowledgeable of the impact of the exposure protocols/parameters of the specific CBCT unit on received doses – especially since these doses can be efficiently reduced when using lower exposure protocols. Moreover, improvements and increased x-ray

beam filtration have proved to reduce the dose, since the low energy photons will be filtered out. Adjusting the exposure parameters to the specific patient's head size (where applicable) and limiting the FOV was shown to considerably reduce radiation doses (Qu et al., 2010). These conclusions concur with observations in this sub-study which compared different fields of view and exposure protocols.

The thyroid collars are recommended by The National Council on Radiation Protection and Measurements (NCRP) for adults and children, as long as it does not obscure the regions of interest. This clinically would be impractical in some instances, as this shielding might impede multiple extra-oral x-ray examinations – e.g. panoramic radiographs (Miles & Langlais, 2004).

“Inconsistent” evidence was obtained from the literature concerning the clinical application of the thyroid shielding, particularly during the CBCT exam (Pauwels et al., 2019). The thyroid tissue is highly sensitive to radiation – particularly for female patients and young ages (Pauwels et al., 2019). It is found that thyroid shielding would cause metallic artefacts only in and just superior and inferior to the thyroid gland shield level (influenced by the primary beam angle), and if this interferes with the diagnostic objective of the radiographic exam, the thyroid shield should be avoided (Pauwels et al., 2019). In other instances, the thyroid shielding is recommended as a routine practice for young ages and of benefit to adults (up to 50 years) (Pauwels et al., 2019).

Although the author acknowledges the sensitivity of the thyroid gland and the importance of its protection, the questionable applicability during extraoral x-ray exams (i.e. panoramic and CBCT) and particularly during implant planning in the mandible discouraged the use of the thyroid collar.

Tsiklakis et al. (2005) found that shielding the thyroid gland and the cervical spine during CBCT acquisitions was sufficient to reduce the mean absorbed dose from 0.32 mGy to 0.18 mGy. The average absorbed dose of the cervical spine (over 3 vertebrae) was also reduced from 1.28 mGy to 0.95 mGy. Although the thyroid gland received a decreased amount of radiation dose, the highest absorbed doses were in the regions of

the salivary glands and bone marrow – which is particularly found in the mandibular molar region and cervical spine (Tsiklakis et al., 2005).

Qu, G Li, et al. (2012) found that the proper use of thyroid shields can result in a slight reduction of overall effective dose. Nonetheless, the significant reduction of the individual organ doses of the thyroid and oesophagus is still considerable.

Attaia et al. (2020) used different shielding techniques, including a leaded head cap, radiation safety glass, and thyroid shield to assess the effects on the received doses during the CBCT examination. Different fields of views and various scanning protocols were assessed. The results disclosed a reduction in the dose when different shielding techniques were used. A substantial dose reduction was found when “low dose” exposures’ parameters/settings were used. Nevertheless, a shielding technique using the head cap, glasses, and thyroid collar together (FOV  $17 \times 11$  cm, 0.4 mm voxel size) significantly reduced the dose of all covered organs except the equivalent dose to the lens of the eyes (-9.5%, -2% reduction using low and standard dose protocols, respectively) and salivary glands. In this sub-study (FOV  $15 \times 12$  cm, standard dose), there was a significant equivalent dose reduction to the eye lens (right side 80.8% and left side 81.3%) when a modified tightly fitting 0.5 mm leaded eye mask was used.

The bone marrow showed significant effective organ dose difference (14% and 21% for  $17 \times 11$  cm (FOV) using low and standard dose protocols, respectively) (Attaia et al., 2020). Compared to findings in this sub-study (FOV  $15 \times 12$  cm, standard dose) the effective organ dose for the bone marrow was  $11.59 \mu\text{Sv}$  and was reduced to  $7.58 \mu\text{Sv}$  (34.59% reduction). The brain effective dose showed significant difference (32% and 38% for  $17 \times 11$  cm (FOV) using low and standard dose protocols, respectively) using the shield (Attaia et al., 2020); this is comparable to 31.7% brain effective dose reduction found in this study (reduction from  $16.4 \mu\text{Sv}$  (unshielded) to  $11.2 \mu\text{Sv}$  (shielded)).

When using only a bismuth-fabricated eye shield placed on a paediatric phantom during CT scan, Mukundan et al., (2007) were able to reduce the absorbed doses to the eye and its lens by 42% and 25% respectively (at 120 kVp).

McLaughlin and Mooney (2004) used a commercially available eye shield that was able to reduce the mean absorbed dose by only 18% to the lens of the eye during CT scans. These authors indicated that the reduction to the eyes was not significant. This was due to the fact the primary x-ray beams leaving the patient's tissues and obstructed by the shield will still increase the absorbed doses received by the attenuated anatomical sites along the x-ray beam's trajectory to the shield. In a similar assessment (Geleijns et al., 2006), the eye shield was able to reduce the dose by 27% to the eye lens and by 1% to the brain.

Goren et al. (2013) assessed the effectiveness of leaded glasses and thyroid shielding on radiation doses during CBCT examinations. They concluded that the implementation of thyroid shielding and leaded glasses during CBCT examination effectively reduce the doses received by the thyroid and the lens of the eye. An absorbed dose reduction of 61% to the left lens of the eye (3.96 reduced to 1.53 mGy) and 71.8% reduction to the right lens (4.69 reduced to 1.32 mGy) was reported by Goren et al., (2013) when a full FOV (17×23 cm) was used. When compared to this study, the absorbed dose reduction was 80.8% and 81.3% to the right and left lens of the eye (respectively) using 15×12 cm (FOV), and 0% when only partial maxilla and mandible collimation was used (8×9 FOV).

The findings of this sub-study regarding the dose reduction to the eye lens are comparable with results found by Prins et al. (2011) who indicated about 67% absorbed dose reduction. These authors (Prins et al., 2011) also mentioned that the glasses did not degrade the radiographic quality of the region of interest.

In a smaller field of view (8×9 cm, acquired by CS<sup>®</sup>8100 3D), the absorbed doses in the nine anatomical sites covered by the shield were originally (without shield) minimal when compared to the larger field of view (acquired by NewTom<sup>®</sup> 5GXL). The shield's ability to reduce these doses were minimal and inconsistent among these sites, nevertheless, the absorbed doses were observed to be reduced in the orbit (50%, left side only), pituitary gland (9.1%), midbrain region (16.7%), and calvarium (50%, left

side). The role of the shield in reducing these doses is uncertain, due to the minimal absorbed doses in both examinations (with/without the shield), in addition to the inconsistency of obtaining a positive dose difference (dose reduction) at the sites concerned. Nevertheless, the overall view tends to indicate the limited value of the shield when a medium field of view (8×9 cm) is used. The sites outside the domain of the radiation field receive only a minimal amount of radiation, which is mostly due to scattered radiation from inside the patient. It was also reported (Tsiklakis et al., 2005) that scattered radiation within the patient radiated the tissues that lie away from the domain of the primary x-ray beam. No effects such as artefacts on the rendered volume were noted (Figure 6-14).

During the panoramic exam (Sirona<sup>®</sup> Orthophos XG3<sup>®</sup>), the absorbed doses in the nine regions of interest were constantly showing no captured exposures, except in the pituitary gland (captured 0.04 mGy with and without the shield) and left eye lens (0.02 mGy reduced to zero with the shield in place). These values indicate that during a panoramic examination with and without the shield, these anatomical sites (9 sites) are, in most instances, zero to minimally exposed, hence, shielding has no clinical value. The shield has no effects on the region of interest (jaw sites), and these sites can still be assessed efficiently with the shield on (Figure 6-15).



**CHAPTER 7 | CONCLUSION**

The modified head shield with the eye mask significantly reduced the absorbed doses to highly sensitive anatomical structures in the cranial cavity and eye lens using the **15 × 12 cm** field of view; with no adverse effect on the rendered volume quality in the region of interest. Admittedly, the total effective dose was minimally reduced using the shield. Primary data acquired from this investigation support the clinical effectiveness and benefit of using this shielding design, especially, where exposure to the orbit and cranium is unavoidable. However, the author concedes that further comprehensive investigations should be performed.

The shield efficacy was limited in the field of view **8 × 9 cm** and smaller, and during panoramic radiography. However, further investigations using different experimental settings should be performed.

**Acknowledgements**

- All the staff members at the Medical Physics Department, Groote Schuur Hospital, Cape Town.
- Dr Christian Traunchet, Division of Medical Physics, Faculty of Health Sciences, Stellenbosch University.



PART 7  
DISCUSSION AND CONCLUSION

UNIVERSITY of the  
WESTERN CAPE

**CONTENTS AT A GLANCE**

**Section 1| Discussion and conclusion**

**Section 2| Proposed draft recommendations on implant imaging in SA.**

- 2.1 Clinical notes to justify and optimise dental exposure.
- 2.2 Phase I: Initial patient assessment
  - 2.2.1 Factors which increase the risk of treatment complications
- 2.3 Phase II: Implant planning
- 2.4 Phase III: Intra-operative, directly post-surgery, and post-prosthetic stages
- 2.5 Phase IV: Follow-up



UNIVERSITY of the  
WESTERN CAPE

## SECTION 1: DISCUSSION AND CONCLUSION

This series of studies was aimed at contributing to the pool of evidence available regarding the factors affecting implant imaging. The data obtained by this research may help establish efficient guidelines in terms of implant therapy. According to the evidence attained during this study together with a review of available published information and within the limitations of this study, the following comments can be deduced:

- Currently, two and three-dimensional imaging modalities are used during various phases of implant treatment – each with advantages and disadvantages (Part 2, Chapter 2). Imaging technology other than that currently available (i.e. panoramic, CT, CBCT, and MRI) does not exist for use during the therapy.
- A single, ideal radiographic modality to use during implant therapy is not available, hence, a combination of modalities is usually prescribed in clinical practice (Tyndall et al., 2012).
- CBCT is considered advantageous when compared with 2D modalities (e.g. PAN & PA). It provides additional, high-quality anatomical details that are needed during the therapy (Bornstein et al., 2017; Benavides et al., 2012; Tyndall et al., 2012).
- This study confirms a submillimetre dimensional accuracy of CBCT examinations with inconsistent measurements (over millimetre mean accuracy) are obtained from panoramic and periapical radiographs (further details are in Part 4, Chapter 5).
- The differences found between the linear and angular physical distances of the arch's arc have emphasised the importance of careful consideration to the type of measurements, and the consequent accurate reproduction of these virtual dimensions to the clinical setting (further details are in Part 4, Chapter 6).
- The survey (Part 3) conducted showed a preference to prescribe a combination of panoramic radiographs and CBCT volumes during implant planning.

- The radiation doses of dental examinations are reported to be far lower than the dose limits which are known to induce deterministic effects, but not stochastic effects (Harris et al., 2012; White & Pharoah, 2013). The evidence on a safe limit of radiation dose is lacking, and thus the implementation of the ALARA (as low as reasonably achievable) is vital with each exposure needing to be justified (Abbott, 2000).
- At the same time, the concerns of “potential surgical misadventures” can deprive patients of beneficial radiographical exams due to the overestimation of the risks of the diagnostic examination (Tubiana et al., 2009). The pre-surgical 3D radiographic assessment of a potential implant site plays a vital role in avoiding the jeopardization of the structures in its vicinity (e.g. cortical borders and maxillary sinuses perforation, and injury to neurovascular bundles), and thus enhancing treatment outcomes (Tyndall et al., 2012; Hatcher et al., 2003; Kraut, 1998).
- In the current analysis, the investigation of the exposure outputs of several x-ray units revealed comparable dose levels to their counterparts in the literature (although reported doses for the exact CBCT machine model studied were not found), and further details are in Part 5, Chapters 2 and 5.
- Limiting the field of view (as practically as possible) and choosing the low-dose exposure protocols (where applicable) were found to efficiently reduce the received doses, and thus are recommended (details in Part 5, Chapter 6).
- Multiple studies indicated a limited impact of lowering exposure settings (i.e. tube current, scanning time) on the resultant volume quality and accuracy sufficient for implant therapy (Sur et al., 2010; Al-Ekrish, 2012; Vandenberghe et al., 2012).
- The relevant literature showed that each x-ray unit can yield variable received doses, hence, each radiographic facility should be aware of these doses and the technical specification (including the exposure protocols), further details are in Part 5, Chapter 2. This information is vital and can readily influence the radiographic protocols

followed at a specific facility – particularly that some CBCT machines were reported to yield comparable effective doses to their conventional counterparts (i.e. as low as a panoramic radiograph).

- Efficient equivalent dose reduction received by the orbits, lens of the eye, and different parts of the brain was confirmed using the shield in CBCT exams ( $15 \times 12$  cm FOV). The modified face shield is thus suggested for any clinical situation that warrants a large field of view examination. Nevertheless, a limited to no protection effectiveness during panoramic radiography and CBCT, with fields of view set at maxilla and mandible ( $\sim 8 \times 9$  cm) was noted (Part 6, Chapter 5).

Inconsistency is evident internationally in terms of using cross-sectional imaging (i.e. CBCT) indiscriminately (Drago & Carpentieri, 2011; Noffke et al., 2011; Tyndall et al., 2012; Ahmad & Chapokas, 2019) or based on necessity during implant planning (Benavides et al., 2012; Harris et al., 2012; European Commission, 2012; Superior Health Council, 2011; Kim et al., 2020). The variation between these imaging guidelines could possibly lead to indifference by many clinicians. Thus, there is compelling need to formulate vigorous guideline-forming methodologies; since the establishing evidence is presumed the same for most of these guidelines, but not the drawn “conclusions” (Horner et al., 2015).

Proving the role of CBCT compared to panoramic radiography in “controlled prospective clinical trials” to reduce potential damages to the vital structures (e.g. inferior alveolar nerve) during the implant therapy, is challenging due to inadequate sample size and ethical issues raised by such a study design (Bornstein et al., 2017). The investigator of this study presumes that this lack of such evidence in legitimising a standard radiographic approach (i.e. to employ 3D imaging during the implant planning phase), has made the available guidelines controversial and without international standardisation – as most are derived from consensus or experts’ opinions.

Emerging technologies as digital implant planning (computer-guided surgeries) particularly its indications, were not investigated, as this was not the aim of this study.

However, it must be acknowledged that if guided implantology was chosen as the best treatment option, three-dimensional imaging (CT or CBCT) would be a pre-requisite.

The investigator of this study speculates that a selective approach based on specific criteria to use CBCT should be practised. As such, a selection criterion is also mostly a result of consensus and clinical opinions, the investigator proposes a working draft protocol (Section 2, Part 7) based on the finding of the various facets of this study; which represents the clinical opinion of the investigator. The indiscriminate use of CBCT during implant planning is valued, only if these CBCT acquisitions proved to expose patients to minimal doses compared to the conventional radiographic exams (i.e. panoramic radiograph).

Whether the consensus arguments lead one to support 2D over 3D imaging (or vice versa) or, even to have combined examinations, justification of these exposures must be determined to benefit the patient and after a thorough dental and medical exam.



#### Disclaimer

The following suggested “working” protocol is a draft that is not ready for clinical employment at this stage. As such, these recommendations are still open to further modifications, amendments, and discussions. This protocol represents the scientifically-based best practices of the investigator of this study. The data obtained should inform the development of formal guidelines in south Africa by relative authorities.

## SECTION 2: PROPOSED DRAFT RECOMMENDATIONS ON IMPLANT IMAGING IN SA (CHART 7-1)

Even though dental radiation doses are minimal, every radiation exposure must be justified. This should be preceded by a thorough history and clinical, medical, and dental examination.

### 2.1 CLINICAL NOTES TO JUSTIFY AND OPTIMISE DENTAL EXPOSURE:

- 1- The most appropriate radiographic modality and exposure protocol should be selected in order to achieve the diagnostic goal and yet yield the least exposure.
- 2- Continuous monitoring of the local diagnostic reference levels (DRL) is recommended in order to confirm that these remain within the ranges of nationally and regionally accepted DRL for the same type of radiographic procedure (Harris et al., 2012).
- 3- Regular evaluation and maintenance of the x-ray machines including radiographic quality assurance procedures and assessment of radiation outputs are encouraged (Harris et al., 2012). Compliance with the guidelines and codes of practice published by The South African Health Products Regulatory Authority (SAHPRA), including the quality control tests for dental diagnostic x-ray imaging systems, is recommended (Radiation control, 2017).
- 4- The use of radiation protective measures such as leaded aprons and thyroid shields where applicable (particularly during intraoral radiography and especially for young patients) is suggested.
- 5- Ensure the right beam characterising factors (e.g. kVp, mAs) are selected, with the lowest-dose exposure protocols that achieve adequate diagnostic quality. The highest quality acquisition is generally not required during implant therapy; the “adequate” quality is the target (Bornstein et al., 2017). However, the use of very low exposure parameters can lead to poor diagnostic images, which will be of no clinical use. The ALARA principles have been modified to ALADA (‘As Low As Diagnostically Acceptable’) to ensure a balance between the resultant image quality and optimisation of the procedure (Bornstein et al., 2017).

- 6- During CBCT acquisitions, it is vital to limit the field of view to the area of interest.
- 7- Ensure optimum and stable head position at all times, since any movement of the patient would compromise the resultant image quality and consequently may require retakes.
- 8- The basic principles of using CBCT proposed by the European Academy of Dental and Maxillofacial Radiology (Horner et al., 2009) should be followed.

## 2.2 Phase I: Initial patient assessment

- 1- Obtain a comprehensive medical and dental history prior to choosing image modalities. Moreover, eliminate any implant candidate whose medical history might preclude successful placement and maintenance of an implant.
- 2- Perform a thorough clinical examination of the oral and maxillofacial structures (including the candidate implant site), and determining if the patient's periodontal status is acceptable for implant placement.
- 3- Undertake a detailed clinical inspection of the potential implant site that includes palpation of the bony structure which will identify any clinically obvious irregular bone architecture, clinically visible soft pathologies, and ridge undercuts. The assessment of the occlusion, and selective ridge mapping of the potential implant site are recommended.
- 4- A stone model (cast) should be made for both jaws. This allows for the confirmation and evaluation of the available spaces, bone and dental morphology, and occlusion. Furthermore, the fabrication of a radiographic guide with embedded radio markers will then be possible, and this is recommended prior to any initial radiographic examination.
- 5- A panoramic view, performed with the radiographic guide in place, is justified at this stage. This is necessary for the evaluation of the jaws, to approximate the initial bone quality and quantity, to detect intraosseous pathology, and to determine the overall risk.
- 6- The process of risk/benefit assessment is mandatory in deciding how to proceed if more sophisticated radiographic modalities are necessary.



---

## 2.2.1 FACTORS WHICH INCREASE THE RISK OF TREATMENT COMPLICATIONS

- 1- If the initial clinical and conventional radiographic assessment raised suspicions of irregular alveolar bone architecture, insufficient bone dimension, and the presence of undercuts, then a CBCT is advised.
- 2- Proximity to vital structures:
  - Mental foramen (MF): the investigator recommends the consideration of a CBCT in cases where implants are to be placed in the vicinity of the MF; since the radiographic presentation of the borders of the MF on conventional 2D imaging could be variable, and measurements performed to these borders are prone to uncertainties (Beshtawi et al., 2020).
  - Inferior alveolar nerve (IAN): if the clinical assessment (e.g. ridge mapping and dental model/casts) supplemented with conventional 2D radiographs revealed an insufficient quantity of bone (excluding the 2 mm safe zone) or irregular architecture, then CBCT is recommended.
  - Maxillary sinuses and nasopalatine canal: if the clinical assessment supplemented with 2D radiographs showed an insufficient quantity of bone and/or irregular architecture, CBCT is recommended.
  - Lingual foramen region: the author recommends CBCT if the dental implants need to be placed in the region of the 32-42.
- 3- If digital implant planning (computer-guided surgery) is considered, CBCT/CT is a prerequisite.
- 4- Aesthetic and prosthetic demands: if the conventional approaches which include dental models (casts) and 2D radiographs proved not to be adequate to optimally assess the aesthetic demands of the patient, and if 3D images are predicted to add information, CBCT is then justified.
- 5- If bone grafting procedures are indicated, CBCT is advised.

### 2.3 Phase II: Implant planning

If implants were considered as an option after a careful initial assessment, the clinician can then proceed to the implant planning phase.

After the risk assessment of the patient, if a low-risk profile was identified, then planning will be based on conventional 2D radiographic modalities only (PAN /and PA). In these circumstances, the following should be considered:

- Prior to the initial panoramic examination, care should be taken in adopting the optimum patient position and adherence to the manufacturer's instruction. Minor head position errors can result in inaccurate dimensions.
- Quality assurance of the resultant panoramic radiograph should be carried out to confirm the absence of any distortions and the attainment of optimum diagnostic quality.
- Calibrating the virtual measurements by comparing them with their corresponding physical measurements performed on a stone model or using the radiographic markers (of predetermined dimensions and angles embedded in the radiographic guide) would help detect distortions and magnifications.
- Dimensional accuracy of conventional modalities is inconsistent (i.e. technique sensitive) and may carry substantial risks, and hence a wide compensatory safe zone (at least 2 mm) is advised. Moreover, care should be taken when measuring the length of the arch (the arc) between two reference points on the panoramic radiographs, particularly between the anterior and posterior segments (at the curvature of the jaw). This entails capturing a linear 2D measurement for an angular three-dimensional structure, hence, incurring possible inaccuracies.
- If periapical radiographs are considered, the parallel technique using a film holder is recommended. A parallel relationship between the long axis of the alveolar bone and the x-ray receptor must be ensured as much as anatomically

possible. Compensation for possible dimensional distortions must be considered, particularly, in maxillary acquisitions.

If the patient showed medium to high-risk profiles, the author advises the use of three-dimensional modalities, with the CBCT being the best option.

If **CBCT** is considered:

- Ensure static and optimum patient head position during the acquisition. Volumes with motion artefacts are risky and unreliable and must not be used for any succeeding dimensional analysis. In the author's experience, subtle patient movements could result in degrading the overall quality of the volume (even without inducing a striking motion artefact), and hence might compromise the identification of borders and subsequent measurements.
- The lead apron should be worn during all CBCT examinations. Although the clinical applicability is sometimes questionable during extraoral x-ray examinations, thyroid collar shields may be considered. In particular, when the patient is at high risk (e.g. young ages, females), the region of interest is further away from the domain of the shield artefacts (e.g. CBCT exam with a field of view collimated only to the maxilla), and if it does not impose a technical challenge (short neck height that may obscure the region of interest).
- The patient's upper and lower teeth should be apart during the examination to avoid overlapping. The patient should be advised to bite on cotton rolls (in a symmetric fashion). Another approach would be to let the patient bite on tissue wax; this will ensure the stability of the jaws while separating upper and lower teeth.
- Adjust the acquisition to the smallest applicable field of view that depicts an adequate area of the candidate implant site (region of interest).
- The lowest exposure parameters that maintain acceptable diagnostic quality should be chosen. One of the main challenges is the presence of Ferro-metallic objects in the region of interest that may induce volumes artefacts, which may

require higher exposure parameters in order to reduce its effect. Revising the exposure protocols provided by each CBCT machine would help identify the available options.

- During virtual dimension analysis, reconstructing cross-sections for the region of interest with measurable and clinically reproducible thickness, is recommended. Awareness of the axial plane orientation (head sagittal titling) before capturing measurements on the cross-sectional slices is necessary. The axial plane should be in line with the cusps of the upper or lower teeth. Deviations in the axial plane orientation will be inherent in the reconstructed cross-sectional images, and this can result in false interpretation when measurements are reproduced clinically.

#### 2.4 Phase III: Intra-operative, directly post-surgery, and post-prosthetic stages

**During and directly after surgery**, periapical radiography is sufficient. After surgery and in conditions when there was extensive dental implant placement (e.g. multiple implants in different jaw segments), a panoramic radiograph can be taken instead of multiple periapical radiographs. Three-dimensional images are not recommended except in an emergency such as loss of sensation (related to the surgery), uncontrolled bleeding, and suspicion of perforation of the surrounding anatomy.

**During the prosthetic phase**, a periapical radiograph can be used to ensure the integrity of the components of the implant, full seating of the crowns, and the efficient elimination of any excess cement. A parallel relationship between the implant axis and the x-ray receptor should be ensured so as to not superimpose any defect between the implant components.

## 2.5 Phase IV: Follow-up

Clinical assessment of the mechanical stability of the implants, the presence of any symptoms, or complications (e.g. pain, unresolving swelling, loss of sensation), should be assessed. In the case of:

---

### 2.5.1 ASYMPTOMATIC PATIENTS

Intraoral periapical radiographs coupled with clinical examination are sufficient and of value in assessing the osteointegration of the implant, the presence of any peri-implant pathology, and the integration of the components of the implant. A panoramic radiograph can be used in the case of extensive implant therapy, with the possible combination of intraoral periapical radiographs only for the questionable implant sites. The use of CBCT is anticipated to cause beam hardening artefacts, which would compromise the optimal assessment of the implant site and, thus, is not advised.

---

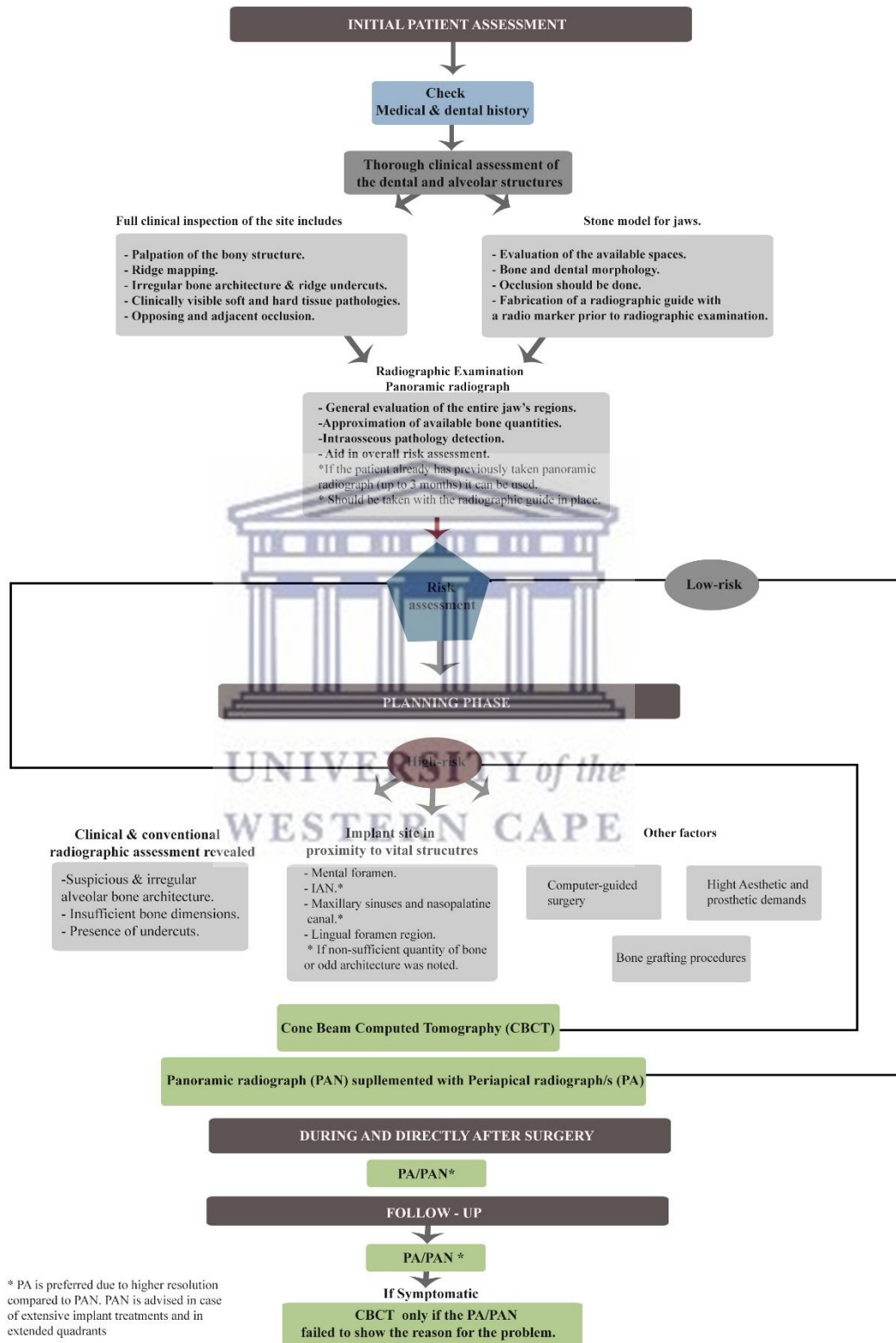
### 2.5.2 SYMPTOMATIC PATIENTS

A periapical or panoramic radiograph can be used initially, and CBCT is then advised if the conventional approaches failed to identify the source of the problem. If the conventional radiographs showed direct or suspicious proximity to vital structures, CBCT is advised, but should be limited to that region of interest.

The recommended frequency of the follow-ups was not evaluated, as this was beyond the scope of this study.

**To conclude, the author presents the following diagrammatic representation of the recommendations, which were informed by the analyses of the findings of this project (Chart 7-1).**

**Chart 7-1. Recommendation on dental implant imaging in SA**



## PART 8 REFERENCES

- Abbott, P. (2000). Are dental radiographs safe?. *Australian Dental Journal*, 45(3): 208–213.
- Academy of Osseointegration. (2010). 2010 Guidelines of the Academy of Osseointegration for the provision of dental implants and associated patient care. *The International journal of oral & maxillofacial implants*, 25(3): 620–7.
- Adibi, S., Shahidi, S., Nikanjam, S., Paknahad, M. & Ranjbar, M. (2017). Influence of Head Position on the CBCT Accuracy in Assessment of the Proximity of the Root Apices to the Inferior Alveolar Canal. *Journal of dentistry (Shiraz, Iran)*, 18(3): 181–186.
- Agrawal, A., Agrawal, G., Nagarajappa, A. kumar, Sreedevi & Kakkad, A. (2014). Journey from 2D to 3D: Implant imaging a review. *International journal of contemporary Dental & Medical Reviews*, 2014.
- Ahmad, O. & Chapokas, A. (2019). *Diagnostic imaging in the treatment planning, surgical, and prosthodontic aspects of implant dentistry*. Chicago: American College of Prosthodontists. Available at: [https://www.prosthodontics.org/assets/1/7/Diagnostic\\_Imaging\\_in\\_the\\_Treatment\\_Planning,\\_Surgical,\\_and\\_Prosthodontic\\_Aspects\\_of\\_Implant\\_Dentistry.pdf](https://www.prosthodontics.org/assets/1/7/Diagnostic_Imaging_in_the_Treatment_Planning,_Surgical,_and_Prosthodontic_Aspects_of_Implant_Dentistry.pdf).
- Aksoy, U., Eratalay, K. & Tözüm, T.F. (2009). The possible association among bone density values, resonance frequency measurements, tactile sense, and histomorphometric evaluations of dental implant osteotomy sites: A preliminary study. *Implant Dentistry*, 18(4): 316–325.
- Al-Ekrish, A.A. (2012). Effect of exposure time on the accuracy and reliability of cone beam computed tomography in the assessment of dental implant site dimensions in dry skulls. *Saudi Dental Journal*, 24(3–4): 127–134.
- Al-Ekrish, A.A. & Ekram, M. (2011). A comparative study of the accuracy and reliability of multidetector computed tomography and cone beam computed

- tomography in the assessment of dental implant site dimensions. *Dentomaxillofacial Radiology*, 40(2): 67–75.
- Al-Okshi, A., Nilsson, M., Petersson, A., Wiese, M. & Lindh, C. (2013). Using Gafchromic film to estimate the effective dose from dental cone beam CT and panoramic radiography. *Dentomaxillofacial Radiology*, 42(7).
- Albrektsson, T., Zarb, G., Worthington, P. & Eriksson, A.R. (1986). The long-term efficacy of currently used dental implants: a review and proposed criteria of success. *The International journal of oral & maxillofacial implants*, 1(1): 11–25.
- Aliasgharzadeh, A., Mihandoost, E., Masoumbeigi, M., Salimian, M. & Mohseni, M. (2015). Measurement of entrance skin dose and calculation of effective dose for common diagnostic x-Ray examinations in Kashan, Iran. *Global journal of health science*, 7(5): 202–207.
- Alnahwi, M., Alqarni, A., Alqahtani, R., Baher Baker, M. & Alshahrani, F.N. (2017). A survey on radiographic prescription practices in dental implant assessment. *Journal of Applied Dental and Medical Sciences*, 3(1): 148–156.
- Amarnath, G.S., Kumar, U., Hilal, M., Muddugangadhar, B.C., Anshuraj, K. & Shruthi, C.S. (2015). Comparison of cone beam computed tomography, orthopantomography with direct ridge mapping for pre-surgical planning to place implants in cadaveric mandibles: An ex-vivo study. *Journal of international oral health*, 7(Suppl 1): 38–42.
- Aminoshariae, A., Su, A. & Kulild, J.C. (2014). Determination of the location of the mental foramen: A critical review. *Journal of Endodontics*, 40(4): 471–475.
- Amis, E.S., Butler, P.F., Applegate, K.E., Birnbaum, S.B., Brateman, L.F., Hevezi, J.M., Mettler, F.A., Morin, R.L., Pentecost, M.J., Smith, G.G., Strauss, K.J. & Zeman, R.K. (2007). American College of Radiology White Paper on Radiation Dose in Medicine. *Journal of the American College of Radiology*, 4(5): 272–284.
- De Andrade, J., Valerio, C., Monteiro, M., Machado, V. & Manzi, F. (2016).



- Comparison of 64-detector-multislice and cone beam computed tomographies in the evaluation of linear measurements in the alveolar ridge. *The International Journal of Prosthodontics*, 29(2): 132–134.
- Aps, J.K.M. & Scott, J.M. (2014). Oblique lateral radiographs and bitewings; estimation of organ doses in head and neck region with Monte Carlo calculations. *Dentomaxillofacial Radiology*, 43(6).
- Arisan, V., Karabuda, Z.C., Avsever, H. & Özdemir, T. (2013). Conventional multi-slice computed tomography (CT) and cone-beam CT (CBCT) for computer-assisted implant placement. Part I: Relationship of radiographic gray density and implant stability. *Clinical Implant Dentistry and Related Research*, 15(6): 893–906.
- Armstrong, R.T. (2006). Acceptability of cone beam CT vs. Multi-detector CT for 3D anatomic model construction. *Journal of Oral and Maxillofacial Surgery*, 64(9): 37.
- Assaf, M. & Gharbyah, A. (2014). Accuracy of Computerized Vertical Measurements on Digital Orthopantomographs: Posterior Mandibular Region. *Journal of Clinical Imaging Science*, 4(2): 7.
- Attaia, D., Ting, S., Johnson, B., Masoud, M.I., Friedland, B., Abu El Fotouh, M. & Abu el Sadat, S. (2020). Dose reduction in head and neck organs through shielding and application of different scanning parameters in cone beam computed tomography: an effective dose study using an adult male anthropomorphic phantom. *Oral Surgery, Oral Medicine, Oral Pathology and Oral Radiology*, 130(1): 101–109.
- Bai, M., Liu, X. & Liu, B. (2013). Effective patient dose during neuroradiological C-arm CT procedures. *Diagnostic and Interventional Radiology*, 19(1): 29–32.
- Bansal, G.J. (2006). Digital radiography. A comparison with modern conventional imaging. *Postgraduate medical journal*, 82(969): 425–8.
- Batista, W. (2016). Use of Monte Carlo simulation software for calculating effective

- dose in cone beam computed tomography. In *16 International Symposium on Solid State Dosimetry*. México: International Symposium on Solid State Dosimetry: 237–246. Available at: [https://inis.iaea.org/collection/NCLCollectionStore/\\_Public/48/016/48016655.pdf](https://inis.iaea.org/collection/NCLCollectionStore/_Public/48/016/48016655.pdf). [Accessed 13 April 2020].
- Baumgaertel, S., Palomo, J.M., Palomo, L. & Hans, M.G. (2009). Reliability and accuracy of cone-beam computed tomography dental measurements. *American Journal of Orthodontics and Dentofacial Orthopedics*, 136(1): 19–25.
- Begoña Ormaechea, M., Millstein, P. & Hirayama, H. (1999). Tube angulation effect on radiographic analysis of the implant-abutment interface. *The International journal of oral & maxillofacial implants*, 14(1): 77–85.
- Behneke, A., Burwinkel, M. & Behneke, N. (2012). Factors influencing transfer accuracy of cone beam CT-derived template-based implant placement. *Clinical Oral Implants Research*, 23(4): 416–423.
- Benavides, E., Rios, H.F., Ganz, S.D., An, C.H., Resnik, R., Reardon, G.T., Feldman, S.J., Mah, J.K., Hatcher, D., Kim, M.J., Sohn, D.S., Palti, A., Perel, M.L., Judy, K.W.M., Misch, C.E. & Wang, H.L. (2012). Use of cone beam computed tomography in implant dentistry: The international congress of oral implantologists consensus report. *Implant Dentistry*, 21(2): 78–86.
- Berglundh, T., Armitage, G., Araujo, M.G., Avila-Ortiz, G., Blanco, J., Camargo, P.M., Chen, S., Cochran, D., Derks, J., Figuero, E., Hämmerle, C.H.F., Heitz-Mayfield, L.J.A., Huynh-Ba, G., Iacono, V., Koo, K.T., Lambert, F., McCauley, L., Quirynen, M., Renvert, S., Salvi, G.E., Schwarz, F., Tarnow, D., Tomasi, C., Wang, H.L. & Zitzmann, N. (2018). Peri-implant diseases and conditions: Consensus report of workgroup 4 of the 2017 World Workshop on the Classification of Periodontal and Peri-Implant Diseases and Conditions. *Journal of Clinical Periodontology*, 45(Suppl 20): 286–291.
- Berrington De González, A., Mahesh, M., Kim, K.P., Bhargavan, M., Lewis, R.,

- Mettler, F. & Land, C. (2009). Projected Cancer Risks from Computed Tomographic Scans Performed in the United States in 2007. *Archives of Internal Medicine*, 169(22): 2071–2077.
- Bertram, F., Bertram, S., Rudisch, A. & Emschoff, R. (2018). Assessment of location of the mandibular canal: Correlation between panoramic and cone beam computed tomography measurements. *The International Journal of Prosthodontics*, 31(2): 129–134.
- Beshtawi, K., Qirresh, E., Parker, M. & Shaik, S. (2020). Custom focal trough in Cone-beam computed tomography reformatted panoramic versus digital panoramic for mental foramen position to aid implant planning. *Journal of Clinical Imaging Science*, 10(34).
- Bornstein, M., Scarfe, W., Vaughn, V. & Jacobs, R. (2014). Cone beam computed tomography in implant dentistry: A systematic review focusing on guidelines, indications, and radiation dose risks. *The International Journal of Oral & Maxillofacial Implants*, 29(Supplement): 55–77.
- Bornstein, M.M., Horner, K. & Jacobs, R. (2017). Use of cone beam computed tomography in implant dentistry: current concepts, indications and limitations for clinical practice and research. *Periodontology 2000*, 73(1): 51–72.
- Bou Serhal, C., Jacobs, R., Flygare, L., Quirynen, M. & Van Steenberghe, D. (2002). Perioperative validation of localisation of the mental foramen. *Dentomaxillofacial Radiology*, 31(1): 39–43.
- Boyce, R.A. & Klemons, G. (2015). Treatment planning for restorative implantology. *Dental Clinics of NA*, 59: 291–304.
- Brenner, D.J. & Hall, E.J. (2007). Computed tomography - An increasing source of radiation exposure. *New England Journal of Medicine*, 357(22): 2277–2284.
- Carrafiello, G., Dizonno, M., Colli, V., Strocchi, S., Pozzi Taubert, S., Leonardi, A., Giorgianni, A., Barresi, M., Macchi, A., Bracchi, E., Conte, L. & Fugazzola, C. (2010). Comparative study of jaws with multislice computed tomography and

- cone-beam computed tomography. *La Radiologia medica*, 115(4): 600–611.
- Carter, J.B., Stone, J.D., Clark, R.S. & Mercer, J.E. (2016). Applications of cone-Beam computed tomography in oral and maxillofacial surgery: An overview of published indications and clinical usage in United States academic centers and oral and maxillofacial surgery practices. *Journal of Oral and Maxillofacial Surgery*, 74(4): 668–679.
- Cassetta, M., Di Giorgio, R. & Barbato, E. (2018). Are intraoral radiographs reliable in determining peri-implant marginal bone level changes? The correlation between open surgical measurements and peri-apical radiographs. *International Journal of Oral and Maxillofacial Surgery*, 47(10): 1358–1364.
- Cassetta, M., Stefanelli, L.V., Pacifici, A., Pacifici, L. & Barbato, E. (2014). How accurate is CBCT in measuring bone density? A comparative CBCT-CT in vitro study. *Clinical Implant Dentistry and Related Research*, 16(4): 471–478.
- Chau, A.C.M. & Fung, K. (2009). Comparison of radiation dose for implant imaging using conventional spiral tomography, computed tomography, and cone-beam computed tomography. *Oral Surgery, Oral Medicine, Oral Pathology, Oral Radiology and Endodontology*, 107(4): 559–65.
- Chinem, L.A.S., Vilella, B.D.S., Maurício, C.L.D.P., Canevaro, L.V., Deluiz, L.F. & Vilella, O.D.V. (2016). Digital orthodontic radiographic set versus cone-beam computed tomography: An evaluation of the effective dose. *Dental Press Journal of Orthodontics*, 21(4): 66–72.
- Colombo, M., Mangano, C., Mijiritsky, E., Krebs, M., Hauschild, U. & Fortin, T. (2017). Clinical applications and effectiveness of guided implant surgery: a critical review based on randomized controlled trials. *BMC oral health*, 17(1): 150.
- Correa, L.R., Spin-Neto, R., Stavropoulos, A., Schropp, L., da Silveira, H.E.D. & Wenzel, A. (2014). Planning of dental implant size with digital panoramic radiographs, CBCT-generated panoramic images, and CBCT cross-sectional

- images. *Clinical Oral Implants Research*, 25(6): 690–695.
- Council, N.R. (2006). *Health risks from exposure to low levels of ionizing radiation: BEIR VII phase 2*. Washington, DC: National Academies Press.
- Cremonini, C.C., Dumas, M., Pannuti, C.M., Neto, J.B.C., Cavalcanti, M.G.P. & Lima, L.A. (2011). Assessment of linear measurements of bone for implant sites in the presence of metallic artefacts using cone beam computed tomography and multislice computed tomography. *International Journal of Oral and Maxillofacial Surgery*, 40(8): 845–850.
- Dattatreya, S., Vaishali, K., Shetty, V. & Suma. (2016). Imaging Modalities in implant dentistry. *Journal of Dental & Oro-facial Research*, 12(1): 22–29.
- Davies, J., Johnson, B. & Drage, N. (2012). Effective doses from cone beam CT investigation of the jaws. *Dentomaxillofacial Radiology*, 41(1): 30–36.
- Dawood, A., Brown, J., Sauret-Jackson, V. & Purkayastha, S. (2012). Optimization of cone beam CT exposure for pre-surgical evaluation of the implant site. *Dentomaxillofacial Radiology*, 41(1): 70–74.
- Deeb, G., Antonos, L., Tack, S., Carrico, C., Laskin, D. & Deeb, J.G. (2017). Is cone-beam computed tomography always necessary for dental implant placement? *Journal of Oral and Maxillofacial Surgery*, 75(2): 285–289.
- Deshpande, A. & Bhargava, D. (2014). Intraoral periapical radiographs with grids for implant dentistry. *Journal of maxillofacial and oral surgery*, 13(4): 603–5.
- Devlin, H. & Yuan, J. (2013). Object position and image magnification in dental panoramic radiography: A theoretical analysis. *Dentomaxillofacial Radiology*, 42(1): 29951683.
- Diniz, A.F.N., Mendonça, E.F., Leles, C.R., Guilherme, A.S., Cavalcante, M.P. & Silva, M.A.G.S. (2008). Changes in the pre-surgical treatment planning using conventional spiral tomography. *Clinical Oral Implants Research*, 19(3): 249–53.

- Dölekoğlu, S., Fişekçioğlu, E., İlgüy, M. & İlgüy, D. (2011). The usage of digital radiography and cone beam computed tomography among Turkish dentists. *Dentomaxillofacial Radiology*, 40(6): 379.
- Drage, N.A., Palmer, R.M., Blake, G., Wilson, R., Crane, F. & Fogelman, I. (2007). A comparison of bone mineral density in the spine, hip and jaws of edentulous subjects. *Clinical Oral Implants Research*, 18(4): 496–500.
- Drago, C. & Carpentieri, J. (2011). Treatment of maxillary jaws with dental implants: Guidelines for treatment. *Journal of Prosthodontics*, 20(5): 336–347.
- Dudhia, R., Monsour, P.A., Savage, N.W. & Wilson, R.J. (2011). Accuracy of angular measurements and assessment of distortion in the mandibular third molar region on panoramic radiographs. *Oral Surgery, Oral Medicine, Oral Pathology, Oral Radiology and Endodontology*, 111(4): 508–516.
- El-Beialy, A.R., Fayed, M.S., El-Bialy, A.M. & Mostafa, Y.A. (2011). Accuracy and reliability of cone-beam computed tomography measurements: Influence of head orientation. *American Journal of Orthodontics and Dentofacial Orthopedics*, 140(2): 157–165.
- European Commission. (2012). *Protection radiation No 172: Cone beam CT for dental and maxillofacial radiology (Evidence-based guidelines)*. Luxembourg. Available at: [http://www.sedentexct.eu/files/radiation\\_protection\\_172.pdf](http://www.sedentexct.eu/files/radiation_protection_172.pdf). [Accessed 19 April 2019].
- European Commission. (2004). *Radiation Protection No 136: European guidelines on radiation protection in dental radiology - The safe use of radiographs in dental practice*. Luxembourg. Available at: <https://ec.europa.eu/energy/sites/ener/files/documents/136.pdf>. [Accessed 16 June 2019].
- Field, M.J. & Lohr, K.N. (1992). *Guidelines for Clinical Practice*. National Academies Press (US).
- Filius, M.A.P., Kraeima, J., Vissink, A., Janssen, K.I., Raghoobar, G.M. & Visser, A.

- (2017). Three-dimensional computer-guided implant placement in oligodontia. *International Journal of Implant Dentistry*, 3(1): 30.
- Flügge, T., Derksen, W., te Poel, J., Hassan, B., Nelson, K. & Wismeijer, D. (2017). Registration of cone beam computed tomography data and intraoral surface scans – A prerequisite for guided implant surgery with CAD/CAM drilling guides. *Clinical Oral Implants Research*, 28(9): 1113–1118.
- Flügge, T.V., Nelson, K., Schmelzeisen, R. & Metzger, M.C. (2013). Three-dimensional plotting and printing of an implant drilling guide: Simplifying guided implant surgery. *Journal of Oral and Maxillofacial Surgery*, 71(8): 1340–1346.
- Fokas, G., Vaughn, V.M., Scarfe, W.C. & Bornstein, M.M. (2018). Accuracy of linear measurements on CBCT images related to presurgical implant treatment planning: A systematic review. *Clinical Oral Implants Research*, 29(Suppl 16): 393–415.
- Fortin, T., Isidori, M. & Bouchet, H. (2009). Placement of posterior maxillary implants in partially edentulous patients with severe bone deficiency using CAD/CAM guidance to avoid sinus grafting: a clinical report of procedure. *The International journal of oral & maxillofacial implants*, 24(1): 96–102.
- Frei, C., Buser, D. & Dula, K. (2004). Study on the necessity for cross-section imaging of the posterior mandible for treatment planning of standard cases in implant dentistry. *Clinical Oral Implants Research*, 15(4): 490–7.
- Ganguly, R., Ramesh, A. & Pagni, S. (2016). The accuracy of linear measurements of maxillary and mandibular edentulous sites in conebeam computed tomography images with different fields of view and voxel sizes under simulated clinical conditions. *Imaging Science in Dentistry*, 46(2): 93–101.
- Ganguly, R., Ruprecht, A., Vincent, S., Hellstein, J., Timmons, S. & Qian, F. (2011). Accuracy of linear measurement in the Galileos cone beam computed tomography under simulated clinical conditions. *Dentomaxillofacial Radiology*,

- 40(5): 299–305.
- Ganz, S.D. (2011). Cone beam computed tomography–assisted treatment planning concepts. *Dental Clinics of North America*, 55(3): 515–536.
- Geleijns, J., Salvadó Artells, M., Veldkamp, W.J.H., López Tortosa, M. & Calzado Cantera, A. (2006). Quantitative assessment of selective in-plane shielding of tissues in computed tomography through evaluation of absorbed dose and image quality. *European radiology*, 16(10): 2334–2340.
- Gomez-Roman, G., Lukas, D., Beniashvili, R. & Schulte, W. (1999). Area-dependent enlargement ratios of panoramic tomography on orthograde patient positioning and its significance for implant dentistry. *The International journal of oral & maxillofacial implants*, 14(2): 248–57.
- Goren, A.D., Prins, R.D., Dauer, L.T., Quinn, B., Al-Najjar, A., Faber, R.D., Patchell, G., Branets, I. & Colosi, D.C. (2013). Effect of leaded glasses and thyroid shielding on cone beam CT radiation dose in an adult female phantom. *Dento maxillo facial radiology*, 42(6): 20120260.
- Granolund, C., Thilander-Klang, A., Ylhan, B., Lofthag-Hansen, S. & Ekestubbe, A. (2016). Absorbed organ and effective doses from digital intra-oral and panoramic radiography applying the ICRP 103 recommendations for effective dose estimations. *British Journal of Radiology*, 89(1066): 20151052.
- Gray, C.F., Redpath, T.W., Smith, F.W. & Staff, R.T. (2003). Advanced imaging: Magnetic resonance imaging in implant dentistry. *Clinical oral implants research*, 14(1): 18–27.
- Grol, R. & Grimshaw, J. (2003). From best evidence to best practice: Effective implementation of change in patients' care. *Lancet*, 362(9391): 1225–1230.
- Grunder, U., Gracis, S. & Capelli, M. (2005). Influence of the 3-D bone-to-implant relationship on esthetics. *The International journal of periodontics & restorative dentistry*, 25(2): 113–9.
- Gupta, A., Devi, P., Srivastava, R. & Jyoti, B. (2014). Intra oral periapical



- radiography-basics yet intrigue: A review. *Bangladesh Journal of Dental Research & Education*, 4(2): 83–7.
- Gupta, S., Patil, N., Solanki, J., Singh, R. & Laller, S. (2015). Oral implant imaging: A review. *The Malaysian journal of medical sciences : MJMS*, 22(3): 7–17.
- Haghnegahdar, A. & Bronoosh, P. (2013). Accuracy of linear vertical measurements in posterior mandible on panoramic view. *Dental research journal*, 10(2): 220–4.
- Halboub, E.S., Barnkgkei, I., Alsabbagh, O. & Hamadah, O. (2015). Radiation-induced thumbs carcinoma due to practicing dental X-ray. *Contemporary Clinical Dentistry*, 6(1): 116–118.
- Harris, D., Buser, D., Dula, K., Gröndahl, K., Jacobs, R., Lekholm, U., Nakielny, R., Van Steenberghe, D. & Van Der Stelt, P. (2002). E.A.O. guidelines for the use of diagnostic imaging in implant dentistry: A consensus workshop organized by the European Association for Osseointegration in Trinity College Dublin. *Clinical Oral Implants Research*, 13(5): 566–70.
- Harris, D., Horner, K., Gröndahl, K., Jacobs, R., Helmrot, E., Benic, G.I., Bornstein, M.M., Dawood, A. & Quirynen, M. (2012). E.A.O. guidelines for the use of diagnostic imaging in implant dentistry 2011. A consensus workshop organized by the European Association for Osseointegration at the Medical University of Warsaw. *Clinical Oral Implants Research*, 23(11): 1243–1253.
- Hatcher, D.C., Dial, C. & Mayorga, C. (2003). Cone beam CT for pre-surgical assessment of implant sites. *Journal of the California Dental Association*, 31(11): 825–33.
- Hidalgo, A., Davies, J., Horner, K. & Theodorakou, C. (2015). Effectiveness of thyroid gland shielding in dental CBCT using a paediatric anthropomorphic phantom. *Dentomaxillofacial Radiology*, 44(3): 20140285.
- Horner, K., Islam, M., Flygare, L., Tsiklakis, K. & Whaites, E. (2009). Basic principles for use of dental cone beam computed tomography: consensus

- guidelines of the European Academy of Dental and Maxillofacial Radiology. *Dento maxillo facial radiology*, 38(4): 187–95.
- Horner, K., O'Malley, L., Taylor, K. & Glenny, A.-M. (2015). Guidelines for clinical use of CBCT: a review. *Dento maxillo facial radiology*, 44(1): 20140225.
- Horner, K. & Shelley, A.M. (2016). Preoperative radiological evaluation of missing single teeth: A review. *European Journal of Oral Implantology*, 9(Suppl 1): 69–88.
- Hounsfield, G. (1973). Computerized transverse axial scanning(tomography):Part I description of system. *British Journal of Radiology*, 46(552): 1016–1022.
- Hu, K.S., Choi, D.Y., Lee, W.J., Kim, H.J., Jung, U.W. & Kim, S. (2012). Reliability of two different presurgical preparation methods for implant dentistry based on panoramic radiography and cone-beam computed tomography in cadavers. *Journal of Periodontal and Implant Science*, 42(2): 39–44.
- Iannucci, J. & Howerton, L.J. (2017). *Dental Radiography*. 5th editio. St. Louis, Missouri: Elsevier.
- International team for implantology. (2014). Contemporary surgical and radiographic techniques: cone beam computed tomography (CBCT). Available at: <https://www.iti.org/academy/consensus-database/consensus-statement/-/consensus/cone-beam-computed-tomography-cbct-/1212>. [Accessed 6 June 2020].
- Jacobs, R., Adriansens, A., Naert, I., Quirynen, M., Hermans, R. & Van Steenberghe, D. (1999). Predictability of reformatted computed tomography for pre-operative planning of endosseous implants. *Dentomaxillofacial Radiology*, 28(1): 37–41.
- Jacobs, R., Salmon, B., Codari, M., Hassan, B. & Bornstein, M.M. (2018). Cone beam computed tomography in implant dentistry: recommendations for clinical use. *BMC oral health*, 18(1): 88.
- Jacobs, R., Vranckx, M., Vanderstuyft, T., Quirynen, M. & Salmon, B. (2018). CBCT vs other imaging modalities to assess peri-implant bone and diagnose

- complications: a systematic review. *European Journal of Oral Implantology*, 11(Suppl 1): 77–92.
- Jayachandran, S. (2017). Digital imaging in dentistry: A review. *Contemporary clinical dentistry*, 8(2): 193–194.
- Kadesjö, N., Lynds, R., Nilsson, M. & Shi, X.Q. (2018). Radiation dose from X-ray examinations of impacted canines: Cone beam CT vs two-dimensional imaging. *Dentomaxillofacial Radiology*, 47(3).
- Karjodkar, F.R. (2009). *Textbook of dental and maxillofacial radiology*. 2nd ed. New Delhi (IND): Jaypee Brothers.
- Katsumata, A., Hirukawa, A., Okumura, S., Naitoh, M., Fujishita, M., Ariji, E. & Langlais, R.P. (2007). Effects of image artifacts on gray-value density in limited-volume cone-beam computerized tomography. *Oral Surgery, Oral Medicine, Oral Pathology, Oral Radiology, and Endodontology*, 104(6): 829–836.
- Kayal, R. (2016). Distortion of digital panoramic radiographs used for implant site assessment. *Journal of orthodontic science*, 5(4): 117–120.
- Khelassi-Toutaoui, N., Berkani, Y., Tsapaki, V., Toutaoui, A.E.K., Merad, A., Frahi-Amroun, A. & Brahim, Z. (2008). Experimental evaluation of PCXMC and prepare codes used in conventional radiology. *Radiation Protection Dosimetry*, 131(3): 374–378.
- Kim, E.K., Han, W.J., Choi, J.W. & Battulga, B. (2018). Estimation of the effective dose of dental cone-beam computed tomography using personal computer-based Monte Carlo software. *Imaging Science in Dentistry*, 48(1): 21–30.
- Kim, M.-J., Lee, S.-S., Choi, M., Ha, E.J., Lee, C., Kim, J.-E. & Heo, M.-S. (2020). Development of an evidence-based clinical imaging diagnostic guideline for implant planning: Joint recommendations of the Korean Academy of Oral and Maxillofacial Radiology and National Evidence-based Healthcare Collaborating Agency. *Imaging Science in Dentistry*, 50(1): 45.

- Kim, Y.K., Park, J.Y., Kim, S.G., Kim, J.S. & Kim, J.D. (2011). Magnification rate of digital panoramic radiographs and its effectiveness for pre-operative assessment of dental implants. *Dentomaxillofacial Radiology*, 40(2): 76–83.
- Kitai, N., Mukai, Y., Murabayashi, M., Kawabata, A., Washino, K., Matsuoka, M., Shimizu, I. & Katsumata, A. (2013). Measurement accuracy with a new dental panoramic radiographic technique based on tomosynthesis. *Angle Orthodontist*, 83(1): 117–126.
- Kobayashi, K., Shimoda, S., Nakagawa, Y. & Yamamoto, A. (2004). Accuracy in measurement of distance using limited cone-beam computerized tomography. *The International journal of oral & maxillofacial implants*, 19(2): 228–31.
- Koivisto, J., Kiljunen, T., Tapiovaara, M., Wolff, J. & Kortensniemi, M. (2012). Assessment of radiation exposure in dental cone-beam computerized tomography with the use of metal-oxide semiconductor field-effect transistor (MOSFET) dosimeters and Monte Carlo simulations. *Oral Surgery, Oral Medicine, Oral Pathology and Oral Radiology*, 114(3): 393–400.
- Kraut, R.A. (1998). Interactive CT diagnostics, planning and preparation for dental implants. *Implant dentistry*, 7(1): 19–25.
- Lagravère, M., Fang, Y., Carey, J., Toogood, R., Packota, G. & Major, P. (2006). Density conversion factor determined using a cone-beam computed tomography unit NewTom QR-DVT 9000. *Dentomaxillofacial Radiology*, 35(6): 407–409.
- Lascala, C.A., Panella, J. & Marques, M.M. (2004). Analysis of the accuracy of linear measurements obtained by cone beam computed tomography (CBCT-NewTom). *Dentomaxillofacial Radiology*, 33(5): 291–294.
- Lee, C., Lee, S.S., Kim, J.E., Huh, K.H., Yi, W.J., Heo, M.S. & Choi, S.C. (2016). Comparison of dosimetry methods for panoramic radiography: Thermoluminescent dosimeter measurement versus personal computer-based Monte Carlo method calculation. *Oral Surgery, Oral Medicine, Oral Pathology and Oral Radiology*, 121(3): 322–329.

- Lee, G.S., Kim, J.S., Seo, Y.S. & Kim, J.D. (2013). Effective dose from direct and indirect digital panoramic units. *Imaging Science in Dentistry*, 43(2): 77–84.
- Lee, K., Lee, W., Lee, J., Lee, B. & Oh, G. (2010). Dose reduction and image quality assessment in MDCT using AEC (D-DOM & Z-DOM) and in-plane bismuth shielding. *Radiation protection dosimetry*, 141(2): 162–167.
- Li, G. (2013). Patient radiation dose and protection from cone-beam computed tomography. *Imaging Science in Dentistry*, 43(2): 63.
- Lin, E.C. (2010). Radiation risk from medical imaging. *Mayo Clinic Proceedings*, 85(12): 1142–1146.
- Lindh, C., Nilsson, M., Klinge, B. & Petersson, A. (1996). Quantitative computed tomography of trabecular bone in the mandible. *Dentomaxillofacial Radiology*, 25(3): 146–150.
- Lindh, C., Obrant, K. & Petersson, A. (2004). Maxillary bone mineral density and its relationship to the bone mineral density of the lumbar spine and hip. *Oral surgery, oral medicine, oral pathology, oral radiology, and endodontics*, 98(1): 102–9.
- Lindh, C., Petersson, A. & Klinge, B. (1995). Measurements of distances related to the mandibular canal in radiographs. *Clinical Oral Implants Research*, 6(2): 96–103.
- Lingam, A., Reddy, L., Nimma, V. & Pradeep, K. (2013). ‘Dental implant radiology’ - Emerging concepts in planning implants. *Journal of Orofacial Sciences*, 5(2): 88.
- Little, M.P., Wakeford, R., Tawn, E.J., Bouffler, S.D. & De Gonzalez, A.B. (2009). Risks associated with low doses and low dose rates of ionizing radiation: Why linearity may be (almost) the best we can do. *Radiology*, 251(1): 6–12.
- Luangchana, P., Pornprasertsuk-Damrongsri, S., Kiattavorncharoen, S. & Jirajariyavej, B. (2015). Accuracy of Linear Measurements Using Cone Beam Computed Tomography and Panoramic Radiography in Dental Implant

- Treatment Planning. *The International Journal of Oral & Maxillofacial Implants*, 30(6): 1287–1294.
- Ludlow, J., Davies-Ludlow, L. & Brooks, S. (2003). Dosimetry of two extraoral direct digital imaging devices: NewTom cone beam CT and Orthophos Plus DS panoramic unit. *Dentomaxillofacial Radiology*, 32(4): 229–234.
- Ludlow, J.B. (2011). A manufacturer's role in reducing the dose of cone beam computed tomography examinations: effect of beam filtration. *Dentomaxillofacial Radiology*, 40(2): 115.
- Ludlow, J.B. (2009). Dosimetry of the Kodak 9000 3D small FOV CBCT and panoramic unit. *Oral Surgery, Oral Medicine, Oral Pathology, Oral Radiology and Endodontics*, 107(4): e29.
- Ludlow, J.B., Davies-Ludlow, L.E. & White, S.C. (2008). Patient risk related to common dental radiographic examinations: the impact of 2007 International Commission on Radiological Protection recommendations regarding dose calculation. *Journal of the American Dental Association (1939)*, 139(9): 1237–43.
- Ludlow, J.B. & Ivanovic, M. (2008). Comparative dosimetry of dental CBCT devices and 64-slice CT for oral and maxillofacial radiology. *Oral Surgery, Oral Medicine, Oral Pathology, Oral Radiology, and Endodontology*, 106(1): 106–114.
- Ludlow, J.B., Timothy, R., Walker, C., Hunter, R., Benavides, E., Samuelson, D.B. & Scheske, M.J. (2015). Effective dose of dental CBCT - A meta analysis of published data and additional data for nine CBCT units. *Dentomaxillofacial Radiology*, 44(1).
- Luk, L.C.K., Pow, E.H.N., Li, T.K.L. & Chow, T.W. (2011). Comparison of ridge mapping and cone beam computed tomography for planning dental implant therapy. *The International journal of oral & maxillofacial implants*, 26(1): 70–4.
- Mah, P., Reeves, T.E. & McDavid, W.D. (2010). Deriving Hounsfield units using

- grey levels in cone beam computed tomography. *Dentomaxillofacial Radiology*, 39(6): 323–335.
- Majid, I., Mukith ur Rahaman, S., Sowbhagya, M., Alikutty, F. & Kumar, H. (2014). Radiographic prescription trends in dental implant site. *Journal of Dental Implants*, 4(2): 140.
- Mall, N. & Pritam, A. (2017). Assessment of current radiographic prescription trends in dental implant treatment planning: A survey based original study. *International Journal of Medical and Health Research*, 3(9): 66–69.
- Manisundar, N., Saravanakumar Hemalatha, B.V., Manigandan, T. & Amudhan, A. (2014). Implant imaging-A literature review. *Biosciences Biotechnology Research Asia*, 11(1): 179–187.
- McCullough, C.H. & Schueler, B.A. (2000). Calculation of effective dose. *Medical Physics*, 27(5): 828–837.
- McLaughlin, D.J. & Mooney, R.B. (2004). Dose reduction to radiosensitive tissues in CT. Do commercially available shields meet the users' needs? *Clinical radiology*, 59(5): 446–450.
- Mehra, A. & Pai, K.M. (2012). Evaluation of dimensional accuracy of panoramic cross-sectional tomography, its ability to identify the inferior alveolar canal, and its impact on estimation of appropriate implant dimensions in the mandibular posterior region. *Clinical Implant Dentistry and Related Research*, 14(1): 100–111.
- Miles, D. & Danforth, R. (2008). A clinician 's guide to understanding cone beam volumetric imaging (CBVI), a peer-reviewed publication. *Academy of Dental Therapeutics and Stomatology*. Available at:  
[https://www.researchgate.net/publication/274681725\\_Comparison\\_of\\_landmark\\_positions\\_between\\_Cone-Beam\\_Computed\\_Tomogram\\_CBCT\\_and\\_Adjusted\\_2D\\_lateral\\_cephalogram/fulltext/55edef908aef559dc4385fc/274681725\\_Comparison\\_of\\_landmark\\_positi](https://www.researchgate.net/publication/274681725_Comparison_of_landmark_positions_between_Cone-Beam_Computed_Tomogram_CBCT_and_Adjusted_2D_lateral_cephalogram/fulltext/55edef908aef559dc4385fc/274681725_Comparison_of_landmark_positi)

ons\_between\_Cone-Beam.

- Miles, D. & Langlais, R. (2004). NCRP report No. 145: New dental X-ray guidelines: their potential impact on your dental practice. *Dentistry today*, 23(9).
- Mora, M.A., Chenin, D.L. & Arce, R.M. (2014). Software tools and surgical guides in dental-implant-guided surgery. *Dental Clinics of North America*, 58(3): 597–626.
- De Moraes, J.A.N.D., Sakakura, C.E., Loffredo, L. de C.M. & Scaf, G. (2007). A survey of radiographic measurement estimation in assessment of dental implant length. *The Journal of oral implantology*, 33(4): 186–90.
- Moraschini, V., da Poubel, L.C., Ferreira, V. & dos Barboza, E.S. (2015). Evaluation of survival and success rates of dental implants reported in longitudinal studies with a follow-up period of at least 10 years: a systematic review. *International Journal of Oral & Maxillofacial Surgery*, 44(3): 377–388.
- Moshfeghi, M., Tavakoli, M.A., Hosseini, E.T., Hosseini, A.T. & Hosseini, I.T. (2012). Analysis of linear measurement accuracy obtained by cone beam computed tomography (CBCT-NewTom VG). *Dental research journal*, 9(Suppl 1): S57-62.
- Mukundan, S., Wang, P.I., Frush, D.P., Yoshizumi, T., Marcus, J., Kloeblen, E. & Moore, M. (2007). MOSFET dosimetry for radiation dose assessment of bismuth shielding of the eye in children. *American Journal of Roentgenology*, 188(6): 1648–1650.
- Di Murro, B., Papi, P., Passarelli, P.C., D’Addona, A. & Pompa, G. (2020). Attitude in radiographic post-operative assessment of dental implants among Italian dentists: A cross-sectional survey. *Antibiotics*, 9(5): 234.
- Nackaerts, O., Maes, F., Yan, H., Couto Souza, P., Pauwels, R. & Jacobs, R. (2011). Analysis of intensity variability in multislice and cone beam computed tomography. *Clinical Oral Implants Research*, 22(8): 873–879.
- Nagalaxmi, V., Swetha, P., Srikanth, K. & Lalitha, C.H. (2015). Implant imaging : A



- review of literature. *IJSS Case Reports & Reviews*, 2(5): 48–54.
- Nagarajan, A., Perumalsamy, R., Thyagarajan, R. & Namasivayam, A. (2014). Diagnostic imaging for dental implant therapy. *Journal of clinical imaging science*, 4(Suppl 2): 4.
- Nair, M.K. & Nair, U.P. (2007). Digital and advanced imaging in endodontics: A review. *Journal of Endodontics*, 33(1): 1–6.
- Naitoh, M., Hirukawa, A., Katsumata, A. & Arijii, E. (2009). Evaluation of voxel values in mandibular cancellous bone: relationship between cone-beam computed tomography and multislice helical computed tomography. *Clinical Oral Implants Research*, 20(5): 503–506.
- National Bureau of Standards. (1964). *Physical Aspects of Irradiation*, NBS Handbook No. 85. Washington DC: US Government Printing Office.
- Nikneshan, S., Aghamiri, M.R., Moudi, E., Bahemmat, N. & Hadian, H. (2016). Dosimetry of three cone beam computerized tomography scanners at different fields of view in terms of various head and neck organs. *Iranian Journal of Radiology*, 13(3): 34220.
- Nikneshan, S., Aval, S.H., Bakhshalian, N., Shahab, S., Mohammadpour, M. & Sarikhani, S. (2014). Accuracy of linear measurement using cone-beam computed tomography at different reconstruction angles. *Imaging Science in Dentistry*, 44(4): 257–262.
- Nitsche, T., Menzebach, M. & Wiltfang, J. (2011). What are the indications for three-dimensional X-ray-diagnostics and image-based computerised navigation aids in dental implantology? *European journal of oral implantology*, 4((Suppl)): 49–58.
- Noffke, C., Farman, A., Nel, S. & Nzima, N. (2011). Guidelines for the safe use of dental and maxillofacial CBCT: a review with recommendations for South Africa. *SADJ : journal of the South African Dental Association = tydskrif van die Suid-Afrikaanse Tandheelkundige Vereniging*, 66(6): 264–6.
- Nomura, Y., Watanabe, H., Honda, E. & Kurabayashi, T. (2010). Reliability of voxel

- values from cone-beam computed tomography for dental use in evaluating bone mineral density. *Clinical Oral Implants Research*, 21(5): 558–562.
- Obed, R.I., Ogbole, G.I. & Majolagbe, S.B. (2015). Comparison of the ICRP 60 and ICRP 103 recommendations on the determination of the effective dose from abdominopelvic computed tomography. *International Journal of Medical Physics, Clinical Engineering and Radiation Oncology*, 04(02): 172–176.
- Oliveira, B., Valerio, C., Jansen, W., Zenóbio, E. & Manzi, F. (2016). Accuracy of digital versus conventional periapical radiographs to detect misfit at the implant-abutment interface. *The International Journal of Oral & Maxillofacial Implants*, 31(5): 1023–1029.
- Özalp, Ö., Tezerişener, H.A., Kocabalkan, B., Büyükkaplan, U.Ş., Özarslan, M.M., Kaya, G.Ş., Altay, M.A. & Sindel, A. (2018). Comparing the precision of panoramic radiography and cone-beam computed tomography in avoiding anatomical structures critical to dental implant surgery: A retrospective study. *Imaging Science in Dentistry*, 48(4): 269–275.
- Pauletto, N., Lahiffe, B.J. & Walton, J.N. (1999). Complications associated with excess cement around crowns on osseointegrated implants: a clinical report. *The International journal of oral & maxillofacial implants*, 14(6): 865–8.
- Pauwels, R., Beinsberger, J., Collaert, B., Theodorakou, C., Rogers, J., Walker, A., Cockmartin, L., Bosmans, H., Jacobs, R., Bogaerts, R. & Horner, K. (2012). Effective dose range for dental cone beam computed tomography scanners. *European Journal of Radiology*, 81(2): 267–271.
- Pauwels, R., Horner, K., Vassileva, J. & Rehani, M.M. (2019). Thyroid shielding in cone beam computed tomography: recommendations towards appropriate use. *Dento maxillo facial radiology*, 48(7): 20190014.
- Pertl, L., Gashi-Cenkoglu, B., Reichmann, J., Jakse, N. & Pertl, C. (2013). Preoperative assessment of the mandibular canal in implant surgery: comparison of rotational panoramic radiography (OPG), computed tomography (CT) and

- cone beam computed tomography (CBCT) for preoperative assessment in implant surgery. *European journal of oral implantology*, 6(1): 73–80.
- Platzer, S., Bertha, G., Heschl, A., Wegscheider, W.A. & Lorenzoni, M. (2012). Three-dimensional accuracy of guided implant placement: indirect assessment of clinical outcomes. *Clinical Implant Dentistry and Related Research*, 15(5): no-no.
- Plooij, J.M., Maal, T.J.J., Haers, P., Borstlap, W.A., Kuijpers-Jagtman, A.M. & Bergé, S.J. (2011). Digital three-dimensional image fusion processes for planning and evaluating orthodontics and orthognathic surgery. A systematic review. *International Journal of Oral and Maxillofacial Surgery*, 40(4): 341–352.
- Popelut, A., Valet, F., Fromentin, O., Thomas, A. & Bouchard, P. (2010). Relationship between Sponsorship and Failure Rate of Dental Implants: A Systematic Approach. *PLoS ONE*, 5(4): e10274.
- Prins, R., Dauer, L.T., Colosi, D.C., Quinn, B., Kleiman, N.J., Bohle, G.C., Holohan, B., Al-Najjar, A., Fernandez, T., Bonvento, M., Faber, R.D., Ching, H. & Goren, A.D. (2011). Significant reduction in dental cone beam computed tomography (CBCT) eye dose through the use of leaded glasses. *Oral surgery, oral medicine, oral pathology, oral radiology, and endodontics*, 112(4): 502–507.
- Qiang, W., Qiang, F. & Lin, L. (2019). Estimation of effective dose of dental x-ray devices. *Radiation Protection Dosimetry*, 183(4): 418–422.
- Qu, X.M., Li, G., Ludlow, J.B., Zhang, Z.Y. & Ma, X.C. (2010). Effective radiation dose of ProMax 3D cone-beam computerized tomography scanner with different dental protocols. *Oral Surgery, Oral Medicine, Oral Pathology, Oral Radiology and Endodontology*, 110(6): 770–776.
- Qu, X.M., Li, G., Sanderink, G.C.H., Zhang, Z.Y. & Ma, X.C. (2012). Dose reduction of cone beam CT scanning for the entire oral and maxillofacial regions with thyroid collars. *Dento maxillo facial radiology*, 41(5): 373–8.

- Qu, X.M., Li, G., Zhang, Z. & Ma, X. (2012). Thyroid shields for radiation dose reduction during cone beam computed tomography scanning for different oral and maxillofacial regions. *European Journal of Radiology*, 81(3).
- Rabi, H., Qirresh, E. & Rabi, T. (2017). Radiographic prescription trends among Palestinian dentists for dental implant placement – A cross sectional survey. *Journal of Dental Problems and Solutions*: 11–14.
- Radiation control, D. of H.S.A. (2017). *Requirements for licence holders with respect to quality control tests for dental diagnostic x-ray imaging systems (version 10)*. Available at: <https://www.sahpra.org.za/wp-content/uploads/2020/01/DIAGNOSTIC-QC-Dental-March-2017-Version-10-2.pdf>.
- Ramakrishnan, P., Shafi, F.M., Subhash, A., Kumara, A.E.G., Chakkarayan, J. & Vengalath, J. (2014). A survey on radiographic prescription practices in dental implant assessment among dentists in Kerala, India. *Oral health and dental management*, 13(3): 826–30.
- Reeves, T., Mah, P. & McDavid, W. (2012). Deriving Hounsfield units using grey levels in cone beam CT: a clinical application. *Dentomaxillofacial Radiology*, 41(6): 500–508.
- Riecke, B., Friedrich, R.E., Schulze, D., Loos, C., Blessmann, M., Heiland, M. & Wikner, J. (2015). Impact of malpositioning on panoramic radiography in implant dentistry. *Clinical Oral Investigations*, 19(4): 781–790.
- Roberts, J.A., Drage, N.A., Davies, J. & Thomas, D.W. (2009). Effective dose from cone beam CT examinations in dentistry. *The British journal of radiology*, 82(973): 35–40.
- Rottke, D., Patzelt, S., Poxleitner, P. & Schulze, D. (2013). Effective dose span of ten different cone beam CT devices. *Dentomaxillofacial Radiology*, 42(7).
- Sahai, S. (2015). Recent advances in imaging technologies in implant dentistry. *Journal of the International Clinical Dental Research Organization*, 7(3): 19.

- Sakakura, C., Morais, J., Loffredo, L. & Scaf, G. (2003). A survey of radiographic prescription in dental implant assessment. *Dentomaxillofacial Radiology*, 32(6): 397–400.
- SCENIHR. (2012). *Scientific Committee on Emerging and Newly Identified Health Risks (SCENIHR): Health effects of security scanners for passenger screening (based on X-ray technology)*. Brussels: European Commission. Available at: [https://ec.europa.eu/health/scientific\\_committees/emerging/docs/scenih\\_r\\_o\\_036.pdf](https://ec.europa.eu/health/scientific_committees/emerging/docs/scenih_r_o_036.pdf).
- Schilling, R. & Geibel, M.A. (2013). Assessment of the effective doses from two dental cone beam CT devices. *Dentomaxillofacial Radiology*, 42(5).
- Schropp, L., Stavropoulos, A., Gottfredsen, E. & Wenzel, A. (2011). Comparison of panoramic and conventional cross-sectional tomography for preoperative selection of implant size. *Clinical Oral Implants Research*, 22(4): 424–9.
- Schropp, L., Wenzel, A. & Kostopoulos, L. (2001). Impact of conventional tomography on prediction of the appropriate implant size. *Oral Surgery, Oral Medicine, Oral Pathology, Oral Radiology, and Endodontics*, 92(4): 458–63.
- Seeram, E. (2009). *Computed tomography: physical principles, clinical applications, and quality control*. 3rd ed. St. Louis: Saunders Elsevier.
- Sewerin, I. (1990). Errors in radiographic assessment of marginal bone height around osseointegrated implants. *European Journal of Oral Sciences*, 98(5): 428–433.
- Shah, N., Bansal, N. & Logani, A. (2014). Recent advances in imaging technologies in dentistry. *World journal of radiology*, 6(10): 794–807.
- Sheikhi, M., Dakhil-Alian, M. & Bahreinian, Z. (2015). Accuracy and reliability of linear measurements using tangential projection and cone beam computed tomography. *Dental research journal*, 12(3): 271–7.
- Shen, P., Zhao, J., Fan, L., Qiu, H., Xu, W., Wang, Y., Zhang, S. & Kim, Y.-J. (2015). Accuracy evaluation of computer-designed surgical guide template in oral implantology. *Journal of Cranio-Maxillofacial Surgery*, 43(10): 2189–2194.

- Shewale, A., Gattani, D., Gudadhe, B. & Meshram, S. (2017). Radiographic imaging assessment prior to implant placement – Choice of dentists in Nagpur city. *Indian J Dent Adv*, 9(3): 139–143.
- Shin, H.S., Nam, K.C., Park, H., Choi, H.U., Kim, H.Y. & Park, C.S. (2014). Effective doses from panoramic radiography and CBCT (cone beam CT) using dose area product (DAP) in dentistry. *Dentomaxillofacial Radiology*, 43(5).
- Silva, M.A.G., Wolf, U., Heinicke, F., Bumann, A., Visser, H. & Hirsch, E. (2008). Cone-beam computed tomography for routine orthodontic treatment planning: A radiation dose evaluation. *American Journal of Orthodontics and Dentofacial Orthopedics*, 133(5): 640.e1-640.e5.
- Singh, R., Singh, S., Nabi, A.T., Huda, I. & Singh, D. (2019). Evaluation of existing radiographic prescription tendencies in planning dental implant therapy: A survey based original study. *Journal of Advanced Medical and Dental Sciences Research*, 7(1): 100–103.
- Smith, D.E. & Zarb, G.A. (1989). Criteria for success of osseointegrated endosseous implants. *The Journal of Prosthetic Dentistry*, 62(5): 567–572.
- Stratemann, S.A., Huang, J.C., Maki, K., Miller, A.J. & Hatcher, D.C. (2008). Comparison of cone beam computed tomography imaging with physical measures. *Dentomaxillofacial Radiology*, 37(2): 80–93.
- Superior Health Council. (2011). *Advisory report of the Superior Health Council No 8705. Dental Cone beam computed tomography*. Brussels. Available at: [https://www.health.belgium.be/sites/default/files/uploads/fields/fpshealth\\_theme\\_file/19068321/Dentale cone beam computed tomography %28february 2011%29 %28SHC 8705%29.pdf](https://www.health.belgium.be/sites/default/files/uploads/fields/fpshealth_theme_file/19068321/Dentale%20cone%20beam%20computed%20tomography%20february%202011%20SHC%208705.pdf).
- Sur, J., Seki, K., Koizumi, H., Nakajima, K. & Okano, T. (2010). Effects of tube current on cone-beam computerized tomography image quality for presurgical implant planning in vitro. *Oral Surgery, Oral Medicine, Oral Pathology, Oral Radiology and Endodontology*, 110(3): 29–33.

- Tang, Z., Liu, X. & Chen, K. (2017). Comparison of digital panoramic radiography versus cone beam computerized tomography for measuring alveolar bone. *Head and Face Medicine*, 13(1): 1–7.
- Tapiovaara, M. & Siiskonen, T. (2008). *PCXMC 2.0 user's guide*. Helsinki: Radiation and Nuclear Safety Authority of Finland (STUK).
- Tepedino, M., Cornelis, M.A., Chimenti, C. & Cattaneo, P.M. (2018). Correlation between tooth size-arch length discrepancy and interradicular distances measured on CBCT and panoramic radiograph: An evaluation for miniscrew insertion. *Dental Press Journal of Orthodontics*, 23(5): 39.e1-39.e13.
- Tharmalingam, S., Sreetharan, S., Brooks, A.L. & Boreham, D.R. (2019). Re-evaluation of the linear no-threshold (LNT) model using new paradigms and modern molecular studies. *Chemico-Biological Interactions*, 301: 54–67.
- Theodorakou, C., Walker, A., Horner, K., Pauwels, R., Bogaerts, R. & Jacobs, R. (2012). Estimation of paediatric organ and effective doses from dental cone beam CT using anthropomorphic phantoms. *The British journal of radiology*, 85(1010): 153–160.
- Torres, M.G.G., Campos, P.S.F., Segundo, N.P.N., Navarro, M. & Crusoé-Rebello, I. (2012). Accuracy of linear measurements in cone beam computed tomography with different voxel sizes. *Implant dentistry*, 21(2): 150–5.
- Tsiklakis, K., Donta, C., Gavala, S., Karayianni, K., Kamenopoulou, V. & Hourdakis, C.J. (2005). Dose reduction in maxillofacial imaging using low dose Cone Beam CT. *European Journal of Radiology*, 56(3): 413–417.
- Tubiana, M., Feinendegen, L.E., Yang, C. & Kaminski, J.M. (2009). The linear no-threshold relationship is inconsistent with radiation biologic and experimental data. *Radiology*, 251(1): 13–22.
- Turkyilmaz, I., Tözüm, T.F. & Tumer, C. (2007). Bone density assessments of oral implant sites using computerized tomography. *Journal of Oral Rehabilitation*, 34(4): 267–272.

- Tyndall, D.A. & Brooks, S.L. (2000). Selection criteria for dental implant site imaging: a position paper of the American Academy of Oral and Maxillofacial radiology. *Oral surgery, oral medicine, oral pathology, oral radiology, and endodontics*, 89(5): 630–7.
- Tyndall, D.A., Price, J.B., Tetradis, S., Ganz, S.D., Hildebolt, C., Scarfe, W.C. & American Academy of Oral and Maxillofacial Radiology. (2012). Position statement of the American Academy of Oral and Maxillofacial Radiology on selection criteria for the use of radiology in dental implantology with emphasis on cone beam computed tomography. *Oral Surgery, Oral Medicine, Oral Pathology and Oral Radiology*, 113(6): 817–826.
- Vandenbergh, B., Luchsinger, S., Hostens, J., Dhoore, E., Jacobs, R., Sedentexct, T. & Consortium, P. (2012). The influence of exposure parameters on jawbone model accuracy using cone beam CT and multislice CT. *Dentomaxillofacial Radiology*, 41(6): 466–474.
- Vazquez, L., Nizamaldin, Y., Combescure, C., Nedir, R., Bischof, M., Dohan Ehrenfest, D.M., Carrel, J.P. & Belser, U.C. (2013). Accuracy of vertical height measurements on direct digital panoramic radiographs using posterior mandibular implants and metal balls as reference objects. *Dentomaxillofacial Radiology*, 42(2).
- Vazquez, L., Saulacic, N., Belser, U. & Bernard, J.P. (2008). Efficacy of panoramic radiographs in the preoperative planning of posterior mandibular implants: A prospective clinical study of 1527 consecutively treated patients. *Clinical Oral Implants Research*, 19(1): 81–5.
- Vercruyssen, M., Cox, C., Coucke, W., Naert, I., Jacobs, R. & Quirynen, M. (2014). A randomized clinical trial comparing guided implant surgery (bone- or mucosa-supported) with mental navigation or the use of a pilot-drill template. *Journal of Clinical Periodontology*, 41(7): 717–723.
- Verdun, F.R., Bochud, F., Gundinchet, F., Aroua, A., Schnyder, P., Meuli, R.,



- Gudinchet, F., Aroua, A., Schnyder, P. & Meuli, R. (2008). Quality initiatives radiation risk: what you should know to tell your patient. *Radiographics*, 28(7): 1807–1816.
- Wadhvani, C.P.K., Schuler, R., Taylor, S. & Chen, C.S.K. (2012). Intraoral radiography and dental implant restoration. *Dentistry today*, 31(8): 66, 68, 70–1; quiz 72–3.
- Walker, C. & van der Putten, W. (2012). Patient dosimetry and a novel approach to establishing Diagnostic Reference Levels in dental radiology. *Physica Medica*, 28(1): 7–12.
- Wall, B.F., Harrison, R.M. & Spiers, F.W. (1988). *Patient dosimetry techniques in diagnostic radiology*. United Kingdom.
- Waltrick, K.B., de Abreu Junior, M.J.N., Corrêa, M., Zastrow, M.D. & D'Avila Dutra, V. (2013). Accuracy of linear measurements and visibility of the mandibular canal of Cone-beam computed tomography images with different voxel sizes: an in vitro study. *Journal of Periodontology*, 84(1): 68–77. Available at: <http://doi.wiley.com/10.1902/jop.2012.110524>. [Accessed 10 August 2020].
- White, S.C. & Pharoah, M.J. (2013). *Oral radiology : principles and interpretation*. 7th editio. St. Louis, Missouri: Mosby,Elsevier.
- Wood, M.R., Vermilyea, S.G. & Committee on Research in Fixed Prosthodontics of the Academy of Fixed Prosthodontics. (2004). A review of selected dental literature on evidence-based treatment planning for dental implants: report of the Committee on Research in Fixed Prosthodontics of the Academy of Fixed Prosthodontics. *The Journal of prosthetic dentistry*, 92(5): 447–62.
- Yassaei, S., Ezoddini-Ardakani, F. & Ostovar, N. (2010). Predicting the actual length of premolar teeth on the basis of panoramic radiology. *Indian Journal of Dental Research*, 21(4): 468.
- Yeh, J.K. & Chen, C.H. (2018). Estimated radiation risk of cancer from dental cone-

beam computed tomography imaging in orthodontics patients. *BMC Oral Health*, 18(1): 131.

Zarch, S., Bagherpour, A., Javadian Langaroodi, A., Ahmadian Yazdi, A. & Safaei, A. (2011). Evaluation of the accuracy of panoramic radiography in linear measurements of the jaws. *Iranian Journal of Radiology*, 8(2): 97–102.



## PART 9 APPENDICES

## 1) ETHICS APPROVAL LETTER



OFFICE OF THE DIRECTOR: RESEARCH  
RESEARCH AND INNOVATION DIVISION

Private Bag X17, Bellville 7535  
South Africa  
T: +27 21 959 4111/2948  
F: +27 21 959 3170  
E: [research-ethics@uwc.ac.za](mailto:research-ethics@uwc.ac.za)  
[www.uwc.ac.za](http://www.uwc.ac.za)

11 March 2019

Dr KR Besthawi  
Faculty of Dentistry

**Ethics Reference Number:** BM19/1/20

**Project Title:** Recommendations for the development of a framework for radiological imaging studies during implant therapy in SA.

**Approval Period:** 07 March 2019 – 07 March 2020

I hereby certify that the Biomedical Science Research Ethics Committee of the University of the Western Cape approved the scientific methodology and ethics of the above mentioned research project.

Any amendments, extension or other modifications to the protocol must be submitted to the Ethics Committee for approval.

**Please remember to submit a progress report in good time for annual renewal.**

The Committee must be informed of any serious adverse event and/or termination of the study.

A handwritten signature in black ink, appearing to read 'Josias'.

*Ms Patricia Josias  
Research Ethics Committee Officer  
University of the Western Cape*

**BMREC REGISTRATION NUMBER -130416-050**

FROM HOPE TO ACTION THROUGH KNOWLEDGE.

## 2) INFORMATION SHEET



UNIVERSITY of the  
WESTERN CAPE

Faculty of Dentistry &  
WHO Oral Health Collaborating Centre  
Department of Diagnostic Science  
Private Bag X17, Bellville 7535, South Africa  
Telephone: +27 21 937 3112



Code: INF1/2018

### INFORMATION SHEET

**Research Project Title:** ‘Recommendations for the development of a framework for radiological imaging studies during implant therapy in SA’

**Principal investigator:** Khaled Beshtawi, B.D.S, M.Sc.

A research Project will be submitted for the fulfilment of the requirements of a PhD degree at the Department of Diagnostic Science, Faculty of Dentistry – University of the Western Cape.

#### What is this study about?

The planned research intends to propose an imaging protocol to be used during implant therapy. The research will assess the international and local guidelines regarding imaging protocols, current radiographic practices in South Africa, radiation doses, and the clinical measurement accuracy of several radiographic modalities. At the end of this study, we aim to develop a protocol for a “lower-dose” and clinically efficient radiographic assessment during implant therapy in South Africa.

### **What will I be asked to do if I agree to participate?**

A consent form to participate should be signed and a questionnaire involves 25 MCQ'S (Multiple Choice Questions) will be supplied. These questions will capture the radiographic practice of the participants according to different clinical scenarios proposed in the questionnaire.

### **Would my participation in this study be kept confidential?**

The researchers undertake to protect your identity and the nature of your contribution. Written informed consent will be obtained from all participants on standardized Forms which will be available in English, Afrikaans, Xhosa and if necessary any other indigenous language. All information will be stored in protected environments. All personal identifiers will not be disclosed and will be kept anonymous when the data are published.

### **What are the risks of this research?**

There is no if any risk at all to you as a research participant. This study necessitates only completing a questionnaire. There is no risk of physical, psychological, social or economic harm to the participant during this study.

### **What are the benefits of this research?**

This research is not designed to help you personally, the findings of this study will contribute to the understanding of the actual radiographic practices in South Africa. At the end of this project, we aim to Construct, adopt and customize a protocol for a “lower-dose” and clinically efficient radiographic assessment during implant therapy; that considers the clinical preferences, equipment, and socioeconomic factors in South Africa.

Your participation in this research is completely voluntary. You may choose not to take part at all. If you decide to participate in this research, you may stop participating

at any time. If you decide not to participate in this study or if you stop participating at any time, you will not be penalized or lose any benefits to which you otherwise qualify

### What if I have questions?

If any questions have raised at any point, please feel free to contact the principal investigator or any of the supervisors. Your input will enrich the content and it is absolutely appreciated

|  |  |   |
|--|--|---|
| <p><b>Khaled Beshtawi</b><br/>B.D.S, M.Sc.</p>   | <p><b>Prof Manogari Chetty</b><br/>BSc, BChD, MChD, Ph.D.</p>  | <p><b>Dr. Mogammad Peck</b><br/>BChD, MSc Dent, MChD,<br/>MRD RCSEd, FDS RCSEd</p>  |
| <p><b>Principal investigator</b><br/>University of the Western<br/>Cape<br/><a href="mailto:kbeshtawi@uwc.ac.za">kbeshtawi@uwc.ac.za</a></p> | <p><b>Supervisor</b><br/>University of the Western<br/>Cape<br/><a href="mailto:mchetty@uwc.ac.za">mchetty@uwc.ac.za</a></p> | <p><b>Co-Supervisor</b><br/>University of the<br/>Western Cape<br/><a href="mailto:mpeck@uwc.ac.za">mpeck@uwc.ac.za</a></p> |

**This research has been approved by the University of the Western Cape's Biomedical Research Ethics Committee/Humanities and Social Sciences Research Ethics Committee. Reference number: BM 19/1/20**

|  |
|--|
| <p><b>BMREC</b><br/>UWC<br/>Private Bag x17<br/>Bellville<br/>7535<br/>Tel: + 27 21 959 4111<br/>Email: <a href="mailto:research-ethics@uwc.ac.za">research-ethics@uwc.ac.za</a></p> |
|--|

### 3) CONSENT FORM: PARTICIPATION IN THE STUDY



UNIVERSITY of the  
WESTERN CAPE

Faculty of Dentistry &  
WHO Oral Health Collaborating Centre  
Department of Diagnostic Science  
Private Bag X17, Bellville 7535, South Africa  
Telephone: +27 21 937 3112



World Health  
Organization

Code: CF1/2018

#### CONSENT FORM: PARTICIPATION IN THE STUDY

**Research Project Title:** ‘Recommendations for the development of a framework for radiological imaging studies during implant therapy in SA’

**Principal investigator:** Khaled Beshtawi, B.D.S, M.Sc.

A research project will be submitted for the fulfillment of the requirements of a Ph.D. degree at the Department of Diagnostic Science, Faculty of Dentistry - University of the Western Cape.

**I hereby certify that:**

The study has been described to me in language that I understand. My questions about the study have been answered. And I understand:

- 1- What my participation will involve and I freely and voluntarily agree to participate.
- 2- That all the information obtained during this study will be kept confidential and no personal identification will be disclosed.
- 3- The data/results of this study can be used for approved research purposes and publications.
- 4- I may withdraw from the study at any time without giving a reason and without fear of negative consequences or loss of benefits.

**Participant’s name**.....

**Participant's Signature**.....

**Date**.....

#### 4) SURVEY (Q1/2018): RADIOGRAPHIC TRENDS DURING DENTAL IMPLANT THERAPY IN SOUTH AFRICA

|                                    | Question   | Choices   |
|------------------------------------|--|---|
| Assessment phase: implant planning | What type of radiograph/s would you prefer to take during the implant planning stage in the posterior mandible (Unilateral, distal to first premolar region)?    | <ol style="list-style-type: none"> <li>1. Periapical radiograph/s (P.A) only</li> <li>2. Panoramic radiograph (PAN) only</li> <li>3. PAN + P.A only</li> <li>4. P.A + CBCT</li> <li>5. Pan + CBCT</li> <li>6. CBCT only</li> <li>7. No Radiographs</li> <li>8. Other</li> </ol>   |
|                                    | What type of radiograph/s would you prefer to take during the implant planning stage in the anterior region of the Maxilla/Mandible (Canine to Canine region)?   |   |
|                                    | What type of radiograph/s would you prefer to take during the implant planning stage in the posterior maxilla region (Unilateral: distal to the first premolar)? |   |
|                                    | What type of radiograph/s would you prefer to take during the implant planning stage in one jaw (Mandible/Maxilla) or both jaws (Full mouth)?                    |   |
|                                    | What type of radiograph/s would you prefer to take during the implant planning stage in the mental foramen region (uni/bilateral)?                               |   |
|                                    | Concerning your previous selections, can you specify the factor/s that influenced your radiographic preference (Multiple answers are allowed)?                   | <ol style="list-style-type: none"> <li>1. lower costs for the patients (If the conventional modalities PAN and/or P.A were preferred previously)</li> <li>2. Availability and ease of access of the radiographic modality (if the conventional modalities PAN and/or P.A were preferred previously)</li> <li>3. Radiation dose concerns of three-dimensional modalities (if the conventional modalities PAN and/or P.A were preferred previously)</li> <li>4. Broad coverage of the designated anatomical area (If PAN and/or CBCT were preferred previously)</li> <li>5. Better dimensional accuracy (if three-dimensional modalities e.g. CBCT were selected previously)</li> </ol> |



|                                  |  |   |
|----------------------------------|--|---|
|                                  |  | <ol style="list-style-type: none"> <li>6. Three-dimensional modalities provide more anatomical information necessary for the success of the therapy</li> <li>7. Only Three-dimensional modalities (e.g. CBCT) if guided implant surgery is considered</li> <li>8. Other:</li> </ol>   |
| <b>Intraoperative / Surgical</b> | <b>What type of radiograph/s would you prefer to take during the implant surgery (i.e. to check the drilling site's position, orientation, and extent, etc., with no suspicion of any operative complication)?</b> | <ol style="list-style-type: none"> <li>1. Periapical radiograph/s (P.A)</li> <li>2. Panoramic radiograph (PAN)</li> <li>3. CBCT</li> <li>4. No radiographs needed</li> </ol>  |
|                                  | <b>What type of radiograph/s would you prefer to take directly after the implant surgery? *</b>  |   |
| <b>Follow-up</b>                 | <b>What type of radiograph/s would you prefer to take during follow-up (Asymptomatic patient)? *</b>   | <ol style="list-style-type: none"> <li>1. Periapical radiograph/s (P.A) only</li> <li>2. Panoramic radiograph (PAN) only</li> <li>3. PAN + P.A only</li> <li>4. P.A + CBCT</li> <li>5. Pan + CBCT</li> <li>6. CBCT only</li> <li>7. No Radiographs</li> <li>8. Other</li> </ol>   |
|                                  | <b>In case of any post-operative complications (e.g. unresolved swelling, pain and/or neurological dysfunction) what type of radiograph/s would you consider?</b>  |   |
|                                  | <b>Concerning your previous selection, can you specify the reason/s why you selected that specific modality/s (Multiple answers are allowed)?</b>  | <ol style="list-style-type: none"> <li>1. Conventional radiographs (especially P.A) are preferred as the CBCT is of limited value if radiographic artefacts (caused by implants e.g. beam hardening and scattering) are evident in the volume</li> <li>2. CBCT provides more information regardless of the limitations of possible beam radiographic artefacts caused by the implants</li> <li>3. Availability and ease of access of the radiographic modality</li> <li>4. Broad coverage of the designated anatomical area</li> <li>5. Other:</li> </ol> |
|                                  | <b>What is the frequency of radiographic follow-up (After the delivery of the prosthesis)?</b>   | <ol style="list-style-type: none"> <li>1. After the first 6 months, 12 months, and then every year for a 10-year period.</li> <li>2. Every year for a 10-year period.</li> <li>3. After 6 months, 12 months and then every year for a 3-year period.</li> <li>4. Every three years for ten years</li> <li>5. Other:</li> </ol>  |